Defining the role of Fibroblast Growth Factor signaling in lung development

By

John Herriges

A dissertation submitted in partial fulfillment of

the requirements for the degree of

Doctor of Philosophy

(Genetics)

at the

UNIVERSITY OF WISCONSIN-MADISON

2014

Date of final oral examination: 05/02/2014

The dissertation is approved by the following members of the Final Oral Committee:
Xin Sun, Associate Professor, Genetics
Arash Bashirullah, Assistant Professor, Pharmacy
Akihiro, Ikeda, Associate Professor, Genetics
Allen, Laughon, Professor, Genetics
Avtar Roopra, Associate Professor, Neuroscience

Table of Contents:

Acknowledgments……iii

Abstract……iv

Chapter I: Introduction ……1
Figures……11

Chapter II: A genome-scale study of transcription factor expression in the branching mouse lung. ……15
Abstract ……16
Introduction……17
Results/Discussion……20
Conclusion……53
Materials and Methods……55
Figures……57

Chapter III: FGF-regulated Etv genes control FGF-SHH feedback loop in branching lung……68
Abstract ……69
Introduction……70
Results……73
Discussion……79
Materials and Methods……83
Figures……88

Chapter IV: Examining the role of *Fgfr3* and Fgfr4 in postnatal lung development……108
Abstract ……109
Introduction……110
Results……114
Discussion……123
Materials and Methods……127
Figures……130

Chapter V: Conclusions and future directions……162

Appendix I: *Etv4* and *Etv5* mediate postnatal lung development through controlling prenatal lung patterning……167
Abstract……168
Introduction……169
Results……172
Discussion……177
Materials and Methods……180
Figures……183

Appendix II: Identification of a novel *Ift140* allele.....201
Introduction……...……..……..202
Results/Discussion…….....203
Conclusion....……...206
Materials and Methods.....207
Figures…….…….....…...209

References: …….....….....219

Acknowledgments:

First, I would like to thank my advisor, Xin Sun, and my committee members: Allen Laughon, Arash Bashirullah, Akihiro Ikeda, and Avtar Roopra, for their helpful insights and suggestions on my research projects. I am especially grateful for Xin for her constant support and guidance.

Second, I would like to thank the American Heart Association Graduate Fellowship Program for supporting two years of my graduate studies at UW-Madison.

Third, I would like to thank my parents and family for all of the support that they have given me, and for reminding me that its ok to leave lab every once and a while.

Lastly, I would like to thank past and present members of the Sun lab for putting up with me these past six years: Jamie Verheyden, Lisa Abler, Zhen Zhang, Liz Hines, Kurt Throckmorton, Kelsey Branchfield, Shige Yokoyamo, David McCulley, Tina Zhang, Mary-kayt Jones, Xouchee Mauo, Sarah Hamilton and Amber Lashua.

Abstract

Defining the role of Fibroblast Growth Factor signaling in lung development

By

John Herriges

Under the supervision of Professor Xin Sun

At the University of Wisconsin-Madison

In mammals the lung is necessary for survival at birth. The development of the lung is an incredibly complex process in which two fluid filled epithelial buds are transformed into millions of alveoli that are able to facilitate oxygen uptake. One of the principle signaling pathways that mediates lung development is the FGF signaling pathway. Here I examine the role of FGF signaling in lung development and maturation.

While a great deal is known about how signaling pathways mediate lung branching morphogenesis on the level of the ligand and receptor, relatively little is known about the transcriptional regulation this process. To identify novel transcription factors involved branching morphogenesis, I took part in a genome scale RNA *in situ* hybridization screen. In this screen we identified sixty-two transcription factors that were expressed during branching morphogenesis. The majority of the transcription factors we identified had not been previously implicated in lung development. Therefore my studies have identified new transcription factors that may regulate branching morphogenesis in the mouse lung.

Previous studies have identified that the FGF signaling pathway is a key mediator of lung development. My results further our knowledge of how FGF signaling mediates lung development by demonstrating that the FGF regulated transcription factors *Etv4* and *Etv5* (hereafter *Etv4;5*) are necessary for embryonic lung development. Interestingly, we found that although *Etv4;5* act downstream of the FGF signaling pathway, FGF signaling was increased in the *Etv4;5* mutant lung. Subsequent genetic experiments demonstrated that this increase in *Fgf10* expression contributes to the *Etv4;5* mutant phenotype. Additionally, we found that SHH signaling was decreased in the *Etv4;5* mutant lung, and that activating the SHH signaling pathway was able to rescue the *Etv4;5* mutant phenotype. Together my data suggests a model in which *Etv4;5* are mediating lung development by acting as intermediates in an FGF-SHH signaling loop.

Previous works have shown that *Fgfr3* and *Fgfr4* (hereafter *Fgfr3;4*) are necessary for alveologenesis in the postnatal lung; however, these studies have not identified how *Fgfr3;4* mediate postnatal lung development. In my studies I have further examined *Fgfr3;4* double knockout mice (hereafter *Fgfr3;4* mutant) in order to elucidate the mechanisms through which they control postnatal lung development. Interestingly, I found that *Fgfr3;4* mutant mice first develop a phenotype during sacculation, which is prior to what has previously been reported. Additionally, through the use of *Fgfr3;4* conditional mutant mice I have found that the primary role of *Fgfr3;4 lies within the mesenchyme of the lung*. Finally, when I examined the *Fgfr3;4* mutant lungs for phenotypic changes, I found that the initial phenotype was an increased deposition of Elastin fibers in the distal alveoli. Together my data expands upon the present

knowledge of how FGFR3;4 mediate postnatal lung development as it shows that through the mesenchyme *Fgfr3;4* mediates postnatal sacculation by controlling the deposition of the Elastin extracellular matrix.

Chapter I: Introduction

Introduction:

Lung development is a complex process, and the mature lung is essential for mammalian survival at birth. In humans, lung-related diseases such as broncho-pulmonary dysplasia (BPD), Idiopathic pulmonary fibrosis (IPF), and chronic obstructive pulmonary disease (COPD) afflict a large portion of the population, and their specific disease mechanisms are poorly understood. Interestingly, many of the phenotypic abnormalities associated with human lung diseases are also found in genetic mouse models. Therefore, by studying these genetic mouse models we can potentially gain a better understanding of the mechanisms behind the development of these diseases. In these studies I utilize genetic mouse models to examine lungs that span a range of stages, with the goal of gaining a comprehensive view of how the lung develops and matures.

Overview of lung development

In mice, lung development and maturation can be divided into five stages: embryonic bud initiation (E9.5-E11.5), pseudoglandular (E11.5-E16.5), canalicular (E16.5-E17.5), saccular (E17.5-P5), and alveolar (P4~P36) (Maeda et al. 2007; Morrisey and Hogan 2010). In mice the respiratory lineage marker *Nkx2.1* is first expressed in the embryonic foregut as early as E8.25 (Lazzaro et al. 1991; Minoo et al. 1999). However, the embryonic lung buds are not visible until more than a day later, when the right and left lung lobes sprout from the ventral foregut. Between E9.5-E11.5 the lung buds elongate and form the secondary branches that will become the four right lobes and the single left lobe of the mouse lung. After bud initiation, the lung buds enter

the pseudoglandular stage where they utilize a reiterative series of three different forms of branching to establish hundreds of epithelial airways (Metzger et al. 2008). During the pseudoglandular stage, specialized epithelial populations, like neuroendocrine bodies (NEBs), club cells (also known as clara cells), and ciliated cells begin to form in the proximal epithelium (Rawlins et al. 2006). Additionally, during this time the distinction between what will become the proximal airways and the distal alveoli becomes more apparent.

Over the final days of embryonic development and during first few days after birth, the lung undergoes a drastic morphological shift that will allow for the uptake of oxygen. Through the process of saccular branching, the distal lung begins to form primitive alveoli, or saccules, that are the functional unit of oxygen uptake (Figure 1A) (Morrisey and Hogan 2010). During this time there are also several changes on the cellular level that will allow for oxygen uptake at birth. In the epithelium, alveolar epithelial (AEC) type I and AEC type II cells mature. AEC type I cells are flat cells that coat the vast majority of the lung surface area, and are the primary epithelial cell type mediating oxygen uptake (Figure 1 yellow cells) (Bourbon et al. 2005; Dobbs et al. 2010). Mature AEC type II cells have a more rounded morphology and produce surfactants, a protein and lipid mixture that lowers surface tension in the lung and allows lung expansion at birth (Figure 1 green cells) (Khoor et al. 1994**;** Whitsett and Weaver 2002**;** Serrano et al. 2006). Additionally, during this stage the vascular network in the distal lung begins to remodel so that a capillary network runs through the walls of each primitive alveoli in close association with the AEC type I cells. This close association between the AEC type I cells and the capillary network will facilitate oxygen uptake and

allow for its transport throughout the body. While the development of the primitive alveoli supports gas-exchange at the end of saccular stage, further development is needed to facilitate the oxygen uptake required in an adult mouse.

At the end of sacculation (P4), the alveolar surface area of the lung accounts for approximately 5% of the total alveolar surface area in an adult mouse (Mund et al. 2008). To increase the alveolar surface, the distal lung undergoes the process known as alveologenesis, in which thousands of septal crests grow from the walls of the primitive alveoli, into the air filled alveolar lumen (Figure 1B). The exact mechanisms through which septal outgrowth occurs is still not fully understood. However recent studies have demonstrated that the smooth muscle expressing interstitial fibroblasts, known as myofibroblasts, are critical for this process (Bostrom et al. 1996; Lindahl et al. 1997). During alveologenesis myofibroblasts localize to outgrowing septal crests, and the loss of this population inhibits septal outgrowth (McGowen et al. 2008).

One of the mechanisms through which myofibroblasts are thought to mediate alveolar development is by establishing the alveolar Elastin extracellular matrix (ECM). Like the myofibroblasts, the Elastin ECM is necessary for alveolar development, with *Elastin* knockout mice developing a severely simplified alveolar structure (Wendel et al. 2000). The Elastin ECM is primarily made from the monomer tropoelastin, which is produced by myofibroblasts (Bostrom et al. 1996; Lindahl et al. 1997; Yeo et al 2010). To form the Elastin fibers that make up the Elastin ECM, tropoelastin is cross-linked into bundles through interactions with the LOX and FBLN proteins and transported onto a microfiber network. Once the tropoelastin bundles are placed on the microfibers, they then undergo further crosslinking to form an Elastin fiber. Many of the proteins

necessary for the formation of the Elastin ECM are also necessary for lung development, as the knockout mice for LOXL1, FBLN5, and FBN1 also develop severe alveolar phenotypes (Yanagisawa et al. 2002;Neptune et al. 2003; Liu et al 2004). The Elastin ECM is thought to control alveolar development through a few different mechanisms. First, the Elastin ECM is though to mediate alveolar development by providing structural integrity and elasticity to the alveolar walls. This role is most obvious in the Elastin knockout mice, where Elastin knockout lungs are indistinguishable from control lungs prior to birth, but cannot maintain their alveolar structure postnatally (Wendel et al. 2000). Second, the Elastin ECM is thought to mediate alveolar development by controlling the diffusion of growth factors like TGF-b (Neptune et al. 2003).

In addition to being necessary for postnatal lung development, the disruption of both myofibroblasts and the Elastin ECM is associated with multiple lung diseases like BPD and COPD (Benjamin et al. 2007; Merrilees et al. 2008; Turino et al. 2011; Karvonen et al. 2013). Thus gaining a better appreciation for their role in development may allow us to better understand how they may be contributing to lung diseases.

FGF Signaling and lung development

Recent studies have demonstrated that several of the core developmental signaling pathways are critical for lung development including the FGF, SHH, BMP, and WNT signaling pathways (Warburton et al 2005; Cardoso and Lu 2006; Morrisey and Hogan 2010). Of these, the FGF signaling pathway is one of the most thoroughly studied. Previous studies have demonstrated that seven FGF ligands and four FGF

receptors are involved in various stages of lung development (Warburton et al. 2005, Cardoso and Lu 2006; Morrisey and Hogan 2010). Furthermore, clinical studies have indicated that several components of the FGF signaling pathway may be contributing to the development of lung diseases like COPD and BPD (Benjamin et al. 2007; Rezvani et al. 2013). Therefore it is important to understand how FGF signaling is mediating normal lung development, as it could give us some insight into the mechanisms through which FGF signaling mediates the development of lung diseases.

In mammals, the canonical FGF signaling pathway runs through four FGF receptors (hereafter FGFRs) and eighteen FGF ligands (FGF1-10 and FGF16-23) (Beenken and Mohammadi 2009). FGFRs are transmembrane tyrosine kinases that are composed of three extracellular immunoglobulin (IG) domains, a single transmembrane helix domain, and an intracellular tyrosine kinase (TK) domain (Eswarakumar and Schlessinger 2005). In addition to the four FGFRs, FGFR1-3, also contain two alternative splice forms in the third IG domain ("IIIb" and "IIIc"), with the FGFR-IIIb and the FGFR-IIIc splice forms being expressed in the epithelium and mesenchyme respectively (Orr-Urtreger et al. 1993). The FGF ligands are secreted glycoproteins that are expressed in both the epithelium and mesenchyme of the developing embryo. The ability of the FGF ligands to interact with the FGFRs is controlled by their ability to interact with the extracellular IG domains. Recent studies have demonstrated that the alternative splicing of FGFR1-3 dramatically affects the ability of FGF ligands to interact with the FGFRs, with the majority of FGF ligands interacting with a single splice form (Ornitz et al. 1996; Eswarakumar and Schlessinger 2005). After a FGF ligand binds to a FGFR, the FGFR dimerizes, and the tyrosine kinase domains of the FGFR are auto-

phosphorylated. In the cell, this leads to the activation of PLC-gamma and FRS2, which activate the PIP2, PI3K, and MAPK intracellular pathways (Turner and Grose 2010). Upon activation, these signaling cascades go onto effect numerous cellular processes including transcription, cellular differentiation, and proliferation.

The majority of studies on the role of FGF signaling in lung development have focused on its function in the embryo, where studies have shown that FGF signaling is necessary for each stage of embryonic lung development. The earliest requirement for the FGF signaling pathway in lung development is in bud initiation, where FGF signaling through FGF10 and FGFR2-IIIb, is required for lung bud outgrowth (Min et al. 1998; Sekine et al. 1999; De Moerlooze et al. 2000). When the lung enters the pseudoglandular stage and begins branching morphogenesis, the FGF signaling pathway mediates numerous processes, including; epithelial branch patterning, the development of the vascular plexus, and airway smooth muscle development (Colvin et al. 2001; Abler et al. 2009; Yi et al 2009; Yin et al. 2011; Volckaert et al. 2013). Finally, as the lung finishes embryonic development, FGF signaling is critical for the formation of primitive alveoli, which are necessary for oxygen uptake at birth (Usui et al 2004; Yu et al. 2010).

In addition to being necessary for lung bud initiation, FGF10 is critical for branching morphogenesis (Abler et al. 2009). During branching morphogenesis, *Fgf10* is expressed in nodules in the distal mesenchyme (Bellusci et al. 1997). Recent studies have suggested that one of the primary mechanisms through which FGF10 is able to mediate branching morphogenesis is by acting as chemoattractant to the distal epithelium (Weaver et al. 2000) (Figure 2). Interestingly, as FGF10 promotes epithelial

outgrowth, the epithelium secretes SHH, which inhibits the expression of *Fgf10* in the adjacent mesenchyme. This causes *Fgf10* to be expressed in dynamically localized nodules that change in response to the outgrowing epithelium (Bellusci et al. 1997). Traditionally, it has been thought that the dynamic localization of *Fgf10* expression is one of the driving forces of epithelial bifurcation during branching morphogenesis, as each newly formed *Fgf10* nodule would serve as separate sources of FGF10 and therefore each outgrowing epithelial tip would be exposed to multiple nodules (Figure 2). However a recent study suggests the *Fgf10* expression level, and not the *Fgf10* expression localization, is important for branching morphogenesis (Volckaert et al. 2013).

In addition to FGF10, FGF9 is the other main FGF ligand to mediate embryonic lung development. *Fgf9* is expressed in both the epithelium and mesothelium during lung development, and is thought to signal through the "IIIc" splice forms of FGFR1 and FGFR2 in the mesenchyme (Yin et al. 2011). *Fgf9* knockout mice have a severely simplified epithelial branch structure, and die postnatally because they cannot efficiently take up oxygen (Colvin et al. 2001; Yi et al 2009; Yin et al. 2011). FGF9 is thought to mediate branching morphogenesis in part through its ability to induce the expression of *Fgf10* in the mesenchyme, with *Fgf9* knockout mice displaying a decrease in *Fgf10* expression (Colvin et al 2001; del Moral et al. 2006). Recent studies using an *Fgf9* conditional allele have also suggested that FGF9 activity in the epithelium can mediate branching morphogenesis independent of FGF10 (Yin et al. 2011). In addition to mediating branching morphogenesis, one of the primary roles FGF9 during lung development is to control mesenchymal differentiation, as recent studies have

demonstrated the FGF9 is a key mediator of airway smooth muscle development (Marie del Moral et al 2006; Yi et al 2009).

Although the focus of most studies on FGF signaling and lung development has been on the embryonic lung, recent studies have begun to examine the role of FGF signaling in postnatal lung development. In rodents, several of the FGF ligands, including FGF1, FGF2, FGF7 and FGF18, have been linked to postnatal lung development (Yi et al. 2006; Padela et al. 2008; Franco-Montoya et al 2011). However, the majority of genetic studies on FGF signaling during postnatal lung development have focused on FGFRs, as three of the four FGFRs (FGFR2-4) have been shown to be essential for postnatal lung development in mice (Weinstein et al. 1998; Hokuto et al 2003; Srisuma et al. 2010).

Of the FGFRs, *Fgfr3* and *Fgfr4* (hereafter *Fgfr3;4*) are the only ones to be specifically required in the postnatal lung, for postnatal lung development. The individual loss of either FGFR3 or FGFR4 activity does not affect lung development; however, the *Fgfr3;4* double mutant (hereafter *Fgfr3;4* mutant) mice develop an emphysematous phenotype by P8 (Weinstein et al 1998; Srisuma et al. 2010). The alveolar simplification in *Fgfr3;4* mutant mice is thought to be cause by the excessive deposition of Elastin fibers in the alveolar walls, which inhibits septal outgrowth. Interestingly, a disruption in Elastin ECM formation is observed in BPD models systems, and a recent study has suggested that FGFR4 is one of the genetic factors linked to a patient's susceptibility to develop BPD (Bland et al. 2008; Rezvani et al. 2013). Therefore a further understanding of how FGFR3;4 mediate postnatal lung development may help us to understand the mechanisms behind BPD development in patients.

Although FGFR2-IIIb is one of the primary FGFRs involved in embryonic lung development, its postnatal activity is not required normal alveologenesis. This was demonstrated by conditionally inhibiting FGFR2-IIIb activity in the postnatal lung, through the expression of a soluble dominant negative FGFR2-IIIb construct (hereafter FGFR2-HFc) (Hokuto et al. 2003). When this construct is expressed at the earliest stages of lung development, it recapitulates the FGFR2-IIIb knockout phenotype. However, the expression of the FGFR2-HFc construct in the postnatal lung has no phenotypic consequences. Although FGFR2-IIIb activity is not specifically required for postnatal lung development, inhibition of FGFR2 activity at either the pseudoglandular or canalicular stages results in an alveolar simplification that resembles the *Fgfr3;4* knockout lung (Weinstein et al 1998; Hokuto et al. 2003 Srisuma et al 2010). Therefore, these results suggest that FGFR2-IIIb has very specific temporal requirements during lung development, and that disrupting the prenatal roles of the FGF signaling pathway can have drastic phenotypic consequences as the lung matures postnatally.

In my studies I have examined how the FGF signaling pathway mediates lung development. My studies have identified that the FGF regulated transcription factors *Etv4* and *Etv5* are necessary for both prenatal and postnatal lung development. Furthermore my studies have expanded upon the mechanisms though which FGFR3;4 are thought to mediate postnatal lung development. Together I feel that my work has expanded the fields understanding of how FGF signaling is involved in lung development.

Figures:

Figure 1: Alveolar development in mice.

(A) At birth (P0) mice contain all the cell types that are necessary for oxygen uptake, including the vasculature (red), type I cells (yellow), and type II cells (green). (B) From P4 to P36 the lung undergoes alveologenesis, in which secondary septae (black arrows) grow from the alveolar wall into the alveolar lumen (white space). The right hand panels represent H&E staining from the representative stages. Modified from Morrisey and Hogan 2010

Figure 1: Alveolar development in mice.

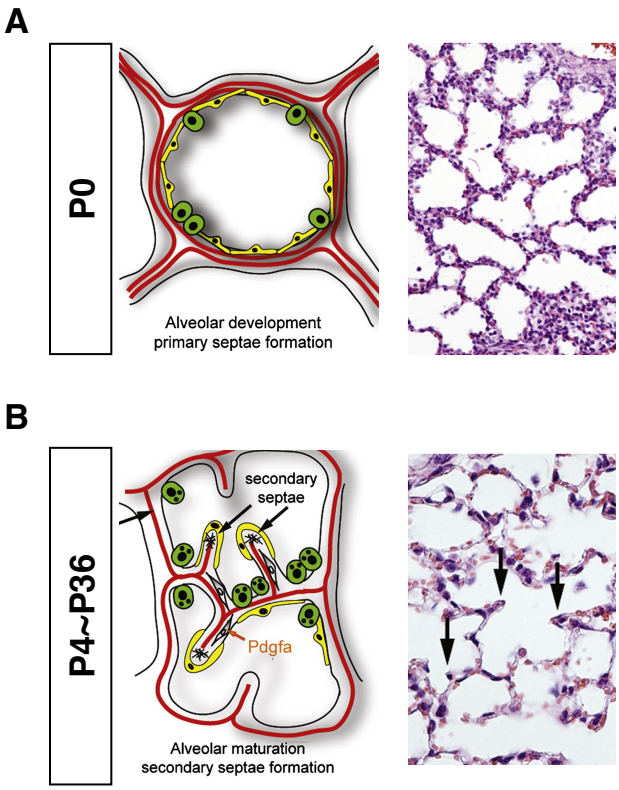

Figure 2: FGF-SHH signaling loop and epithelial bifurcation

Fgf10 is expressed in the distal mesenchyme (yellow) of the developing lung (Red). FGF10 signals to the lung epithelium (blue/green) to promote epithelial outgrowth. In response the epithelium secretes factors, like SHH, which inhibit the expression of *Fgf10* in the adjacent mesenchyme. This causes *Fgf10* to be dynamically expressed in nodules that shift and split in response to the outgrowing epithelium. Traditionally, the dynamic localization of *Fgf10* expression was thought to be one of the driving forces of epithelial bifurcation during branching morphogenesis, as the each newly formed *Fgf10* nodule would serve as separate sources of FGF10 and therefore each outgrowing epithelial tip would be exposed to multiple nodules. This figure was modified from Domyan et al. 2011.

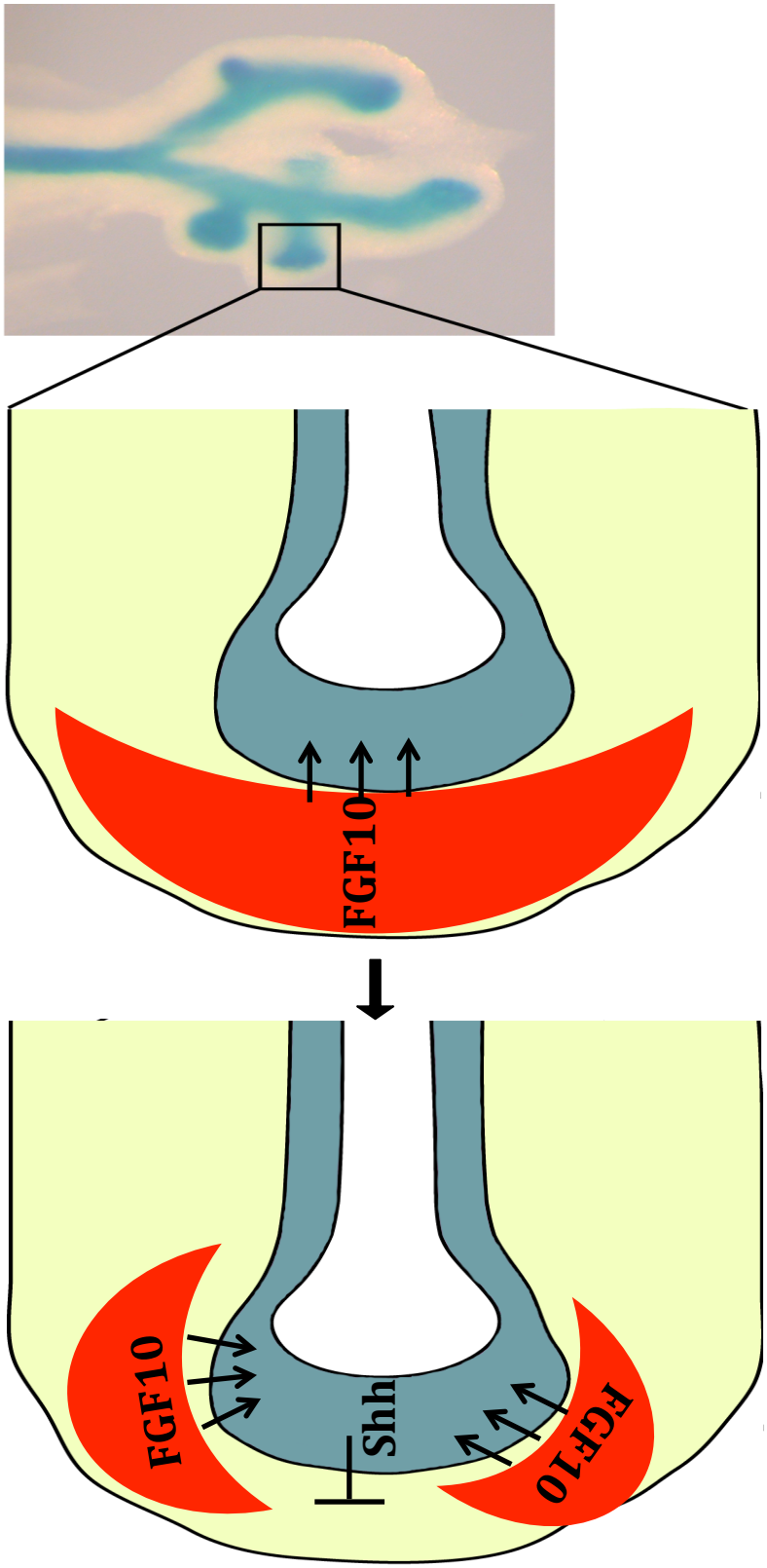

Figure 2: FGF-SHH signaling loop and epithelial

Chapter II: A genome-scale study of transcription factor expression in the branching mouse lung

This chapter has been published as: **Herriges JC**, Yi L, Hines EA, Harvey JF, Xu G, Gray PA, Ma Q, Sun X. 2012. Genome-scale study of transcription factor expression in the branching mouse lung. Dev Dyn. 2012.9:1432-53.

Abstract:

Background: Mammalian lung development consists of a series of precisely choreographed events that drive the progression from simple lung buds to the elaborately branched organ that fulfills the vital function of gas exchange. Strict transcriptional control is essential for lung development. Among the large number of transcription factors encoded in the mouse genome, only a small portion of them are known to be expressed and function in the developing lung. Thus a systematic investigation of transcription factors expressed in the lung is warranted.

Results: To enrich for genes that may be responsible for regional growth and patterning, we performed a screen using RNA *in situ* hybridization to identify genes that show restricted expression patterns in the embryonic lung. We focused on the pseudoglandular stage during which the lung undergoes branching morphogenesis, a cardinal event of lung development. Using a genome-scale probe set that represents over 90% of the transcription factors encoded in the mouse genome, we identified sixty-two transcription factor genes with localized expression in the epithelium, mesenchyme or both. Many of these genes have not been previously implicated in lung development.

Conclusions: Our findings provide new starting points for the elucidation of the transcriptional circuitry that controls lung development.

Introduction:

The mammalian lung is essential for survival starting at birth. It is a prominent branching organ, with an endoderm-derived epithelium supported by a mesoderm-derived mesenchyme. In the mature lung, the epithelial tubules assume the shape of a tree-like structure, where the proximal portion forms the conducting airways and the distal portion forms the gas-exchanging alveoli. The mesenchyme consists primarily of the vasculature, smooth muscles, and tracheal/bronchial cartilage that forms intimate contacts with the epithelial tree and are also critical for respiration (Cardoso and Whitsett, 2008; Shi et al. 2009; Warburton et al. 2010).

In mice, lung development and maturation can be divided into five stages: embryonic bud initiation (Embryonic Day, or E9.0-E11.5), pseudoglandular (E11.5-E16.5), canalicular (E16.5-E17.5), saccular (E17.5-P5), and alveolar (P5-P28) stages (Maeda et al. 2007). The first sign of respiratory specification is marked by the expression of a transcription factor encoding gene, *Nkx2-1* in a small group of ventral foregut endoderm cells at E9.0 (Lu et al. 2004). Signals from the surrounding cardiac and prospective lung mesenchyme are critical for this specification (Domyan and Sun 2011). The first morphologically distinct respiratory structure, the primary lung buds, are observed at E9.5. From E9.5-11.5, these buds elongate and undergo secondary branching to establish the basis of one left lung lobe and four right lung lobes. The bulk of branching morphogenesis occurs during the pseudoglandular stage, and follows a strict program (Metzger et al. 2008). Towards the end of this stage and continuing into the canalicular stage, the conducting airway epithelium differentiates into specialized cell types, including Clara and ciliated cells (Rawlins et al. 2006). Drastic changes occur in the

saccular stage as the lung transitions from being fluid filled to air breathing. The distal epithelium undergoes saccular branching and subdivides into primary alveolar sacs that allow for gas exchange. Meanwhile, the vascular network surrounding the alveolar sacs remodels to facilitate oxygen uptake. Within the distal epithelium, type II pneumocytes mature and start to produce surfactants, a protein and lipid mixture that lowers surface tension within the lung and allows lung expansion at birth (Whitsett and Weaver 2002). The expression of channel proteins also increases at birth, leading to rapid clearing of the fluid from the lung. While the lung can carry out gas-exchange at the end of saccular stage, it only contains approximately 5% of the final alveolar surface area. During alveologenesis, thousands of secondary septae rise from the walls of the primary alveolar sac into the lumen; each serving as a new surface for gas-exchange (Mund et al. 2008).

Transcription factors have been shown to play critical roles in lung development (Warburton et al. 2000; Whitsett and Matsuzaki 2006; Maeda et al. 2007). They control diverse processes, including epithelial branching, epithelial and mesenchymal cell differentiation, surfactant and channel gene expression, and septae formation. Thus studies of transcription factor function in lung development have been a fruitful direction of research in the field. There are over 1,400 transcription factors encoded in the mouse genome. To date only a small faction of these are known to be expressed and play a role in the lung. A systematic investigation of transcription factor expression in the lung is necessary, as it will help to elucidate the genetic control of lung development.

We performed an RNA *in situ* hybridization screen to identify transcription factor genes expressed within the branching mouse lung. There are several previously

published expression screens in the branching lung (Liu and Hogan 2002, Lu et al. 2004, Lu et al. 2005, Metzger et al. 2007). Some of these focus on genes differentially expressed in particular regions of the wildtype lung (Liu and Hogan 2002, Lu et al. 2004), while others focus on genes that are regulated by specific signals essential for branching, such as FGF (Lu et al. 2005, Metzger et al. 2007). In addition to these studies, there are public databases such as GenePaint (www.genepaint.org) where gene expression patterns in tissue sections are available on a genome scale (Visel et al. 2004). However, these large-scale databases are not focused on any particular tissue. Therefore, annotation of the expression pattern is not always precise. For example, in GenePaint, *Sox17* is listed as not expressed in E14.5 lung, while it is clearly expressed at this stage and plays a critical role in lung development (Park et al. 2006).

To enrich the existing datasets, we utilized a mouse transcription factor probe collection that represents approximately 90% of all transcription factors encoded in the mouse genome (Gray et al. 2004). We conducted wholemount *in situ* hybridization using over 1,100 probes on E13.5 mouse lungs. Using a stringent standard, we identified sixty-two genes that are expressed in a subset of the cells within the lung epithelium, mesenchyme, or both. It should be noted that not all transcription factor genes are represented in the cDNA collection. Furthermore, since one probe per gene was screened, it is likely that a fraction of the probes do not produce the optimal hybridization signal with the specific transcript. Due to these limitations, our data only account for a subset of the transcription factor genes expressed in the branching lung. However, as many of the genes identified in our screen have not been previously

implicated in lung development, our findings make an important contribution to existing gene expression datasets in the branching lung.

Results/Discussion:

We chose to carry out our screen in E13.5 lungs for several reasons. First, a meticulous mapping of the lung epithelial ductal system during development shows that epithelial branching follows a stereotypical program, suggestive of strict genetic control including transcriptional regulation (Metzger et al. 2008). E13.5 is a stage in the middle of pseudoglandular branching, and is thus representative of the process. Second, several key signaling pathways that are essential for lung branching, including the fibroblast growth factor (FGF), sonic hedgehog (SHH) and bone morphogenetic protein (BMP) signaling pathways, are all active in the E13.5 lung. Members of these pathways are known to influence each other's transcription through feedback loops, yet few transcription factors that mediate these regulations have been identified. Third, E13.5 is a stage when active patterning of the epithelium and mesenchyme occurs. These broad patterns then serve as blueprints for fine-scale cellular differentiation that occurs at later stages of lung development. Finally, we chose to carry out an *in situ* screen because we are particularly interested in genes expressed in subsets of cells in the lung as they may direct regional growth and patterning events. We determined that E13.5 is the latest, and therefore most advanced stage when distinct patterns can still be consistently discerned from wholemount *in situ* hybridization.

As we are interested in genes that may drive regional patterning and morphogenesis in the lung, we focused on genes that show restricted expression patterns. Overall, we

identified sixty-two genes with differential expression in distinct sub-regions of the lung (Table 1, Figs. 1-4). Some of these factors have previously been shown to play a role in lung development (Maeda et al. 2007). However, the majority of these genes do not have a well-characterized association with the branching lung. We grouped these genes into four categories to present their expression patterns and discuss known or potential functions. The first three categories are distinguished based on their expression site: genes that are expressed solely in the epithelium (Category 1) or mesenchyme (Category 2), and genes that are expressed in subregions of both tissue layers (Category 3). Hox genes are presented as a separate group (Category 4) to facilitate a direct comparison of their overlapping expression patterns (Fig.4). For each gene, gene expression patterns in the wholemount lung were confirmed by the pattern in vibratome sections.

Category 1-genes expressed in the lung epithelium:

Twenty-three transcription factor genes were identified as having epithelial specific expression patterns within the lung (Fig. 1A-W). We found more than one member in each of the following families containing specific domains: homeobox, zinc finger, forkhead box (FOX), SRY box (SOX), and E-twenty six (ETS).

Homeobox containing: Irx3, Nkx2-1, Nkx2-9, Nkx1-2, Hnf1b, and Mnx1

Homeobox containing transcription factors are essential for patterning throughout the developing embryo. In the E13.5 lung, we identified five genes belonging to this

family that are expressed solely in the epithelium (Fig. 1A-F). Of these, only *Irx3* and *Nkx2*-1 have been previously shown to play roles in embryonic lung development.

The Iroquois homeobox (Irx) transcription factor family consists of six members that have extensive overlaps in expression within the developing mouse embryo (Bosse et al. 1997; Christoffels et al. 2000; Cohen et al. 2000; Houweling et al. 2001). At E13.5, *Irx3* expression is detected at a high level in the distal portion of the lung epithelium (Fig. 1A). Three other Irx transcription factors (*Irx1,2,5*) are also expressed within the lung epithelium in a similar pattern as *Irx3* (Becker et al. 2001; Van Tuyl et al. 2006; Diez-Roux et al. 2011). No lung abnormalities have been reported in any existing Irx single gene mutant mice (Lebel et al. 2003). However, knockdown of all *Irx* transcription factors using antisense oligonucleotides in lung explants causes branching defects (Van Tuyl et al. 2006), suggesting that Irx factors may act redundantly to regulate lung branching.

Three Nkx transcription factors were identified within our screen, *Nkx2-1*, *Nkx2-9*, and *Nkx1-2* (Fig. 1B-D). *Nkx2-1* (also termed *TTF-1*) is one of the earliest genes expressed in the nascent respiratory lineage (Lazzaro et al. 1991). Knockdown or knockout of *Nkx2-1* leads to early lung branching arrest (Minoo et al. 1995; Minoo et al. 1999). However, lung buds form in each case, suggesting that *Nkx2-1* is dispensable for lung budding, but essential for secondary branching morphogenesis. Furthermore, *Nkx2-1* mutants show a failed formation of the trachea, suggesting that this gene is essential for trachea specification (Minoo et al. 1999, Que et al. 2007). *Nkx2*-9 knockout mice form functional lungs and survive to adulthood, but show tracheobronchial epithelial hyperplasia (Tian et al. 2006). Further analysis of the *Nkx2*-9 mutants

demonstrates that *Nkx2-9* maintains the cellular architecture of the upper airway by restricting cell proliferation in the epithelium. Little is known regarding the role of *Nkx1-2* in development, including in the lung. No knockout mouse line has been reported. In the *Foxa2* mutant mouse gastrula, *Nkx1-2* expression is downregulated (Tamplin et al.2008). Since *Foxa2* is a key factor in the lung required for alveologenesis and epithelial differentiation (Wan et al. 2005), these results raise the possibility that *Nkx1-2* may function downstream of *Foxa2* in the lung.

The roles of either *Hnf1b* or *Mnx1* in lung development have not been closely interrogated. Within the developing lung, *Hnf1b* shows higher expression within the distal region of the lung epithelium, while *Mnx1* expression appears more evenly spread throughout the proximal/distal regions of the lung epithelium (Fig. 1E). Homozygous null mutants of *Hnf1b* (also known as *vHnf1* and *Tcf2*) are lethal at the early post-implantation stage due to defects in extra-embryonic endoderm differentiation (Barbacci et al. 1999; Coffinier et al 1999). Using a conditional allele, it has been shown that inactivation of *Hnf1b* in the bile duct led to a change from cuboidal to pseudostratified squamous epithelium (Coffinier et al. 2002). Conditional inactivation of *Hnf1b* within the kidney results in a polycystic kidney phenotype, suggesting that *Hnf1b* is essential in controlling planar cell polarity (Fischer et al. 2006; Verdeguer et al. 2010). A recent study has demonstrated the importance of planar cell polarity in lung development (Yates et al. 2010), raising the possibility that *Hnf1b* may play a role in this process in lung. *Mnx1* (also known as *Hb9*) knockout mice die at birth due to an inability to inflate the lung (Arber et al. 1999). However, it remains unresolved whether this is the result of a lung-specific defect or a neuronal defect in diaphragm innervation. In the epithelium of

other tissues, such as the pancreas, *Mnx1* is known to regulate cell differentiation, raising the possibility that *Mnx1* may regulate a similar process within the lung (Harrison et al. 1999; Li et al. 2001).

Zinc finger containing*: Gata6, Lmo1, Zfp746, and Tcea2*

Four zinc finger containing transcription factors were found to be expressed within the E13.5 lung epithelium: *Gata6, Lmo1, Zfp746,* and *Tcea2,* and (Figure 1G-J). Of these, only *Gata6* has been shown to be essential for lung development (Keijzer et al. 2001; Yang et al. 2002; Liu et al. 2002; Zhang et al. 2008). For example, *Gata6* controls the number of bronchioalveolar stem cells (BASCs), a lineage that is activated to repopulate bronchial cell populations in response to injury (Kim et al. 2005).

Homozygous *Lmo1* null mutants are viable and show no obvious defects including in the lung (Tse et al. 2004). This lack of a phenotype within the lung may result from redundancy with other *Lmo* transcription factors, as several other Lmo members are also expressed within the lung, including *Lmo4* and *Lmo7* (Sum et al. 2005; Ott et al. 2008). In neural tissues such as the hindbrain, LMO factors regulate proximal-distal patterning (Matis et al. 2007). This raises the possibility that LMO factors may function collectively to control lung epithelium patterning.

Zfp746 has not been shown to be expressed or have a function within the developing lung. A recent study using overexpression and knockdown techniques show that *Zfp746* (also termed *PARIS*) promotes neural degeneration in Parkinson's disease models (Shin et al. 2011). No *Zfp746* mutant mouse has been reported.

Tcea2 is strongly expressed within the distal region of the lung epithelium and is one of two transcriptional elongation factors identified within this screen, (together with *Tcea1*, see below). Existing evidence suggests that *Tcea2* promotes transcription by preventing the arrest of RNA polymerase (Reines et al. 1996). It remains unclear how this molecular role impacts tissue development, as no *Tcea2* mutant mice have been reported. It is interesting to note that *Tcea2* is not expressed within the adult lung (Umehara et al. 1997), suggesting that it may act specifically in cells and tissues that are undergoing active proliferation and expansion.

FOX domain containing: Foxa1, Foxd4

A number of forkhead box (FOX) domain transcription factors are expressed within the developing lung (Maeda et al. 2007). Our screen highlights two that are detected within the lung epithelium at E13.5, *Foxa1* and *Foxd4* (Fig. 1K,L). *Foxa1*, along with the closely related *Foxa2*, has been shown to be critical for branching and epithelial differentiation in the lung (Wan et al. 2004a; Wan et al. 2004b; Wan et al. 2005). Inactivation of *Foxa1* and *Foxa2* in the mouse lung epithelium leads to fewer, and more dilated epithelial branches than the control. Furthermore, markers of differentiated cell types in both the proximal airway (CC10 or SCGB1A1, and FOXJ1) and distal alveoli (SFTPC and SFTPB) are no longer expressed in the absence of these FOX factors, suggesting that *Foxa1;Foxa2* are required broadly in the lung epithelium for cell differentiation. On the protein level, it has been shown that FOXA1 interacts with NKX2-1 to regulate the expression of *Sftpc* in the lung epithelium (Minoo et al. 2007). Moreover, examination of major signaling pathways essential for lung development

demonstrates that *Foxa1* and *Foxa2* may act to control the expression of *Shh* in the lung epithelium (Wan et al. 2005).

While *Foxd4* has been shown to be expressed at a low level in the adult lung (Kaestner et al. 1993), its expression has not been reported in the embryonic lung (Fig. 1L). In yeast, *Foxd4* controls the cell cycle by regulating the G2/M transition (Kumar 2000). Whether it plays a similar role in mice has not been tested, and no knockout mouse has been reported. Outside of the lung, within the gastrula stage embryo, the expression of *Foxd4* is positively regulated by FOXA2 (Tamplin et al. 2008). Thus it is possible that *Foxd4* may function downstream of *Foxa2* in the lung.

Although not identified by probes used in our screen, several other FOX domain transcription factors are expressed within the developing lung epithelium, including the Foxp sub family (Lu et al. 2002). *Foxp1*, *Foxp2* and *Foxp4* exhibit overlapping expression patterns within the lung epithelium and mesenchyme (Shu et al. 2001; Lu et al. 2002). Inactivation of *Foxp1* and one allele of *Foxp2* (*Foxp1*$^{-/-}$*;Foxp2*$^{+/-}$) produces a smaller lung due to a decrease in cell proliferation (Shu et al. 2007). At later stages these mice also develop a simplified alveolar network. FOXP factors act mainly as transcriptional repressors and this effect is mediated through interaction with HDAC proteins (Chokas et al 2010). In the adult lung, double heterozygous *Foxp1*$^{+/-}$*;HDAC2*$^{+/-}$ mice are resistant to hyperoxia-induced lung injury compared to control. These data together suggest that FoxP genes play critical roles in both lung development and homeostasis.

ETS **domain containing*****: Etv5*** **and** ***Elf5***

Two genes encoding ETS domain proteins, *Etv5* and *Elf5*, were identified as being expressed solely in the lung epithelium (Fig. 1M,N). Both have been shown to be expressed in the distal lung epithelium, and play a role in lung development (Liu et al. 2003; Metzger et al. 2007; Metzger et al. 2008a). Likewise, both have been shown to act downstream of FGF signaling, which could explain their expression within the distal epithelium, as Fgf10 is strongly expressed within the distal mesenchyme during branching morphogenesis (Liu et al. 2003; Metzger et al. 2007). ETV5 belongs to the three-member Pea3 subgroup of ETS domain containing proteins (ETV1 also known as ER81, ETV4 also known as PEA3, and ETV5 also known as ERM), which share homology not only in the ETS domain, but also throughout the rest of the protein. Within the lung *Etv4* and *Etv5* expression is positively regulated by FGF signaling (Liu et al. 2003). Expression of a dominant-negative form of *Etv5* in the epithelium of late branching stage lung causes proximal-distal patterning defects (Liu et al. 2003). No overt lung phenotype was found in *Etv5* loss-of-function mutants (Chen et al. 2005), likely due to redundancy with *Etv1* and *Etv4*.

Like *Etv5*, the expression of *Elf5* is positively regulated by FGF signaling (Metzger et al. 2007). Overexpression of *Elf5* within the distal epithelium of the lung causes dilated branching tips, and disrupted differentiation into type II cells (Metzger et al. 2008). On the molecular level, overexpression of *Elf5* leads to decreased expression of *Etv5* and increased expression of *Spdef*, another ETS family gene. This result suggests the presence of an intricate feedback regulation among ETS family members. Homozygous null mutants of *Elf5* die by E7.5, prior to lung initiation (Zhou et al. 2005). Lung epithelium-specific inactivation of *Elf5* produces no overt lung development

defects (X. Sun unpublished results), possibly due to redundancy with other ETS containing genes expressed in the lung epithelium.

SRY box containing: Sox2 and Sox9

Two genes encoding SRY box (SOX) transcription factors, *Sox2* and *Sox9*, were identified as being expressed in the epithelium (Fig. 1O,P). They are known to exhibit complementary expression patterns in the epithelium, with *Sox2* expression localized to the proximal epithelium and *Sox9* expression localized to the distal epithelium. Conditional inactivation of *Sox2* within the respiratory epithelium leads to disrupted differentiation of various cell types along the upper airways (Que et al. 2009; Tompkins et al. 2009). Loss of *Sox2* leads to a decrease in ciliated and Clara cells in both the trachea and bronchiole, but it leads to an increase in goblet cells in the trachea and a decrease in goblet cells in the bronchiole. Furthermore in the adult, loss of *Sox2* in the trachea disrupts the ability to repair after sulfur dioxide (SO2)-induced epithelial damage, possibly due to a reduced number of basal stem cells in the mutant epithelium (Que et al. 2009). Similarly, loss of *Sox2* in the adult bronchiole disrupts the increase in goblet cell differentiation and mucus production in response to allergen challenge (Tompkins et al. 2009). Compared to these loss-of-function phenotypes, overexpression of *Sox2* in the lung epithelium causes altered branching morphogenesis, proximalization of epithelial cell fate, and a slight decrease in cell proliferation (Gontan et al. 2008).

Inactivation of *Sox9* in the lung epithelium does not result in any reported defects (Perl et al. 2005), suggesting that by itself, *Sox9* is not required in the epithelium for lung development. However, *Sox9* is also expressed in the proximal mesenchyme,

specifically in the precursor and differentiated cartilages of both the trachea and main bronchi (Elluru et al. 2004). As *Sox9* is a key gene essential for cartilage development (Bi et al. 2001), it may play a role in airway cartilage ring formation.

Miscellaneous epithelial genes: Kat2b, Ash2l, Tfap2c, Nab1, Id2, Irf6, and *Grhl2*

Seven of the epithelium-expressed transcription factors, *Kat2b*, *Ash2l1*, *Tfap2c, Nab1, Id2, Irf6,* and *Grhl2*, were identified in our screen as the sole member of their respective families (Fig. 1Q-W). The roles of these genes in lung development are largely unknown.

Kat2b

Kat2b (also known as *Pcaf*) is a bromodomain-containing acetyl transferase. *Kat2b* knockout mice survive postnatally, and no lung defect has been reported (Yamauchi et al. 2000). The absence of an apparent lung phenotype may be due to redundancy with a close family member *Kat2a*. In support of this possibility, while *Kat2a* is expressed at a relatively low level in the wild-type lung, its level increases dramatically in the *Kat2b* mutant lung (Yamauchi et al. 2000). As *Kat2a* global knockout mice die prior to E11.5, identification of a possible combined role of *Kat2a* and *Kat2b* in lung awaits the generation of tissue-specific double mutants. A recent study identifies *Kat2b* as a potential target of miR302/367, two GATA6-regulated miRNAs that control saccular branch patterning and the balance between proliferation and differentiation in the lung (Tian et al. 2011). Whether misexpression of *Kat2b* contributes to the defects in the miR302/367 overexpression or knockdown lungs has yet to be established.

Ash2l

Ash2l is a SPRY domain containing methyl-transferase that promotes the trimethylation of lysine 4 of histone 3 (H3K4), an epigenetic signature of actively transcribed regions (Steward et al. 2006). RNAi knockdown of *Ash2l* in HeLa cells causes decreased trimethylation of H3K4, and decreased transcription of target genes (Steward et al. 2006). *Ash2l* knockout mice die at a stage when lung buds initiate (Stoller et al. 2010), and its role in lung development has not been studied. Despite this, *Ash2l* has been shown to regulate the expression of several genes implicated in lung development. For example, in muscle differentiation, *Ash2l* regulates the expression of *MyoG* (Rampalli et al. 2007). Previous studies show that *MyoG* is required in the lung for transition from pseudoglandular to saccular stages (Tseng et al. 2000). *Ash2l* has also been shown to regulate the expression of *Fgfr3* in a neuroblastoma cell line (Tan et al. 2009). *Fgfr3*, together with *Fgfr4*, are required for lung alveologenesis (Weinstein et al. 1998; Srisuma et al. 2010). These data raise the possibility that *Ash2l* may act upstream of these factors during lung development.

Tfap2c

Tfap2c (also known as *Ap-2g*) is an Ap2 family gene. The role of *Tfap2c* in the developing lung remains unknown. Knockout mice are lethal between E7 and E9, prior to lung budding (Werling et al. 2002). Conditional ablation of *Tfap2c* in the skin show that *Tfap2c* is important for terminal differentiation of epidermal cells (Wang et al. 2008). This role is executed through an interaction with members of the NOTCH signaling

pathway. In the lung, NOTCH signaling is essential for epithelial patterning and differentiation (Tsao et al. 2008; Guseh et al. 2009; Tsao et al. 2009; Morimoto et al. 2010). Furthermore, recent data show that CEBPa, a critical factor for the maturation of the distal epithelium, is a downstream target of TFAP2C (Martis et al. 2006; Xu et al. 2008). Thus, it is plausible that TFAP2C may interact with these genes to control lung development. It should be noted that another *Tfap2* transcription factor, *Tfap2a* (also known as *Ap-2a*), is expressed within the lung epithelium (Visel et al 2004). Double knockout mice for these two TFAP2 factors die prior to the lethality of either single mutant, suggesting that they function redundantly during development, possibly also in the lung (Winger et al. 2006).

Nab1

Nab1 single mutant mice are viable, fertile, and no lung defect has been reported (Le et al. 2005). In contrast, double mutants of both *Nab1* and the related *Nab2* develop labored breathing. It is not clear if the respiratory defect results from the loss of *Nab1* and *Nab2* within the lung or in other tissues required for breathing, as histology of the double mutant lungs has not been examined (Le et al. 2005). On the molecular level, *Nab1* is a transcriptional repressor of early growth response proteins 1 and 2 (EGR1 and EGR2) (Swirnoff et al. 1998; Le et al. 2005). Loss of *Egr1* protects the lung from bleomycin-induced fibrosis, a mouse model for idiopathic pulmonary fibrosis (IPF) (Lee et al. 2004). Furthermore, *Egr1* has been implicated in mediating cell death in smoking-induced chronic obstructive pulmonary disease (COPD) (Chen et al. 2008). *Egr2* knockout mice develop increased breathing rates (Desmazieres et al. 2008). These

findings suggest that *Nab1* and *Nab2* may control lung maturation through their ability to regulate the activity of *Egr1* and *Egr2*.

Id2

Id2 is a member of the inhibitor of differentiation (Id) family of bHLH domain transcription factors. There are four Id transcription factor genes and all are expressed within the lung: *Id2* and *Id4* are expressed in the distal and proximal epithelium, respectively, while *Id1* and *Id3* are expressed within the mesenchyme (Fig. 1U, Fig. 2Q; Jen et al. 1996). Lineage tracing using an *Id2*-creER^{T2} has shown that *Id2*-expressing cells represent a multipotent progenitor population within the lung epithelium that contributes to both the proximal airway epithelial and the distal alveolar epithelial cell populations (Rawlins 2009). The expression of Id genes is regulated by BMP signaling (Miyazono and Miyazawa 2002; ten Dijke et al. 2003). Previous work has demonstrated that genetic inactivation of BMP signaling leads to trachea specification, proximal-distal lung patterning as well as lung cell differentiation defects (Bellusci 1996; Weaver et al. 1999; Eblaghie et al. 2006; Que et al. 2006; Li et al. 2008; Sun et al 2008; Domyan et al. 2011). These results suggest that the Id genes may mediate the critical roles of BMP signaling in lung. However, there are no reported lung developmental defects associated with single Id gene mutants, including *Id2* mutants. These results suggest that either these Id genes function redundantly amongst themselves, or with other bHLH factors during lung development (Yokota et al. 1999).

Irf6

Irf6 is an interferon regulatory factor whose human homolog has been associated with Van der Woude syndrome, a craniofacial disease characterized by the formation of a cleft lip (Kondo et al. 2002). Irf6 is expressed throughout both the proximal and distal portions of the lung epithelium (Fig. 1V). *Irf6* knockout mice develop skin defects as a result of increased proliferation, and decreased terminal differentiation of epidermal progenitor cells (Ingraham et al. 2006). *Irf6* knockout mice also display esophageal closure and limb-tail fusion as a result of increased adhesion between epidermal layers. At the molecular level, *Irf6* has been shown to act as a downstream mediator of NOTCH signaling (Restivo et al. 2011). Since NOTCH signaling is critical for lung epithelial patterning and differentiation (Tsao et al. 2008; Guseh et al. 2009; Tsao et al. 2009; Morimoto et al. 2010), it is plausible that *Irf6* may also function downstream of NOTCH in the lung epithelium.

Grhl2

Grhl2 is one of three Grainyhead homologs (*Grhl1*-3), and all are expressed within the developing lung epithelium (Fig. 1W; Auden et al. 2006). While *Grhl2* targeted knockout mutants die at the stage of development that precludes a study of their requirement in lung (Rifat et al 2010), mice carrying a *Grhl2* point mutant hypomorphic allele exhibit reduced lung size and inability to inflate the lung at birth (Pyrgaki et al. 2011). In *Grhl2* point mutant lungs, cell adhesion proteins including E-Cadherin, b-Catenin, and Ezrin are detected at lower levels and/or mislocalized. Regulation of cellular adhesion molecules appears to be a general function of *Grhl2* during development, as a similar role was also found in the epidermis and the neural tube

(Werth et al. 2010; Boglev et al. 2011;). These data together suggest that *Grhl2* is essential for lung development via controlling the adhesion properties of the lung epithelium.

Category 2-genes expressed in the lung mesenchyme:

From our screen, twenty-three genes were identified as showing mesenchyme-specific expression patterns in the lung (Fig. 2A-W). Most of these factors have not been characterized for their role in early lung development. We found multiple transcription factors that contained the following domains: zinc finger, homeobox, SOX, ETS, bHLH, and FOX.

The mesenchymal lineages are not well defined within the pseudoglandular stage lung. However of the twenty-three transcription factors that showed mesenchymal expression, seven have been shown to mediate endothelial development within mice and are expressed in a pattern similar to the endothelial network of the lung (Fig. 2E, I-N, Lazarus et al. 2011). This suggests that these transcription factors could be used as markers of the endothelial lineages in the lung. These seven transcription factors are members of the zinc finger, homeobox, SOX, and ETS domain groups, and include *Nr2f2*, *Hhex*, *Sox7*, *Sox18*, *Elk3*, *Ets1*, and *Ets2*. The endothelial network is an important regulator of lung branching (Lazarus et al. 2011), however none of these transcription factors have been shown the mediate lung development within mice.

Zinc finger containing: Gli2, Snai1, Baz1b, Nr2f1, and Nr2f2

Five zinc finger-containing transcription factors were identified within the mesenchyme (Fig. 2A-E). Of these, only *Gli2* is known to be required for early lung development. *Gli2*, together with *Gli1* and *Gli3,* are core components of the Hedgehog signaling pathway. Loss of *Gli2* leads to reduced lung branching (Motoyama et al. 1998). Further inactivation of *Gli3* in a *Gli2* knockout background (generating *Gli2*$^{-/-}$*;Gli3*$^{-/-}$embryos) results in trachea and lung agenesis, suggestive of shared function (Motoyama et al. 1998).

Snai1 is abundantly expressed in the subepithelial mesenchyme of the lung mesenchyme (Fig. 2B). Its function in lung has not been directly assessed, as *Snai1* knockout mutants are lethal prior to E8.5 due to aberrant conversion of epiblast cells into mesoderm cells during gastrulation (Carver et al. 2001). As exemplified by its role during gastrulation, SNAI1 is part of the core machinery that promotes epithelial to mesenchymal transitions (EMT) throughout development as well as in postnatal events such as turmorigenesis (Vincent et al. 2009). In normal lung development, a known EMT event is the transition of mesothelium into cells in the mesenchyme (Que et al. 2008). Whether *Snai1* plays a role in this event remains to be tested using conditional gene inactivation approaches. In pathological conditions of the lung, it has been shown that *Snai1* promotes EMT in lung epithelium-derived cell lines (Jayachandran et al. 2009). This suggests that *Snai1* may contribute to lung fibrosis in diseases such as Idiopathic Pulmonary Fibrosis (IPF) (Kim et al. 2006; Coward et al. 2010). However, a recent study throws into question the involvement of EMT in lung fibrosis (Rock et al 2011).

Baz1b has been shown to be expressed within the adult lung through Northern blot analysis (Peoples et al. 1998). Here, we localize its expression to the E13.5 lung mesenchyme (Fig. 2C). On the molecular level, BAZ1B controls transcription by interacting with a number of chromatin remodeling proteins including the SWI/SNF-type WINAC and ISWI-type WICH complexes (Oya et al. 2009). This interaction is regulated by MAPK signaling. In humans, *BAZ1B* deletions have been associated with the congenital disorder Williams Syndrome (WS), where patients develop supravalvular aortic stenosis along with neurological abnormalities (Williams et al. 1961; Lu et al. 1998; Riby and Porter 2010; Mohan et al. 2011). Consistent with disease symptoms, *Baz1b* knockout mice develop heart abnormalities, including atrial/ventricular septation defects and abnormal trabeculation (Yoshimura et al. 2009). However no lung phenotype has been reported in these mice.

Nr2f1 and *Nr2f2* (also known as *Coup-TfI* and *Coup-TfII*) encode zinc finger-containing steroid/thyroid hormone nuclear receptor proteins. In the lung, they are expressed in overlapping patterns with *Nr2f1* being more restricted to the sub-epithelial mesenchyme (SEM) while *Nr2f2* being more widely expressed in the mesenchyme (Fig. 2D,E). *Nr2f1* has primarily been shown to control neural development, where it regulates both the patterning of neural tissues as well as the differentiation of progenitor cells into mature neurons (Qiu et al. 1997; Faedo et al. 2008). Despite neural differentiation phenotypes, *Nr2f1* knockout mice survive postnatally, with no report of cyanosis or labored breathing. *Nr2f2* knockout mice show abnormal angiogenesis and heart patterning, and are lethal by E10.0 (Pereira et al. 1999). Conditional knockout of *Nr2f2* in the foregut mesentery using Nkx3-2-cre produces defects that mimic congenital

diaphragmatic hernia (CDH), a human birth defect characterized by failed closure of the diaphragm, herniation of abdominal content into the chest cavity, and hypoplastic lungs (You et al. 2005). It remains to be determined whether this lung defect is due to a primary requirement for *Nr2f2* in lung, or is secondary to the mechanical pressure exerted by the herniating tissues on the lung.

Homeobox domain containing: Meis1, Pou3f1, Lhx6 and Hhex

We identified four homeobox containing genes that are expressed within the mesenchyme of the E13.5 lung: *Meis1, Pou3f1, Lhx6 and Hhex* (Fig. 2F-I). While there are no reported role for the latter three factors in the developing lung, a previous study indicates that *Meis1* is required for normal lung development (Hisa 2004).

The Meis family of transcription factors is primarily recognized as Hox cofactors in their regulation of gene expression (Moens and Selleri 2006). In mice, all three *Meis* genes are expressed in the developing lung mesenchyme, with Meis1 being expressed evenly throughout the mesenchyme (Fig. 2F and data not shown). The expression of *Meis1* throughout the lung mesenchyme, suggests that the expression of different Hox genes is going to determine the specific requirement of Meis1 within any given segment of the lung mesenchyme. Multiple Hox genes are expressed within the lung mesenchyme and all are possible partners of Meis (Fig.4). *Meis1* knockout mice die around E14.5 due to hematopoietic and microvascular defects, and exhibit hypoplastic lungs (Hisa et al. 2004). However the primary role of *Meis1* in lung development has not been determined.

Pou3F1 (also known as *Oct6*) is primarily known for its function in neuronal differentiation (Bermingham et al. 1996; Bermingham et al. 2002; Ghazvini et al. 2002). *Pou3f1* mutants are unable to form myelinating Schwann cells within the embryonic peripheral nervous system. These mutants die at birth due to respiratory distress but examination of the lungs revealed no gross defect. Instead, it was proposed that the respiratory deficiency is caused by a possible decrease in number and function of phrenic motor neurons, which may lead to failed diaphragm function during respiration (Bermingham et al. 1996). However, given its expression in the lung, a more thorough analysis of the lung defects in these mutants and a tissue-specific inactivation of *Pou3F1* in lung may be worthwhile to rule out a direct requirement for *Pou3F1* in lung development.

Lhx6 belongs to a large family of genes encoding LIM homeodomain containing transcription factors. *Lhx6* knockout mice die shortly after two weeks of age due to unknown causes (Liodis et al. 2007). Whether these mice develop lung defects has not been shown. Functional redundancy among Lhx factors is observed during development. For example, during neural development, *Lhx6*;*Lhx7* double knockout mutants, but neither of the single mutants, show decreased number of differentiated interneurons and abnormal distribution of GABAergic interneurons (Loidis et al. 2007; Fragkouli et al. 2009). During dentition, *Lhx6*;*Lhx7* double mutants display molar agenesis due to failed mesenchyme differentiation (Denaxa et al. 2009). Following the detection of *Lhx6* expression in lung (Fig. 2H), a search of existing databases revealed that *Lhx4*, *Lhx5*, and *Lhx9* are also expressed in the lung mesenchyme (Visel et al.

2004). These results suggest that *Lhx6* may function redundantly with other Lhx members to control lung mesenchyme development.

Hhex (also known as *Hex*) is expressed in the lung in a pattern that resembles the vascular network (Fig. 2I, Lazarus et al. 2011). *Hhex* knockout mice die prior to E14.5 due to abnormal development of the heart and vascular network (Keng et al. 2000; Hallaq et al. 2004). In the heart, *Hhex* mutants show abnormal outflow tract and valve formation as a result of persistent EMT of endocardial cells. This persistent EMT is thought to be mediated, at least in part, by increased VEGFA protein levels. In the vascular network of *Hhex* knockout mice, blood vessels initiate normally. However, the vascular lumens become dilated, possibly due to a decrease in vascular smooth muscle. Whether *Hhex* mutants development any lung defects has not been reported.

SOX domain containing: Sox7 and Sox18

From our screen, we identified two genes encoding F subgroup SOX domain containing transcription factors, *Sox7* and *Sox18*. These genes, together with the remaining F subgroup member *Sox17*, are expressed in overlapping, but non-identical patterns in the overall vasculature (Fig. 2J,K) (Park et al. 2006; Sakamoto et al. 2007; François et al. 2010). For example, in a normal embryo, *Sox18*, but not *Sox7* or *Sox17*, is expressed in the lymphatic endothelial cells. Interestingly, in the absence of *Sox18*, *Sox7* becomes ectopically expressed in the lymphatics (Hosking et al. 2009). Consistent with this, these genes play redundant roles in endothelial cell differentiation in blood and lymphatic vessels in both mice and zebrafish (Cermenati et al. 2008; Sakamoto et al. 2007). In humans, a dominant-negative mutation in human *SOX18*, which likely

interferes with the function of multiple SOX genes, is known to cause Hypotrichosis-Lymphedema-Telangiectasia, a congenital lymphatic disorder (Irrthum et al. 2003). The specific requirement for these genes in the lung vasculature has not been directly addressed. Moreover, *Sox17*, but not *Sox18* or *Sox7*, is expressed in the epithelium beginning at E18.5. Overexpression of *Sox17* in the epithelium of early stage lungs results in defects in both branching and epithelial cell differentiation (Park et al. 2006).

ETS domain containing: Elk3, Ets1, and Ets2

We identified three ETS domain containing transcription factors that are expressed within the lung mesenchyme: *Elk3*, *Ets1*, and *Ets2* (Fig.2 L-N). While their function in the lung remains unclear, the expression patterns of all three of these genes are consistent with their known roles in endothelial development.

Elk3 (also known as *Net*) knockout mice survive past birth and show no lung defects (Ayadi et al. 2001). While these mutant mice do eventually die due to respiratory distress, the cause is not believed to be intrinsic to the lung, but rather due to a build up of chyle in the thoracic body cavity from a defective lymphatic system (Zheng et al. 2003; McGrath et al. 2010). In addition to its role in lymphatic development, *Elk3* has also been shown to be necessary for endothelial response to pro-angiogenic growth factors such as FGF2 during wound healing (Ayadi et al. 2001).

While *Ets1* knockout mice are viable, *Ets2* knockout embryos die around E8.5 due to a defect in extra-embryonic tissue development (Muthusamy et al. 1995; Yamamoto et al. 1998). Double mutant mice of *Ets1* and *Ets2* that utilize a null allele of *Ets1*, and

either a partial loss of function allele or a conditional deletion of *Ets2* within the epiblast, are lethal at approximately E14.5 and display severe hemorrhaging due to a drastic decrease of embryonic vasculature (Wei et al. 2009). While no lung phenotypes have been reported in these mice, it is possible that these Ets genes play a role in the formation of the pulmonary vasculature.

bHLH containing: Tcf21, Hif3a, Id3, and Heyl

We identified four bHLH family transcription factors that were expressed within the lung mesenchyme: *Tcf21, Hif3a*, *Id3 and Heyl* (Fig. 2O-R). Of these, *Tcf21* and *Hif3a* have known roles in lung development.

Previous work has shown that *Tcf21* (also known as *Pod1*) is essential for lung branching morphogenesis (Quaggin et al. 1999). *Tcf21* knockout mice develop fewer epithelial branches compared to control lungs and these mutant branches do not go on to form terminal sacs. The lack of terminal sacs is likely due to proximalization of the lung epithelium, as evidenced by the expansion of the proximal marker *Scgb1a1* and reduction of the distal marker *Sftpc.* Additionally, *Bmp4* expression is decreased within the *Tcf21* mutant lung. Previous work has demonstrated that inhibition of BMP signaling results in a similar phenotype as the *Tcf21* knockout (Bellusci 1996; Weaver et al. 1999; Sun et al 2008). Thus, *Tcf21* may control lung branching and proximal-distal patterning through promoting *Bmp4* expression.

Hif3a is a well-known hypoxia induced factor (HIF) that is expressed within the distal portion of the lung mesenchyme (Fig. 2P). *Hif3a* knockout mutants show impaired alveologenesis with an increase in the amount of vasculature lining the alveolar walls

(Yamashita et al. 2008). Whether the vasculature defect is the mechanism underlying the alveolar phenotype remains to be determined.

Id3, similar to *Id2* mentioned above, is a member of the Id family of genes (Fig. 2Q). *Id3* knockout mice are viable and no lung defect has been reported (Pan et al.1999). The lack of an apparent developmental phenotype is likely due to its redundancy with *Id1*, which shows overlapping expression patterns with *Id3* throughout the embryo, including in the mesenchyme of the lung (Jen et al. 1996). In support of this, *Id1*;*Id3* double knock out mice die by E13.5 and develop severe vascular and neural defects (Lyden et al. 1999). Whether these mutants exhibit lung defects has not been reported. A recent study within the postnatal lung shows that *Id3* expression is increased in *Id1* knockout lungs, further suggesting that these two genes may share a redundant function (Lowery et al. 2010). Given that their expression is regulated by BMP signaling (Miyazono and Miyazawa et al. 2002; Ten Dijke et al. 2003), it is possible that together they may mediate the essential role of BMP signaling in lung development.

Heyl is a downstream component of the NOTCH signaling pathway (Nakagawa et al. 2000; Leimeister et al. 2000). As mentioned above, extensive work has demonstrated that the NOTCH signaling pathway regulates lung proximal-distal patterning and cell differentiation (Tsao et al. 2008; Guseh et al. 2009; Tsao et al. 2009; Morimoto et al. 2010). In the lung, *Heyl* expression is restricted to the vascular smooth muscle (Fig. 2R), likely overlapping with the expression of *Notch3*, which plays an essential role in vascular smooth muscle differentiation and maturation (Domenga et al. 2004). While knockout mice for *Heyl* have no reported lung phenotype, *Heyl* may function together

with other components of the Notch signaling pathway during lung vascular smooth muscle development.

FOX domain containing: Foxf1a and Foxf2

Foxf1a (also known as *Foxf1*) and *Foxf2* encode closely related FOX domain containing factors and have very similar expression patterns within the lung (Fig. 2S,T). This expression is positively regulated by SHH signaling and negatively regulated by BMP signaling (Mahlapuu et al. 2001; Lim et al. 2002), both critical signals for lung development. *Foxf1a* has previously been shown to be essential for lung development in a haploinsufficient manner, since mice carrying one mutant allele (*Foxf1a*$^{+/-}$) display lobe fusion, altered epithelial branching, and postnatal lethality due to pulmonary hemorrhaging (Mahlapuu et al. 2001; Lim et al. 2002). Tissue-specific inactivation of both copies of *Foxf1a* in the lung has not been reported. *Foxf2* knockout mice have no reported lung phenotype and die postnatally due to inability to feed (Wang et al. 2003). *Foxf1a* and *Foxf2* have been shown to act redundantly in the intestine, where they regulate extracellular matrix production through their ability to mediate WNT signaling (Ormestad et al. 2006). Whether *Foxf1a* and *Foxf2* have redundant roles in lung development has not been reported.

Miscellaneous: Lef1, Creb3l1, and Tbx3

Three of the mesenchyme-expressed transcription factors, *Lef1*, *Creb3l1* and *Tbx3*, were identified in our screen as the sole member of their respective families (Fig. 2U-

W). Of these, *Lef1* is the only gene known to regulate lung development (Okubo et al. 2004).

***Lef1*:**

Lef1 is an HMG domain-containing transcription factor, and a downstream component of the WNT signaling pathway. Within the lung, lef1 expression is higher within the distal mesenchyme, which corresponds to the distal expression of Wnt2 and Wnt7b within the mesenchyme and epithelium respectively (Visel et al. 2004). Both canonical (e.g. *Wnt2*, *Wnt2b* and *Wnt7b*) and non-canonical (e.g. *Wnt5a*) WNT signaling has been shown to control branching morphogenesis, patterning, and differentiation in the developing lung (Li et al. 2002; Li et al. 2005; Cohen et al. 2009; Goss et al. 2009; Goss et al. 2011). Consistent with this, expression of a b-Catenin-Lef1 fusion protein within the lung epithelium leads to constitutive activation of WNT signaling and a change of cell fate of the lung epithelium into the intestinal epithelium (Okubo et al. 2004). *Lef1* knockout mice die after birth and before weaning (van Genderen et al. 1994), however no lung defect has been reported. The lack of a lung phenotype in *Lef1* knockout mice may result from its overlapping expression with the highly related *Tcf1*, which is also expressed within the lung mesenchyme (Oosterwegel et al. 1993).

Creb3ll:

Creb3l1 (also known as *Oasis*) is a bZIP (basic leucine zipper) domain containing transcription factor that is tethered to the endoplasmic reticulum (ER) and cleaved in response to ER stress (Murakami et al. 2006). Upon cleavage, the DNA binding

domain-containing portion of the protein can be transported to the nucleus where it regulates downstream gene expression. *Creb3l1* cleavage can also be regulated by signaling ligands such as BMPs (Murakami et al. 2009). Consistent with this regulation, *Creb3l1* knockout mice show decreased bone formation due to reduced secretion of bone matrix proteins. *Creb3l1* has also been shown to regulate extracellular matrix production within the pancreas (Vellanki et al. 2010). *Creb3l1* mutant mice are viable and no lung defect has been reported (Murakami et al. 2006; Murakami et al. 2009).

***Tbx3*:**

Tbx3 is one of the four members of the T-box transcription factor family genes, *Tbx2-5* that have been shown to be expressed within the lung mesenchyme (Fig. 2W, Chapman et al. 1996; Li et al. 2004). Their expression is promoted by SHH signaling, which is critical for lung epithelial branching and mesenchymal differentiation (Pepicelli et al. 1998; Li et al. 2004). However, no lung phenotype has been reported in *Tbx3* knockout mice (Davenport et al. 2003), potentially due to overlapping expression with *Tbx2*,*4,5*.

Category 3-genes expressed in both the epithelium and mesenchyme:

We identified ten transcription factors as being expressed in both the epithelium and the surrounding mesenchyme (Fig. 3A-J). Within this group, there are multiple members of the homeobox and FOX domain containing transcription factors.

Homeobox domain-containing: Pitx2, Zfhx3, and Pou2f1

Of the three homeobox domain-containing transcription factors found to be expressed in both the epithelium and the mesenchyme (Fig. 3A-C), *Pitx2* is the only gene known to be required for normal lung development. *Pitx2* knockout mice exhibit a left-right asymmetry defect, which manifests in the transformation of the normally single-lobed left lung into the multi-lobed right lung (Lu et al. 1999; Liu et al. 2001). It remains to be determined whether this phenotype is due to a primary role of *Pitx2* in the lung, or an earlier requirement in the node or lateral plate mesenchyme for overall determination of left-right asymmetry. Of note, *Pitx2* is expressed in only the left lobe of the E9.5 lung, but it becomes bilaterally expressed throughout the lung epithelium and mesenchyme by E13.5 (Kitamura et al. 1999 and data not shown). Two other Pitx transcription factor genes, *Pitx1* and *Pitx3*, are also expressed in regions of the lung mesenchyme that overlap with the *Pitx2* expression domain, suggesting possible redundancy (Fig. 3A; De Langhe et al. 2008). It has also been shown that the expression of both *Pitx2* and *Pitx3* are positively regulated by WNT signaling in the lung (De Langhe et al. 2008), raising the possibility that Pitx genes may mediate the essential functions of WNT signaling during lung development.

Zfhx3 (also known as *Atbf1*) shows strong expression in the epithelium and subepithelial mesenchyme of the developing lung (Fig. 3B) (Ido et al. 1996). It has been shown that *Zfhx3* promotes *Pdgfrß* expression in P19 mouse embryonic carcinoma cells, protecting these cells from oxidative stress (Kim et al. 2010). *Pdgfrß* is expressed within the subepithelial mesenchyme of the lung, and a recent study suggests that signaling through PDGFRB promotes smooth muscle development in the lung (Cohen

et al. 2009). Mice carrying a gene-trap allele of *Zfhx3* have been produced, but no lung phenotype has been described (Stryke et al. 2003; Qi et al. 2008).

Pou2f1 (also known as *Oct1*) is strongly expressed in the lung epithelium, and weakly expressed in the adjacent mesenchyme (Fig. 3C). *Pou2f1* knockout embryos are smaller in size, underrepresented after E13.5, and none survive after birth (Wang et al. 2004). No lung phenotype has been reported. However, in lung derived NCI-H441 cells, *Pou2f1* has also been shown to directly bind to the promoter of *SCGB1A1* (also known as *CC10* or *CCSP*), a key marker for Clara cells (Sawaya et al. 1993). Furthermore, in the lens and nasal placode, *Pou2f1* genetically interacts with *Sox2* to promote the induction of these tissues (Donner et al. 2007). *Sox2* is essential for the differentiation of airway epithelial cells (Gontan et al. 2008; Que et al. 2009; Tompkins et al. 2009). Whether similar interactions occur in the lung remains to be determined.

FOX domain containing: Foxm1 and Foxh1

Two FOX domain containing transcription factor genes, *Foxm1* and *Foxh1* are identified as being expressed in both the epithelium and mesenchyme of the lung (Fig. 3D,E). The expression level of *Foxm1* in lung diminishes from E11.0-E18.5, but peaks again during the initiation of alveologenesis in the postnatal lung (Wang et al. 2010). During lung development, *Foxm1* promotes blood vessel formation, epithelial cell differentiation, and inhibits arterial smooth muscle formation. Conditional inactivation of *Foxm1* in the lung mesenchyme leads to an increase of smooth muscle around the proximal airways and a decrease of pulmonary microvasculature (Kim et al. 2005). Conditional inactivation of *Foxm1* in the lung epithelium leads to a decrease in sacculation and a delay in the differentiation of alveolar type I cells (Kalin et al. 2008).

Expression of a constitutively active form of *Foxm1* within the embryonic lung epithelium results in impaired sacculation and epithelial hyperplasia in the major airways (Wang et al. 2010). These results demonstrate that precise control of *Foxm1* level is crucial to multiple processes of lung development.

Similar to the loss of *Pitx2*, inactivation of *Foxh1* in the lateral plate mesoderm leads to left-right asymmetry defects, which includes the transformation of the one-lobe left lung into the four-lobe right lung (Hoodless et al. 2001; Yamamato et al. 2003; Kofron et al. 2004; Von Both et al. 2004). And like in *Pitx2* mutants, it is unclear whether this transformation of lung lobes is due to the requirement for *Foxh1* in the lung, or at earlier stages in cells essential for left-right determination. In other tissues, *Foxh1* has been shown to interact with several signaling pathways that are critical for lung development. For example, in the brain, *Foxh1* acts downstream of TGFβ and upstream of retinoic acid signaling (Silvestri et al. 2008). However, whether similar relationships operate within the lung has not been shown.

Miscellaneous: E2f1, Hif1a, Smarca5, Brd7, and Tcea1

Of the five single family member transcription factors expressed in both the epithelium and mesenchyme (Fig. 3F-J), *E2f1* and *Hif1a* have previously been shown to play a role in lung development.

E2f1:

E2f1 is one of eight E2f transcription factor genes present in the mouse genome. E2F transcription factors play very diverse roles including the control of cell proliferation, cell death, and cell differentiation (Wang et al. 1998; Fajas et al. 2002; Sharma et al.

2006; Chong et al. 2009). The function of the E2F1 transcription factor within the lung may be through its ability to interact with the retinoblastoma (RB) on the protein level (Swiss et al. 2010). Recent studies have identified that Rb is an important negative regulator of cell proliferation in the lung (DS Simpson DS et al.; Masson-Riche et al. 2008). In the lung, *E2f1* is more strongly expressed within the distal epithelium and mesenchyme, suggesting that E2f1 could regulate the differentiation/proliferation of cells within these two sub regions of the lung (Fig. 3F). While *E2f1* single knockout mice show no lung phenotype, *E2f1;E2f3* double knockout mice have simplified alveoli (Tsai et al. 2008). The precise role of these E2f factors in lung development has not been determined.

***Hif1a*:**

Like *Hif3a* described above, *Hif1a* is a member of the HIF group. It is known to promote vascular growth in response to low oxygen levels (Tian et al. 1997; Semenza et al. 2001a; Semenza et al. 2001b). Knockout mice are lethal by E11.0, due to defective vascular development and cardiac patterning (Iyer et al. 1998; Compernolle et al. 2003). Both conditional inactivation and conditional induction of Hif1a within the lung epithelium results in lethality shortly after birth (Saini et al. 2008; Bridges et al. 2011). The alveolar wall is much thicker in both lines, and both lines also have decreased alveolar epithelial differentiation. This suggests that the regulation of *Hif1a* is critical to alveolar epithelial differentiation within the lung . The specific function of *Hif1a* within the lung mesenchyme has not been examined.

***Smarca5* and *Brd7*:**

Two of the transcription factors expressed in the epithelium and mesenchyme, *Smarca5* and *Brd7* are known chromatin regulators (Fig. 3H,I). SMARCA5 is a SWI/SNF related protein that is highly expressed within the distal epithelium and mesenchyme, while BRD7 is a bromodomain containing protein that acts as a component of the SWI/SNF complex and is expressed more uniformly with the lung (Fig. 3H, I and Stopka et al. 2003; Kaeser et al. 2008). *Smarca5* global knockout mice are lethal during the pre-implantation stage of development (Stopka et al. 2003). *Smarca5*$^{+/-}$ embryonic stem cells or spermatocytes exhibit a global decrease in H3K9Ac and H3K79Me2 levels, indicating an inactive gene expression state (Vargova et al. 2009). These results suggest that the general role of *Smarca5* within the embryo is to promote an active chromatin state. No *Brd7* knockout mutant has been reported, and the function of either of these genes during lung development awaits to be determined.

***Tcea1*:**

Similar to *Tcea2* described above, *Tcea1* is a transcriptional elongation factor that assists RNA polymerases to read through transcriptional blocks (Wind et al. 2000). *Tcea1* is strongly expressed within the distal tips of the outgrowing lung bud epithelium, and within the distal lung mesenchyme (Fig. 3J). Recent work has suggested that *Tcea1* can also boost RNA polymerase function through regulation of histone modifications (Nagata et al. 2009). *Tcea1* knockout mice die prior to E16.5, with defects in the maintenance and differentiation of hematopoietic progenitor cells (Ito 2006). No lung phenotype has been reported, which may be due to redundancy with *Tcea2*, which

is also expressed in the lung epithelium (Fig. 1J). It is interesting to note that these factors, which have seemingly, house keeping functions show tissue specific expression.

Category 4-Hox genes:

Hox genes encode an evolutionarily conserved family of transcription factors that control pattern formation in animals. Thirty-nine *Hox* genes are encoded in the mouse genome. Previous results obtained using multiple approaches including Northern blotting, RT-PCR/qRT-PCR and *in situ* hybridization suggest that as many as twenty *Hox* genes are expressed in the lung during development (Cardoso 1995; Mollard and Dziadek 1997; Grier et al. 2009). Despite the clear presence of expression, the function of Hox genes during lung development is largely unknown as only a single *Hox* mutant, *Hoxa5,* displays primary lung defects (Aubin et al. 1997; Kinkead et al 2004; Mandeville et al. 2006). *Hoxa5* mutant mice exhibit respiratory distress and partial lethality at birth, likely due to reduced surfactant production and/or reduced and disorganized tracheal cartilage, which may lead to tracheal occlusion. *Hoxa5* mutants that survive postnatally were found to have impaired alveologenesis. The lack of a lung phenotype in other single Hox mutants suggests that Hox factors may act redundantly. Furthermore, the range of defects observed in *Hoxa5* mutants demonstrates that Hox factors may regulate a variety of processes over the course of lung development. To elucidate the function of Hox in lung branching morphogenesis, we assessed the expression of fourteen *Hox* genes (*Hoxa1, Hoxa2, Hoxa5, Hoxa9, Hoxb2, Hoxb3, Hoxb5, Hoxb6, Hoxb8, Hoxb9, Hoxc5, Hoxc6, Hoxd4* and *Hoxd9*) previously noted for their expression

in the lung. We identified six genes, *Hoxa1, Hoxa2, Hoxa5, Hoxa9, Hoxb5,* and *Hoxb8* that showed restricted expression patterns in E11.5, and either E12.5 or E13.5 lung and trachea (Fig. 4A-L).

While most of the Hox genes we assayed show similar expression between the two stages that we analyzed, *Hoxa1* expression changes over time. At E11.5, similar to at E10.5, *Hoxa1* expression is readily detected, particularly in the distal mesenchyme of both the medial and accessory buds (Fig.4A and data not shown). However, this expression tapers off by E13.5 (Fig. 4B). Progressive loss of *Hoxa1* expression is also supported by data from northern blot analysis (Mollard and Dziadek 1997). Northern blot data further indicate that other genes, *Hoxa7, Hoxb3,* and *Hoxb4* also exhibit temporally dynamic expression (Mollard and Dziadek 1997). It should be noted that *Hoxa1* mutants develop breathing abnormalities at birth (Lufkin et al. 1991). However, existing evidence has attributed the defect to a requirement for *Hoxa1* in patterning the respiratory neuronal circuits in the brain (Chatonnet et al. 2002; Gray 2008).

Different Hox genes are often expressed in distinct cell lineages. For example, *Hoxa2*, *Hoxa5,* and *Hoxa9* are expressed in the trachea/bronchi region, while *Hoxb5* and *Hoxb8* are not. At both E11.5 and E13.5, *Hoxa2* and *Hoxa5* are observed in the trachea and main bronchi in a pattern consistent with cartilage precursors (Fig. 4C-F). Interestingly, while no tracheal cartilage defects have been reported in *Hoxa2* mutants, *Hoxa5* mutants do exhibit cartilage malformations, suggesting that *Hoxa5* may be the primary Hox factor that controls cartilage patterning (Aubin et al. 1997). Although *Hoxa9* is also expressed in the trachea/bronchi region, its expression is primarily in the epithelium (Fig. 4G,H). The epithelial expression of *Hoxa9* continues into the lung,

where it is also detected in the proximal lung mesenchyme. In contrast to this proximal bias, *Hoxa2*, *Hoxa5,* and *Hoxb5* expression in the lung is more widespread throughout the mesenchyme at E12.5/E13.5 (Fig. 4D,F,J).

A vast majority of the genes that have been studied in the mouse lung show similar expression in the five lung lobes. Hence, it is interesting that several of the Hox genes that we have assayed exhibit biased expression in the different lobes. For example, at E11.5, both *Hoxa1* and *Hoxa5* show concentrated expression in the distal mesenchyme of the medial and accessory lobes (Fig. 4A,E). At both E11.5 and E12.5, *HoxB8* show concentrated expression in the distal mesenchyme of the left lobe and in the cranial and caudal lobes of the right lung (Fig. 4K,L). Whether these transcription factors coordinate the shape and size of the lung lobes remains unknown. It is important to note that Hox genes were first identified as genes that provide segmental identity in *Drosophila*. In mouse, *Hox* gene expression often marks particular sub-regions within a tissue lineage such as in the anterior/posterior axis, the brain and the limb bud. Our results suggest that *Hoxa1, Hoxa5* and *Hoxb8* can be used as markers of early lobe compartments within the developing lung.

Conclusions:

Using a probe collection that represents a majority of the transcription factors encoded in the mouse genome, we identified sixty-two transcription factors that show patterned expression in the pseudoglandular stage mouse lung. Many of the transcription factors that we identified have not been previously implicated in lung development. Furthermore, characterization of the expression pattern of some of these

genes, such as *Grhl2* and *Lhx6*, has led to consideration of other members of the gene families. We envision that our findings will promote future studies by: providing additional genes to be investigated for their roles in lung development; increasing nodes of the transcriptional circuits that act either upstream or downstream of known factors; and suggesting putative markers for specialized cell populations in the lung at multiple stages of development and maturation.

Going beyond development, our dataset may be of value to lung disease research such as the studies of lung cancer. Recent investigations of lung cancer have revealed strong correlations between patient survival rates and miss-expression of a number of the transcription factors highlighted in our screen. For example, increased nuclear localization of *ID2* or increased expression of *FOXM1*, *HIF1A*, *SNAI1* or *HOXA9* is associated with higher mortality rates (Choi et al. 2006; Rauch et al. 2007; Gialmanidis et al. 2009; Hung et al. 2009; Rollin et al. 2009). These findings also raise the possibility that while the expression of many of these factors is downregulated at the completion of development, they are reactivated in tumor cells. Thus, our dataset may suggest candidate biomarkers that can be used to accelerate lung cancer diagnosis.

Materials and Methods:

Tissue Collection*:*

The embryos used in these experiments were harvested from time-mated females, with noon the day of the vaginal plug counted as E0.5. Dissected lung tissues were fixed in 4% paraformaldehyde for 4 hours to overnight at 4°C. After fixation the right lungs were embedded in 4% low melt agarose and sectioned at 100um thickness using a vibratome. Intact left lung lobes and the right lung sections were dehydrated through a methanol series and stored at -20 ^{o}C in 100% methanol until RNA in situ hybridization.

RNA in situ hybridization:

RNA in situ probes were generated from a published plasmid collection (Gray 2004). RNA in situ hybridization was performed following a protocol that was adapted from previously published protocols (Wall and Hogan 1995; Abler et al. 2011). Briefly, either wholemount of vibratome-sectioned tissues stored in methanol were rehydrated using PBS with 0.1% Tween (PBT). Tissues were then permeabilized using 10μg/ml proteinase K in PBT for 10 minutes. Tissues were fixed with 4% paraformaldehyde, 0.2% glutaraldehyde in PBT for 20 minutes. They were then washed and allowed to hybridize with probes at 70°C overnight. After the hybridization, tissues were washed three times, twenty minutes each in 2x SSC, 0.1% CHAPS, and then in 0.2x SSC, 0.1% CHAPS at 70°C. Tissues were then washed in KTBT and blocked for 2 hours in 2% blocking solution (Roche) and 20% heat inactivated sheep serum (Sigma) in KTBT at room temperature. The tissues were then incubated overnight at 4˚C in the primary

antibody, AP conjugated α-DIG, Fab fragment (Roche) at a dilution of 1:2000 using 2% blocking solution and 20% heat inactivated sheep serum in KTBT. The tissues were then washed 5 times, 1hour each in KTBT at room temperature. Following this, the tissues were washed twice, 5 minutes each with 0.1% Tween, 1mM Levamisole in ddH_2O. Finally the tissues were stained in BM purple (Roche) containing 0.1% Tween and 1mM levamisole. The staining was carried out for varying amount of time depending on the probes until desired intensity, from 30 minutes to 8 hours.

Figures:

Figure 1. Patterns of transcription factor genes with primarily epithelial expression within the developing lung.

(A-W) Twenty-three genes were identified by RNA *in situ* hybridization as having epithelium-specific expression patterns in the E13.5 lung. For each gene, the left panel is a wholemount *in situ* hybridization of a left lung lobe, and the right panel is a vibratome section of a right lung lobe.

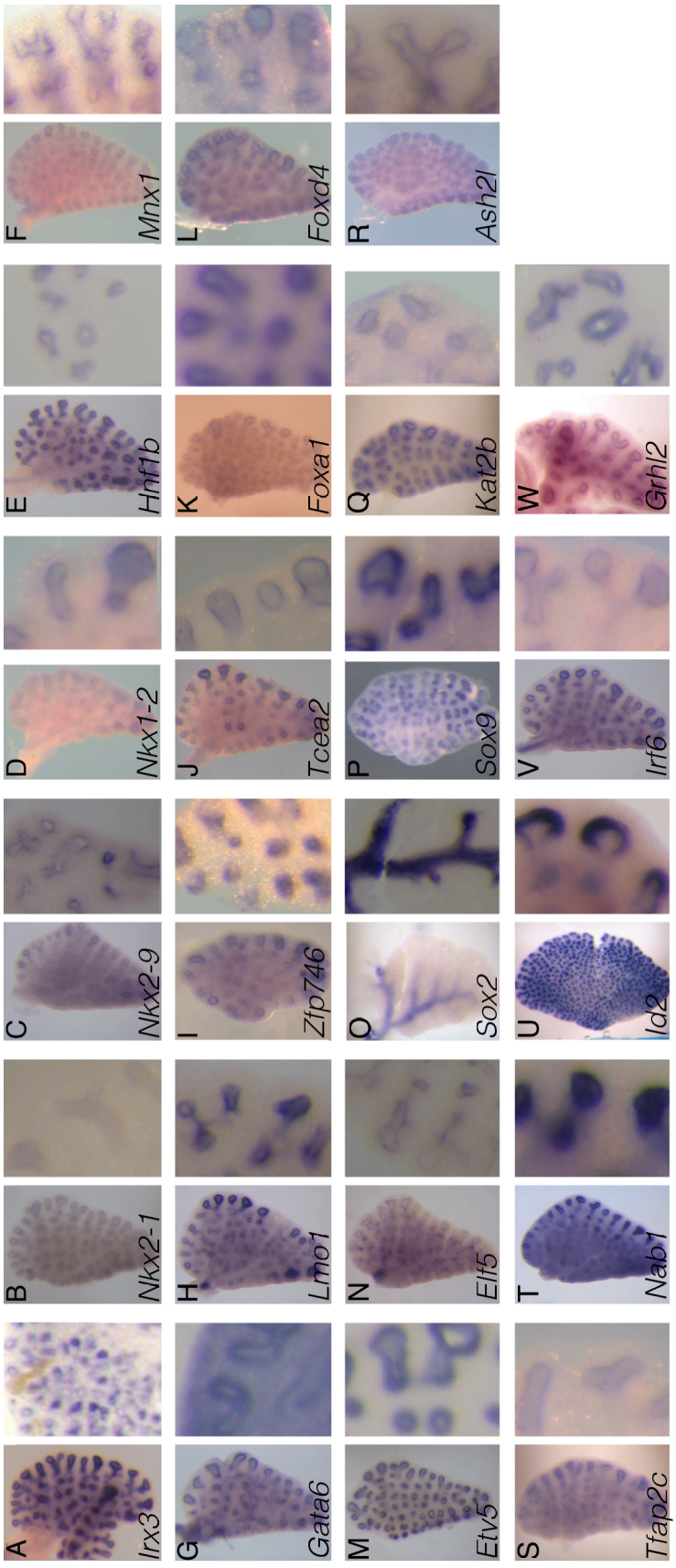

Figure 1: Patterns of transcription factor genes with primarily epithelial expression within the developing lung.

Figure 2. Patterns of transcription factor genes with primarily mesenchymal expression within the developing lung.

(A-W) Twenty-four genes were identified by RNA *in situ* hybridization as having mesenchyme-specific expression patterns in the E13.5 lung. For each gene, the left panel is a wholemount *in situ* hybridization of a left lung lobe, and the right panel is a vibratome section of a right lung lobe.

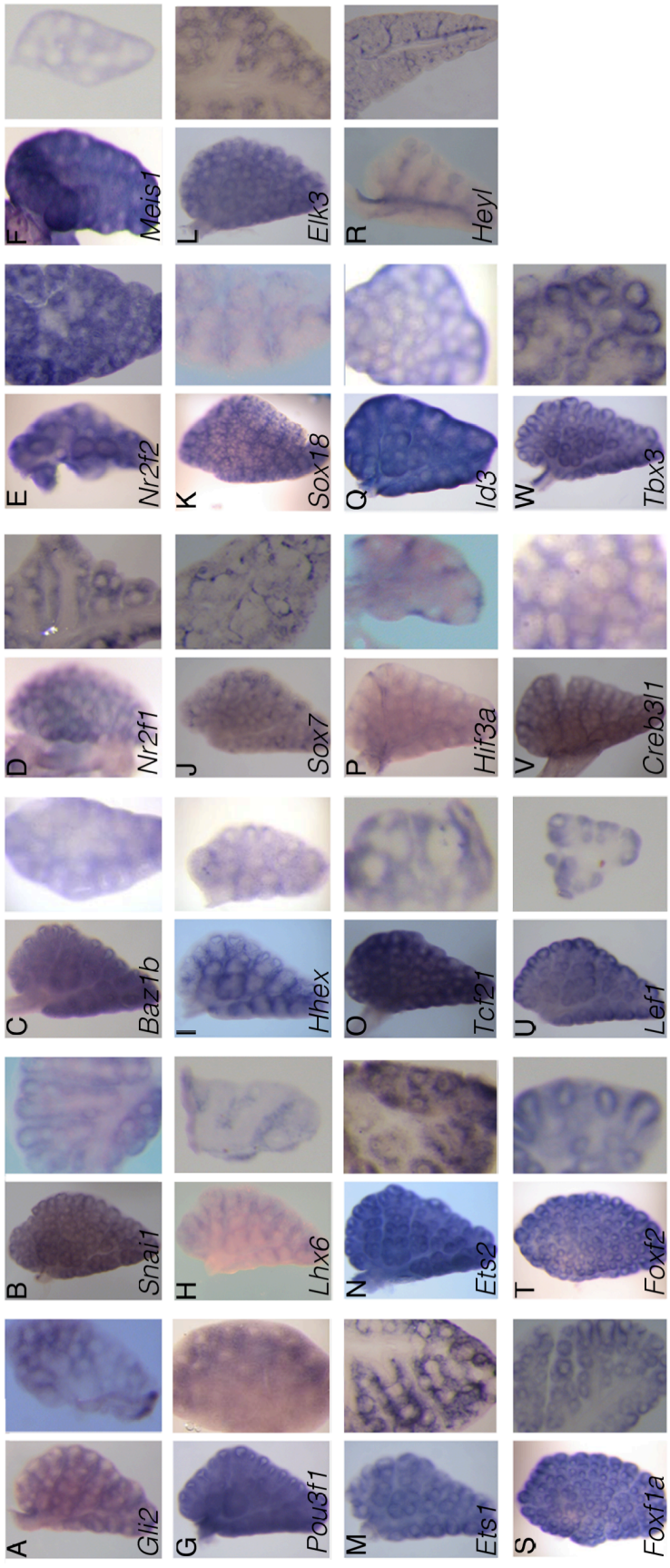

Figure 2. Patterns of transcription factor genes with primarily mesenchymal expression within the developing lung.

Figure 3: Patterns of transcription factor genes with both epithelial and mesenchymal expressions within the developing lung.

(A-J) Ten transcription factor genes were identified by RNA *in situ* hybridization to be expressed within both the epithelium and the mesenchyme of the E13.5 lung. For each gene, the left panel is a wholemount *in situ* hybridization of a left lung lobe, and the right panel is a vibratome section of a right lung lobe.

Figure 3: Patterns of transcription factor genes with both epithelial and mesenchymal expressions within the developing lung.

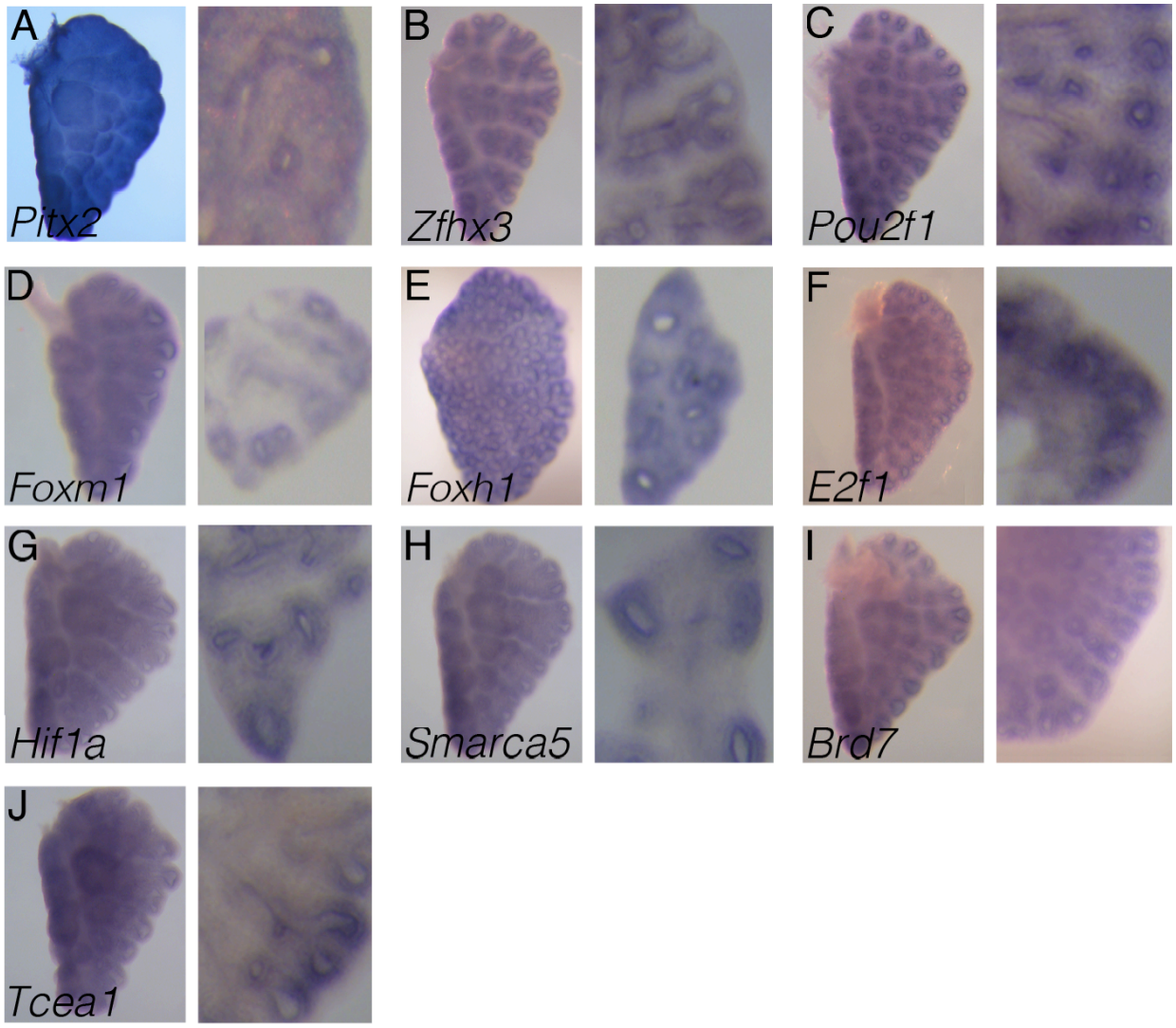

Figure 4: Patterns of Hox transcription within the developing lung.

(A-L) Six Hox genes were identified by RNA *in situ* hybridization to be expressed within the E11.5 (A,C,E,G,I,K) and either E12.5 (J,L) or E13.5 (B,D,F,H) lung and trachea. Each gene is a wholemount *in situ* hybridization of both the trachea and lung.

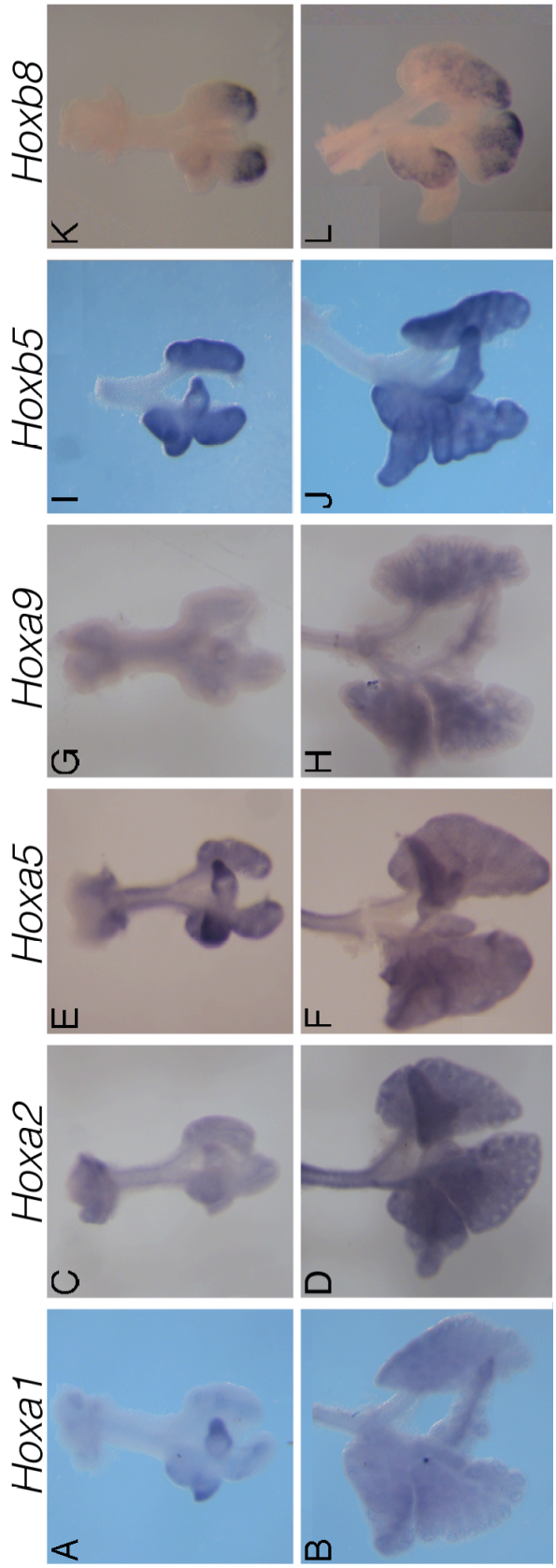

Figure 4. Patterns of Hox transcription within the developing lung.

Table 1. A summary of transcription factors identified in the screen:

Gene Name	Sites of expression in lung	Function during lung development	References	Figure
Ash2l	Epithelium	KO: dies at lung bud initiation stage.	Stoller et al. 2010	1R
Baz1b	Mesenchyme	KO: die at birth with heart defects, no reported lung defect.	Yoshimura et al. 2009	2C
Brd7	Epithelium and Mesenchyme	No knockout line available.	Kaeser et al. 2008	3I
Creb3l1	Mesenchyme	KO: viable and no reported lung defect.	Murakami et al. 2009	2V
E2f1	Epithelium and Mesenchyme	KO: no reported lung defect. Double KO of *E2f1;E2f3* develops simplified alveoli.	Tsai et al. 2008	3F
Elf5	Epithelium	OE: dilated branching tips and disrupted epithelial differentiation. KO: no reported lung defect.	Metzger et al. 2008 and Xin Sun unpublished	1N
Elk3	Mesenchyme	KO: survive birth, but eventually die due to respiratory distress secondary to chyle built up in thorax.	Ayadi et al. 2001	2L
Ets1	Mesenchyme	KO: viable and no reported lung defect.	Muthusamy et al. 1995	2M
Ets2	Mesenchyme	KO: embryonic lethal at E8.5.	Yamamoto et al. 1998	2N
Etv5	Epithelium	DN: proximalization of the lung epithelium in late branching stage. KO: no reported lung defect.	Liu et al. 2003; Chen et al. 2005	1M
Foxa1	Epithelium	KO: crucial for epithelial branching and differentiation.	Wan et al. 2005	1K
Foxd4	Epithelium	No knockout line available.	Kaestner et al. 1993	1L
Foxf1a	Mesenchyme	Heterozygous KO: lung lobe fusion and altered branch pattern.	Mahlapuu et al. 2001	2S
Foxf2	Mesenchyme	KO: dies postnatally with no reported lung defect.	Wang et al. 2003	2T
Foxh1	Epithelium and Mesenchyme	KO: left-right asymmetry lung defect.	Yamamato et al. 2003; Hoodless et al. 2001	3E
Foxm1	Epithelium and Mesenchyme	KO: defects in vascular and epithelial cell differentiation and inhibit arterial smooth muscle formation in lung.	Kim et al 2005; Kalin et al. 2008	3D
Gata6	Epithelium	KO: precocious formation of bronchial alveolar stem cells (BASCs).	Keijzer et al 2001; Yang et al. 2002	1G
Gli2	Mesenchyme	KO: reduced lung branching.	Motoyama et al. 1998	2A
Grhl2	Epithelium	Point mutant: reduced lung size and lung collapse at birth. KO: dies at beginning of lung development.	Pyrgaki et al. 2011	1W
Heyl	Mesenchyme	KO: viable and no reported lung defect.	Fischer et al. 2007	2R
Hhex	Mesenchyme	KO: dies at E14.5, no reported lung defect.	Hallaq et al. 2004	2I

Hif1a	Epithelium and Mesenchyme	CKO in epithelium: lethal at birth due to low surfactant gene expression.	Saini et al 2008	3G
Hif3a	Mesenchyme	KO: impaired alveologenesis with an increase of the vasculature lining the alveolar walls.	Yamashita et al. 2008	2P
Hnf1b	Epithelium	KO: embryonic lethal at post implantation stage.	Coffinier et al. 2002	1E
Id2	Epithelium	KO: dies postnatally, no reported lung defect.	Yokota et al. 1999	1U
Id3	Mesenchyme	KO: viable and no reported lung defect.	Pan et al. 1999	2Q
Irf6	Epithelium	Unknown. KO: no reported lung defect.	Ingraham et al. 2006	1V
Irx3	Epithelium	KD: abnormal branching.	Van Tuyl et al. 2006	1A
Kat2b	Epithelium	KO: no reported lung defect.	Yamauchi et al. 2000	1Q
Lef1	Mesenchyme	KO: dies postnatally, no reported lung defect.	van Genderen et al. 1994	2U
Lhx6	Mesenchyme	KO: dies around 2 weeks postnatally, no reported lung defect.	Liodis et al. 2007	2H
Lmo1	Epithelium	KO: viable and no reported lung abnormalities.	Tse et al. 2004	1H
Meis1	Mesenchyme	KD: dies at E14.5 and exhibit lung hypoplasia.	Hisa et al. 2004	2F
Mnx1	Epithelium	KO: postnatal lethal due to failure to inflate lungs.	Arber et al. 1999	1F
Nab1	Epithelium	KO: viable and no reported lung defect.	Le et al. 2005	1T
Nkx1-2	Epithelium	No knockout line available.	Tamplin et al.2008	1D
Nkx2-1	Epithelium	KO or KD: failed trachea specification and lung branching arrest.	Minoo et al.1995; Minoo et al. 1999	1B
Nkx2-9	Epithelium	KO: tracheobronchial epithelium hyperplasia in adult lung.	Tian et al. 2006	1C
Nr2f1	Mesenchyme	KO: postnatal lethal with no reported lung defect.	Qiu et al.1997	2D
Nr2f2	Mesenchyme	KO: dies at E10.0. CKO: lung hypoplasia.	Pereira et al 1999; You et al. 2005	2E
Pitx2	Epithelium and Mesenchyme	KO: left-right asymmetry lung defect.	Lu et al. 1999; Liu et al. 2001	3A
Pou2f1	Epithelium and Mesenchyme	KO: prenatal lethal with erythropoiesis defect, no reported lung defect.	Wang et al. 2004	3C
Pou3f1	Mesenchyme	KO: dies at birth due to respiratory distress possibly secondary to neuronal defects.	Bermingham et al. 1996	2G
Smarca 5	Epithelium and Mesenchyme	KO: lethal at pre-implantation stage.	Stopka et al. 2003	3H
Snai1	Mesenchyme	KO: lethal at E8.5.	Carver et al. 2001	2B
Sox18	Mesenchyme	KO: variable prenatal lethality, cardiovascular defects, no reported lung defect.	Dunn et al. 1995	2K

Sox2	Epithelium	CKO: disruption of cell differentiation. OE: altered branching morphogenesis.	Gontan et al. 2008; Tompkins et al. 2009; Que et al. 2009	1O
Sox7	Mesenchyme	No knockout line available.	Cermenati et al 2008	2J
Sox9	Epithelium	CKO: no reported lung defect.	Perl et al. 2005	1P
Tbx3	Mesenchyme	KO: dies before birth, no reported lung defect.	Davenport et al. 2003	2W
Tcea1	Epithelium and Mesenchyme	KO: dies before E16.5 and no reported lung defect.	Ito et al. 2006	3J
Tcea2	Epithelium	No knockout line available.	Reines et al. 1996	1J
Tcf21	Mesenchyme	KO: branching defects with proximalization of the lung epithelium.	Quaggin et al. 1999	2O
Tfap2c	Epithelium	KO: dies at E7-9.	Werling et al. 2002	1S
Zfhx3	Epithelium and Mesenchyme	Gene-trap mutant: no reported lung defect.	Stryke et al. 2003	3B
Zfp746	Epithelium	No knockout line available.	Shin et al 2011	1I

Abbreviations:

KO	Knock Out
KD	Knock Down
CKO	Conditional Knock Out
DN	Dominant Negative
OE	Over Expression

*Hox gene expression patterns are presented separately in Figure 4.

Chapter III: FGF-Regulated Etv Genes Control FGF-SHH Feedback Loop in Branching Lung

The transgenic lungs used in this study were generated with the help of Ying Zhang, Matthew J. Anderson, Deborah A. Swing, and Mark Lewandoski.
All other data was produced by John Herriges.

Abstract:

The FGF signaling pathway plays critical roles in both prenatal and postnatal lung development. However how FGF controls lung development at the transcriptional level is poorly understood. Here, we conditionally inactivated FGF regulated transcription factor genes *Etv4* and *Etv5* (*Etv4;5*) in the lung epithelium, and demonstrate that they are necessary for prenatal lung development. Unexpectedly, rather than phenotypes that mimic loss-of-function FGF mutants, the mutant lungs exhibited increased *Fgf10* expression and corresponding increased ERK1/2 phosphorylation. Subsequent genetic experiments demonstrated that this increase in *Fgf10* expression contributes to the *Etv4;5* mutant phenotype. We show further, evidence that this ETV inhibition of *Fgf10* is likely mediated by ETV promotion of *Shh* expression in the lung epithelium, which in turn inhibits *Fgf10* expression in the adjacent mesenchyme. As ETV inhibits *Shh* expression in the limb bud, our results in the lung indicate that the nature of ETV regulation of *Shh* is context dependent. Together, our findings show that Etv genes are an important node of the FGF-SHH signaling loop that balances between growth and branching of the lung epithelium.

Introduction:

The mammalian lung is essential for survival at birth. In mice, lung development initiates around embryonic day 9.5 (E9.5), with the outgrowth of the epithelial lung buds from the embryonic foregut (Cardoso and Lu 2006; Morrisey and Hogan 2010). Shortly after lung bud initiation the lung buds elongate and enter the pseudoglandular stage, where the epithelium begins the process known as branching morphogenesis. During branching morphogenesis a complex network of epithelial airways arises through the stereotypical application of three different modes of epithelial branching (Metzger et al. 2008). The stereotypical nature through which branching morphogenesis occurs suggests that there is a strict genetic component that regulates this process.

Many signaling pathways play critical roles in lung formation (Warburton et al. 2005; Cardoso and Li 2006; Morrisey and Hogan 2010). Of these, the fibroblast growth factor (hereafter FGF) signaling pathway is one of the most thoroughly studied. In total, seven FGF ligands and four FGF receptors are expressed in the lung at varying stages of development (Warburton et al. 2005; Yu et al. 2010; Cardoso and Lu 2006; Morrisey and Hogan 2010). The earliest requirement for the FGF signaling pathway in lung development is during bud initiation, where FGF10 and FGFR2-IIIb, are required for the formation of the initial lung buds (Min et al. 1998; Sekine et al. 1999; De Moerlooze et al. 2000). During branching morphogenesis the mesenchymally expressed *Fgf10* continues to be necessary for epithelial development, as *Fgf10* hypomorphs and *Fgf10* conditional knockout mice develop a greatly simplified epithelial branching structure (Mailleux et al. 2005; Abler et al 2009). Recent studies have suggested that one of the primary mechanisms through which FGF10 mediates epithelial development is through

an FGF10 to SHH negative feedback loop (Bellusci et al. 1997; Pepicelli et al. 1998; Abler et al. 2009). In this loop, the mesenchymally expressed *Fgf10* signals to the distal epithelium to promote epithelial outgrowth (Weaver et al. 2000). In response to FGF10, the epithelium grows towards the distal mesenchyme and produces SHH, which inhibits the expression of *Fgf10* in the adjacent mesenchyme (Abler et al. 2009). This causes *Fgf10* to be expressed in nodules that are constantly shifting and splitting in response to the outgrowing epithelium. Traditionally the dynamic localization of *Fgf10* expression has been thought to be one of the driving forces of epithelial bifurcation during branching morphogenesis, as each newly formed *Fgf10* expression nodule serves as a separate source of FGF10 and each outgrowing epithelial tip is exposed to multiple nodules. However, recent data has suggested that the expression level of *Fgf10*, and not its expression pattern, is critical for branching morphogenesis (Volckaert et al. 2013). Regardless of these recent studies though, the FGF-SHH feedback loop is still thought to be one of the key mediators of branching morphogenesis, as it controls *Fgf10* expression levels.

Interestingly, although many studies have been devoted to examining the function of pathway ligands and receptors during lung development, relatively few studies have examined how the downstream components of these signaling pathways mediate branching morphogenesis. To begin to understand the molecular mechanisms that control branching morphogenesis we had previously performed a genome scale transcription factor *in situ* hybridization screen (Herriges et al. 2012). From this screen we identified the PEA3 group ETS domain transcription factor ETV5, which is expressed in the distal epithelium. ETV5 is one of three PEA3 group transcription factors, all of

which are expressed in the developing lung, however, only *Etv4 and Etv5 (hereafter Etv4;5)* are strongly expressed in the lung epithelium (Liu et al 2003; Chotteau-LelieÁvre et al. 1997; Herriges et al. 2012). Previous studies have shown that the expression of *Etv4;5* are regulated by FGF signaling, making them attractive candidates for mediating FGF function during lung development (Liu et al. 2003; Lin et al. 2006; Zhang et al. 2009). A recent study examined the role of PEA3 group transcription factors in lung development through the overexpression of a dominant negative ETV5-Engrailed repressor fusion protein (hereafter *Etv5-Engl*) (Liu et al. 2003). The overexpression of the *Etv5-Engl* construct resulted in several phenotypic abnormalities, including a disruption in epithelial patterning and epithelial differentiation; however, the potential role of PEA3 group transcription factors during branching morphogenesis was not addressed. We were therefore interested in further examining the role of Etv4;5 during branching morphogenesis, in hopes that it would allow for a better understanding of how FGF signaling controls epithelial development in the lung.

In this study we used a conditional knockout approach to examine the role of *Etv4;5* in the embryonic and pseudoglandular stages of lung development. Here we demonstrate that *Etv4;5* are necessary for epithelial branching morphogenesis. Previous work has suggested that FGF signaling controls branching morphogenesis through an FGF-SHH negative feedback loop, however how FGF signaling mediates *Shh* expression is unknown (Abler et al. 2009). Our data suggests that ETV4;5 act as intermediates in the FGF-SHH negative feedback loop in the pseudoglandular stage lung, by acting downstream of FGF signaling and promoting the activity of a long range *Shh*-enhancer. Collectively our data demonstrates that ETV4;5 are necessary for early

epithelial branching in the lung, and provide a more thorough understanding of how FGF signaling is mediating embryonic lung development.

Results:

Inactivation of *Etv4* and *Etv5* leads to reduced branch morphogenesis

To investigate the requirement for *Etv4* and *Etv5* (hereafter *Etv4;5*) during lung development, we inactivated both in the embryonic lung epithelium. This was achieved by conditionally inactivating *Etv5* using an $Etv5^{fl}$ allele and an epithelial-specific Shh^{cre} , in combination with a null allele of *Etv4*, which generated $Shh^{cre/+};Etv5^{fl/fl};Etv4^{-/-}$ (hereafter *Etv4;5* mutant) embryos (Laing et al. 2000; Harfe et al. 2004; Harris et al. 2006; Zhang et al. 2009). We found over 80% reduction of the full-length *Etv5* transcript by E11.5, demonstrating that inactivation is efficient in the presence of the cre-recombinase (Figure 1A).

While *Etv4;5* mutants do survive, they display smaller lungs at birth (data not shown). In tracing the source of the lung hypoplasia phenotype, we found that *Etv4;5* mutant lungs display branching defects as early as E10.5, shortly after budding initiates. The distal tips of nascent buds, especially the larger right lung bud, are dilated in the mutant compared to control (Fig. 1C,D). This tip dilation phenotype remains prominent throughout branching morphogenesis, and the increase in tip size is statistically significant at both E12.5 and E13.5 (Fig. 1E-K). In addition, epithelial branching is delayed in the *Etv4;5* mutant lungs, which contributes to a reduction in branch number starting at E11.5 (Figure 1E,F). This phenotype persists during development, resulting in a greatly simplified epithelial branch structure and partial fusion of the rostral, medial,

and caudal lobes of the right lung (Figure 1C-F and data not shown). *Etv4;5* mutants also have a disruption of branch positioning, the most prominent of which is a posterior shift of the secondary branch that will form the accessory lobe (Figure 1F). This shift will later result in the fusion of the accessory and caudal lobes in the mutant lung (Fig. 1F). Taken together, these results led us to conclude that *Etv4;5* are necessary for establishing epithelial branch patterning during the early stages of lung development.

Etv4;5 mutant lungs show increased FGF signaling.

Interestingly, some of the epithelial defects, that we observed in *Etv4;5* mutant lungs are more similar to the phenotypes that have been reported in mutants with increased, rather than decreased, FGF signaling (Abler et al. 2009;Tang et al. 2011; Volckaert et al. 2013). To determine if FGF signaling was altered in the *Etv4;5* mutant lung, we examined the pattern of phosphorylated-ERK (hereafter pERK), a commonly assayed readout for FGF activity. We found that the pERK signal is elevated in intensity and expanded in its domain in the mutant epithelium compared to the control (Fig. 2A-F). To trace the cause of this increase in FGF activity, we examined the expression of *Fgf10*, the principle FGF ligand that regulates early lung branching. Using quantitative RT-PCR (hereafter qRT-PCR), we found that *Fgf10* expression is significantly increased in the *Etv4;5* mutant lung (Figure 2G). Consistent with this, we found that there was an expansion of the *Fgf10* expression domain in the mutant lung (Figure 2H-I).

The above results suggested that the increase in FGF activity would contribute to the branching defects that arise in the mutant lung. To address this possibility, we

reduced FGF signaling in the mutant lung by inactivating one copy of *Fgf10* in the *Etv4;5* mutant background, generating *Shh*$^{cre/+}$*; Etv5*$^{fl/fl}$*;Etv4*$^{+/-}$;*Fgf10*$^{+/-}$ (hereafter *Etv4;5;Fgf10*) embryos (Sekine et al. 1999). This rescued the pERK staining in the *Etv4;5;Fgf10* lungs, suggesting that introducing Fgf10$^{+/-}$ is sufficient to decrease FGF signaling in the epithelium (Sup Figure 1A-B). Compared to *Etv4;5* mutants, the *Etv4;5;Fgf10* mutants exhibit a mild but consistent attenuation of the distal dilation defect as early as E11.5 (Figure 3A,B). By E13.5, the epithelial tips of *Etv4;5;Fgf10* mutants are roughly 50% smaller than those of *Etv4;5* mutants ($P<0.05$ N=4) (Figure 3C-E). These results are consistent with findings in a recent publication, which demonstrated that FGF signaling controls lung epithelial lumen size (Tang et al. 2011). Interestingly, the branch number was not attenuated in the *Etv4;5;Fgf10* mutant lungs compared to control (Figure 3 C-D,F). Taken together, these data suggest that the increase in FGF signaling contributes to the epithelial phenotypes seen in the *Etv4;5* mutant lungs.

Etv4;5 mutant lungs exhibit a decrease in SHH signaling

The above data revealed that *Etv4;5* are part of a negative feedback loop, where FGF10 promotes the expression of *Etv4;5* in the distal epithelium, and ETV4;5 inhibit the expression of *Fgf10* in the distal mesenchyme. As ETV4;5 are transcription factors that act cell-autonomously, their inhibition of *Fgf10* expression in the mesenchyme must be through an intermediate factor that is expressed in the epithelium, but impacts the mesenchyme. One of the candidate mediators was FGF9, which has previously been shown to promote *Fgf10* expression in the mesenchyme (Colvin et al. 2001; del Moral et

al. 2006). However, we found that *Fgf9* expression was not statistically changed in the mutant lung (Data not shown). A second candidate mediator was *Shh*. Like *Etv4;5*, *Shh* is expressed in the epithelium, and its expression is regulated by FGF10 acting through FGFR2-IIIb in the epithelium (Abler et al. 2009). This raises that possibility that, ETV4;5 may act as the missing transcription factor that mediate the interaction between FGF10 and *Shh*. Further fitting this role, *Shh* has been shown to inhibit *Fgf10* expression (Bellusci et al. 1997; Pepicelli et al. 1998). Together, these data led us to hypothesize that a direct role of *Etv4;5* in the FGF feedback loop is to promote *Shh* expression in the distal epithelium.

To test this hypothesis, we examined whether SHH signaling is altered in the *Etv4;5* mutant lung. By *in situ* hybridization, we found that the staining intensity of *Shh,* as well as the SHH pathway readouts, *Gli1* and *Ptch1,* are decreased in *Etv4;5* mutant lungs (Figure 4A-F). This decrease is supported by qRT-PCR results (Figure 4G), suggesting that *Etv4;5* are required to promote *Shh* expression in the distal epithelial tips.

Increasing SHH signaling activity attenuates lumen size phenotype in *Etv4;5* mutant lungs

To determine if the decrease in SHH signaling in the *Etv4;5* mutant contributes to the phenotype, we enhanced SHH activity in the *Etv4;5* mutant lung and assessed the epithelial branch structure. This enhancement was achieved by using a potent pharmacological activator of the SHH co-receptor, Smoothened (Smoothened agonist, hereafter SAG) in an *in vitro* lung culture system (Chen et al. 2002). The treatment of lungs with SAG was able to induce the expression of the SHH pathway readout *Ptch1*

after twenty-four hours in lung culture (Sup Figure 2A-B). Furthermore, *Etv4;5* mutant lungs cultured in control media develop a dilated epithelial tip after only twenty-four hours, recapitulating the *in vivo* phenotype (P<0.02 N=3 Figure 5A-B, E-F,I). Together these data demonstrate that this *in vitro* lung culture system can allow us to examine how SHH signaling is contributing to the epithelial phenotype in the mutant lung.

To test whether activating the SHH pathway would attenuate the epithelial phenotype, we cultured lungs in media containing SAG ($7.26x10^{-6}$ug/ul). The treatment of control lungs with SAG at this concentration does not affect the epithelial tip size (Figure 5A-D). However, treatment of *Etv4;5* mutant lungs with SAG at this concentration, significantly decreased the mutant epithelial tip size (P<0.02 N=3 Figure E-I). Furthermore, in SAG treated *Etv4;5* mutant lungs, the size of the epithelial tip of *was* not significantly different from either DMSO or SAG treated control lungs (P>0.15 N=3 Figure 5I). These results support the conclusion that the decrease in SHH signaling is contributing to the *Etv4;5* mutant lung phenotype, and also suggest that ETV4;5 are acting in the distal lung epithelium to mediate a FGF-SHH signaling loop.

Etv4;5 directly regulate *Shh* expression through a long range *Shh* enhancer

A recent study identified a long range *Shh* enhancer expressed in the lung epithelium (Sagai et al. 2009). In the *Shh*-enhancer we were able to identify three highly conserved ETV4;5 DNA binding sites, using the previously described ETV4;5 DNA binding matrices (Wei et al. 2010) (Figure 6A). The conservation of these ETV4;5

binding sites suggests that they are functionally relevant for the activity of the *Shh*-enhancer.

To assess whether ETV4;5 regulate the *Shh*-enhancer's activity, we performed a series of luciferase reporter assays in MLE12 cells. In cell culture, we found that ETV5 induced the activity of the *Shh*-enhancer (Figure 6A). Furthermore, removing the N-terminal of the ETV5 ETS DNA binding domain eliminated the ability of ETV5 to act on the *Shh*-enhancer (Figure 6C). This suggests that the binding of ETV5 to the *Shh*-enhancer sequence is required for ETV*5* to promote the enhancer's activity. To determine whether the three conserved *Etv4;5* binding sites are required to induce the activity of the *Shh*-enhancer, we mutated the core ETV4;5 binding sequence from GGAA/T (CCTT/A) to CCAA/T (GGTT/A) (Figure 6B). Previous studies have demonstrated that this can alleviate the ability of ETV5 to bind to a conserved binding site (de Launoit et al. 1998). After mutating the ETV5 binding sites, we found that ETV5 could no longer induce *Shh*-enhancer activity, suggesting that the conserved binding sites are necessary for normal *Shh*-enhancer activity in vitro (Figure 6B). From these data, we conclude that in a lung epithelial cell line, ETV5 is able to induce the activity of the *Shh*-enhancer through interacting with three highly conserved ETV5 DNA binding sites.

In addition to the ETV4;5 binding sites in the *Shh* enhancer, we identified a highly conserved NKX2.1 binding site (Figure 6A). A previous study had demonstrated that ETV5 can interact with NKX2.1 on the protein level to promote the expression of *Sftpc* in a lung epithelial cell line (Lin et al. 2006). In cell culture we found that NKX2.1 was able to induce the activity of the *Shh* enhancer (Sup. Fig 3A). We also found that the

co-culture of NKX2.1 with ETV5 resulted in an increase in luciferase activity that was greater than the luciferase values seen when we cultured cells with ETV5 or NKX2.1 individually. Together these data suggest that ETV4;5 are able to control the activity of the SHH enhancer through interacting with NKX2.1.

To assess the role of the ETV4;5 binding sites in an *in vivo* context, we carried out a transgenic assay in which we examined b-galactosidase (hereafter b-gal) activity in lungs from embryos containing either the control or mutant *Shh*-enhancer linked to a *LacZ* open reading frame. In total, we examined 68 control embryos and 125 mutant embryos, which resulted in 20 control transgenic lines and 23 mutant transgenic lines for the *Shh*-enhancer. In agreement with a previous study, we found that the control *Shh*-enhancer was able to drive b-gal activity throughout the lung epithelium (Sagai et al. 2009)(Figure 6D). We were still able to visualize the b-gal activity in transgenic lungs that carried the mutant *Shh*-enhancer, however the overall staining intensity was greatly reduced (Figure 6E). Furthermore, although we did observe some variability in the strength of the staining in the transgenic lungs containing both the control and mutant *Shh*-enhancer, we consistently saw lighter staining in the transgenic lungs containing the mutant *Shh*-enhancer (Sup figure 4A-C). Together these data suggest that the conserved ETV4;5 binding sites are necessary for the normal activity of the *Shh*-enhancer in an *in vivo* context, and that this may be the mechanism through which *Etv4*;*5* are able to regulate *Shh* expression.

Discussion:

While many studies have examined the function of FGF ligands and FGFRs during lung development, relatively few studies have examined how the FGF pathway controls lung development on the transcriptional level. In this study we utilized a conditional knockout approach to establish a clear and specific requirement for the FGF regulated transcription factors *Etv4;5* during the initial stages of lung development. Our data demonstrates that *Etv4;5* are necessary for branching morphogenesis in the embryonic lung. Furthermore, our data suggests that *Etv4;5* control epithelial branch patterning in part by acting as intermediate components of the FGF-SHH signaling loop, which is thought to be one of the primary mediators of branching morphogenesis. Additionally, our data suggests that *Etv4;5* also control epithelial branch patterning through an unknown mechanism that is independent of the FGF-SHH signaling loop.

Surprisingly, although *Etv4;5* are downstream components of the FGF signaling pathway, we found that FGF signaling was increased in the *Etv4;5* mutant lung. Previous studies have shown that hyperactive FGF signaling can cause the lung epithelium to dilate (Abler et al. 2009;Tang et al. 2011). Therefore the increase in FGF signaling provided a plausible mechanism through which the *Etv4;5* mutant lungs were developing a dilated epithelium. By genetically decreasing FGF signaling in the lung, through removing one copy of *Fgf10*, we were able to confirm that the increase in the lumen size was caused by heightened FGF signaling. We therefore propose that one of the principle roles of *Etv4;5* during lung development is to mediate an FGF negative feedback loop in the distal lung (Figure 6F). Interestingly, previous studies have demonstrated that *Etv4;5* also mediate an FGF negative feedback loop in the limb,

suggesting that a general role of *Etv4;5* is to control the feedback inhibition of FGF signaling during development (Zhen et al. 2009; Junhao et al. 2009).

Since ETV4;5 are transcription factors, their regulation of FGF signaling in the mesenchyme had to be through an intermediate factor. Recent studies provide evidence that SHH signaling acts downstream of FGF signaling in the epithelium, and that SHH signaling negatively regulates *Fgf10* expression in the mesenchyme (Pepicelli et al. 1998; Abler et al. 2009). This made it a plausible medium through which *Etv4;5* could regulate *Fgf10* expression. In agreement with this, we found that SHH signaling was decreased in *Etv4;5* mutant lungs. Furthermore, like the *Etv4;5;Fgf10* rescue, we found that activating the SHH pathway was able to attenuate the lumen dilation phenotype. These findings illustrated that a decrease in SHH activity is contributing to the *Etv4;5* mutant lung phenotype, and suggested that *Etv4;5* are intermediate factors in the FGF-SHH signaling loop that controls lung development.

The question then arose as to how *Etv4;5* are able to mediate SHH expression in the epithelium. Through a combination of *in vitro* and *in vivo* studies we were able to demonstrate that *Etv4;5* promote the activity of a long range *Shh* enhancer in the lung. Interestingly, previous studies have suggested that *Etv4;5* also control FGF signaling in the limb by regulating *Shh* expression. However, in the limb ETV4;5 negatively regulate *Shh* expression, and SHH signaling promotes the FGF pathway (Zhen et al. 2009; Junhao et al. 2009). We believe that the discrepancy between how *Etv4;5* mediate *Shh* expression can be explained by the fact that the SHH-FGF regulation is the opposite in the lung and limb. Therefore, in order for *Etv4;5* to repress FGF signaling in both tissues, *Etv4;5* must have an opposite effect on *Shh* expression in the two tissues.

Additionally, our data suggests that *Etv4;5* mediate *Shh* expression through different mechanism in the two tissues. The majority of reports have indicated that *Etv4;5* positively regulate gene expression (De Launoit et al. 2006). Thus, *Etv4;5* are though to indirectly regulate *Shh* expression in the limb, through inhibiting the formation of a TWIST1-HAND2 heterodimer, which negatively regulates *Shh* expression (Firulli et al. 2007; Zhang et al. 2010). Our data suggests that ETV4;5 directly promote *Shh* expression in the lung through three highly conserved ETV4;5 binding sites in the MACS1 *Shh* enhancer. Furthermore, unlike in the limb, our data suggests that ETV4;5 are able to mediate the transcription of *Shh* by augmenting the ability of NKX2.1 to activate the *Shh* enhancer. This agrees with previous findings that have demonstrated that ETV5 interacts with NKX2.1 to promote the expression of *Sftpc* in lung epithelial cells (Lin et al. 2006). Thus we believe that the different mechanisms through which ETV4;5 are mediating *Shh* expression do not contradict one another, instead these mechanisms are two different means to the same end, which is to restrict FGF signaling.

Along with mediating epithelial lumen size, recent studies have demonstrated that both the FGF and SHH signaling pathways are critical mediators of epithelial branch patterning (Bellusci et al. 1997a; Bellusci et al. 1997b; Park et al. 1998; Pepicelli et al. 1998; Weaver et al. 2000; Volckaert et al. 2013). Originally we had hypothesized that the miss-regulation of the FGF and SHH signaling pathways would be contributing to the epithelial branch phenotype. However, our results from genetically removing one copy of *Fgf10* and pharmacologically activating SHH signaling, suggest that the disrupted epithelial branch patterning in the *Etv4;5* mutant lung is independent of the

FGF-SHH signaling loop. Thus we believe that *Etv4;5* are able to mediate lung branching through mechanisms that are downstream of FGF signaling, but do not involve the FGF-SHH signaling loop (Figure 6F). Other groups that have examined the role of *Etv4;5* in similar epithelial branching organs, like the kidney, and have suggested that *Etv4;5* may be able to mediate epithelial branching through controlling epithelial cell placement and by regulating the expression of matrix metalloproteases (MMP) (Lu et al. 2009; Kuure et al. 2010). Previous studies have also demonstrated that ETV4 controls MMP production in the postnatal lung macrophages, which suggests that *Etv4;5* may be controlling a MMP production in the embryonic lung (Lee et al. 2011). However, how *Etv4;5* are controlling epithelial development independent of the FGF-SHH signaling loop will be the focus of future studies.

Materials and Methods:

Mice

The mutant alleles used in this study are Etv5fl (Zhang at al. 2009), Etv4- (Laing at al. 2000), Fgf10- (Sekine et al. 1999), and Shh-cre (Harfe et al. 2004). The embryos used in these experiments were harvested from time-mated females, with noon the day of the vaginal plug counting as E0.5. Shh-cre;Etv5fl/+;Etv4+/- embryos were used as controls.

Antibody staining:

Embryos were fixed in 4% PFA at 4°C overnight. After fixation, the lungs were dehydrated in methanol and stored at -20 deg C until use. For antibody staining, a standard protocol was followed (Yi et al .2009). The primary antibodies used for this

study were rabbit anti-E-cadherin (Cell Signaling, 1:200 dilution), rat anti-E-cadherin (DECMA source, 1:100 dilution), rabbit anti-Phosphorylated-Erk (Cell Signaling, 1:200 dilution). The secondary antibodies used were Cy3-conjugated goat anti-mouse, FITC-conjugated goat anti-rabbit, HRP-conjugated goat anti-rabbit, and Biotin-conjugated goat anti-rabbit (Jackson Immuno Research, 1:200 dilution). The tertiary antibody used to detect pERK in whole mount lungs was FITC conjugated-Streptavidin (Jackson ImmunoResearch, 1:200 dilution).

RNA *in situ* Hybridization

RNA *in situ* hybridization was performed following a protocol that was adapted from previously published protocols (Wall and Hogan 1995; Herriges 2012). Briefly, wholemount tissues stored in methanol were rehydrated using PBS with 0.1% Tween (PBT). Tissues were then permeabilized using 10µg/ml proteinase K in PBT for 10 minutes. Tissues were fixed with 4% paraformaldehyde, 0.2% glutaraldehyde in PBT for 20 minutes. They were then washed and allowed to hybridize with probes at 70oC overnight. After the hybridization, tissues were washed three times, twenty minutes each in 2x SSC, 0.1% CHAPS, and then in 0.2x SSC, 0.1% CHAPS at 70oC. Tissues were then washed in KTBT and blocked for 2 hours in 2% blocking solution (Roche) and 20% heat inactivated sheep serum (Sigma) in KTBT at room temperature. The tissues were then incubated overnight at 4˚C in the primary antibody, AP conjugated α-DIG, Fab fragment (Roche) at a dilution of 1:2000 using 2% blocking solution and 20% heat inactivated sheep serum in KTBT. The tissues were then washed 5 times, 1hour each in KTBT at room temperature. Following this, the tissues were washed twice, 5 minutes

each with 0.1% Tween, 1mM Levamisole in ddH2O. Finally the tissues were stained in BM purple (Roche) containing 0.1% Tween and 1mM levamisole. The staining was carried out for varying amount of time depending on the probes until desired intensity, from 30 minutes to 8 hours.

Quantitative RT-PCR:

Total RNA was extracted from three control and three mutant samples using Trizol and an RNeasy-micro Qiagen RNA extraction kit(Invitrogen, Qiagen). RNA was reverse-transcribed using Superscript-III first-strand synthesis system (Invitrogen). cDNA was PCR amplified and quantified using SYBRgreen (Applied Biosystems). The primers used were: *β-actin* (5′-CGGCCAGGTCATCACTATTGGCAAC-3′ and 5′-GCCACAGGATTCCATACCCAAGAAG-3′), *Etv5* (5'-GGTATTTCTCCAGCAGCCATGAAGG
-3' and 5'-TCTCGGGTACCACGCAAGTATCATC-3')
, *Fgf10* (5'-GATTGAGAAGAACGGCAAGGTCAG-3' and 5'-TTGACGGCAACAACTCCGATTTCC-3'), *Shh* (5'-GGCTGATGACTCAGAGGTGCAAAG-3' and 5'-GCTCGACCCTCATAGTGTAGAGAC-3'), *Gli1* (5'-GCACGTTTGAAGGCTGTCGGAAGTC-3' and 5'-CGCGGTCACTGGCATTGCTAAAGGC -3'), *Ptch1* (5'-GCACATGTTTGCTCCCGTTCTGGAC-3' and 5'-ATGGCCAGGACGGCAAAGAAGTATC-3'). Three biological replicates and two technical replicates were performed for all qPCR. Expression values were normalized using *β-actin* and results were compared using the Student's t-test.

Luciferase reporter assay:

To make the luciferase reporter containing the MACS1 *Shh* enhancer was amplified and cloned into the Pgl3 vector (Promega). To make the mutated version of the MACS1 Shh enhancer, the GGAA/T core binding sequence was mutated to CCAA using a QuikChange Site-Directed Mutagenesis Kit (Agilent). The plasmids containing the control Etv5 open reading frame and a mutated Etv5 open reading frame have been previously described (Zhang et al. 2009).

MLE-12 cells were transfected with the reporter vector (200ng) and either an empty vector, Etv5 vector, or Etv5 mutant vector (600ng) using lipofectamine 2000 (Invitrogen). A Renilla luciferase plasmid was used as a transfection control. Luciferase activity was analyzed using the Dual-Luciferase reporter system (Promega). Three biological replicates and two technical replicates were performed and results were compared using the Student's t-test.

***In vitro* Lung culture:**

Lungs from control and Etv4;5 mutant embryos were harvested at E11.5. Lungs were placed on a Nucleopore Trak-Etch membrane (Whatman, 8um), and cultured at the air/liquid interface of 500ul of DMEM-F12, supplemented with 10% FBS. To activate SHH signaling smoothened agonist (SAG) was added at a concentration of $7.26x10^{-6}$ug/ul, with DMSO being used as a diluent control. Lungs were incubated at 37°C in 5% CO2 for 24 hours.

Transgenic lung assay:

The transgenic construct was produced by amplifying the MACS1 enhancer and cloning it into the Hsp68-LACZ vecoter (Addgene). Production of transgenic mice was performed as previously reported in Anderson et al. 2013

Figures:

Figure 1: Loss of Etv4;5 activity in the lung epithelium inhibits branching in the embryonic lung.

The flox excision rate from the *Etv5* transcript is significant as early as E11.5 in the Etv4;5 mutant lung (A). (B-I) Representative whole mount E-cadherin immunohistochemical stains from control (B,D,F,H) and *Etv4;5* Mutant (C,E,G,I). As early as E10.5 *Etv4;5* mutant lungs display a dilation of the lung epithelium (B,C). When the lung enters the pseudoglandular stage, disruption in epithelial branch patterning become apparent (D,E). In the control lung the secondary branches that will give rise to the four lobes of the right lung form (D). In the *Etv4;5* mutant lung, the epithelial buds grow out more slowly and the lobes of the right lung are not as apparent (E). Additionally in the *Etv4;5* mutant lung the secondary branch that will give rise the accessory lobe is shifted proximally (arrowhead D,E). Dorsal views of the control and mutant lung reveal that the epithelial branch phenotypes persist into the later stages, with *Etv4;5* mutant lungs showing less epithelial branches that have a larger distal lumen tip (F-I). An example of how the distal tip is defined in shown in the insets in F-G. Quantification of the left lung tip number and the left lung tip area revealed that Etv4;5 mutant lungs have fewer distal epithelial tips and that these tips are larger in area (N=4+ for all stages *P<.05) (J,K). Data are presented as means (+SEM).

Figure 1: Loss of Etv4;5 activity in the lung epithelium inhibits branching in the embryonic lung.

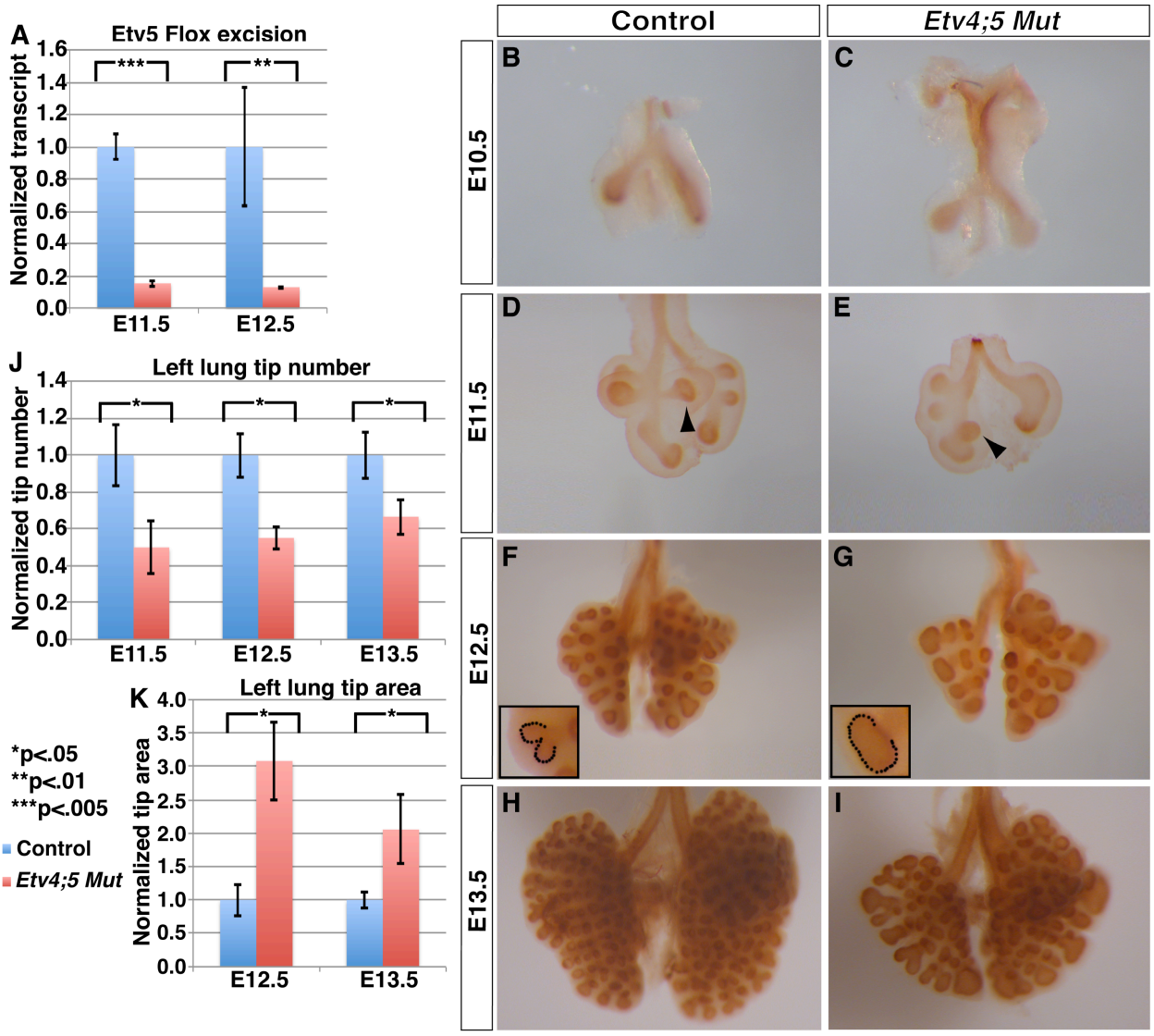

Figure 2: *Etv4;5* mutant lungs display an increase in FGF signaling activity. (A-F) Representative E11.5 whole mount immunofluorescent staining for ECAD (red) and the FGF readout pERK (green). In the control lung pERK localizes to the distal tip of the outgrowing epithelium (A-C). The *Etv4;5* mutant lungs show an expanded pERK staining and an increase in the pERK staining intensity (D-F). *Fgf10* gene expression analysis was performed in control and mutant lungs using qRT-PCR (G) and RNA *in situ* hybridization (H,I). qRT-PCR revealed that at E11.5 and E12.5 the *Fgf10* transcript level is over two fold higher in the *Etv4;5* mutant lungs (G). Data are presented as means (+SEM). Whole mount RNA *in situ* hybridization for *Fgf10* revealed that the *Etv4;5* mutant lungs have an expanded FGF10 expression domain at E12.5 (H,I).

Figure 2: *Etv4;5* mutant lungs display an increase in FGF signaling activity.

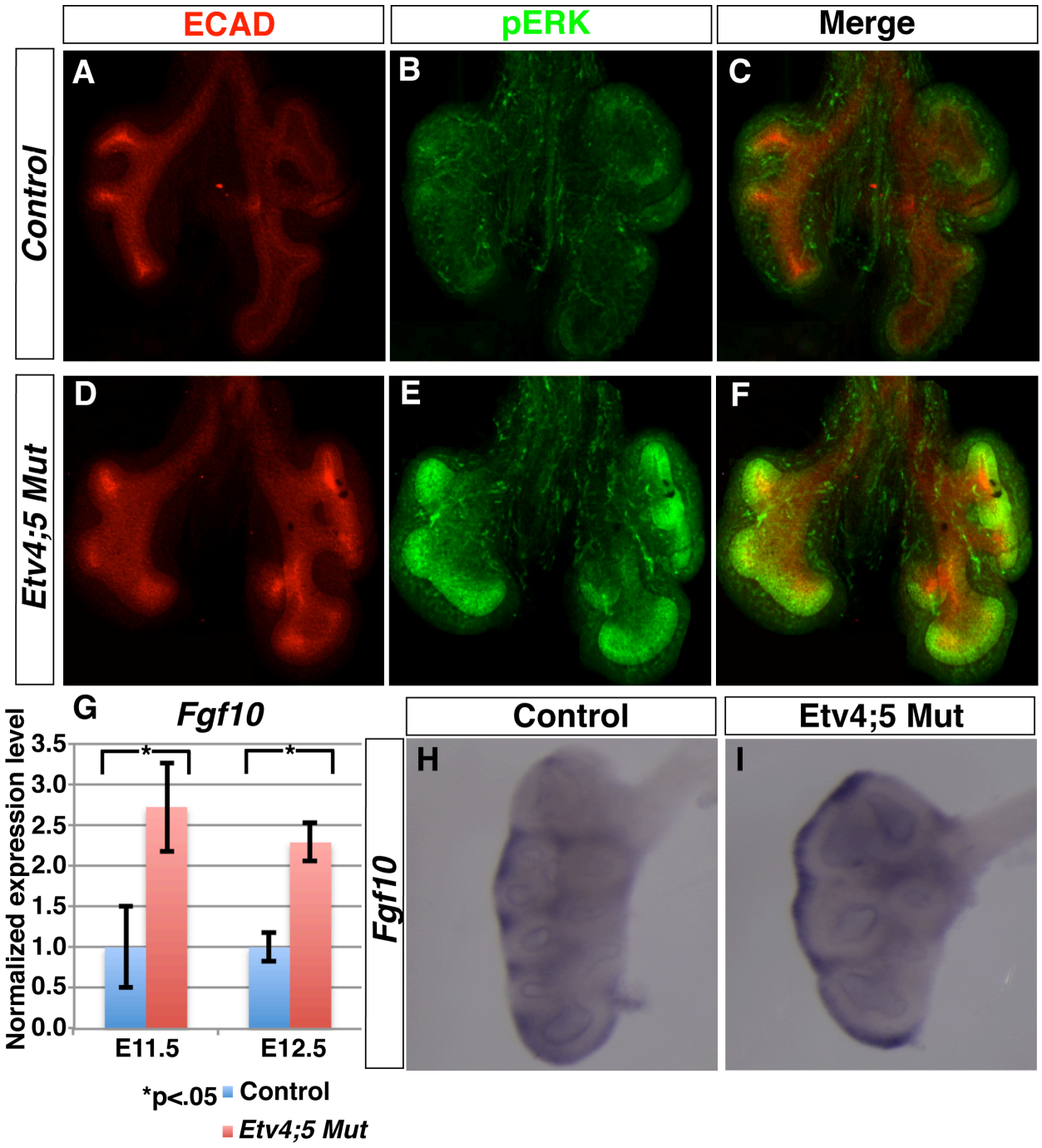

Figure 3: Introducing one mutant copy of *Fgf10* is able to attenuate the *Etv4;5* branching phenotype.

(A-D) Representative dorsal views of E11.5 and E13.5 whole mount ECAD immuno-histochemical stains from *Etv4;5* control and *Etv4;5;Fgf10* mutant embryos. At E11.5 the *Etv4;5;Fgf10* mutant lungs have a slightly narrower epithelial lumen (A,B). By E13.5 the *Etv*4;5 mutant distal dilation phenotype shows a more significant attenuation in the *Etv4;5;Fgf10* mutant lung (C,D). An example of how the distal tip is defined in shown in the insets in C-D. Quantification of the distal branching phenotypes revealed that the distal lung tip area is approximately 50% smaller in the *Etv4;5;Fgf10* mutant lung than the Etv4;5 mutant lung ($P<.05$ N=4) (E). Interestingly, the epithelial branch tip number was not rescued in the *Etv4;5;Fgf10* mutant lung (F). Data are presented as means (+SEM).

Figure 3: Introducing one mutant copy of Fgf10 is able to attenuate the *Etv4;5* branching phenotype.

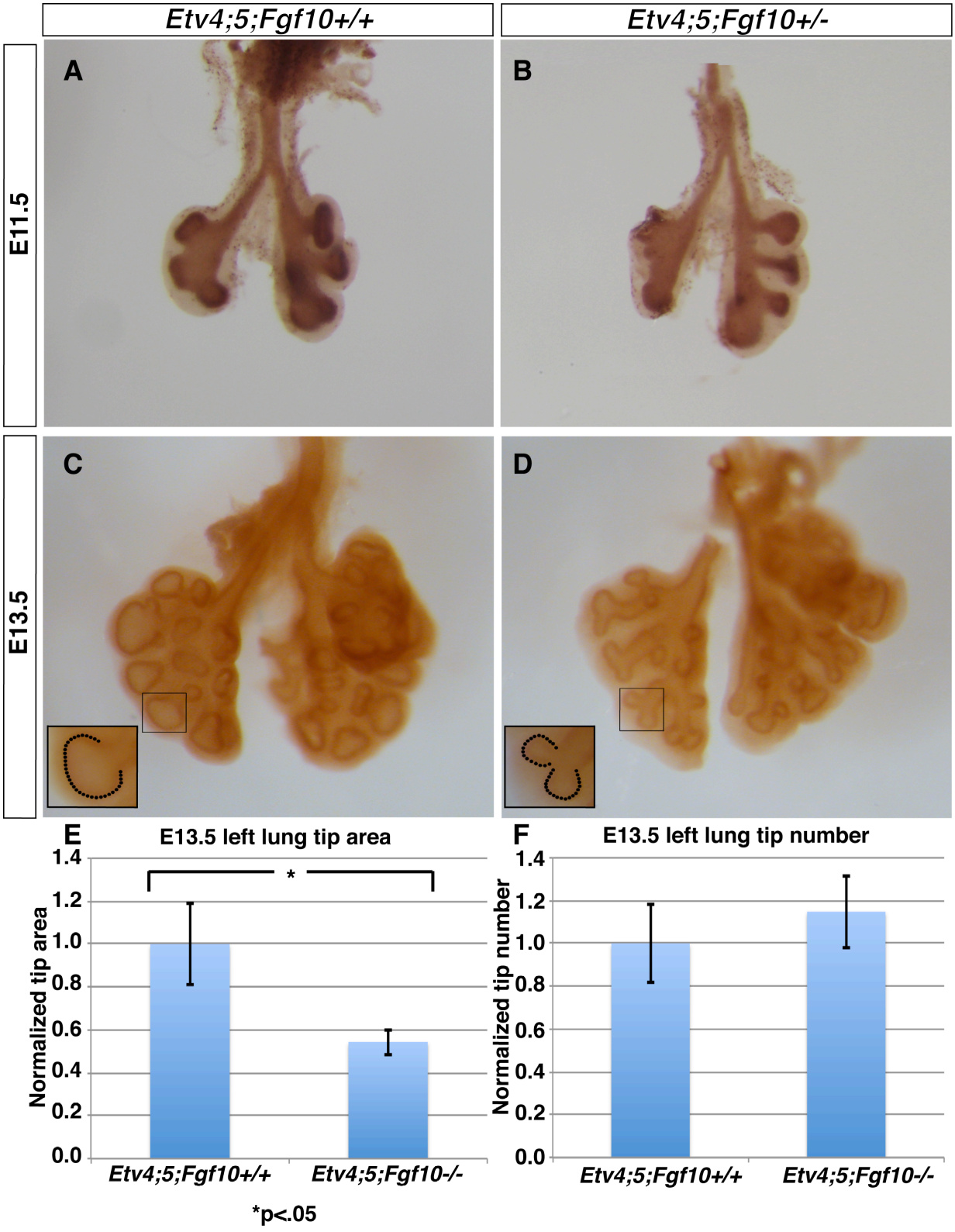

Figure 4: Expression analysis reveals a decrease in SHH signaling in the *Etv4;5* mutant lung.

(A-F) Representative whole mount RNA *in situ* hybridizations were preformed on the left lung of control and *Etv4;5* mutant lungs at E12.5. The expression of *Shh* was decreased in the epithelium of the *Etv4;5* mutant, when compared to cre-positive controls (A,B). SHH signaling in the mesenchyme was also decreased in the *Etv4;5* mutant lung. The expression of the SHH readouts *Gli1* (C,D) and *Ptch1* are decreased in the Etv4;5 mutant lungs at E12.5 when compared to Cre-positive controls (E,F). Quantification of the expression of *Shh*, *Gli1*, and *Ptch1* was performed using qRT-PCR, and all showed a statistically significant decrease in expression in the *Etv4;5* mutant lung when compared to Cre-positive controls (N=3 $P<0.05$) (G). Data are presented as means (+SEM).

Figure 4: Expression analysis reveals a decrease in SHH signaling in the *Etv4;5* mutant lung.

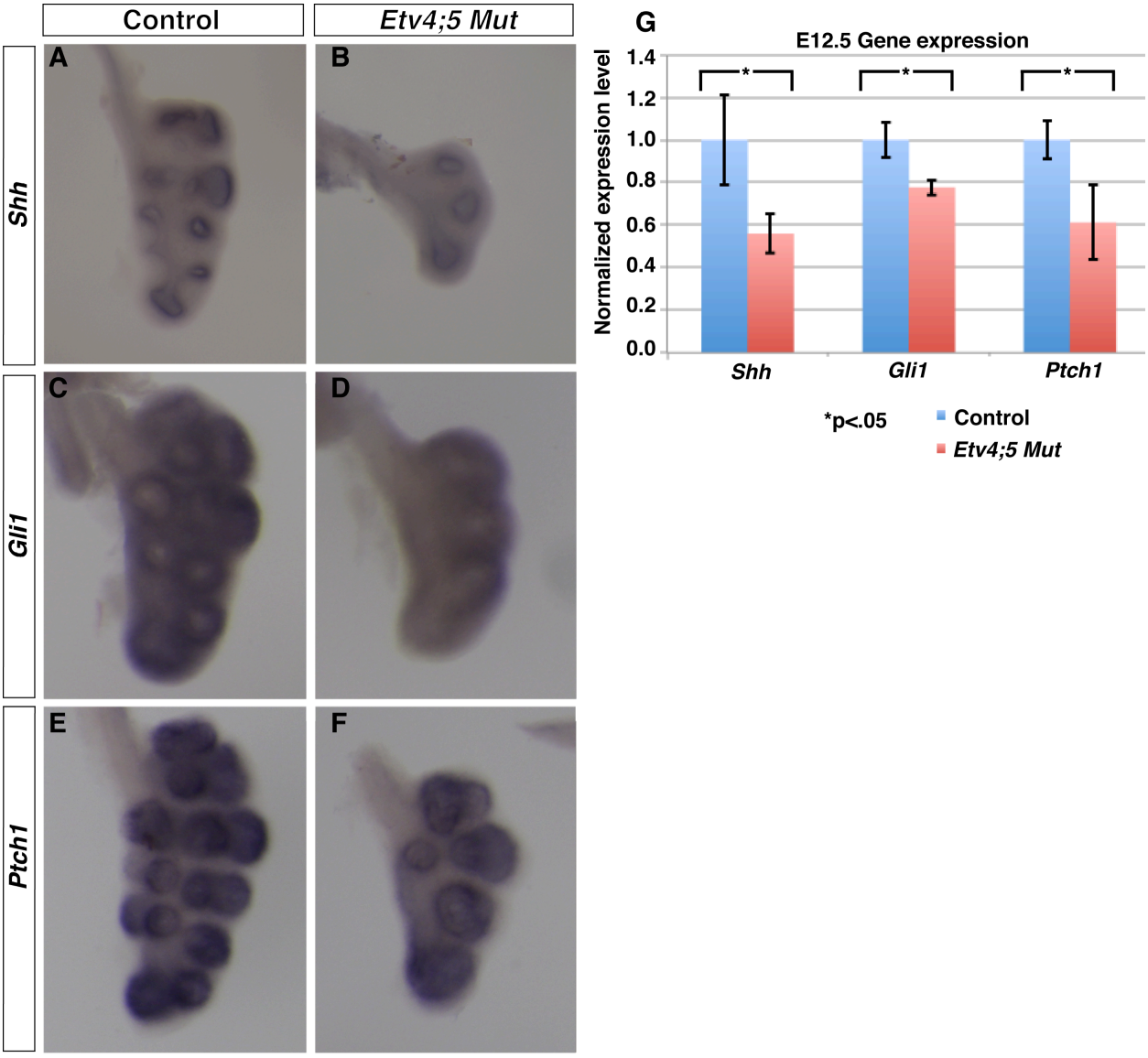

Figure 5: SAG treatment of control and Etv4;5 mutant lungs.

(A-H) Representative images of E11.5 lungs cultured for 24 hours in either DMSO (A,B, E,F) or SAG (C,D,G,H). SAG treatment did not affect the epithelial tip size (outlined in black) after 24 hours lung culture (A-D). *Etv4;5* mutant lungs cultured in DMSO display larger epithelial tip after 24hours lung culture (E,F,I). Culturing *Etv4;5* mutants in SAG was able to attenuate the dilation of the distal tips (G,H). The distal tip epithelium of SAG cultured *Etv4;5* mutant and control lungs was not different (D,H). Quantification of the right lung epithelial tip size showed that SAG treatment was able to significantly attenuate the epithelial lumen size defect (N=4 $P<.05$) (I). Data are presented as means (+SEM).

Figure 5: SAG treatment of control and *Etv4;5* mutant lung

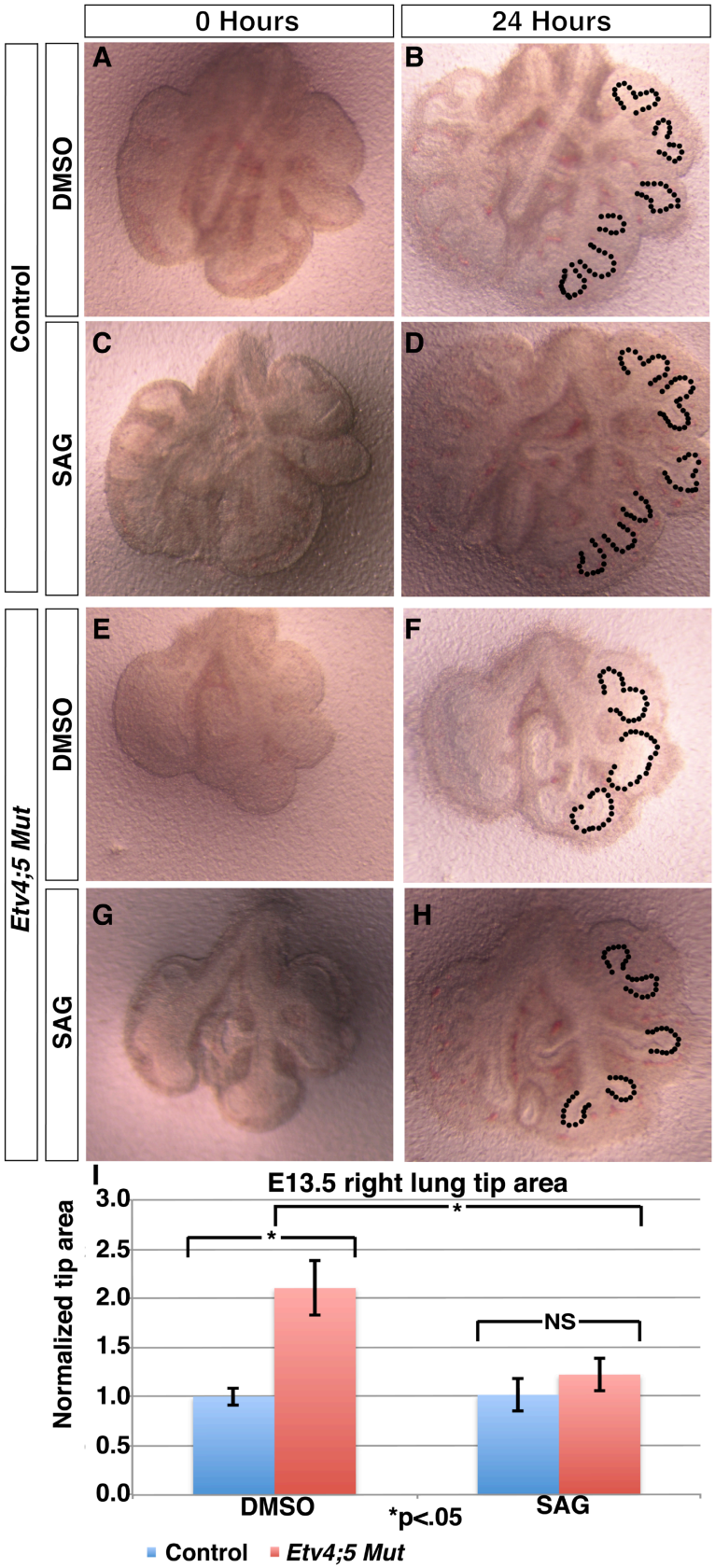

Figure 6: Etv4;5 mediate Shh expression through a long range *Shh* enhancer. (A) The MACS1 lung epithelium enhancer lies in an intron of *Rnf32* that is approximately 800kb upstream of the *Shh* open frame. The MACS1 enhancer contains three highly conserved ETV4;5 binding sites and one NKX2.1 binding site. (B) The ETV4;5 binding sites were mutated to remove the core ETV4;5 binding sequences (GGAA/T) within each site. (C) Using a luciferase assay in MLE-12 cells, we found that ETV5 was able to induce the activity of the MACS1 enhancer *in vitro*. (C) Loss of the ETV5 ETS DNA binding domain inhibited the ability of ETV5 to induce the activity of the MACS1 enhancer. (C) Mutating all three of the ETV5 binding sites inhibited the ability of Etv5 to induce the activity of the MACS1 enhancer. (D,E) Representative John staining of E11.5 whole lungs from transgenic mouse embryos containing either the control and mutant MACS1 *Shh* enhancer. (D) The control enhancer strongly drove LacZ expression throughout the lung epithelium. (E) The mutant enhancer display less robust LacZ expression in the epithelium. (G) Together our data suggests a model in which Etv4;5 are key mediators of an FGF-SHH negative feedback loop. In this loop Etv4;5 act downstream of FGF10 to mediate Shh expression in the distal lung epithelium. The loss of *Etv4;5* results in a decrease in SHH signaling which then causes an increase in *Fgf10* expression in the mesenchyme, which affects the lung lumen size. Additionally, our data suggest that Etv4;5 mediate epithelial branch patterning independent of this loop.

Figure 6: Etv4;5 mediate Shh expression through a long range *Shh* enhancer.

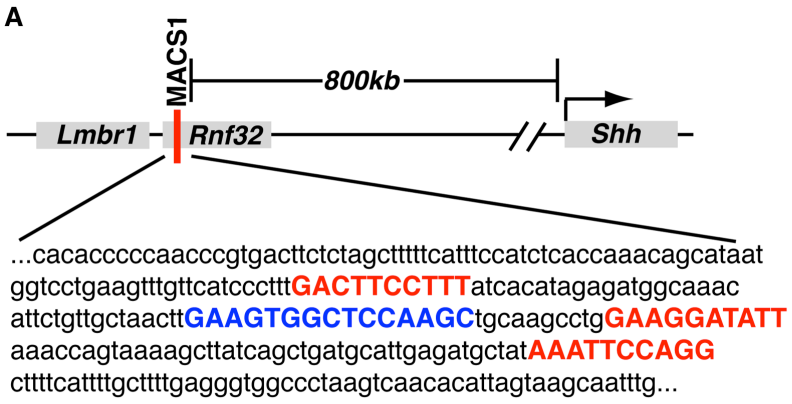



B

	Site 1	Site 2	Site3
Control sequence	GACTTCCTTT	GAAGGATATT	AAATTCCAGG
Mutant sequence	GACTTGGTTT	GAACCATATT	AAATTCCAGG

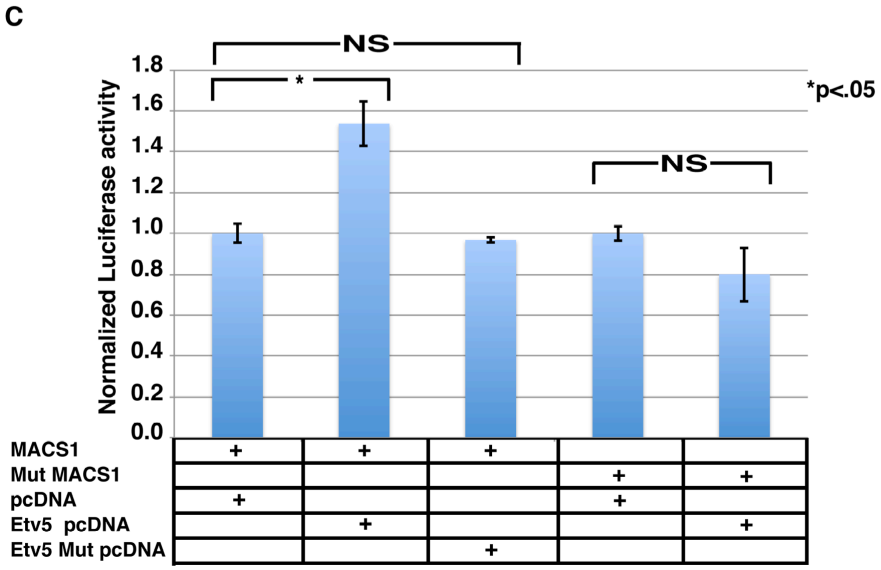

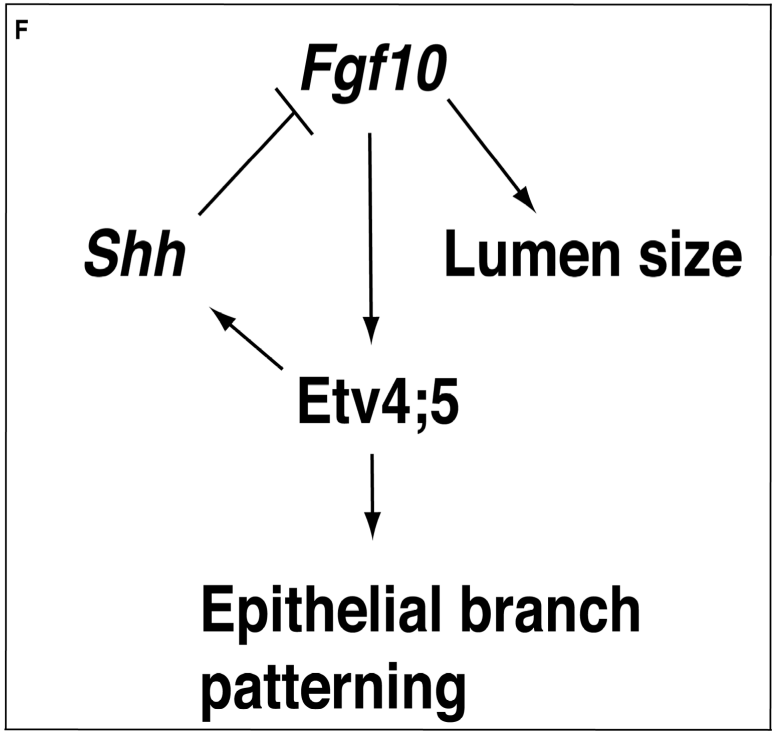

Supplemental Figure 1: The increase in pERK levels is attenuated in the Fgf10;Etv4;5 Mutant lungs.

(A-B) Representative images of an E11.5 left lung lobe from *Etv4;5* Mutant and *Etv4;5;Fgf10* mutant embryo stained for pERK (green) and ECAD (red). In the *Etv4;5* mutant lung there is strong pERK staining throughout the lung epithelium (A). The *Etv4;5;Fgf10* mutant lungs have a decrease in pERK staining when compared to *Etv4;5* mutant lungs (A-B).

Supplemental Figure 1: The increase in pERK levels is attenuated in the *Fgf10;Etv4;5* Mutant lungs.

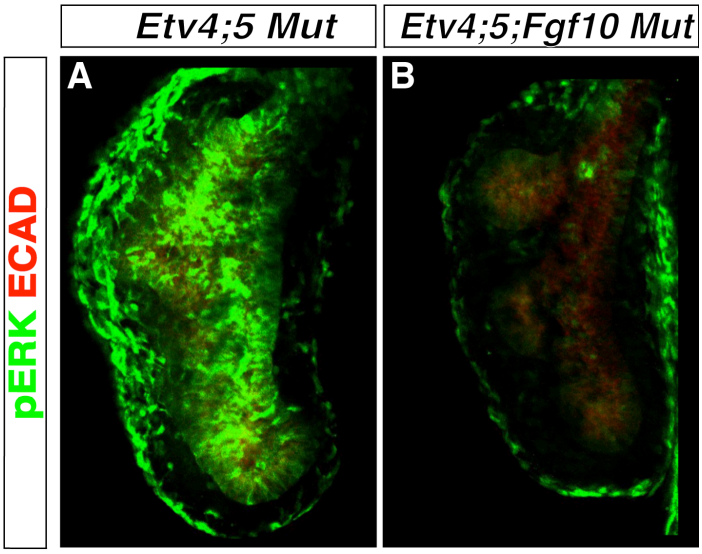

Supplemental Figure 2: Treatment of lungs with SAG induces SHH signaling activity.

(A-B) Representative images of *Ptch1 in situ* hybridization performed on E11.5 lungs that had been cultured 24 hours. FVB lungs were cultured in media containing either DMSO (Control) (A) or the SHH activator smoothened agonist (SAG) (B). In lungs cultured in the control media, *Ptch1* localizes the mesenchyme (A). In lungs cultured in media containing SAG, SHH signaling was increased, as the expression of *Ptch1* was increased (B).

Supplemental Figure 2: Treatment of lungs with SAG induces SHH signaling activity.

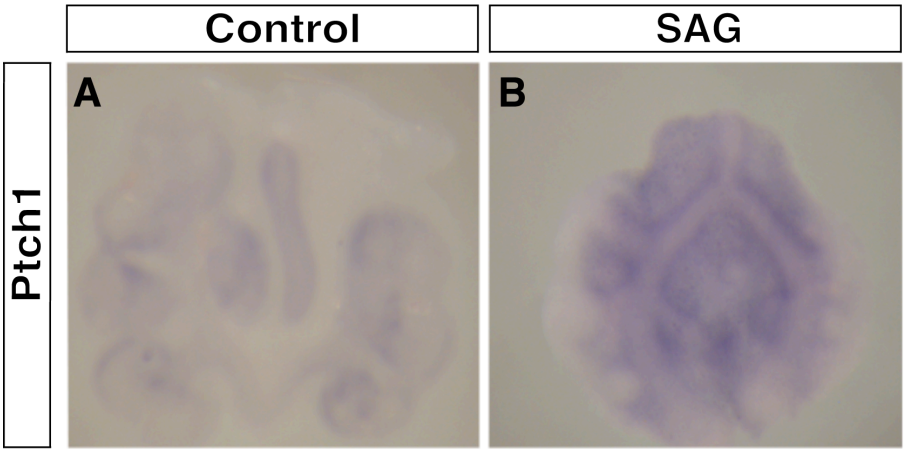

Supplemental Figure 3: ETV5 is able to augment the ability of NKX2.1 to induce the activity of the MACS1 *Shh*-enhancer element.

Using a luciferase assay we found that NKX2.1 was able to induce the activity of the MACS1 Shh-enhancer in the MLE-12 cell line. The co-culture of NKX2.1 with ETV5 was able to induce the activity of the MACS1 *Shh*-enhancer to a greater degree than either NKX2.1 or ETV5 individually ($P<.01$). Data are presented as means (+SEM).

Supplemental Figure 3: ETV5 is able to augment the ability of NKX2.1 to induce the activity of the MACS1 *Shh*-enhancer element.

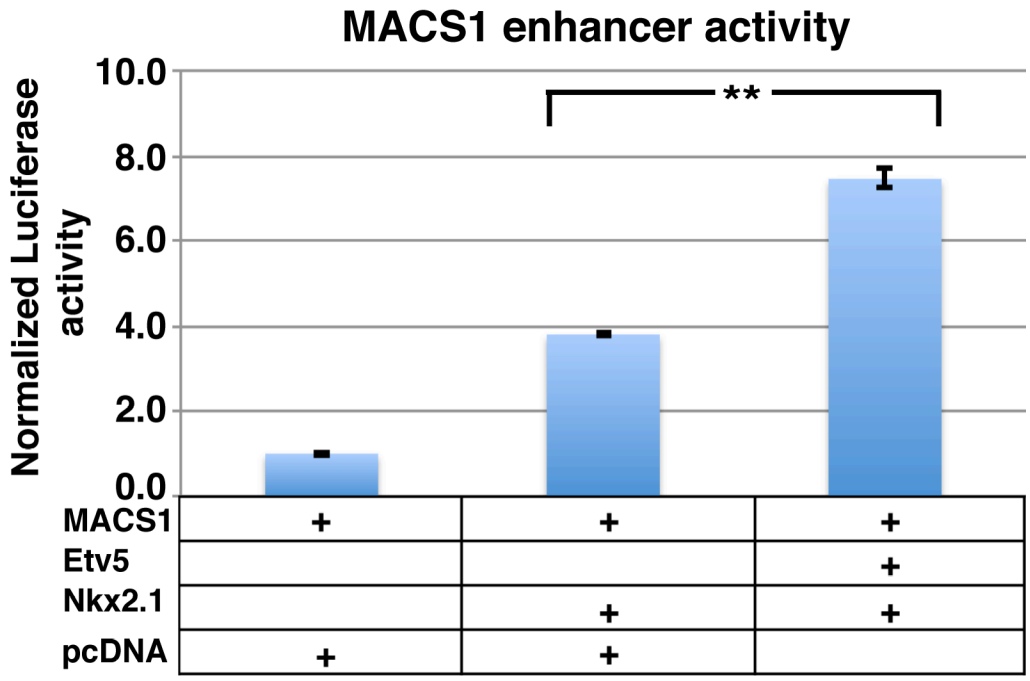

Supplemental Figure 4: Loss of the ETV4;5 sites leads to decreased activity of the Shh-enhancer in vivo.

(A-B) b-Gal staining performed on E11.5 transgenic lungs containing either the control or mutant *Shh* enhancer. In total we identified 20 control and 23 mutant transgenic lines that contained the enhancer construct. The control *Shh* enhancer was active throughout the lung epithelium, with the majority of lungs showing either strong of medium epithelial b-Gal activity (A). After mutating the ETV4;5 binding sites, the *Shh* enhancer continued to be expressed throughout the lung epithelium, however, none of the transgenic lungs showed strong staining in the epithelium (B). Quantification of the transgenic number lungs that showed staining in the lung epithelium revealed that the control and mutant enhancers had approximately the same number of weak and medium b-Gal stained lungs, however, only the control enhancer had lungs that showed strong b-Gal staining (C).

Supplemental Figure 4: Loss of the ETV4;5 sites decreases Shh-enhancer *in vivo*.

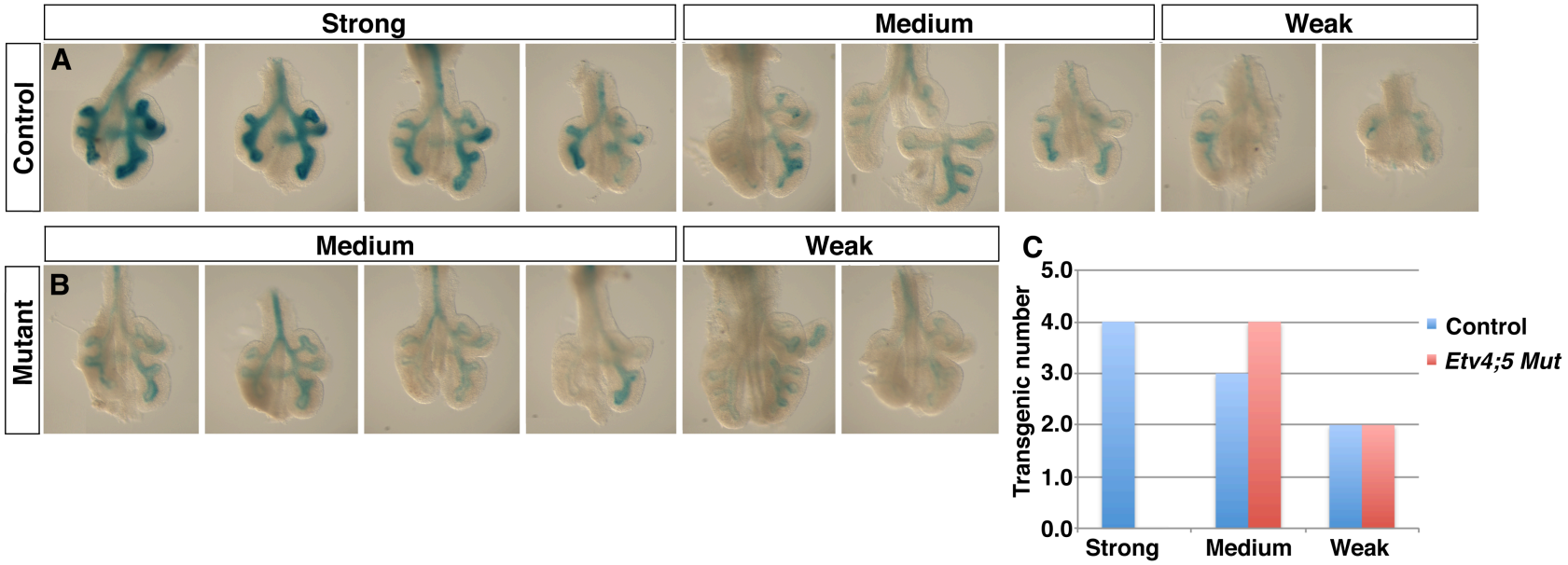

Chapter IV: Examining the role of *Fgfr3* and *Fgfr4* in postnatal lung development

Data for this chapter was generated by John Herriges.

Abstract:

Previous studies have shown that *Fgfr3* and *Fgfr4* (hereafter *Fgfr3;4*) are critical for alveolar development in the postnatal lung development, however the mechanism through which they mediate lung development is unclear. In this study we address how *Fgfr3;4* control lung development by examining both global and conditional *Fgfr3*;4 mutant mice. Interestingly, we found that the loss of *Fgfr3;4* activity disrupts postnatal sacculation, which is prior to what had previously been reported. Furthermore we found that although *Fgfr3;4* are expressed in both the mesenchyme and the epithelium, their activity is only required in the mesenchyme for postnatal lung development. Finally, our data suggests that the primary role of *Fgfr3;4* in the postnatal lung, is to mediate the formation of the extracellular matrix (hereafter ECM), by regulating the deposition of Elastin fibers and by controlling the production of the microfiber associated glycoprotein, MFAP5. Together our data provides a model in which *Fgfr3;4* activity in the mesenchyme is necessary for restricting the formation of the Elastin ECM during early postnatal lung development, which is necessary for proper alveolar development.

Introduction:

In humans, disruption of lung development can lead to a number of postnatal lung diseases, such as bronchopulmonary dysplasia (BPD) and chronic obstructive pulmonary disease (COPD). Although these diseases affect a large portion of the population, and can lead to lifelong respiratory problems, the molecular mechanisms behind their development are poorly understood. Recent studies have suggested that the Fibroblast Growth Factor (FGF) pathway is associated with the development and severity of these diseases; however, how the FGF pathway is be contributing to these diseases is still unknown (Kranenburg et al. 2002; Kranenburg et al. 2005; Rezvani et al. 2013). Additionally, while much is known about the role of the FGF signaling pathway during prenatal lung development, relatively little is known about the role of FGF signaling in postnatal lung development. Therefore, to begin to understand how FGF signaling may be contributing postnatal lung diseases we must first gain a better appreciation for how FGF signaling mediates postnatal lung development.

In mice, lung development begins at embryonic day 9.5 (E9.5) with the outgrowth of the initial epithelial buds (Cardoso and Lu 2006; Morrisey and Hogan 2010). After lung initiation, the epithelial buds elongate and enter the pseudoglandular stage, where from E11.5-E16.5, the epithelium undergoes the stereotypical process known as branching morphogenesis. During this five-day span, hundreds of epithelial airways are generated and the distinctions between what will become the proximal conducting airways and distal alveoli become more apparent. Over the final days of gestation (E16.5-E18.5) the distal lung undergoes a drastic morphological transformation that results in the formation of saccules, or primitive alveoli, which are the functional unit

responsible for oxygen uptake. Each primitive alveoli is lined by alveolar epithelial type I cells and a capillary network which help to facilitate oxygen uptake and transport throughout the body. These primitive alveoli can support oxygen uptake during the first few days of life, however they only account for approximately 5% of the alveolar surface area in an adult mouse (Mund et al. 2008). The final stage of lung development is the alveolar stage, which occurs between postnatal day 4 (P4) and P36. During this stage, the lung undergoes the process known as alveologenesis, in which thousands of secondary septae sprout from the walls of the primitive alveoli into the alveolar lumen. Approximately 55% of the alveolar surface area in an adult mouse is formed during alveologenesis, therefore this process is critical for the formation of a fully functional lung.

One of the primary components that mediates alveolar development is the Elastin extracellular matrix (hereafter ECM). The Elastin ECM is made largely from polymerized Tropoelastin, which is produced by myofibroblasts and then deposited onto an extracellular microfiber network (Bostrom et al. 1996 ; Lindahl et al. 1997;Yeo et al. 2010). The establishment of the Elastin ECM is an incredibly complex process that involves a number of proteins including; the lysyl oxidase enzymes (LOX) and Fibulins (FBLN), which mediate the polymerization of tropoelastin, and the microfiber associated glycoprotein (MFAP) and latent TGF-b binding proteins (LTBP), which mediate the deposition of the polymerized tropoelastin onto the microfiber network (Wagenseil and Mecham 2007; Cirulis et al 2008; Yeo et al 2010). The developmental requirement of the Elastin ECM in the lung appears to primarily be in the postnatal lung, as Elastin knockout mice exhibit severe postnatal, but not prenatal, lung defects (Wendel et al.

2000). Furthermore, the loss of key Elastin ECM assembly proteins, like LOXL1, FBLN5, and FBN1 results in postnatal alveolar simplifications (Yanagisawa et al. 2002;Neptune et al. 2003; Liu et al 2004). In addition to its role in lung development, the Elastin ECM has shown to be disrupted in patients with COPD (Deslee et al 2009; Turino et al. 2011).

Studies have shown that all of the major developmental signaling pathways, including FGF, WNT, SHH and BMP, are necessary for lung development (Kumar et al 2005; Cardoso and Lu 2006; Morrisey and Hogan 2010). Of these, the FGF signaling pathway is one of the most thoroughly characterized; however, the focus of the majority of the developmental studies on FGF signaling in the lung have been on how this pathway mediates embryonic lung development. These studies have demonstrated that numerous FGF ligands; including FGF8, FGF9, FGF10, and FGF18, as well as the FGF receptors, FGFR1 and FGFR2, are necessary for embryonic lung development (Sekine et al 1999; Colvin et al. 2001; Usui et al 2004; del Moral et al. 2006; Abler et al. 2009; Yi et al. 2009; Yu et al. 2010). Recently, studies have begun to examine the role of FGF signaling in the postnatal lung. These studies have demonstrated that the activity of several FGF ligands is necessary for postnatal lung development in rodents, including FGF1, FGF2, and FGF7 (Yi et al. 2006; Padela et al. 2008). Inhibition of either FGF1 or FGF2 activity in the postnatal rat lung leads to a thickening of the alveolar walls and a decrease in the formation of the secondary septae, which is thought to be caused by decrease in cell death (Yi et al 2006). Inhibiting FGF7 activity also causes an alveolar simplification phenotype; however, FGF7 is thought to mediate alveolar development by regulating the formation of the lung vasculature (Padela et al. 2008). Additionally, the

FGFRs, FGFR2-4, have also been shown to be necessary for postnatal lung development (Weinstein et al. 1998; Hokuto et al. 2003; Srisuma et al. 2010). However, unlike in the embryo, where lung development is dependent on FGF signaling through FGFR1 and FGFR2, in the postnatal mouse, lung development is dependent on FGF signaling through FGFR3 and FGFR4 (hereafter FGFR3;4).

Fgfr3;4 are expressed throughout the epithelium and mesenchyme of the developing mammalian lung, with their expression peaking during the saccular and alveolar stages (Weinstein et al. 1998; Mariani et al. 2002; Boucherat et al. 2007). Loss of either *Fgfr3* or *Fgfr4* individually does not disrupt postnatal lung development; however, the combined loss of both *Fgfr3;4* inhibits septal outgrowth during alveologenesis, which causes *Fgfr3;4* mutant lungs to develop a severely simplified alveolar network (Weinstein et al 1998; Srisuma et al 2010). Previous studies have suggested that the primary role of FGFR3;4, is to repress the expression of the extracellular matrix protein Tropoelastin, during the final days of alveologenesis. However, the increase in Tropoelastin production is only seen during the final stages of alveolar development, therefore the question of what causes the initial inhibition of septal outgrowth is still unknown.

In this study we further examine the role of *Fgfr3;4* during postnatal lung development. Our findings expand on the previous studies on *Fgfr3;4* by demonstrating that *Fgfr3;4* are required in the postnatal lung prior to the initiation of alveologenesis. Furthermore our studies demonstrate that although *Fgfr3;4* are expressed in both the alveolar epithelium and the alveolar mesenchyme, their activity is only required in the mesenchyme for normal postnatal lung development. Finally, our data suggests that

the primary role of *Fgfr3;4* is to control the formation of the extracellular matrix, by mediating the deposition of Elastin fibers and by controlling the production of the microfiber associated glycoprotein, MFAP5.

Results:

***Fgfr3;4* mutant mice develop a lung phenotype prior to the initiation of alveologenesis.**

Previous studies have demonstrated that *Fgfr3;4* are necessary for alveolar development in the postnatal lung (Weinstein et al. 1998; Srisuma et al. 2010). However, these studies have focused on the role of *Fgfr3;4* in the final stages of lung development, and have not identified the primary cause of the alveolar simplification. The earliest reported phenotype for *Fgfr3;4* mutant lungs is P8, however, by P8, *Fgfr3;4* mutant lungs have already developed a severe alveolar simplification, which suggests that the phenotype arises at an earlier time point (Srisuma et al. 2010) (Figure 1A,B). When we traced the mutant phenotype back to earlier stages, we found that the *Fgfr3;4* mutant mice had a simplified alveolar structure at P3, however by P2 the mutant lungs were histologically indistinguishable from the lungs of littermate controls (Figure 1C-F). To confirm these results we measured that mean linear intercept (MLI), and found that at P8 and P3, the mutant lungs had a 60% and 20% increase in the relative MLI, respectively (Figure 1E $P<0.005$ and $P<0.05$ $N=4$). However, at P2, the MLI of *Fgfr3;4* mutant lungs was not statistically different from the controls (Figure 1E $P>0.60$ $N=3$). Additionally, we found that the alveolar simplification at P3 is seen prior to any change in overall body weight, demonstrating that the initial alveolar simplification is not a

secondary defect caused by a decrease in the size of the mutant mice (Figure 2). Together these data demonstrate that *Fgfr3;4* are required in the postnatal lung prior to the initiation of alveologenesis, and that the *Fgfr3;4* mutant lung phenotype can first be seen between P2 and P3.

***Fgfr3;4* mutant mice do not have altered proliferation or cell death:**

Recent studies have suggested that alterations in cell proliferation and cell death can contribute to the development of alveolar simplification in the postnatal lung (Yi et al 2006; Srisuma 2010; Dabovic et al. 2012). To address whether proliferation or cell death is contributing to the *Fgfr3;4* mutant phenotype, we examined both of these functions in control and mutant lungs at P2 and P3. Although a previous report had demonstrated that *Fgfr3;4* knockout lungs have decreased proliferation between P8-P21, we did not find a significant change in the proliferation rates at P2 or P3 (Figure 3A-E) (Sirsuma et al 2010). Furthermore, we did not see any difference in the cell death rate at either P2 or P3 (Figure 3F-I). Together these results suggest that the initial alveolar simplification in the *Fgfr3;4* mutant lung is not due to a disruption in cell proliferation or cell death.

***Fgfr3;4* mutant lungs develop a myofibroblast spreading phenotype.**

In the distal lung, alveologenesis is the result of a series of complex interactions between the alveolar epithelium and mesenchyme. To understand the how the alveolar simplification arises in the *Fgfr3;4* mutant lung, we first examined how the alveolar; epithelium, endothelium, and fibroblasts are affected by the loss of FGFR3;4 activity.

The alveolar epithelium is made up of two lineages, the alveolar type I cells which mediate oxygen uptake, and the alveolar type II cells which secrete surfactants that help control surface tension in the lung (Khoor et al. 1994; Bourbon et al 2005; Serrano et al. 2006; Dobbs et al 2010). Several studies have demonstrated that FGF signaling controls alveolar type I and type II cell differentiation at the end of gestation; however, a previous study suggested that the alveolar type II cells are not affected by the loss of FGFR3;4 activity in the adult lung (Weinstein et al. 1998; Liu et al. 2003, Yu et al. 2010). To address whether the alveolar epithelium is affected in the mutant lungs during early postnatal lung development, we performed immunofluorescent staining for the makers PDPN and SFTPC, which label alveolar type I and type II cells, respectively. We found that alveolar type I cells were unaffected in the mutant lungs at both P2 and P8; with type I cells coating the alveolar walls in both the mutant and control lungs (Figure 4A-D). In addition, we found that the loss of FGFR3;4 activity did not affect the alveolar epithelial type II cell population (Figure 4A-D). Together these data demonstrate that the alveolar epithelial lineages are unaffected by the loss of FGFR3;4 activity.

In addition to being necessary for lung function, the endothelial network is essential for alveolar development (DeLisser et al. 2005; Joza et al. 2013). Previous studies have also shown that the FGF signaling pathway regulates endothelial development in the lung, suggesting that the endothelium may be altered in the *Fgfr3;4* mutant (Padela et al. 2008; Yi et al. 2009). To examine whether the endothelium is altered in the mutant lung we performed immunofluorescent staining for the endothelial marker PECAM. In the *Fgfr3;4* mutant lung, we found that the gross structure and

density of the capillary network was unchanged at both P2 and P8 (Figure 4E-H). This data suggests that the *Fgfr3;4* mutant phenotype is not caused by an alteration in the endothelial network.

The myofibroblast lineage is a critical mediator of alveolar development, with the loss of myofibroblasts leading to a severe alveolar simplification (Bostrom et al. 1996 ; Lindahl et al. 1997). A previous group suggested that the loss of FGFR3:4 activity leads to an increase in the number of myofibroblasts in the *Fgfr3;4* mutant lung (Srisuma et al. 2010). To examine whether the myofibroblast lineage was altered during early postnatal lung development, we performed immunofluorescent staining for the myofibroblast marker TAGLN (also known as *SM22*a). We found that TAGLN staining was increased in the *Fgfr3;4* mutant lungs at both P8 and P3 (Figure 5A-D). However, we found that it was unchanged at P2, suggesting that the increase in TAGLN staining is a secondary defect (Figure 5C-F). Furthermore, although we see an increase in TAGLN staining at P3, when we quantified the myofibroblast lineage by mating a $Pdgfra^{GFP/+}$ reporter allele into the *Fgfr3;4* mutant background, we found that there was no difference in the percentage of myofibroblasts in the mutant lung at P3 (Figure 6A-C) (Hamilton et al. 2003). These results demonstrate that the myofibroblasts are not increased in number in the *Fgfr3;4* mutant lung. Instead they suggest that the altered staining may be due to an alteration in fibroblast morphology. Furthermore these results suggest that the initial alveolar simplification in the *Fgfr3;4* mutant lung is not caused by the alterations in myofibroblast morphology, as the phenotype does not precede the alveolar simplification.

***Fgfr3;4* mutant lungs show an alteration in Elastin extracellular matrix formation.**

Previous studies have demonstrated that the morphology of fibroblasts is controlled in part by the ECM (Gobin and West 2003; Rnjak et al 2009; Patel et al. 2012). Like the myofibroblast lineage, the ECM is necessary for alveolar development in the postnatal lung (Wendel et al. 2000; Yanagisawa et al 2002; Neptune et al. 2005). One of the major components of the ECM in the lung, are the Elastin fibers, which are primarily composed of the monomer Tropoelastin (Yeo et al 2011). The initial reports on *Fgfr3;4* in the postnatal lung have established that *Fgfr3;4* regulate Elastin ECM formation during the final stages of alveologenesis (Weinstein et al 1998; Srisuma et al. 2010). However, it is unknown whether *Fgfr3;4* control a similar process during the initial stages of postnatal lung development.

To access whether *Fgfr3;4* mediate Elastin ECM formation in the early postnatal lung we examined the three dimensional structure of the Elastin ECM. In the P8 control lung, we found that the Elastin ECM localized preferentially to the outer portions of the alveolar wall (Figure 7A). However, we found that the Elastin ECM showed little organization in the P8 mutant lungs, with multiple fibers running through each alveolar wall (Figure 7B). In addition, unlike the myofibroblast spreading phenotype, we found that the Elastin ECM was also disorganized at both P3 and P2, prior to when the first histological abnormalities were observed (Figure 7C-F, Figure 1E-F). Interestingly, although we observed more Elastin fibers in the *Fgfr3;4* mutant lung, there was no difference in the production of *Tropoelastin* in the mutant lungs at either P2 or P8 (Figure 8 Together these data demonstrate that *Fgfr3;4* are critical for Elastin ECM

formation; however, unlike what has been reported in the adult lung, *Fgfr3;4* do not appear to be mediating the production of Tropoelastin. Instead, our data suggests that *Fgfr3;4* are necessary for the normal deposition and organization of the Elastin ECM.

Fgfr3;4 **are required in the lung mesenchyme during postnatal lung development**

Fgfr3;4 are expressed in the both the epithelium and the mesenchyme of the postnatal lung, but how their activity in the two tissues is contributing to postnatal lung development is unknown (Weinstein et al. 1998). Given that the Elastin ECM is produced by the mesenchyme of the lung, our data suggests that the mesenchymal activity of *Fgfr3;4* is required for postnatal lung development (Bostrom et al. 1996 ; Lindahl et al. 1997). However, a recent study has suggested that *Fgfr3;4* activity in the epithelium is required for postnatal lung development (Srisuma et al. 2010). To determine the tissue specific roles of *Fgfr3;4* during postnatal lung development we conditionally inactivated *Fgfr3;4* in the epithelium and the mesenchyme. This was achieved by combining the epithelial specific $Nkx2.1^{Cre/+}$, or the mesenchymal specific $Dermo^{Cre/+}$ with a conditional $Fgfr3^{fl}$ allele and the *Fgfr3* and *Fgfr4* knockout alleles, creating $Cre^{+/-};Fgfr3^{fl/-};Fgfr4^{-/-}$ (hereafter *Cre*;*Fgfr3;4* conditional) mice (Sosic et al. 2003; Xu et al. 2008; Su et al. 2010). The activity of both of these Cre-recombinases has been well characterized in the embryonic lung, with the $Nkx2.1^{Cre/+}$ showing strong activity in the lung epithelium as early as E13.5, and the $Dermo^{Cre/+}$ showing robust activity in the lung mesenchyme as early as E11.5 (De Langhe et al. 2008;Tiozzo et al. 2009). Together these data suggest that these Cre-recombinases should allow us to examine the tissue specific roles of *Fgfr3;4* in the postnatal lung.

To asses whether the loss of FGFR3;4 activity in either tissue would affect postnatal lung development, we examined *Fgfr3;4* conditional lungs at P8. We found that *Nkx2.1;Fgfr3;4* conditional lungs were histologically indistinguishable from control lungs at P8, and showed a normal Elastin ECM and myofibroblast morphology (Figure 9A,B,E; Figure 10A,B; Figure 11A,B). Furthermore, *Nkx2.1;Fgfr3;4* conditional mice did not develop any alveolar phenotypes by P28, suggesting that the epithelial activity of FGFR3;4 is not required for alveologenesis (Figure 12A,B). To confirm that the absence of a lung phenotype in the *Nkx2.1;Fgfr3;4* conditional mutant is not caused by an ineffective Cre-recombinase, we tested the activity of the Nkx2.1$^{Cre/+}$ in the postnatal lung. To do this we first mated a Rosa^{EYFP} reporter allele into the *Nkx2.1;Fgfr3;4* conditional background, and found that the Nkx2.1$^{Cre/+}$ is active throughout the airway epithelium and had an almost 100% overlap with alveolar type I and type II cells (data not shown and Figure 12C). Following that, we measured the *Fgfr3^{fl}* excision rate in isolated P2 lung epithelial cells from *Nkx2.1$^{Cre/+}$;Fgfr3$^{fl/+}$* lungs, and found that the excision rate of the *Fgfr3*^{fl} transcript was approximately 50%, which when combined with the *Fgfr3* knockout allele would lead to a complete loss of FGFR3 activity in the lung epithelium (Figure 12D). Together these data demonstrate that the epithelial activity of FGFR3;4 is not required for alveolar development in the postnatal lung.

The Elastin ECM defect that we observed in the *Fgfr3;4* knockout lungs suggested that the mesenchymal activity of FGFR3;4 is required for postnatal lung development. When we conditionally inactivated FGFR3;4 in the mesenchyme using the *Dermo$^{Cre/+}$*, we found that the *Dermo;Fgfr3;4* conditional lungs develop a simplified alveolar structure by P8 that greatly resembles the P8 *Fgfr3;4* mutant phenotype (Figure

9D,E; Figure 1A,B). To confirm these results, we quantified the MLI, and found that the *Dermo;Fgfr3;4* conditional lungs had an approximately 50% increase in the relative MLI at P8 (N=4 P<.05)(Figure 9F). Additionally, we found that the Elastin ECM was disorganized and that the myofibroblasts were more spread out in the *Dermo;Fgfr3;4* conditional lungs (Figure 10C,D, Figure 11C,D). Together these data demonstrate that although *Fgfr3;4* are expressed in both the epithelium and the mesenchyme of lung, only the mesenchymal activity of FGFR3;4 is required for the initial stages of postnatal lung development.

Elastin fiber formation in the *Fgfr3;4* mutant lung.

The formation of the Elastin ECM matrix is an incredibly complex process that involves a number of different structural proteins and enzymes (Vrhovski and Weiss 1998; Wagenseil and Mecham 2007; Yeo et al. 2011). To understand what could be causing the disorganized Elastin ECM we used qRT-PCR to examine the expression of the major components that control Elastin ECM formation. We found that two genes showed altered expression in the *Fgfr3;4* mutant lung, *Fbn2 and Mfap5* (Figure 13A,B).

Fbn2 encodes one of two proteins (FBN1 and FBN2) that form the microfiber network, on which the Elastin ECM is deposited (Yeo et al. 2011). Previous work has demonstrated that microfiber proteins are critical for postnatal lung development, with mutations in FBN proteins causing alveolar simplification in mice and Marfans syndrome in humans (Neptune et al 2003; Carta et al. 2006; Cañadas et al. 2010). To examine whether FBN proteins were altered in *Fgfr3;4* mutant lung, we performed immunohistochemical staining for both FBN1 and FBN2 in P2 lungs. We found that

although the Elastin ECM is disorganized at this stage, there was no appreciable difference in either the level or organization of FBN1 or FBN2 in the mutant lung (Figure 14A-F). Interestingly, although neither of the microfiber proteins were affected in the *Fgfr3;4* mutant lung, we found that the localization of the FBN1 and FBN2 fibers was more scattered than the Elastin fibers of the control lung (Figure 14A'-F'). This observation that the microfiber network runs throughout the alveolar wall in both the control and mutant lung suggests that the loss of FGFR3;4 activity could affect Elastin ECM formation by altering the deposition of Elastin onto the microfiber network.

One protein that mediates the deposition of the Elastin ECM onto the microfiber network is the microfiber-associated glycoprotein, MFAP5 (Lemaire et al. 2007). In the *Fgfr3;4* knockout lung we see an increase in *Mfap5* expression on the protein level at P2 and P8 (Figure 13B). Previous groups have demonstrated that the overexpression of *Mfap5* causes an increase in Elastin fiber formation in cell culture (Lemaire et al. 2007). To test whether the increase in *Mfap5* expression could be causing the alveolar simplification in the *Fgfr3;4* mutant lung, we introduced a *Mfap5* knockout allele into the *Fgfr3;4* mutant background, creating the *Mfap5*$^{-/-}$*;Fgfr3;4* triple mutant mouse (hereafter *Mfap5;Fgfr3;4*) (Combs et al. 2013). We found that the alveolar simplification of the *Fgfr3*;4 mutant lung was attenuated in the *Mfap5;Fgfr3;4* lung, with the *Mfap5;Fgfr3;4* mutant lungs having more complex alveolar network that consisted of smaller alveoli (Figure 15A,B). The attenuation of the alveolar simplification was confirmed by measuring the MLI, which showed that the *Mfap5;Fgfr3;4* lungs had an approximately 20% decrease in the MLI, when compared to *Fgfr3;4* mutants (Figure 15C). Interestingly, although introducing *Mfap5*$^{-/-}$ was able to attenuate the alveolar

simplification in the *Fgfr3;4* mutant, we continued to see a disorganized Elastin ECM in the *Mfap5;Fgfr3;4* knockout lung (Figure 15D,E). Together these results demonstrate that the increase in *Mfap5* expression is contributing to the *Fgfr3;4* mutant phenotype. However, based on the rescue phenotype, our data also suggests that MFAP5 is not the only factor contributing to the alveolar simplification in the *Fgfr3;4* mutant.

Discussion:

In this study we further examined the role of *Fgfr3;4* in postnatal lung development. We demonstrated that the *Fgfr3;4* mutant phenotype can first be seen prior to the initiation of alveologenesis, and that this phenotype is preceded by the disorganization of the alveolar Elastin ECM. Furthermore, we demonstrated that FGFR3;4 activity is required in the mesenchyme, and not the epithelium, during postnatal lung development. Finally, we demonstrated that the *Fgfr3;4* knockout phenotype is caused in part by an increase in the expression of the ECM protein MFAP5.

Although previous studies have examined the role of *Fgfr3;4* in the postnatal lung, this is the first study to demonstrate that *Fgfr3;4* are required during the saccular stage of lung development (Weinstein et al 1998; Srisuma et al 2010). Data from the *Fgfr3;4* mutant lungs demonstrate that the loss of FGFR3;4 activity causes a disruption in lung development beginning at P3. We found this interesting as P3 is prior to the initiation of septal outgrowth/alveologenesis, which begins at P4, but well after the initiation of saccular development, at E17.5. Previous groups have shown that *Fgf8*,

Fgf18, and *Fgfr2* are necessary for normal sacculation; however, all of these have prenatal requirements for normal lung development, while *Fgfr3;4* are only required for postnatal sacculation (Hokuto et al 2003; Usuia et al 2004; Yu et al 2010). One plausible explanation for the *Fgfr3;4 mutant* only having a postnatal lung phenotype is that although *Fgfr3;4* are both expressed in the prenatal lung, their expression peaks right before birth and during alveologenesis (Mariani et al 2002). Thus the loss of FGFR3;4 activity may not have developmental consequences in the embryonic lung, but severe consequences when FGFR3;4 activity does not ramp up at the beginning of sacculation.

Pervious studies have demonstrated that FGF signaling mediates the differentiation of the alveolar epithelium and mesenchyme, as well as the formation of the vasculature in the embryonic and postnatal lung (Hokuto et al 2003; Liu et al. 2003; Yi et al. 2009; Yu et al 2010;). Because the alveolar structure of the lung was so drastically affected, we anticipated that several alveolar lineages would be affected by the loss of FGFR3;4 activity. Interestingly, we did not observe many noticeable differences in the alveolar lineages, with the one difference being that we detected a spreading of the alveolar myofibroblasts (Figure 2). However, this phenotype was only recognizable after the mutant lungs developed an alveolar simplification. Therefore, although the spreading of the myofibroblasts may be contributing to alveolar simplification, it is not the primary defect.

Previous groups have demonstrated that the Elastin ECM can mediate fibroblast spreading, which suggested that there may be an alteration in the Elastin ECM in the *Fgfr3;4* mutant lung (Gobin and West 2003; Rnjak et al 2009; Patel et al. 2012). In

agreement with this, the initial *Fgfr3;4* mutant studies have suggested that one of the primary roles of *Fgfr3;4* during lung development is to mediate the formation of the Elastin ECM (Weinstein et al 1998; Srisuma et al. 2010). Our data agrees with the findings from previous groups, in that we found that *Fgfr3;4* are necessary for Elastin ECM formation in the early postnatal lung (Figure 3). Furthermore, we found that the disruption of the Elastin ECM is the first phenotypic abnormality associated with the *Fgfr3;4* knockout lung, suggesting that it may be the primary defect. However, unlike the previous studies, which have suggested that *Fgfr3;4* mediate Elastin ECM formation by regulating the production of Tropoelastin, we found no difference in Tropoelastin expression in the early knockout lung. Instead, our data suggests that FGFR3;4 mediate Elastin ECM formation by controlling the deposition of Elastin onto the microfiber network. Although our results suggest a different role for *Fgfr3;4* in Elastin ECM formation, they do not contradict the results from previous studies, as their studies have focused on the role of *Fgfr3;4* at the end alveologenesis, while we were looking at the initial stages of alveolar development.

Fgfr3;4 are expressed in both the epithelium and the mesenchyme of the postnatal lung, so the mutant lung phenotype could be derived from the loss of FGFR3;4 activity in either tissue. In the lung, the fibroblast lineage is necessary for Elastin ECM formation, and the expression of *Fgfr3;4* peaks in rodent lung fibroblasts during the initial stages of alveolar development (Bostrom et al. 1996; Lindahl et al. 1997; Boucherat et al. 2007). These finding suggested that the mesenchymal activity of FGFR3;4 is required for normal lung development. However it has been hypothesized that the loss of FGFR3;4 activity in the alveolar epithelium is contributing to the alveolar

simplification, by indirectly mediating the expression of Tropoelastin in the mesenchyme (Srisuma et al 2010). Interestingly, when we knocked *Fgfr3;4* using the Nkx2.1$^{cre/+}$ and the Dermo$^{Cre/+}$, we found the *Dermo;Fgfr3;4* conditional lung almost completely recapitulated the alveolar simplification seen in the straight *Fgfr3;4* mutant lung (Figure 1E-F;Figure 9A-F). Additionally, we found that the *Nkx2.1;Fgfr3;4* conditional lungs were indistinguishable from littermate controls. This suggests a model in which the loss of FGFR3;4 activity in the mesenchyme is the primary contributor to the alveolar simplification in the *Fgfr3;4* mutant lung. Furthermore because we continue to see a disruption in the Elastin ECM in the *Dermo;Fgfr3;4* conditional lung, our data suggests that the root of the Elastin ECM defect lies within the mesenchymal tissue of the *Fgfr3;4* mutant lung.

Our studies suggest that the primary defect in the *Fgfr3;4* knockout lung is a disruption in the formation of the Elastin ECM. Therefore we examined the expression of genes involved in Elastin ECM formation and identified that the microfiber associated glycoprotein, MFAP5 was increased in the *Fgfr3;4* knockout lung. The MFAP group consists of five members MFAP1-5, but *Mfap5* was the only that showed altered expression in the *Fgfr3;4* mutant lung (Figure 13). Interestingly, knocking out *Mfap5* was able to attenuate the alveolar simplification seen in *the Fgfr3;4* mutant lung. However, we found that the Elastin ECM was not significantly rescued in the *Mfap5;Fgfr3;4* mutant lung. This suggests that the increase in *Mfap5* is not the primary factor that leads to aberrant Elastin ECM formation in the mutant lung.

Combined our data suggests that the primary role of *Fgfr3;4* is to mediate the establishment of the Elastin ECM in the lung. In a control lung, the Elastin ECM lines

the alveolar walls (Figure 16A). The normal deposition of the Elastin ECM results in the lung myofibroblasts having a normal morphology, which permits the outgrowth of the septal crests and leads to a normal alveolar structure. Our data suggests that the mesenchymal activity of *Fgfr3;4* is necessary for the normal deposition of the Elastin ECM. Therefore, when the mesenchymal activity of *Fgfr3;4* is lost in the *Fgfr3;4* mutant lung, the deposition of the Elastin ECM is disrupted, so that multiple fibers run through the walls of the primitive alveoli (Figure 16B). The disorganized Elastin ECM causes the myofibroblasts to develop an abnormal morphology, which inhibits septal outgrowth, and leads to the alveolar simplification. Future studies will focus on identifying the mechanisms through *Fgfr3;4* are able to mediate Elastin ECM formation.

Materials and Methods:

Mice:

Pups were dissected postnatally, with the date of birth being marked as postnatal day zero (P0). Fgfr3-/-, Fgfr3fl/fl, Fgfr4-/-, Pdgfra-GFP/+, Magp2 -/- , and Dermo-Cre/+, have been previously described (Sosic et al. 2003). Nkx2.1-cre/+ was purchased from the Jackson Laboratories (Xu et al. 2008). The primers used for genotyping can be found in the original publications.

Histology:

For histological analysis, lungs were inflation fixed with 4%PFA overnight, equilibrated into 30% Sucrose overnight, and then embedded in OCT and sectioned at 5um. Lung sections were then allowed to sit at room temperature for 2 hours and were stained

using a standard H&E protocol. Quantification of lung simplification was performed using the mean linear intercept (MLI) method, as previously described (Chen et al. 2012). Three randomly selected sections from at least three lungs were used to calculate the MLI for mutant and control samples at every stage. Statistical analysis was done using the students T-test.

Immunofluorescent:

For immunofluorescent staining, lungs were inflation fixed overnight in 4% PFA. After fixation, the right lung was cut into 75um thick sections using a vibratome and stained using a standard immunofluorescent protocol (Yi et al. 2009). From each vibratome section a 50um z-stack was taken and then processed into a two-dimensional image using Image-J (CITE). The primary antibodies used were: SFTPC (seven hills), TAGLN (millipore), Elastin (Robert Mecham), Fbn1 (Lynn Sakai), and Fbn2 (Lynn Sakai).

Quantitative RT-PCR

Total RNA was collected from the right lung of at least three control and three mutant mice using a Qiagen RNeasy mini-Plus kit. RNA was reverse transcribed into cDNA using Invitrogen's superscript III-First strand kit. cDNA was then amplified and quantified using a the SYBRgreen kit from applied biosciences. In addition to the three biological replicates, two technical replicates were performed, and statistical analysis of the results was done using the students T-Test.

Western

Total Protein was collected from the right lung of at least three control and three mutant mice. Protein samples were homogenized using the Qiagen TissueLyser II and were then run out on a 8-15% SDS page gel and transferred to a PVDF membrane. The PVDF membrane was blocked in 5% dried Milk powder in TBST for at least 1 hour, incubated in the primary antibody overnight at four degrees, and then incubated with the secondary antibody for one hour at room temperature. Visualization of the western was done using the LI-COR system. The primary antibodies that were used were Mfap5 (1:1000), tropoelastin (1:500), B-actin (1:10000). Protein levels were all normalized to B-actin. Two technical replicates and three biological replicates were performed for each antibody.

Figures:

Figure 1:*Fgfr3;4* mutant lungs develop a simplified alveolar structure during early postnatal lung development.

(A-F) Representative H&E stained frozen sections from the alveolar regions of control (A,C,E) and mutant (B,D,F) lung at P2, P3 and P8. At P8 the distal lung of *Fgfr3;4* mutant lungs is more simplified than that of the control lung, with the *Fgfr3;4* mutant lung developing fewer alveoli that are larger in size (A-B). The simplified alveolar structure of the *Fgfr3;4* mutant lung is still noticeable at P3 (C-D), however by P2 the mutant and control lungs are histologically indistinguishable (E-F). The alveolar simplification at P2, P3, and P8 was quantified by measuring the MLI at P2, P3 , P8 (G). *Fgfr3;4* mutant lungs showed a statistically significant increase in the relative MLI at both P8 ($P<.005$ N=4) and P3 ($P<.05$ N=4), but the relative MLI was unchanged at P2 ($P>.6$ N=3). Data are presented as means (+SEM).

Figure 1:*Fgfr3;4* mutant lungs develop a simplified alveolar structure during early postnatal lung development.

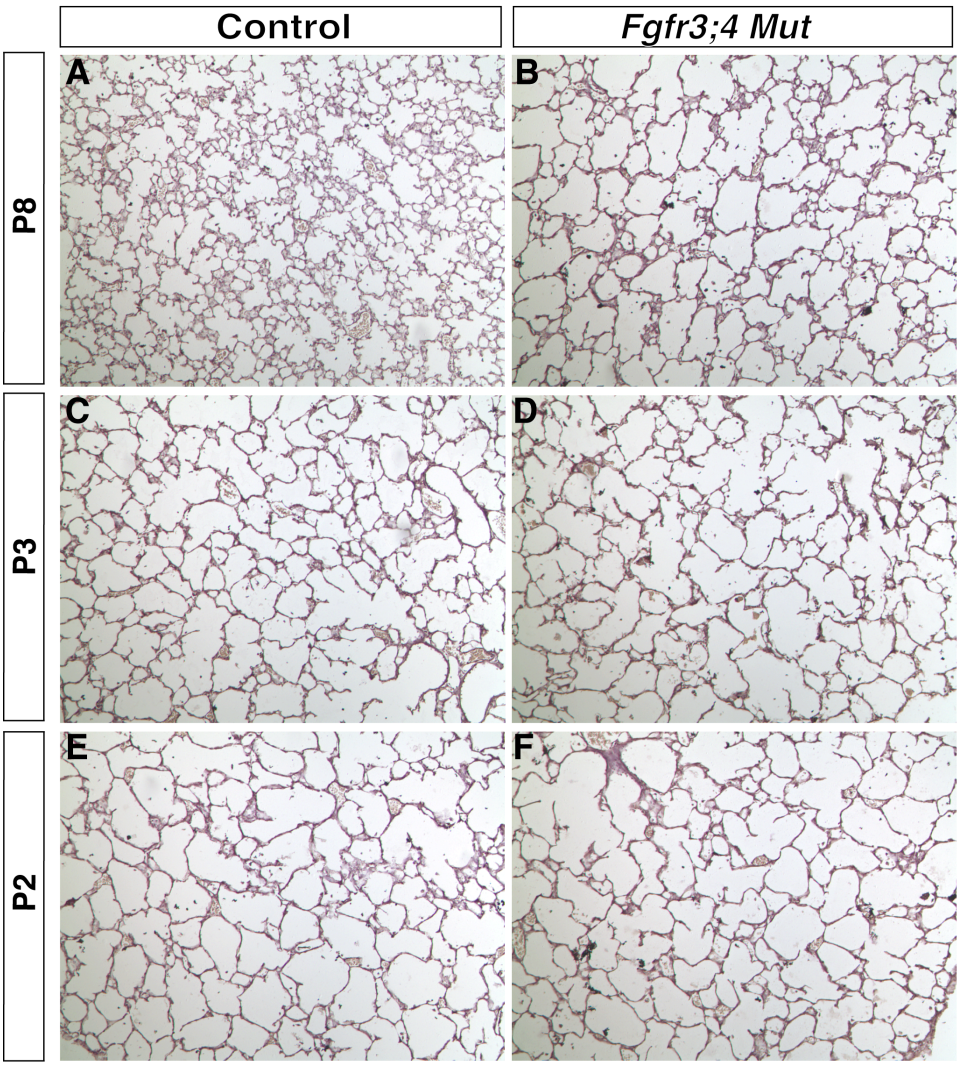

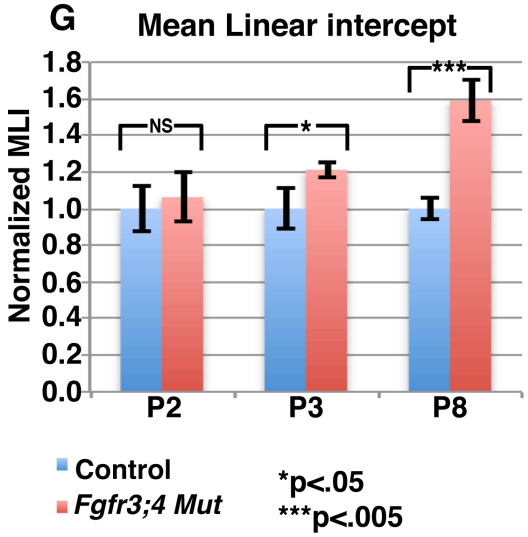

Figure 2: The change in *Fgfr3;4* mutant mouse size is not preceded by an alteration in total mouse weight.

Control and mutant live mice were weighed at P3. There was no apparent difference between the mutant and control mouse size at this stage. Data are presented as means (+SEM).

Figure 2: The change in *Fgfr3;4* mutant mouse size is not preceded by an alteration in total mouse weight.

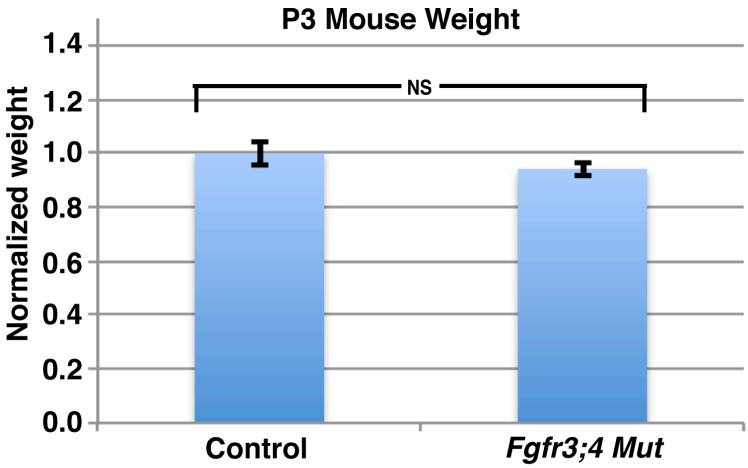

Figure 3: Cell proliferation and Cell death are not altered in *Fgfr3;4* mutant mice between P2 and P3.

(A-D) Representative immunofluorescent staining for the proliferation marker pHIS (red) and nuclei (blue) at P2 and P3. At both P2 and P3, cellular proliferation is unaltered in the mutant lung (A-D). Quantification of the proliferation rate revealed that it was unchanged in the mutant at P2 and P3 (E). Data are presented as means (+SEM). (F-I) Representative immunofluorescent staining for the cell death marker cleaved Casp3 (red) and nuclei (blue) at P2 and P3. At both P2 and P3, there was no noticeable difference in the cell death rate of the control and mutant lung (F-I).

Figure 3: Cell proliferation and Cell death are not altered in *Fgfr3;4* mutant mice between P2 and P3.

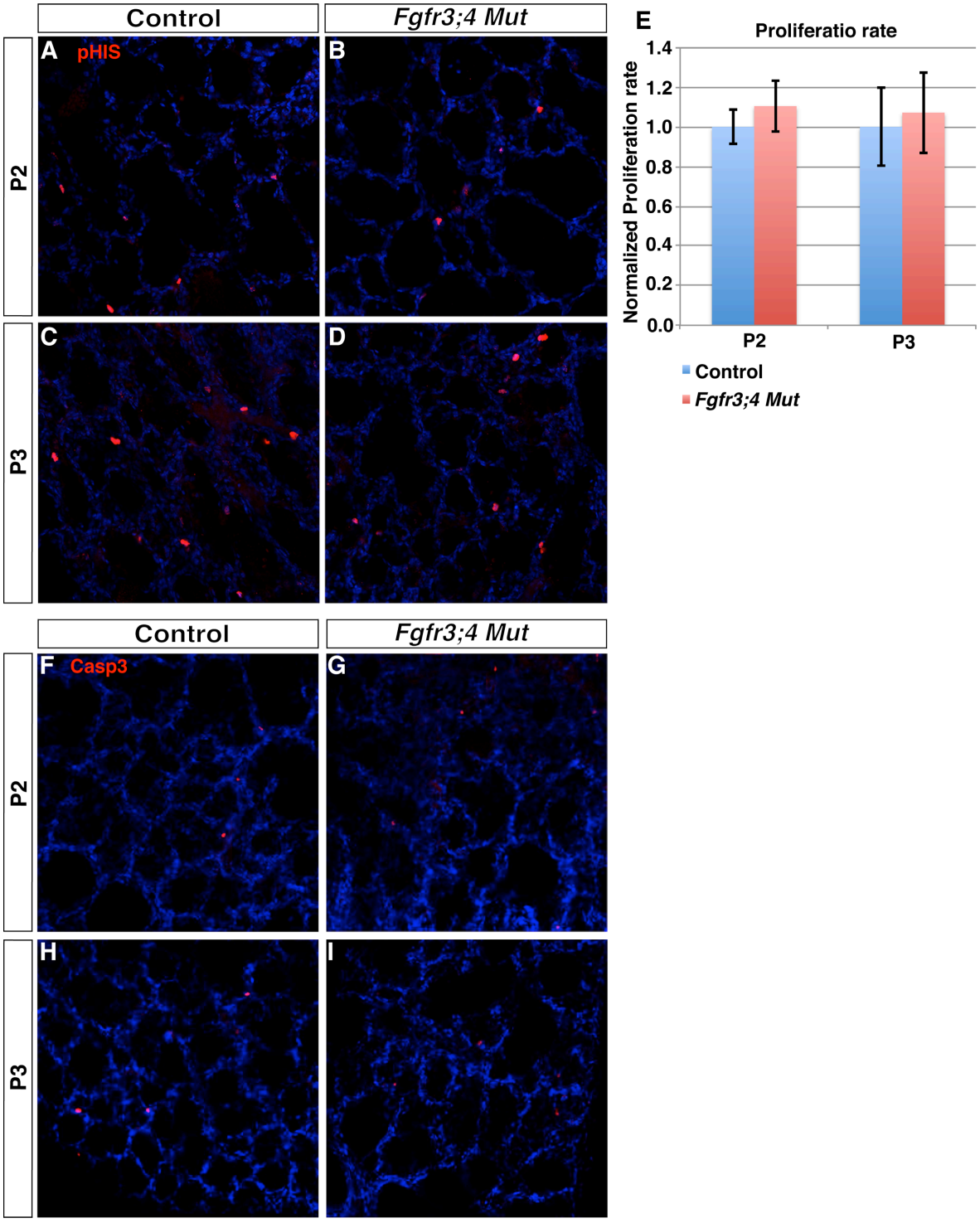

Figure 4: The epithelial and endothelial lineages are unaltered in the *Fgfr3;4* mutant lungs.

(A-D) Representative immunofluorescent staining for alveolar type I cells (PDPN (red)) and alveolar type II cells (SFTPC (green)) in the alveolar region of P2 and P8 lungs. When comparing the control and mutant lungs a P2 and P8, we did not notice any difference in the localization of type I cells or type II cells. (E-H) Representative immunofluorescent staining for the capillary network (PECAM) in the alveolar region of the lung. There is no difference between the localization of the capillary network in the control and mutant lungs at P2 (E,F) There are fewer total capillaries in the Fgfr3;4 mutant lung at P8; however, the complexity of the capillary bed in an individual alveolar wall appears unchanged (G,H).

Figure 4: The epithelial and endothelial lineages are unaltered in the *Fgfr3;4* mutant lungs.

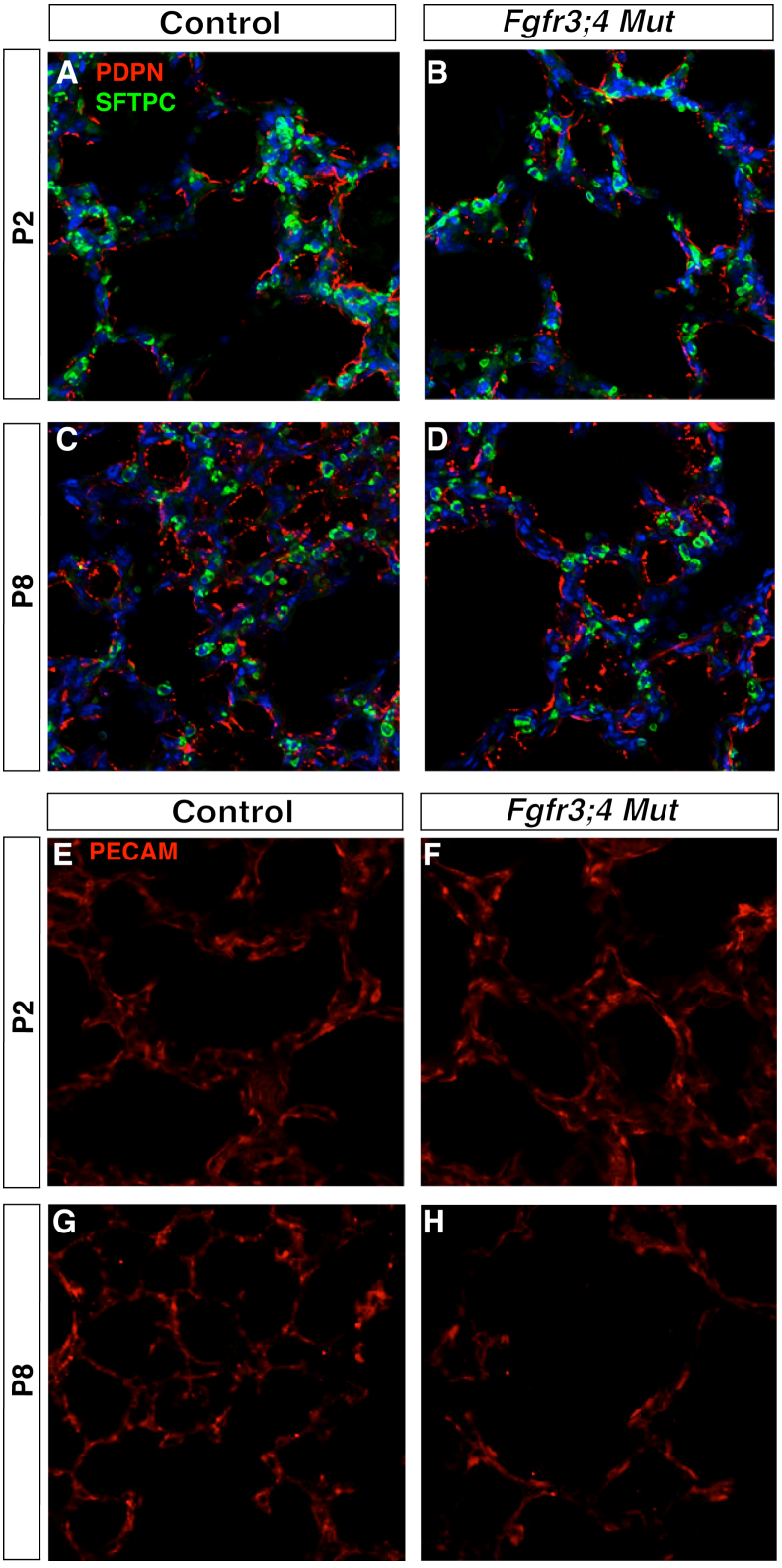

Figure 5: Myofibroblasts are more spread out in the *Fgfr3;4* mutant lung.

(A-F) Reconstructed 50um Z-stacks of immunofluorescent staining for TAGLN (red) in the alveolar region of control and mutant lungs. At P8, *Fgfr3;4* mutant lungs display an increased TAGLN staining, and an altered myofibroblast morphology (A-B). At P3, the mutant lungs continue to develop an altered TAGLN staining (C-D). In the mutant lungs at both P8 and P3 the TAGLN staining is much more spread out in the alveolar regions of the lung (A-D). By P2 the alveolar the staining for myofibroblasts is indistinguishable from that of control lungs (E-F).

Figure 5: Myofibroblasts are more spread out in the *Fgfr3;4* mutant lung.

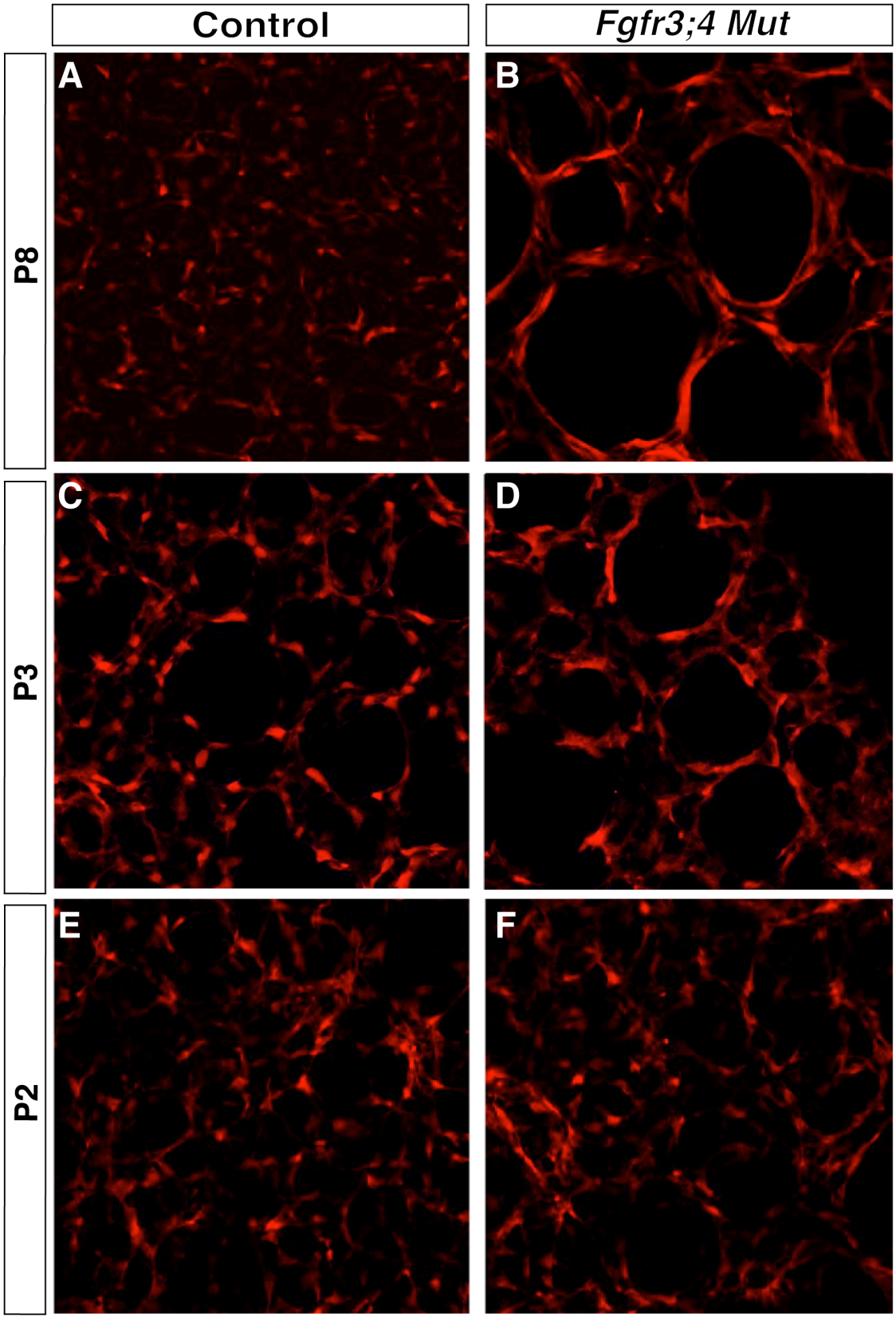

Figure 6: *Fgfr3;4* mutant lungs do not have more myofibroblasts.

(A,B) Representative images of the alveolar region of Pdgfra-GFP positive cells (green) in the control (A) and mutant (B) lung at P3. At P3 there appear to be fewer total Pdgfra-GFP positive cells in the mutant lung (A,B). However, quantification of the percentage of GFP positive cells revealed that the percentage of myofibroblasts is unchanged in the mutant lung (N=3) (C). Data are presented as means (+SEM).

Figure 6: *Fgfr3;4* mutant lungs do not have more myofibroblasts.

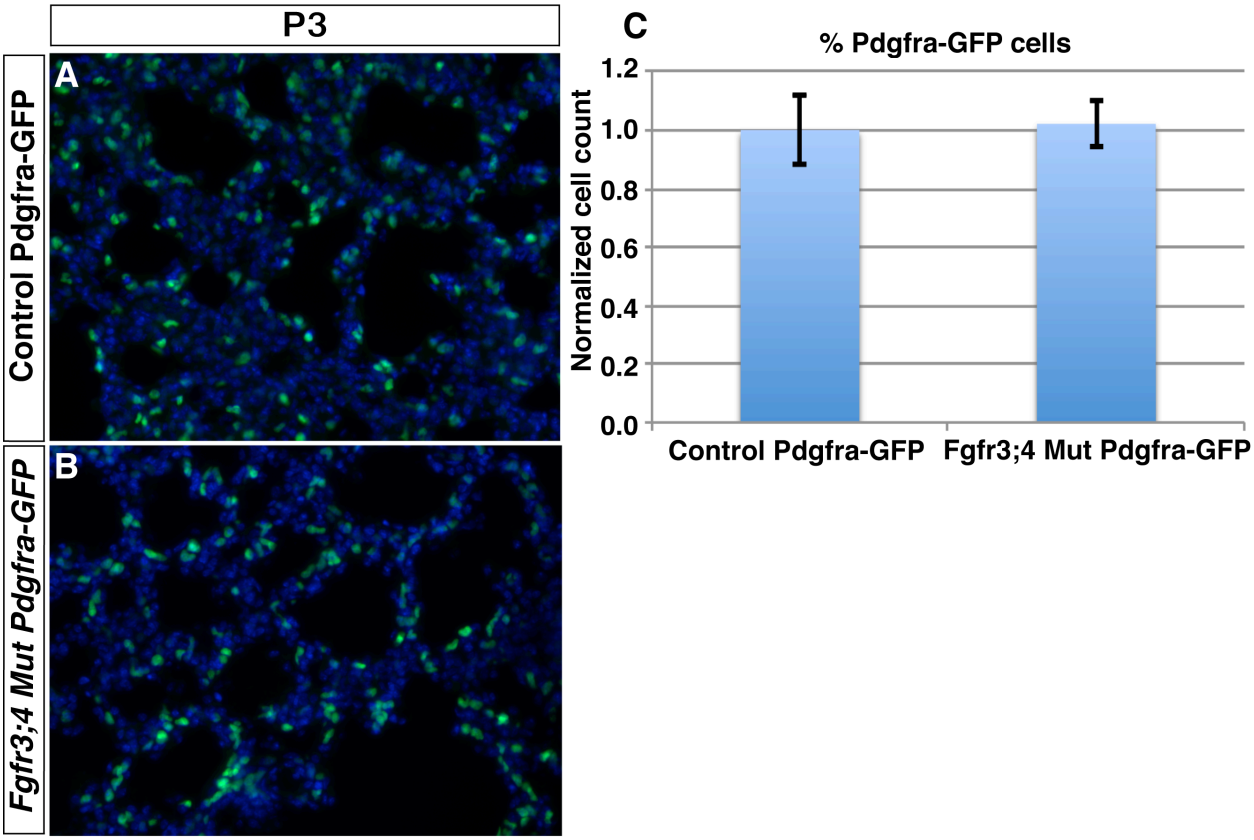

Figure 7: The Elastin ECM is disorganized in the *Fgfr3;4* mutant lung.

(A-F) Reconstructed 50um Z-stacks of immunofluorescent staining for Elastin (red) in the alveolar region of control and mutant lungs. At P8, the Elastin ECM normally lines the alveolar wall (A). In the *Fgfr3;4* mutant lung the Elastin ECM is disorganized, with multiple Elastin fibers running through the alveolar walls (B). At P3 we continue to see a disorganized Elastin ECM in the alveolar region of the mutant lung (C,D). Unlike the TAGLN staining, we continue to see a disorganized Elastin ECM in the alveolar region of the mutant lung at P3.

Figure 7: The Elastin ECM is disorganized in the *Fgfr3;4* mutant lung.

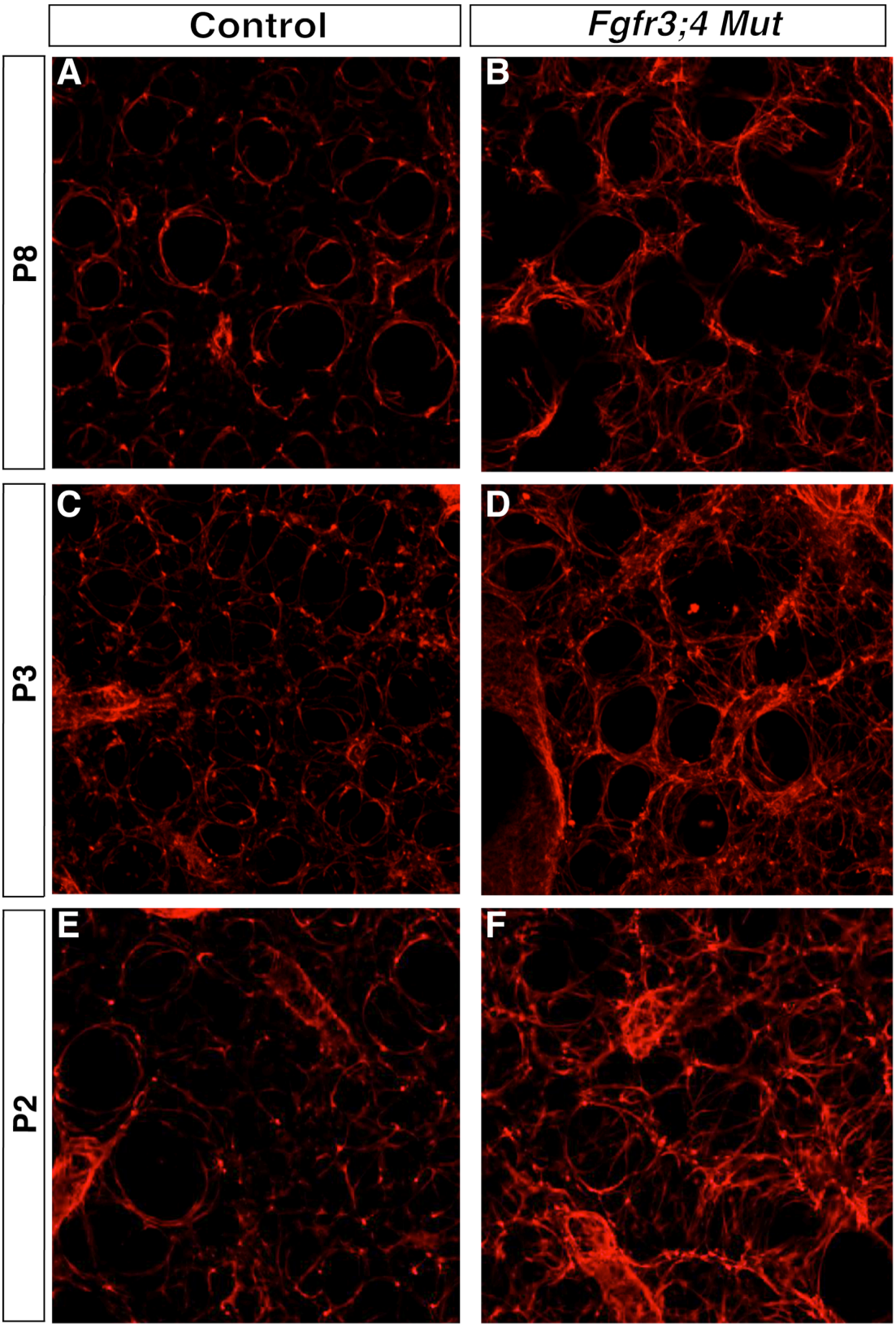

Figure 8: *Fgfr3;4* Mutant mice do not produce more tropoelastin at either P2 or P8 Representative western blots for tropoelastin (green) and B-actin (red) at P2 and P8. At both P2 and we found no difference in the production of the Tropoelastin monomer.

Figure 8: *Fgfr3;4* Mutant mice do not produce more tropoelastin at either P2 or P8

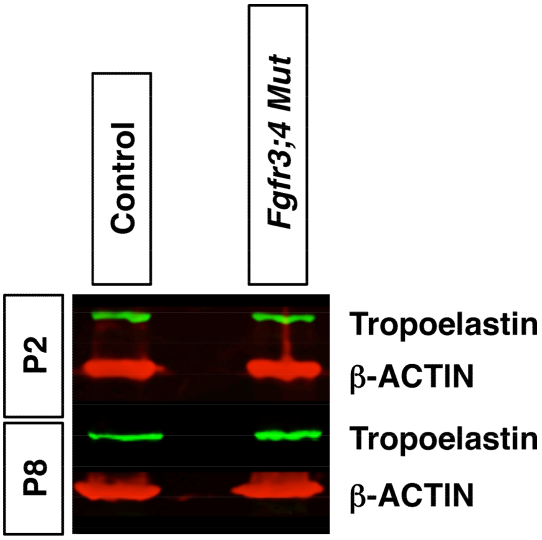

Figure 9: FGFR3;4 activity is required in the mesenchyme and not the epithelium during postnatal lung development.

(A-B, D-E) Representative H&E stained frozen sections from the alveolar regions of P8 Cre-control (A,D) and *Cre*$^{+/-}$*;Fgfr3;4* conditional mutant lungs (B,E). At P8 *Nkx2.1;Fgfr3;4* conditional mice have not developed any histological abnormalities (A-B). The alveolar density was quantified in the *Nkx2.1;Fgfr3;4* conditional lungs by measuring the MLI. At P8 the MLI of *Nkx2.1;Fgfr3;4* conditional lungs was not statistically different from the Cre control lung (C) (P>.95 N=3). At P8 *Dermo;Fgfr3;4* conditional have developed a simplified alveolar structure that is reminiscent of the *Fgfr3;4* mutant phenotype (D-E). The alveolar density was quantified in the *Dermo;Fgfr3;4* conditional lungs by measuring the MLI. At P8 the MLI of *Dermo;Fgfr3;4* conditional lungs was significantly increased, when compared to Cre control lungs (F) (P>.95 N=4). Data are presented as means (+SEM).

Figure 9: FGFR3;4 activity is required in the mesenchyme and not the epithelium during postnatal lung development.

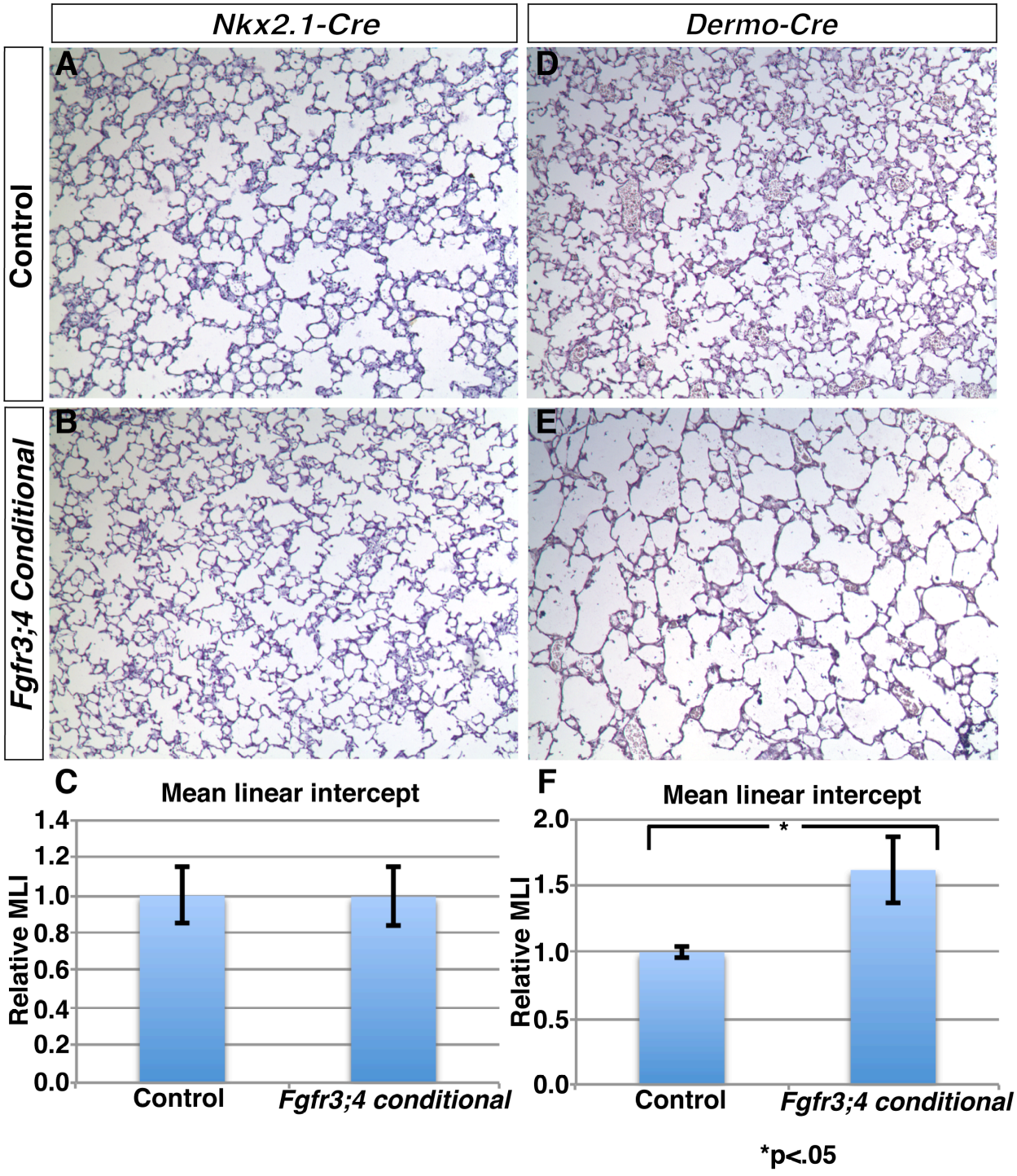

Figure 10: Loss of FGFR3;4 activity in the mesenchyme leads to a disorganized Elastin ECM.

(A-D) Reconstructed 50um Z-stacks of immunofluorescent staining for Elastin (red) in the alveolar region of P8 Cre-control and *Cre*$^{+/-}$*;Fgfr3;4* conditional mutant lungs. At P8 the Elastin ECM shows normal organization in the *Nkx2.1;Fgfr3;4* conditional lung, as the Elastin fibers are primarily found around the outer portion of the alveolar wall (A-B). By P8, *Dermo;Fgfr3;4* conditional lungs develop a disorganized Elastin ECM with multiple Elastin fibers running through the alveolar walls (C-D). This phenotype is reminiscent of disorganized Elastin ECM phenotype seen in *Fgfr3;4* mutant lungs.

Figure 10: Loss of FGFR3;4 activity in the mesenchyme leads to a disorganized Elastin ECM.

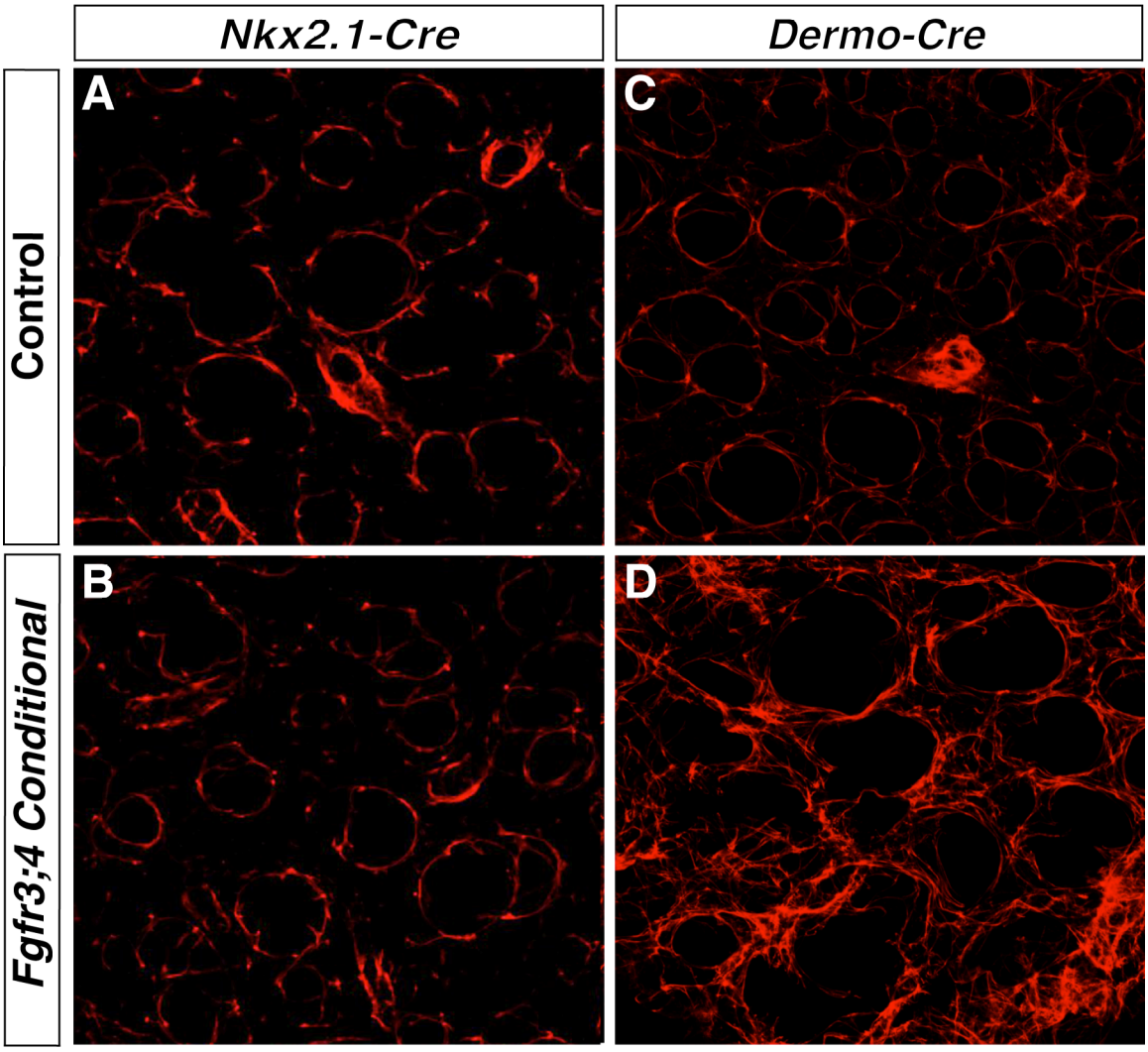

Figure 11: Loss of FGFR3;4 activity in the mesenchyme alters the myofibroblast morphology.

(A-D) Reconstructed 50um Z-stacks of immunofluorescent staining for TAGLN (red) in the alveolar region of P8 Cre-control and *Cre*$^{+/-}$*;Fgfr3;4* conditional mutant lungs. At P8, TAGLN staining is unaltered in the *Nkx2.1;Fgfr3;4* conditional lung (A-B). Myofibroblasts in P8 *Dermo;Fgfr3;4* conditional lungs develop a more spread out morphology than Cre-control lung myofibroblasts (C-D). This phenotype is reminiscent of myofibroblast spreading phenotype seen in *Fgfr3;4* mutant lungs.

Figure 11: Loss of FGFR3;4 activity in the mesenchyme alters the myofibroblast morphology.

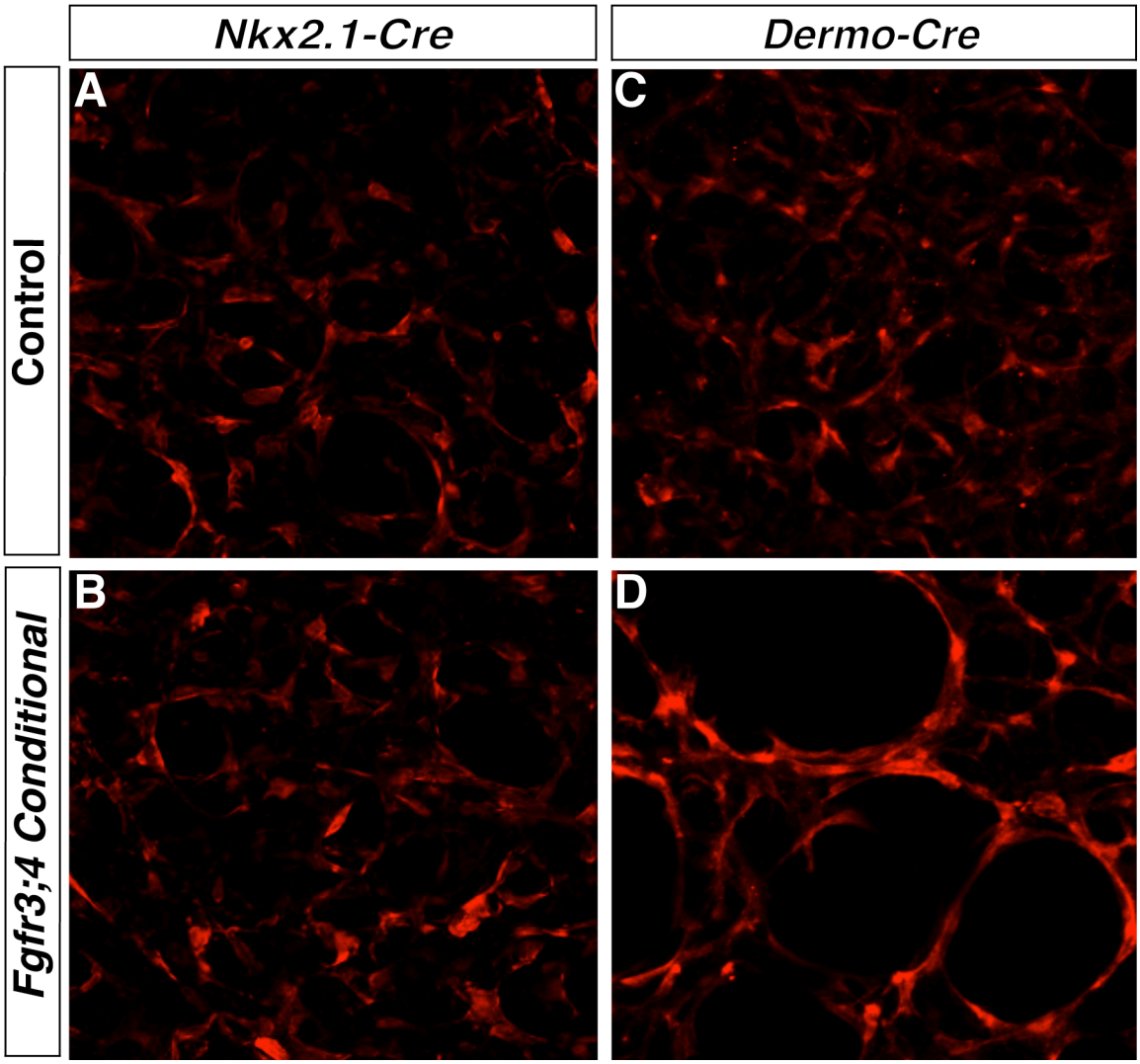

Figure 12: Although the Nkx2.1$^{Cre/+}$ is highly active in the lung epithelium, *Nkx2.1;Fgfr3;4* conditional mice do not develop an alveolar phenotype.
(A-B) Representative H&E stained frozen sections from the alveolar regions of P28 Nkx2.1$^{Cre/+}$ control (A) and *Nkx2.1;Fgfr3;4* conditional lungs (B). At P28 *Nkx2.1;Fgfr3;4* conditional mice do not display any histological abnormalities (A-B). The normal appearance of the *Nkx2.1;Fgfr3;4* conditional lung does not appear to be due to a lack of Nkx2.1$^{Cre/+}$ activity, as it is highly active in the alveolar region of the lung (green), where it colocalizes with SFTPC (red; type II cells) (D). Furthermore the Nkx2.1 cre is able to efficiently excise the floxed region from the Fgfr3^{fl} transcript (N=3). Data are presented as means (+SEM).

Figure 12: Although the Nkx2.1$^{Cre/+}$ is highly active in the lung epithelium,

Nkx2.1;Fgfr3;4 conditional mice do not develop an alveolar phenotype.

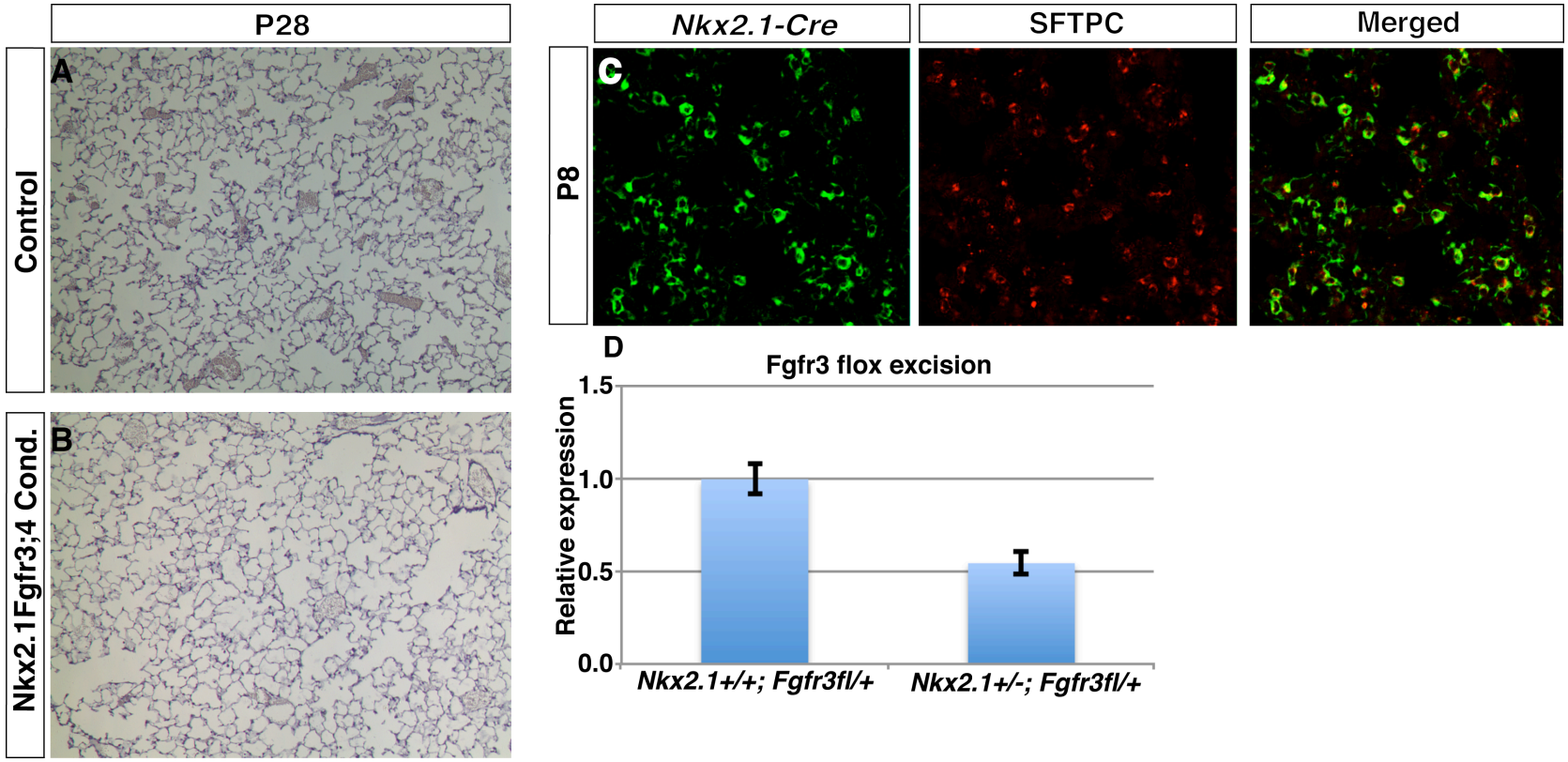

Figure 13: *Fgfr3;4* mutant lungs display an increase in *Mfap5* and *Fbn2* expression.

(A) To identify potential genes that could be causing the disorganized Elastin ECM we performed qRT-PCR for genes involved in Elastin ECM formation. This screen revealed that *Fbn2* and *Mfap5* expression was increased in the *Fgfr3;4* mutant lung at P2 ($P<0.05$ $N=3$). (B) Western analysis of MFAP5 revealed that *Fgfr3;4* mutant also show an increase in MFAP5 protein levels at both P2 and P8. B-actin was used as a loading control.

Figure 13: *Fgfr3;4* mutant lungs display an increase in *Mfap5* and *Fbn2* expression.

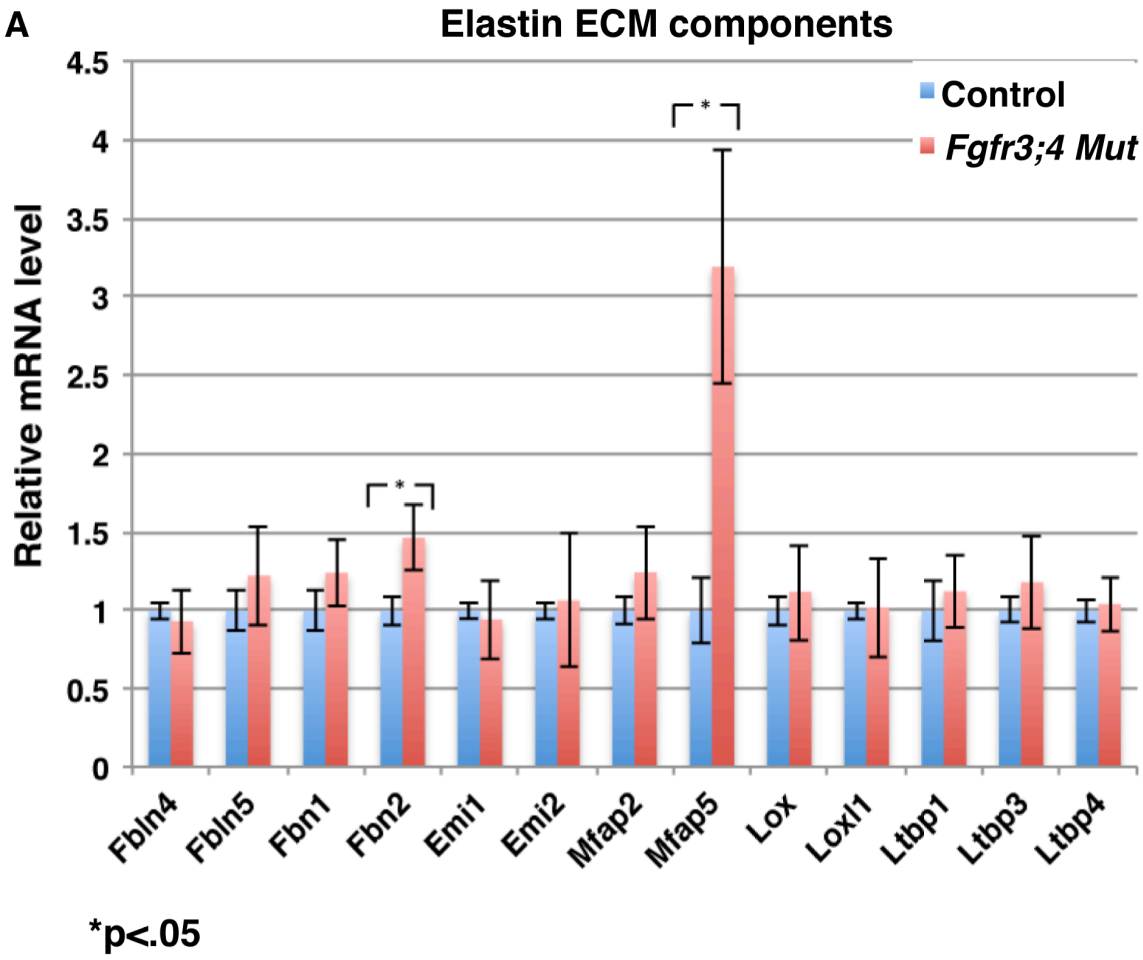

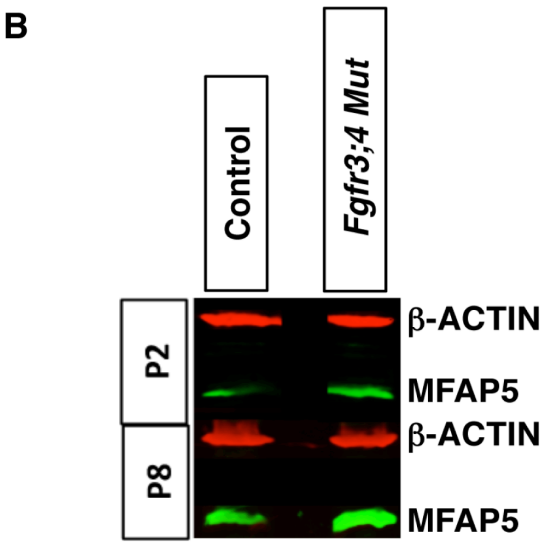

Figure 14: The microfiber network is unaffected in the *Fgfr3;4* mutant lung. (A-F, A'-F') Reconstructed 10um Z-stacks of alveolar region of P2 lungs stained for Elastin (A,B, A',B'), FBN1 (C,D,C'D'), and FBN2 (E,F,E'F') and nuclei (blue). At P2, ELN (red) is localized to the outer region of the alveolar wall in control mice (A, A'). *Fgfr3;4* mutant lungs have a disorganized Elastin ECM at P2 with multiple fibers running through the alveolar wall (B, B'). The organization of FBN1 (red) is unaffected by the loss of FGFR3;4 (C,D, C',D'). The organization of FBN2 (red) is unaffected by the loss of FGFR3;4 (E,F, E',F'). In both the control and mutant lungs FBN1 and FBN2 do not appear to be preferentially located to the alveolar wall (C'-F'). Instead the localization of FBN1 and FBN2 appears to be more like that of the Elastin ECM in the Fgfr3;4 mutant lung (B').

Figure 14: The microfiber network is unaffected in the *Fgfr3;4* mutant lung.

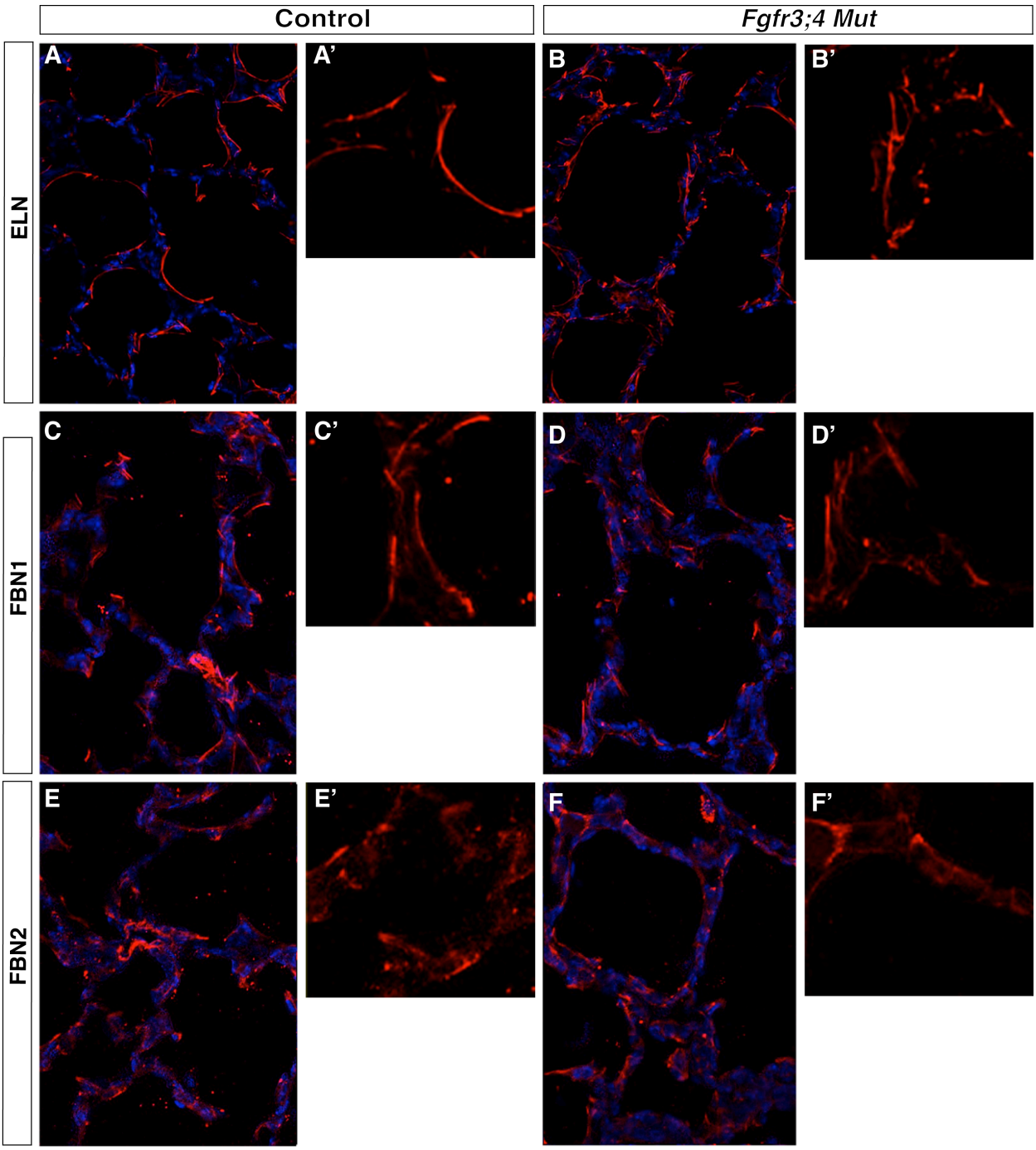

Figure 15: Introducing an *Mfap5* knockout allele into the *Fgfr3;4* mutant background is able to attenuate the alveolar simplification.

(A,B) Representative H&E stained frozen sections from the alveolar regions of P8 *Fgfr3;4* mutant and *Mfap5;Fgfr3;4* mutant lungs. At P8, Fgfr3;4 mutant lungs have a simplified alveolar network with very large alveoli (A). Knocking out *Mfap5* in the *Fgfr3;4* mutant background was able to partially attenuate the alveolar simplification *seen in the Fgfr3;4* mutant lungs (B). The alveolar density was quantified in the *Mfap5;Fgfr3;4* conditional lungs by measuring the relative MLI. At P8 the relative MLI of *Mfap5;Fgfr3;4* lungs was significantly decreased, when compared to *Fgfr3;4* mutant lungs (F) ($P<.05$ $N=4$). (C,D) Reconstructed 50um Z-stacks of immunofluorescent staining for Elastin (green) in the alveolar region of P8 *Fgfr3;4* mutant and *Mfap5;Fgfr3;4* lungs. At P8, we found that the Elastin ECM was disorganized in both the *Fgfr3;4* mutant and *Mfap5;Fgfr3;4* (C,D). In both conditions, we see multiple fibers running through the alveolar walls.

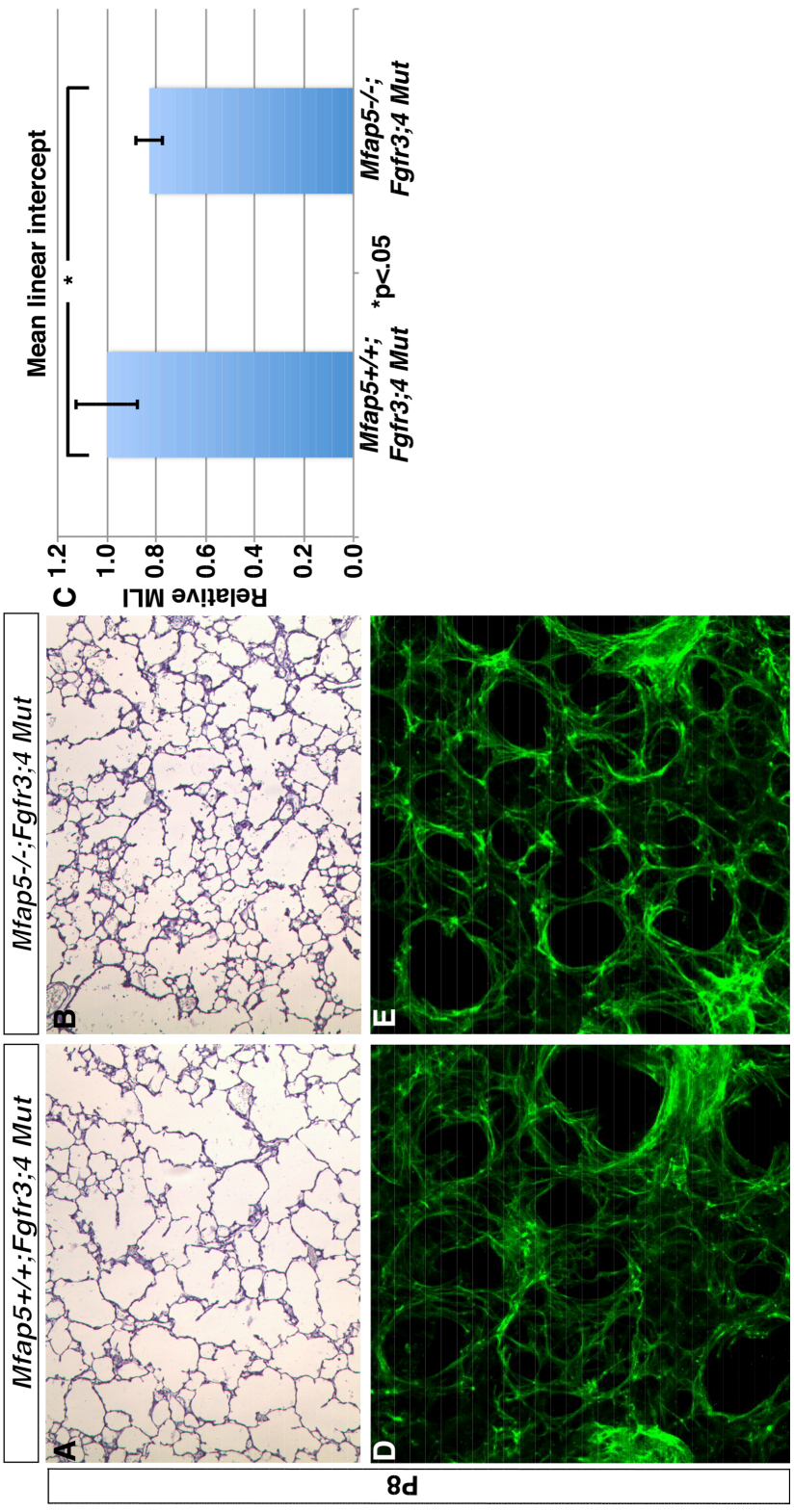

Figure 15: Introducing an *Mfap5* knockout allele into the *Fgfr3;4* mutant background is able to attenuate the alveolar simplification.

Figure 16: Model

(A) In the control lung, the Elastin ECM lines the alveolar walls. The normal deposition of the Elastin ECM results in the myofibroblasts of the lung having a normal localization and morphology. The normal myofibroblast localization and morphology then permits the outgrowth of the septal crests, leading to a normal alveolar structure. (B) In the *Fgfr3;4* mutant lung, the deposition of the Elastin ECM is disrupted, so that multiple fibers run through the walls of the primitive alveoli. The disorganized Elastin ECM leads to an abnormal myofibroblast morphology, which inhibits septal outgrowth, and leads to the alveolar simplification.

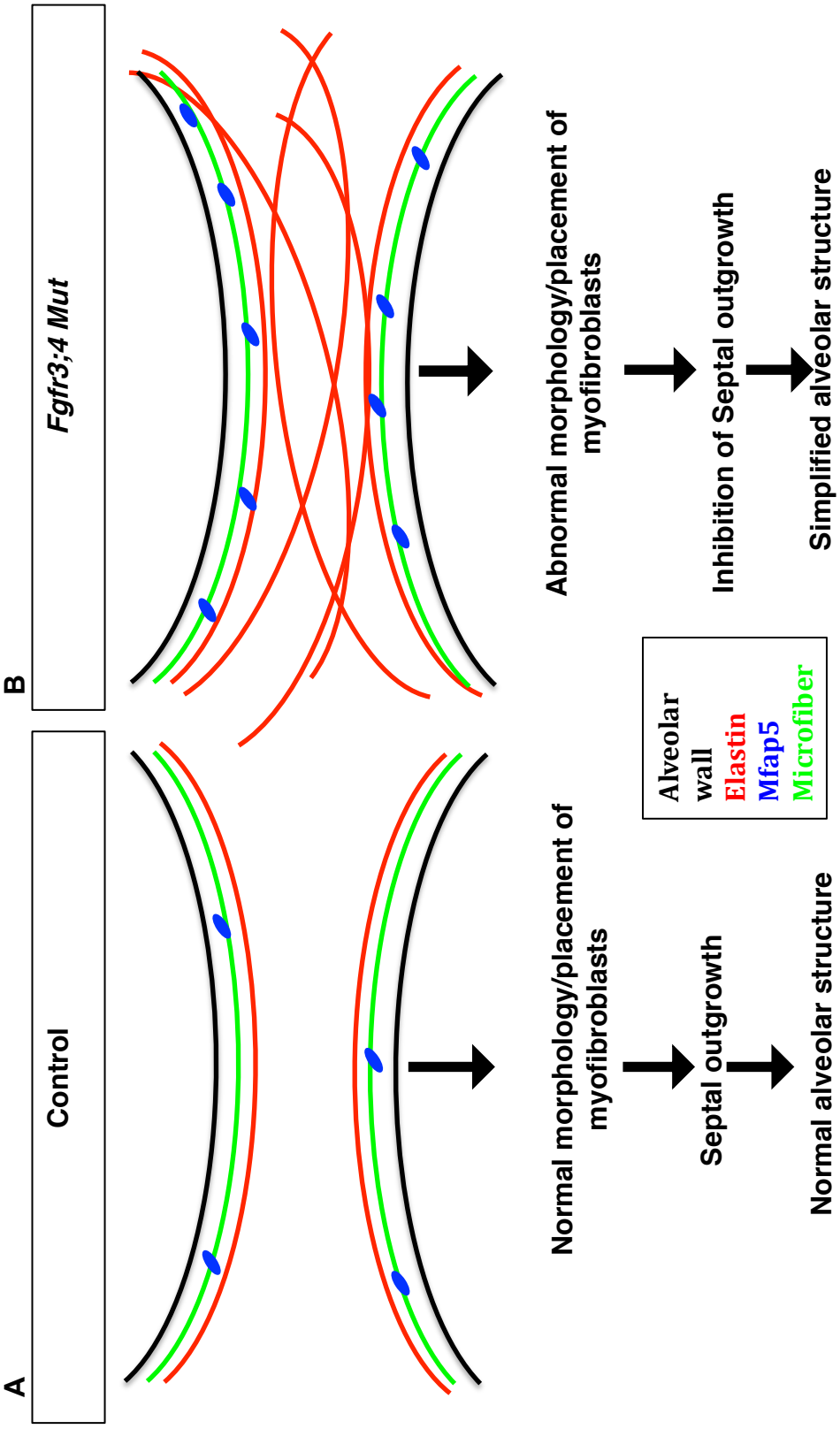

Figure 16: Model

Chapter V: Conclusions and future directions.

Conclusions:

Overall my data enhances the fields understanding of how the lung develops and matures. First, by performing an *in situ* hybridization screen, my findings have helped to elucidate the transcriptional circuitry in the embryonic lung. We found approximately 60 transcription factors that were expressed in the lung at E13.5, most of which have not been shown to mediate lung development during branching morphogenesis. Therefore I think we have identified novel transcription factors that could be the focus of future studies.

Other than knocking out some of the transcription factors we identified and characterizing their role in lung development, I think that it would be really useful to perform a similar screen at later stages of lung development, with an emphasis in the postnatal lung. One of the biggest issues with studying the postnatal lung is that there are not many markers for the different cell populations. One of the things that we were able to pull out of the embryonic screen were potential markers for the vasculature and lymphatic system. I feel that if similar screen was performed in the postnatal lung, we would be able better define the lineages that are necessary for alveolar development.

My work also demonstrates that the FGF regulated transcription factors *Etv4;5* are necessary for epithelial branching morphogenesis. By using a conditional knockout approach we were able to identify that *Etv4;5* mediate epithelial branch patterning and epithelial lumen size in the embryonic lung. Further analysis of the *Etv4;5* mutant lung revealed that FGF signaling was increased in the mutant lung, while SHH signaling was decreased. By using genetic techniques to decrease FGF signaling activity and pharmacological techniques to activate SHH signaling, we were able to rescue the

epithelial lumen phenotype in the *Etv4;5* mutant lung. Furthermore, we were able to use a combination of *in vitro* and *in vivo* techniques to demonstrate *Etv4;5* are able to mediate *Shh* expression in the lung through a long range *Shh* enhancer. Collectively our data suggests that one of the primary functions of *Etv4;5* in the lung is to mediate an FGF-SHH negative feedback loop.

One of the questions that is still unclear is how do *Etv4;5* mediate general branch patterning. Our rescue data suggests that the FGF-SHH signaling loop is not mediating the general branch patterning defect in the *Etv4;5* mutant lung. We had attempted to identify other targets of Etv4;5 in the lung by running gene expression arrays on the whole lung. Unfortunately we did not find any candidates that could be contributing to the *Etv4;5* mutant phenotype. One of the potential reasons for this could be that the gene expression changes in the lung epithelium are being dampened in the arrays by the presence of the mesenchymal tissues. A potential way to get around this would be to dissociate the lung epithelium from the mesenchyme and run an array solely on the lung epithelium. Additionally, we could identify other potential direct targets by performing ChIP-seq. Once these targets are identified we could then use genetic or pharmacological means to assess whether these targets are contributing to the lung phenotype.

Lastly, my work has expanded upon the model of how FGF signaling mediates lung development. We found that *Fgfr3;4* are necessary for the development of the primitive alveoli during the saccular stage of lung development. Our data suggests that the primary role of *Fgfr3;4*, during the saccular stage, is to mediate the deposition of the Elastin ECM. Additionally we demonstrated that the mesenchymal activity of *Fgfr3;4* is

necessary for postnatal lung development. Finally we showed that the alveolar simplification in the *Fgfr3;4* mutant lung is caused in part by an increase in the *Mfap5* expression level.

One of the future directions for this project would be further examine how knocking out *Mfap5* is able to rescue the *Fgfr3;4* mutant phenotype. We had originally hypothesized that knocking out *Mfap5* would attenuate the alveolar phenotype by rescuing the disorganized Elastin ECM, however the elastin ECM is still disorganized in the *Mfap5;Fgfr3;4* mutant lung. In addition to mediating Elastin ECM formation, Mfap5 has been shown to interact with TGFb proteins and to facilitate a cells response to FGF signaling; however, I see no differences in the global level pSMAD2, pAKT, pERK, and pPLC-gamma in the *Fgfr3;4* knockout lung. Therefore I had not pursued this further. However it possible that the alteration in TGF/FGF signaling is only in a subset of the cells, therefore we could examine these pathway a little more closely in the mutant, by looking at whether these pathways are altered in specific cell populations. By looking at this we would gain a better appreciation for how knocking out *Mfap5* can attenuate the *Fgfr3;4* knockout phenotype.

Another future direction for this project would be to identify other factors that could be mediating the development of the alveolar simplification and the alterations in the Elastin ECM. Knocking out *Mfap5* was able to attenuate the alveolar phenotype, however the rescue was not complete, suggesting there are other factors that are mediating the development of the phenotype. To identify these, we have run an array on P2 *Fgfr3;4* mutant and control lungs have identified a number of genes that are associated with the extracellular matrix. One of these genes is IGF1, which has been

shown to promote Elastin expression. Although we don't see an increase in Elastin expression in the *Fgfr3;4* mutant lungs at P2 or P8 it is possible that IGF1 may also mediate the deposition of the Elastin ECM. Once we have confirmed that these genes have an altered expression, the next step would be to knock these genes out in the *Fgfr3*;*4* mutant background to see if it attenuates the phenotype.

The final future direction for this project would be to identify the ligands that are acting on FGFR3;4 in the postnatal lung. The majority of studies that have examined the role of FGF signaling in postnatal lung development have either focused on the role of the FGFRs or have used chemicals to inhibit the activity of the some of the FGF ligands. Ligand specificity studies have demonstrated that FGF1,FGF2, FGF4, FGF8, FGF9, FGF17, FGF18 are able to interact with FGFR3;4 (Eswarakumar et al. 2005). Of these, FGF1, FGF2, FGF8, FGF9, FGF18 have been shown to be expressed in the lung. FGF1, FGF2, have knockout lines, however neither of them have an associated lung defect. FGF8, FGF9 and FGF18 also have knockout lines available, and all three knockout lines have prenatal lung phenotypes. Therefore in order to study their role during postnatal lung development they would have to be conditionally knocked out within the postnatal lung. Currently, there are conditional alleles for both FGF9 and FGF18 and neither of them has been studied for their role in postnatal lung development. By examining what FGF ligands are involved in postnatal lung development, we would gain an appreciation for how FGFR3;4 are mediating postnatal lung development.

Appendix I: *Etv4* and *Etv5* mediate postnatal lung development through controlling prenatal lung patterning.

Images in this chapter were collected by John Herriges with the help of Kelsey Branchfield.

Abstract:

Although the FGF signaling pathway has been shown to be required for both embryonic and postnatal lung development, the transcriptional regulation of FGF signaling activity is still poorly understood. In a previous study we showed that the FGF regulated transcription factors *Etv4* and *Etv5* (Hereafter *Etv4;5*) are necessary for epithelial branching in the embryonic lung. Here we examine the role of *Etv4;5* in late embryonic and early postnatal lung development. Our results demonstrate that the loss of ETV4;5 activity during embryonic lung development results in a simplified proximal airway tree and a simplified alveolar network. Interestingly, when we knockout *Etv4;5* in the postnatal lung, we see no phenotypic abnormalities. Together our data suggests that although *Etv4;5* are expressed in the postnatal lung, their primary role in the lung is to mediate embryonic lung development.

Introduction:

In mice, the lung buds sprout from the ventral foregut at embryonic day 9.5 (Cardoso and Lu 2006; Morrisey and Hogan 2010). Between E9.5-E11.5, the lung epithelium elongates and branches to form the four lobes of the right lung and the single lobe of the left lung. From E11.5-E16.5, the lung enters the pseudoglandular stage where the epithelium will form hundreds of airways through the stereotypical process known as branching morphogenesis (Metzger et al. 2008). Towards the end of branching morphogenesis, specialized cell populations like ciliated cells and clubs begin to form within the proximal regions of the lung, and the distinctions between the cells destined to become the proximal airways, and the distal alveoli become much more apparent (Morrisey and Hogan 2010). Over the final days of embryonic lung development and during the first few days of life, the lung undergoes saccular branching to form the primitive alveoli, which will facilitate oxygen uptake at birth. The final stage of lung development is the alveolar stage, which takes place between P4-P36 (Mund et al. 2008). During this stage approximately 55% of the adult alveolar surface area is established through a process known as alveologenesis, in which thousands septal crests emerge from the walls of the primitive alveoli and grow into the alveolar lumen.

All of the conserved signaling pathways including WNT, SHH, FGF, BMP, and NOTCH have been shown to be critical for different stages of lung development (Cardoso and Lu 2006; Morrisey and Hogan 2010). Of these, the FGF signaling pathway is one of the most thoroughly characterized, as it has been linked to every stage of lung development (Sekine et al 1999; De Moerlooze et al. 2000;Colvin et al. 2001; Hokuto et al. 2003; Usui et al 2004; del Moral et al. 2006; Abler et al. 2009; Yi et

al. 2009; Yu et al. 2010). The earliest required FGF ligand is FGF10, which is necessary for lung bud initiation (Min et al. 1998; Sekine et al. 1999). During the pseudoglandular stage FGF9 and FGF10 mediate branching morphogenesis as well as mesenchymal patterning and the formation of the airway smooth muscle (Abler et al. 2009; Yi et al. 2009). Finally, FGF8 and FGF18 are necessary for the formation of functional primitive alveoli during the final days of gestation (Usui et al 2004; Yu et al. 2010).

In the postnatal lung, the focus of studies on FGF signaling has primarily been on the FGFRs. Recent studies have demonstrated that *Fgfr2*, *Fgfr3,* and *Fgfr4* are all required for postnatal lung development (Weinstein et al. 1998; Hokuto et al. 2003; Srisuma et al. 2010). Interestingly, FGFR2 mediates postnatal lung development through its developmental requirement in the prenatal lung, and specifically inhibiting the activity of FGFR2 postnatally does not have any phenotypic consequences (Hokuto et al. 2003). Recent studies have shown that *Fgfr3* and *Fgfr4* (Hereafter *Fgfr3;4*) function redundantly in the postnatal lung, with *Fgfr3* or *Fgfr4* individual knockout mice showing no phenotypic abnormalities (Weinstein et al. 1998). However, *Fgfr3;4* double knockout lungs do not undergo alveologenesis, resulting in a severely simplified alveolar network in the adult lung (Srisuma et al. 2010).

Although much is known about how FGF signaling mediates lung development on the level of the ligand and the receptor, the transcriptional regulation of FGF signaling in the lung is still poorly understood. In a previous study to identify novel transcription factors involved in lung development, we identified that the FGF regulated transcription factor *Etv5* is expressed in the distal lung epithelium (Herriges et al. 2012).

Etv5 is one of three members of the PEA3 group of transcription factors, which consists of *Etv1*, *Etv4*, and *Etv5* (Liu et al 2003; Chotteau-LelieÁvre et al. 1997; Herriges et al. 2012). All three PEA3 group transcription factors are expressed in the lung; however, *Etv4;5* are the only ones that are strongly expressed in the lung epithelium. In a previous study we examined the role of *Etv4;5* during branching morphogenesis by using a conditional knockout approach (Herriges unpublished). In this study we showed that *Etv4;5* mediate epithelial branching by acting as intermediates in a FGF-SHH negative feedback loop. Recently, a study examined the role of PEA3 group transcription factors during the later stages of embryonic lung development by overexpressing an ETV5-Engrailed repressor fusion protein (hereafter *Etv5-Engl*) (Liu et al. 2003). In the proximal airways, the overexpression of the *Etv5-Engl* construct led to an increase in the number of ciliated cells. While in the alveolar region, the overexpression of the *Etv5-Engl* construct inhibited the differentiation of both the alveolar type I and type II cells. Therefore, we wanted to use our conditional knockout approach to further examine the roles of *Etv4;5* in the late embryonic and early postnatal lung.

In this study we used a conditional knockout approach to examine the role of *Etv4;5* in late embryonic and early postnatal lung development. We demonstrate that the embryonic function of *Etv4;5* is necessary for the establishment of the proximal airways and the distal alveoli in the postnatal lung. Furthermore, in the distal alveoli, our data suggests that *Etv4;5* are not necessary for cell fate determination in the epithelium, but instead are part of an epithelial to mesenchymal crosstalk that mediates the formation of the Elastin extracellular matrix. Finally, through the use of a tamoxifen

inducible cre, we demonstrate that the postnatal activity of Etv4;5 is not required for lung development. Collectively, our data demonstrates that although *Etv4;5* mutant lungs develop a strong postnatal lung phenotype, their activity is not required in the postnatal lung for normal alveologenesis.

Results:

Our previous work has demonstrated that *Etv4;5* are necessary for the pseudoglandular stages of lung development (Herriges unpublished). However, FGF signaling continues to be active in the lung well beyond the end of branching morphogenesis. To investigate the role of *Etv4;5* during the final stages of lung development we conditionally inactivated *Etv4;5* in the lung epithelium. This was achieved by using an $Etv5^{fl}$ allele and an epithelial-specific Shh^{cre} , in combination with an *Etv4* null allele , which generated $Shh^{cre/+};Etv5^{fl/fl};Etv4^{-/-}$ (hereafter *Etv4;5* mutant) embryos (Laing et al. 2000; Harris et al. 2006; Goss et al. 2009; Zhang et al. 2009). We have previously demonstrated that the $Shh^{cre/+}$ can efficiently excise the floxed region of the *Etv5* conditional allele as early as E11.5, so utilizing the $Shh^{cre/+}$ should allow us to examine how *Etv4;5* are involved in the development and maturation of the late embryonic and early postnatal lung.

***Etv4;5* are necessary for the formation of the proximal airways**

While *Etv4;5* mutant mice do survive postnatally, we found that they develop smaller lungs at birth (Figure 1A-B). At birth, *Etv4;5* are expressed in the alveolar region of the lung (Lin et al. 2006). However a previous study has demonstrated that

PEA3 group transcription factors are necessary for the development of both the proximal airways and the distal alveoli (Liu et al. 2003). To examine whether *Etv4;5* are necessary for the general airway structure, we first performed a whole mount *in situ* hybridization for the proximal airway maker *Scgb1a1* on postnatal day zero (P0) lungs. We found that major airways were drastically simplified in the *Etv4;5* mutant lungs, with mutant lungs having fewer airways that were wider in diameter and contained fewer secondary branches (Figure 2 A-C). Interestingly, although we observed such a strong phenotype in the airway structure, the cell populations that make up the airway epithelium including; club cells, NEBs, and ciliated cells, were unaffected (Figure 2D-I). These results suggest that although *Etv4;5* are necessary for the establishing the structure of the proximal airways, they are not necessary for establishing the cellular niches that populate these airways.

Etv4;5 **are necessary for the formation of the distal alveoli**

Previous research has demonstrated that FGF signaling is necessary for the alveolar development (Weinstein et al. 1998; Hokuto et al. 2003; Srisuma et al. 2010). In the postnatal lung *Etv4;5* are expressed in the distal alveoli suggesting that they may also regulate alveolar development. To determine if *Etv4;5* mediate alveolar development we examined the histology of *Etv4;5* mutant lungs at P0 and P7. We found that there is a slight simplification in the alveolar structure at P0, with *Etv4;5* mutant lungs having slightly fewer total alveoli that are larger in size (Figure 3 A,B). This phenotype worsened as the mouse enters the alveolar stage of lung development, with *Etv4;5* mutant lungs showing a more drastic alveolar simplification at P7 (Figure 3C-D).

To confirm these results we measured that mean linear intercept (MLI), and found that at P7, the *Etv4;5* mutant lungs had a 60% increase in the relative MLI (Figure 3E $P<0.05$ N=3). Together these data suggest that ETV4;5 are necessary for alveolar development in the postnatal lung.

Etv4;5 control fibroblast formation in alveolar region of the lung

Alveolar development in the distal lung is the result of a series of complex interactions between the epithelium and mesenchyme. In order to better understand how the alveolar phenotype develops in the *Etv4;5* mutant lung we examined how the different cellular lineages that make up the alveoli are affected by the loss of ETV4;5 activity.

The alveolar epithelium is composed of two different cell types, alveolar epithelial type I (hereafter type I) cells and alveolar epithelial type II (hereafter type II) cells. A previous study had suggested the PEA3 group transcription factors are necessary for the differentiation of both type I and type II cells at E18.5 (Liu et al. 2003). However, we found that type II cells were unaffected by the loss of *Etv4;5* activity in the lung epithelium, with type II cells in *Etv4;5* mutant lungs having a normal localization (Figure 4A-D). Furthermore, we found no noticeable difference in the localization or differentiation of type I cells in the *Etv4;5* mutant lungs (Figure 4A-D). Together these results suggest that although *Etv4;5* are expressed in the alveolar epithelium of the postnatal lung, they are not required for the development of either type I or type II cells.

Previous studies have demonstrated that the fibroblast lineages are necessary for alveolar development in the postnatal lung (Bostrom et al. 1996 ; Lindahl et al.

1997). Furthermore several studies have suggested that FGF signaling can mediate alveolar fibroblast differentiation during normal development and in lung regrowth models (Srisuma et al. 2010; Chen et al. 2012). To determine whether the fibroblast lineages are altered in the *Etv4;5* mutant lungs, we mated a Pdgfra$^{GFP/+}$ reporter allele into the *Etv4;5* mutant background (Hamilton et al. 2003; McGowen et al. 2008). In the *Etv4;5* mutant lungs, we found that there were approximately 30% fewer fibroblasts at both P0 and P7 (Figure 5A-E $P<0.05$ N=3) Interestingly though, when we examined the expression pattern of the myofibroblast using the marker TAGLN, we found no difference in its general localization at P7 (Figure 6A,B). Together these data suggest that although *Etv4;5* are expressed in the epithelium of the lung, the primary tissue that is affected in the *Etv4;5* mutant lung is the mesenchyme.

One of the primary functions of the fibroblast lineage in the postnatal lung is to establish the Elastin extracellular matrix (hereafter ECM) (Bostrom et al. 1996; Lindahl et al. 1997). Previous studies have also demonstrated that the FGF signaling pathway mediates the production of the Elastin ECM (Weinstein et al 1998; Srisuma et al 2010). Interestingly, although we noticed no difference in the Elastin ECM that surrounded the airways, the Elastin ECM in the alveolar region was disorganized at P7 (Figure 7A,B). Unlike what is seen in the *Fgfr3;4* mutant lung, the Elastin ECM in the *Etv4;5* mutant does appear to be abnormally localized in the alveolar walls, instead it appears as though the fibers are not as tightly bundled. This data suggests that one of the mechanisms through which *Etv4;5* may mediate postnatal lung development is by controlling the formation of the Elastin ECM.

Etv4;5 are not required in the alveolar epithelium of the postnatal lung

In the lung, FGF signaling regulates alveolar development through the FGF-receptors; *Fgfr2*, *Fgfr3*, and *Fgfr4* (Weinstein et al. 1998; Hokuto et al. 2003; Srisuma et al 2010). Interestingly, *Fgfr2* conditional inhibition studies have shown that although the inhibition of FGFR2 activity in the embryonic lung leads to a simplified alveolar structure, the inhibition of FGFR2 activity in the postnatal lung has no developmental consequences (Hokuto et al. 2003). Furthermore, although *Fgfr3* and *Fgfr4* (hereafter Fgfr3;4) are expressed in the prenatal lung, previous studies have demonstrated that they are only required for postnatal lung development (Weinstein 1998; Srisuma 2010; Herriges unpublished). Together these studies have suggested that FGF signaling can affect postnatal lung development through two separate mechanisms. The first is exemplified by the *Fgfr2* mutants, in which a disruption of prenatal lung patterning/development causes an abnormal postnatal lung phenotype. The second is seen in the *Fgfr3;4* mutants, where FGF signaling is strictly involved in postnatal lung development.

We have previously shown that *Etv4;5* are required for prenatal lung development (Herriges unpublished). To determine whether the alveolar simplification phenotype we see in the *Etv4;5* mutant is due to the requirement of *Etv4;5* in prenatal or postnatal lung, we utilized the tamoxifen inducible cre-recombinase system to specifically inactivate *Etv4;5* in the postnatal lung epithelium. This was achieved by combining the tamoxifen inducible $Id2^{Cre/Ert2}$ with a conditional $Etv5^{fl}$ allele and an $Etv4^{-}$ knockout allele, generating $Id2^{Cre/Ert2}$;$Etv5^{fl/fl}$;$Etv4^{-/-}$ (hereafter *Etv4;5* inducible mutant) mice. $Id2^{Cre/Ert2}$ is active in the alveolar epithelium, and we found significant $Id2^{Cre/Ert2}$

activity after only four rounds of tamoxifen injections, over the first five days of life (Rawlins et al. 2009) (Figure 8A-B). Furthermore, we found a 60% reduction in the full length Etv5 transcript by P8, demonstrating that the $Id2^{Cre/Ert2}$ is active in the postnatal lung (Figure 8C). To ensure that we would detect any potential alveolar phenotypes in the *Etv4;5* inducible mutant lungs, we collected lungs near the end of alveolar development, at P28. When we compared *Etv4;5* inducible mutant lungs to injected control mice, there were no obvious phenotypic abnormalities at P28. (Figure 9A,B). These results were later confirmed by quantifying the mean linear intercept for control and mutant lungs (Figure 9C). From these data, we conclude that postnatal activity of *Etv4;5* in the lung epithelium is not required for lung development.

Discussion:

In this study we examined the role of *Etv4;5* in postnatal lung development. We were able to demonstrate that the loss of Etv4;5 activity in the embryonic lung, causes a severe alveolar simplification that is reminiscent of the phenotype seen in the lungs of *Fgfr2-HFc* and *Fgfr3;4* mutants (Weinstein et al. 1998; Hokuto et al 2003; Srisuma et al. 2010). However, when we knocked out *Etv4;5* in the postnatal lung, we found that *Etv4;5* are not required in the lung epithelium for normal postnatal lung development. Our findings therefore suggest that *Etv4;5* are able to regulate postnatal lung development through their role in patterning the embryonic lung.

***Etv4;5* mediate general airway patterning but not cellular differentiation.**

A recent study provided evidence which suggested that *Etv4;5* may mediate airway cell differentiation in the embryonic lung (Liu et al. 2003). Additionally, our studies on *Etv4;5* in early lung development, had demonstrated that *Etv4;5* mediate epithelial branch patterning (Herriges unpublished). Therefore we had hypothesized that the patterning of the major airways would be altered on both the cellular level and structural level. Interestingly, although we found that the structural patterning of the airways was disrupted in the mutant lung, the cellular patterning in the airways unaffected (Figure 2). These results suggest that although *Etv4;5* are necessary for establishing the major airway network, they are not necessary for the development of cellular lineages that populate it. One plausible explanation for this is that *Etv4;5* are mainly expressed within the distal lung epithelium during lung develop. Therefore although the cells that localize to the proximal airways would have been derived from ETV4;5 positive cells, they themselves would not be expressing *Etv4;5* when they are differentiating. Thus the loss of *Etv4;5* would not affect the differentiation of these airway cell populations.

Etv4;5 are required for alveolar development

In addition to the disruption of the patterning of the major airways, we found that *Etv4;5* mutant lungs had a simplified alveolar structure. Interestingly, in the *Etv4;5 mutants*, we found that although *Etv4;5* are expressed in the lung epithelium, the primary alveolar lineage affected in the *Etv4;5* mutant lung were the mesenchymal myofibroblasts. We have previously shown that *Etv4;5* mediate epithelial to mesenchymal crosstalk during branching morphogenesis, and *Etv4;5* have also been

shown to mediate epithelial to mesenchymal crosstalk during limb development (Zhang et al. 2009; Herriges). These results suggest that one of the primary roles of *Etv4;5* during development is to mediate epithelial to mesenchymal crosstalk. Previous studies have shown that myofibroblasts are necessary for alveolar development within the postnatal lung, thus the disruption of this population in the *Etv4;5* mutant lung may be contributing to the alveolar simplification. Furthermore given the importance of the Elastin ECM to postnatal lung development it is likely that the myofibroblasts are mediating postnatal lung development through their ability to regulate Elastin ECM formation.

The function of *Etv4;5* is within the embryonic lung.

Previous studies have demonstrated that FGF signaling can control postnatal lung development by being specifically required for postnatal roles, or by mediating the development of the embryonic lung, which will affect how the postnatal lung develops. An example of the former are *Fgfr3;4* which have no mutant phenotypes within the embryonic lung, but develop a severe alveolar simplification by P8 (Weinstein et al. 1998; Srisuma et al. 2010). An example of the latter is *Fgfr2*, which is only necessary for prenatal lung development, but the prenatal roles of *Fgfr2* are not necessary for normal lung development (Hokuto et al. 2003). To test how *Etv4;5* are mediating postnatal lung development, we conditionally inactivated Etv4;5 in the postnatal lung using $Id2^{Cre/Ert2}$. Interestingly, we didn't find any phenotypic abnormalities in the *Etv4;5* conditional mutant lungs, demonstrating that the postnatal expression of *Etv4;5* is not required for postnatal lung development. Additionally, several lines of evidence suggest that *Etv4;5*

may act downstream of *Fgfr2* during postnatal lung development. First, during embryonic lung development *Etv4;5* are thought to act downstream of FGF10 and FGFR2-IIIb in the lung epithelium (Liu et al. 2003). Second, although both *Etv4;5* and *Fgfr2* are expressed in the distal epithelium of the postnatal lung, their activity is not required for postnatal lung development (Hokuto et al. 2003). Therefore, it is not surprising that *Etv4;5* would mediate postnatal lung development through a mechanism similar to *Fgfr2*.

Future directions:

With this project one of the future directions would be to further map out the temporal requirement of *Etv4;5* for lung development. In our studies we cannot differentiate a potential role of *Etv4;5* during branching morphogenesis from a role of Etv4;5 during prenatal sacculation. We had tried to do this with the Id2-cre, but found that tamoxifen injections embryonically resulted in abortion rates that did not make it feasible to study this question. To get around this problem we can mate in a doxycycline induce SpC-cre which would easily allow us to examine the role Etv4;5 play in prenatal sacculation.

Materials and Methods:

Mice:

The mutant alleles used in this study are Etv5fl (Zhang 2009), Etv4- (Laing 2000), Shh-cre (Harfe 2004), and Id2-Cre/Ert2 (Rawlins et al. 2009). The pups used in these experiments were harvested postnatally, with the day of birth being considered P0.

Histology:

For histological analysis, lungs were inflation fixed with 4%PFA overnight, equilibrated into 30% Sucrose overnight, and then embedded in OCT and sectioned at 5um. Lung sections were then allowed to sit at room temperature for 2 hours and were stained using a standard H&E protocol. Quantification of lung simplification was performed using the mean linear intercept (MLI) method, as previously described (Chen et al. 2012). Three randomly selected sections from at least three lungs were used to calculate the MLI for mutant and control samples at every stage. Statistical analysis was done using the students T-test.

Immunofluorescent:

For immunofluorescent staining, lungs were inflation fixed overnight in 4% PFA. After fixation, lungs were equilibrated in 30% Sucrose overnight, embedded in OCT and sectioned at 5um. Sections were then stained using a standard immunofluorescent protocol (Yi et al. 2009). The primary antibodies used were: SpC (seven hills), T1a (seven hills), Elastin (Mecham), and SMA (Abcam).

RNA *in situ* Hybridization

RNA in situ hybridization was performed following a protocol that was adapted from previously published protocols (Wall and Hogan 1995; Abler et al. 2011; Herriges 2012). Briefly, wholemount tissues stored in methanol were rehydrated using PBS with 0.1% Tween (PBT). Tissues were then permeabilized using 10µg/ml proteinase K in PBT for

10 minutes. Tissues were fixed with 4% paraformaldehyde, 0.2% glutaraldehyde in PBT for 20 minutes. They were then washed and allowed to hybridize with probes at 70oC overnight. After the hybridization, tissues were washed three times, twenty minutes each in 2x SSC, 0.1% CHAPS, and then in 0.2x SSC, 0.1% CHAPS at 70oC. Tissues were then washed in KTBT and blocked for 2 hours in 2% blocking solution (Roche) and 20% heat inactivated sheep serum (Sigma) in KTBT at room temperature. The tissues were then incubated overnight at 4˚C in the primary antibody, AP conjugated α-DIG, Fab fragment (Roche) at a dilution of 1:2000 using 2% blocking solution and 20% heat inactivated sheep serum in KTBT. The tissues were then washed 5 times, 1hour each in KTBT at room temperature. Following this, the tissues were washed twice, 5 minutes each with 0.1% Tween, 1mM Levamisole in ddH2O. Finally the tissues were stained in BM purple (Roche) containing 0.1% Tween and 1mM levamisole. The staining was carried out for varying amount of time depending on the probes until desired intensity. Once the staining was completed, lungs were dehydrated through a MeOH gradient, cleared with BABB, and were imaged.

Figures:

Figure 1: *Etv4;5* mutant lungs are smaller than control lungs at birth.

(A,B) Dorsal view of whole mount control and *Etv4;5* mutant lungs taken from P0 pups. At birth *Etv4;5* mutant lungs are noticeably smaller than control lungs (A,B).

Figure 1: *Etv4;5* mutant lungs are smaller than control lungs at birth.

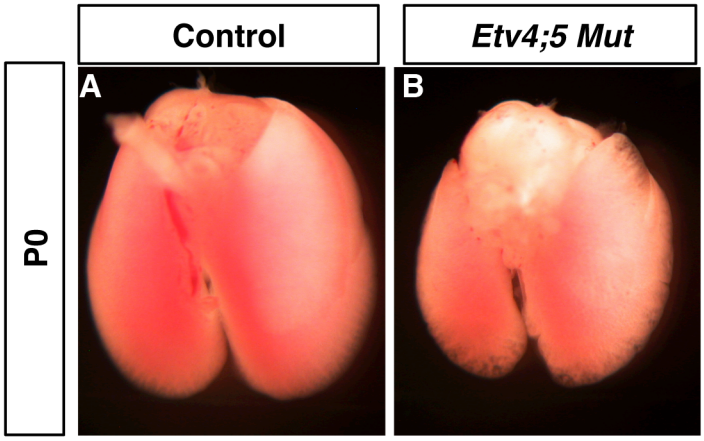

Figure 2: The structure of the airways in the Etv4;5 mutant lungs is simplified, but the cells that populate these airways are unaffected.

(A,B) Representative P0 whole mount *in situ* hybridization for the proximal airway marker *Scgb1a1*. At P0 the staining intensity of the *Scgb1a1* is unchanged in the *Etv4;5* mutant lung; however, the in situ hybridization revealed that the mutant lung has a simplified airway structure (A-B). Quantification of the proximal airways revealed that the *Etv4;5* mutant airways are approximately 40% wider, than the control lungs (N=3 $P<0.03$) (C). Additionally, the airways in the mutant lung contained approximately 40% fewer secondary bronchioles (N=3 $P<0.03$) and approximately 55% fewer airway tips (broncho-alveolar duct junctions or BADJs) (N=3 $P<0.001$) (C). Data are presented as means (+SEM). (D-I) Immuno staining for SCGB1A1 (green), CGRP (green), acetylated tubulin (red), and nuclei (DAPI) in transverse sections of the proximal airways. In the mutant lung, the there appears to be no difference in the localization or differentiation of club cells (D,E), neuroendocrine cells (F,G), or ciliated cells (H,I).

Figure 2: The structure of the airways in the *Etv4;5* mutant lungs is simplified, but the cells that populate these airways are unaffected.

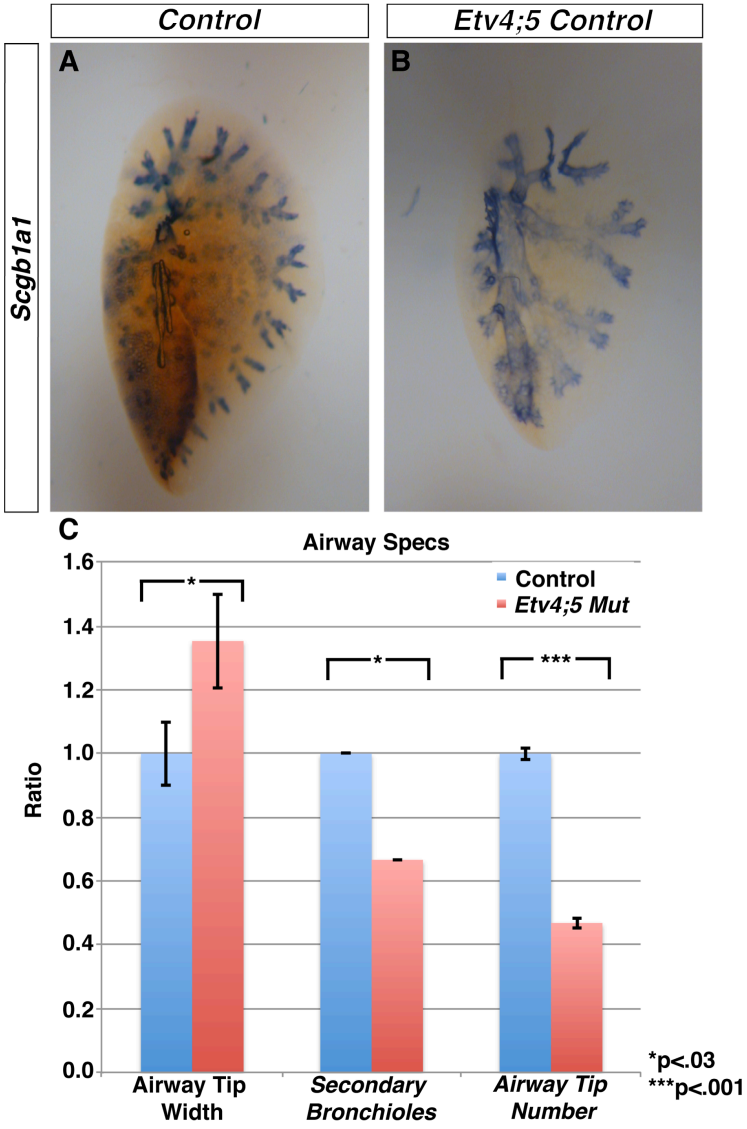

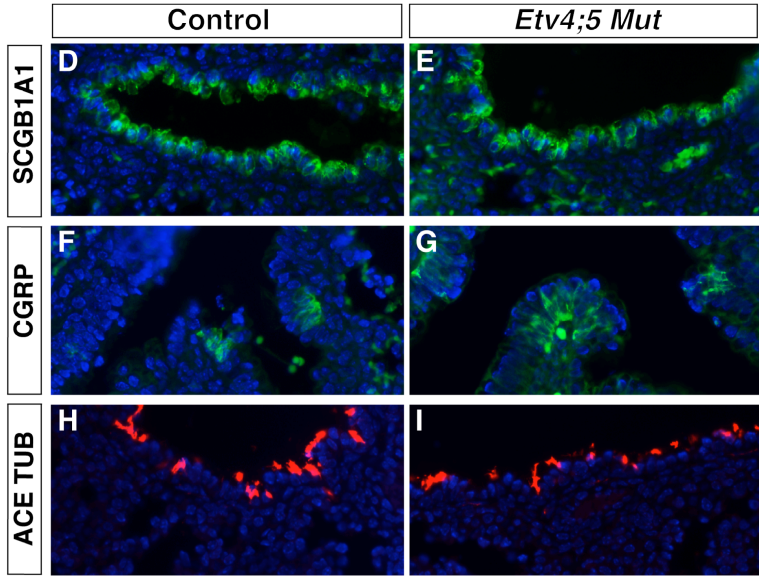

Figure 3: Distal lung histology of *Etv4;5* mutant lungs at birth and during alveologenesis.

(A-D) Representative H&E stained frozen sections from the alveolar regions of *Etv4;5* mutant and control lungs at P0 and P7. At P0 *Etv4;5* mutant lungs have fewer alveoli that are larger in size (A,B). At P7, a much complex alveolar network is found in the control lung, as the result of the beginning of alveologenesis (C). Alveologenesis does not precede normally in the Etv4;5 mutant lung, which results in a simplified alveolar network (D). The alveolar simplification was quantified by measuring the mean linear intercept (MLI) as detailed in the materials/methods section (E). A significant increase in the relative MLI was observed in the *Etv4;5* mutant lungs ($P<0.05$ $N=3$). Data are presented as means (+SEM).

Figure 3: Distal lung histology of *Etv4;5* mutant lungs at birth and during alveologenesis.

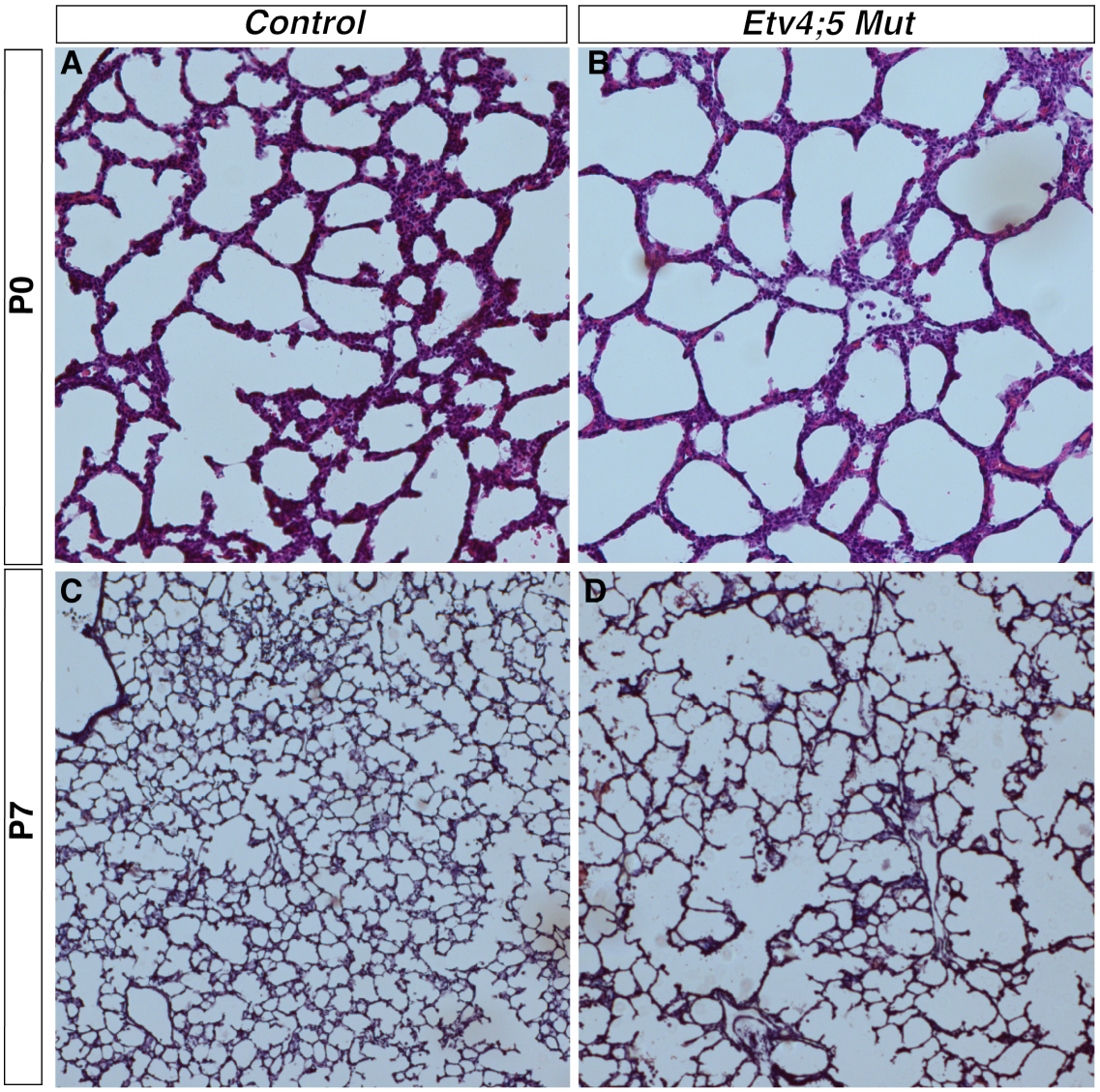

Figure 4: The alveolar epithelial cell lineages are not affected in the *Etv4;5* mutant lung.

(A,B) Representative immunofluorescent images of SFTPC (green), PDPN (red), and nuclei (blue) on the alveolar region of P0 control (A) and *Etv4;5* mutant (B) lungs. At P0 *Etv4;5* mutant lungs show no difference in the localization of either alveolar type I (PDPN) or alveolar type II (SFTPC) cells (A,B). Quantification of the percentage of alveolar type II cells at P0 confirmed that there was no difference (N=3) (C). Data are presented as means (+SEM).

Figure 4: The alveolar epithelial cell lineages are not affected in the *Etv4;5* mutant lung.

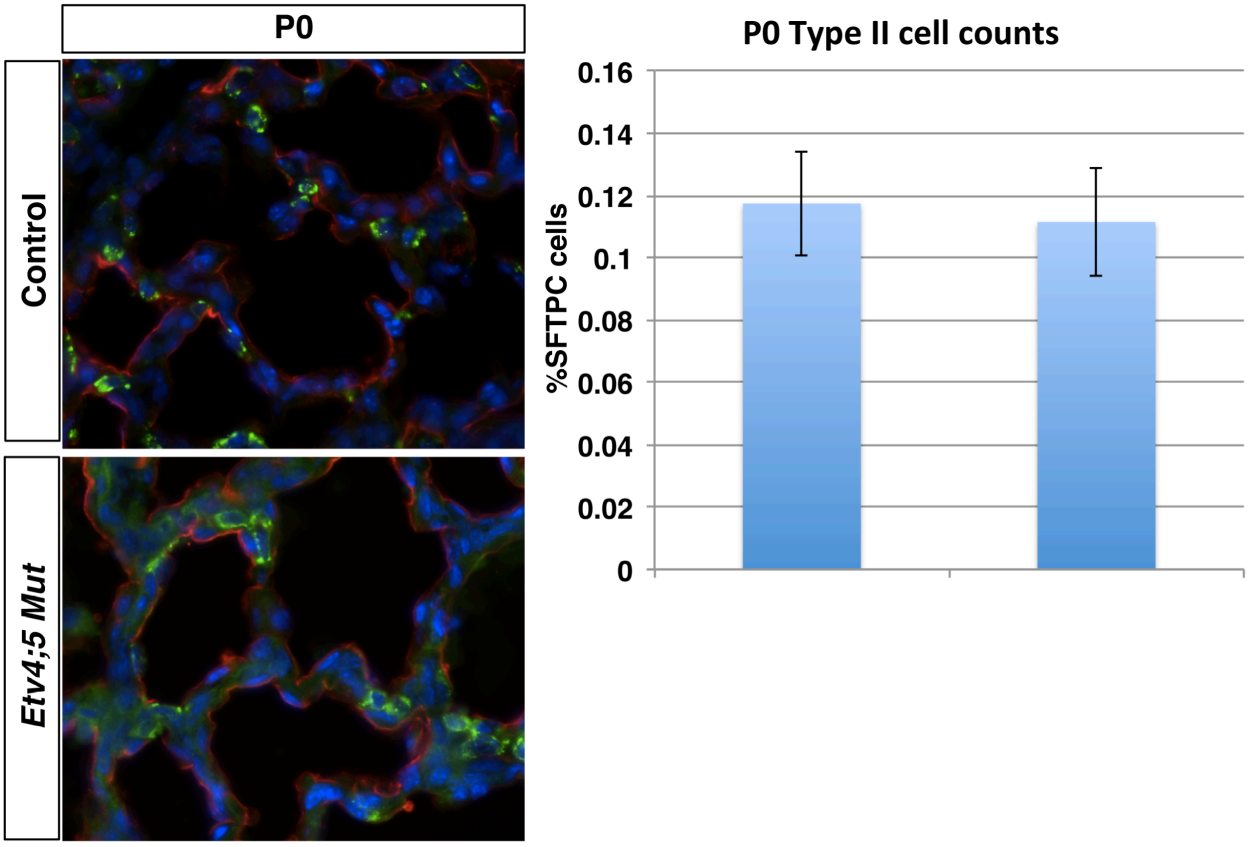

Figure 5: *Etv4;5* mutant lungs have fewer fibroblasts at P7.

(A-D) Representative images from frozen sections showing Pdgfra-GFP (green) reporter activity in either the control (A,C) or mutant (B,D) background. At P0 and P7 *Etv4;5* mutant lungs have fewer Pdgfra-GFP bright cells than control lungs (A-D). Quantification of the percentage of Pdgfra-GFP positive cells revealed that there is no difference in the ratio of Pdgfra-GFP positive cells to total number of cells in the *Etv4;5* mutant lung at P0 (N=3) (E). There is a statistically significant decrease in the percentage of Pdgfra-GFP positive cells in the *Etv4;5* mutant lung at P7 (N=3 $P<0.05$) (E). Data are presented as means (+SEM).

Figure 5: *Etv4;5* mutant lungs have fewer fibroblasts at P7.

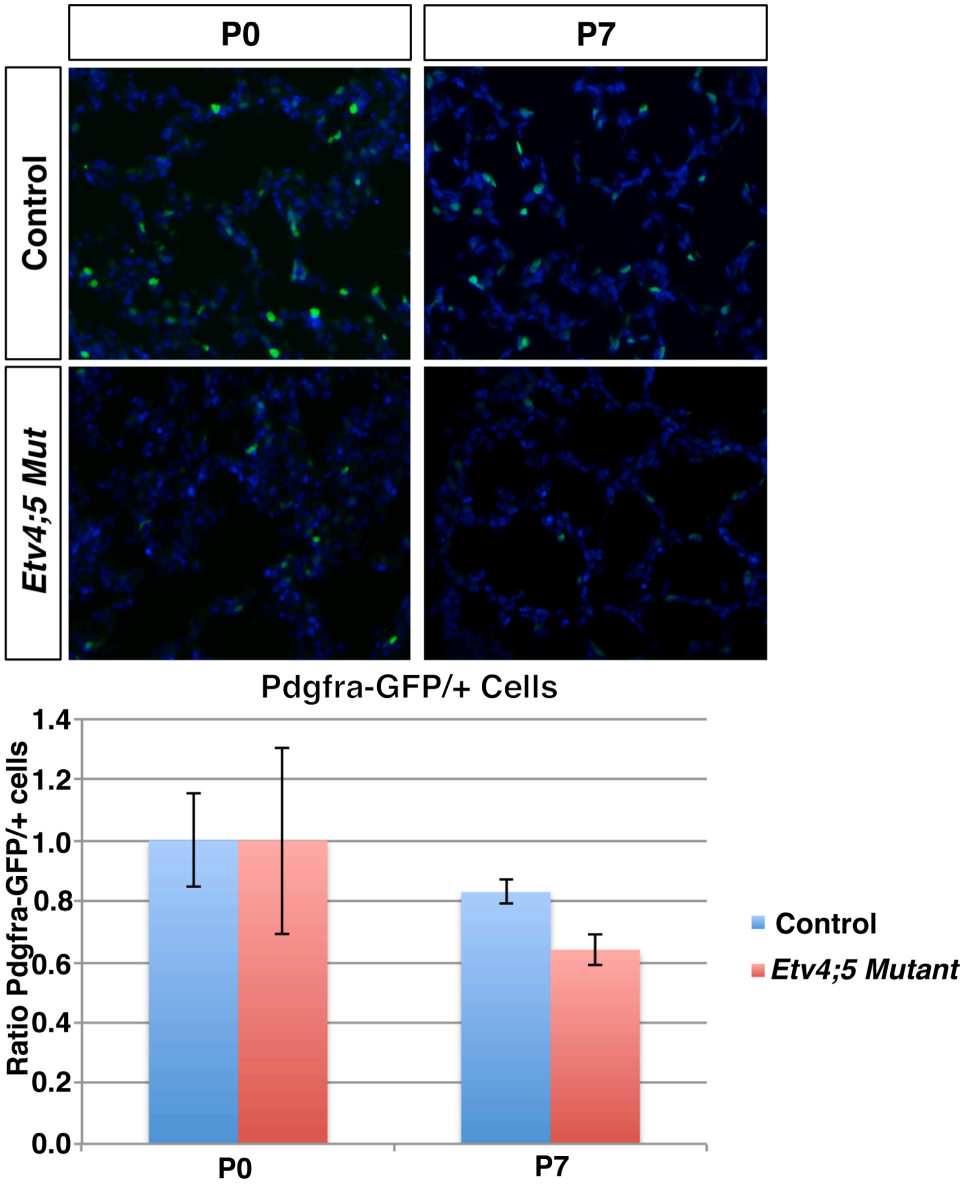

Figure 6: TAGLN staining is unaltered in the *Etv4;5* mutant lung.

(A,B) Representative immunofluorescent images of TAGLN (red) and nuclei (blue) on the alveolar region of P7 control (A) and *Etv4;5* mutant (B) lungs. Although we found that there were fewer myofibroblasts, we did not see any difference in the localization of the TAGLN staining in the alveolar region of the lung (A,B).

Figure 6: TAGLN staining is unaltered in the *Etv4;5* mutant lung.

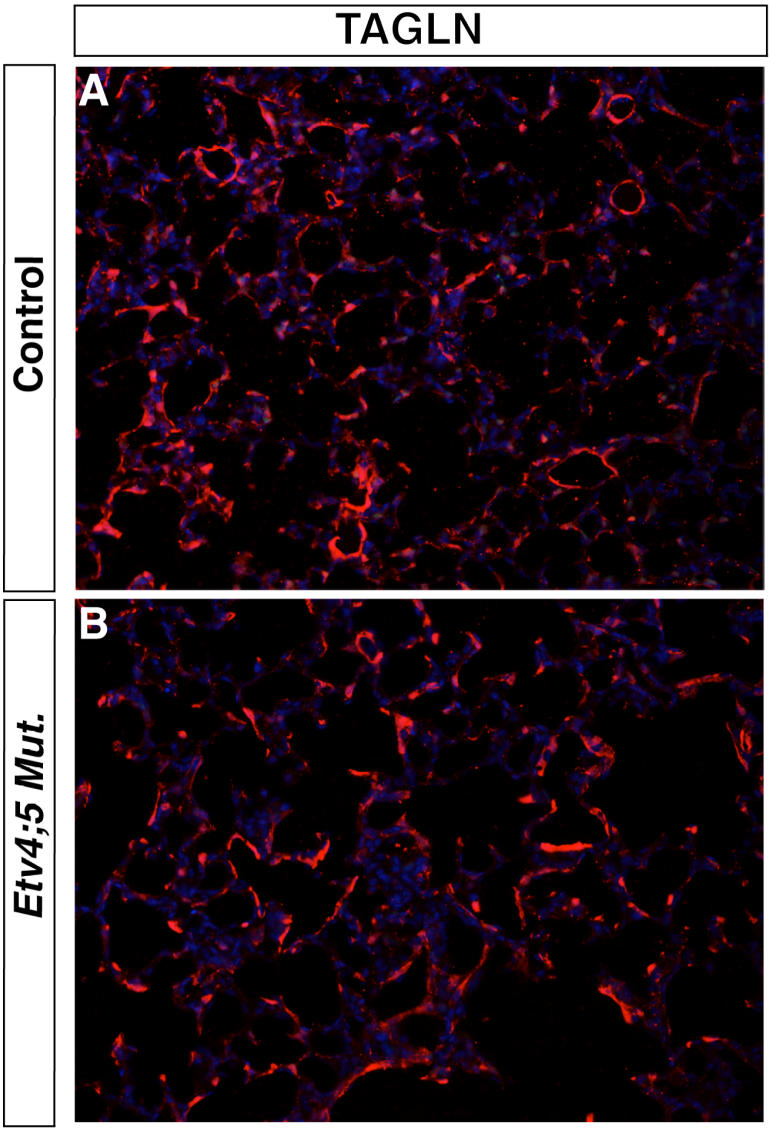

Figure 7: The Elastin ECM is not normally bundled in the alveolar walls of the *Etv4;5* mutant.

(A,B) Representative immunofluorescent images of Elastin (green) around the airways and in the alveolar region (inset) of P7 control (A) and *Etv4;5* mutant (B) lungs. At P7 the Elastin ECM is found in tight bundles lining the airways (A) and the alveolar walls (inset arrowheads). The fibers in the mutant lung appear to be normally localized around the airway and alveolar walls (B), but in the alveolar region of the lung, they do not appear to be bundled properly (arrowheads).

Figure 7: The Elastin ECM is not normally bundled in the alveolar walls of the *Etv4;5* mutant.

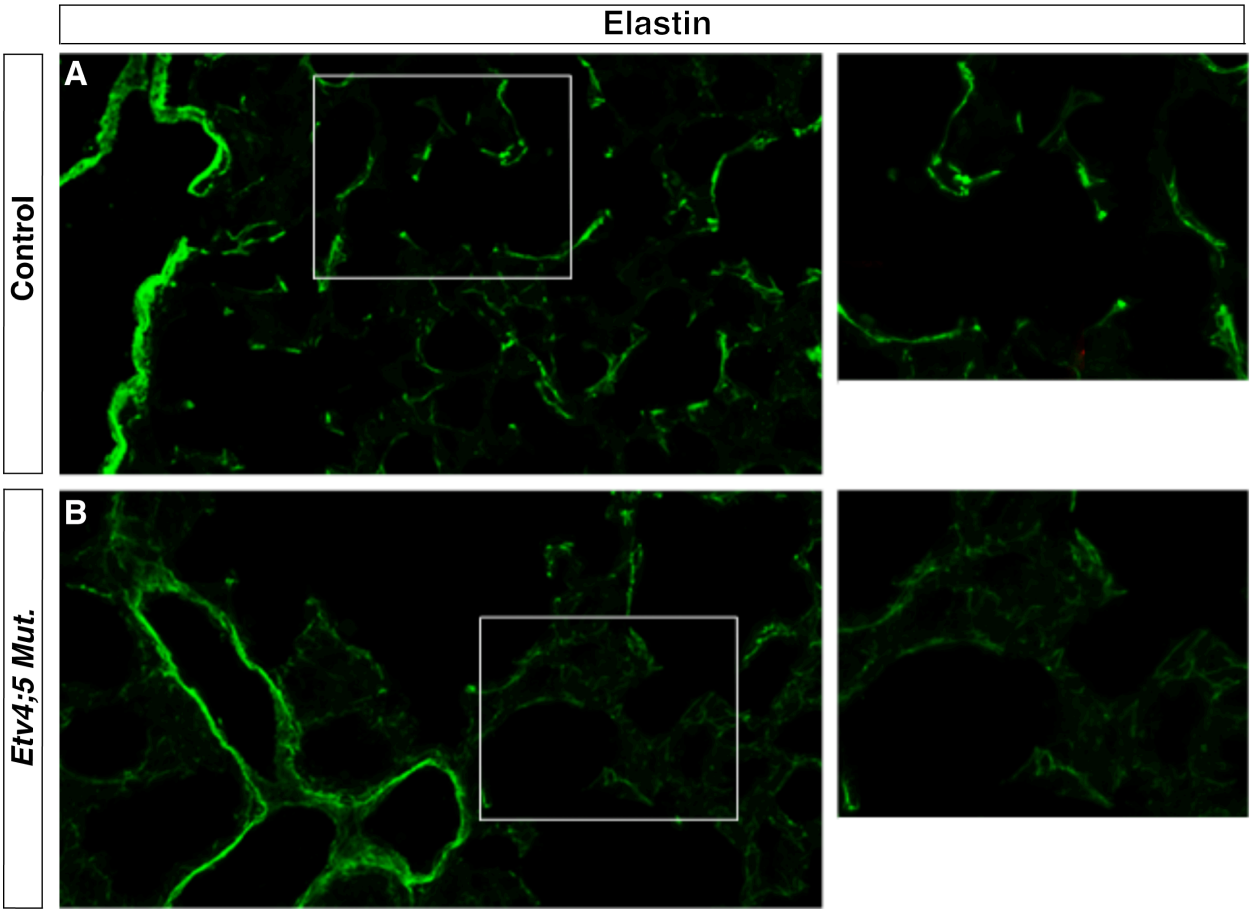

Figure 8: $Id2^{Cre/Ert2}$ shows high activity in the postnatal lung

(A,B) Representative whole mount images of Beta-Gal staining for Id2cre activity in control (A) and tamoxifen injected (B) lungs. After injections the $Id2^{Cre/Ert2}$ showed high activity in the distal regions of the lung (A,B). (C) The activity of the $Id2^{Cre/Ert2}$ was quantified by examining the *Etv5* flox excision rate in the *Etv5* transcript. At P8, The *Etv5* flox excision rate was approximately 60% in mutant lung (C). Data are presented as means (+SEM).

Figure 8: Id2$^{Cre/Ert2}$ shows high activity in the postnatal lung

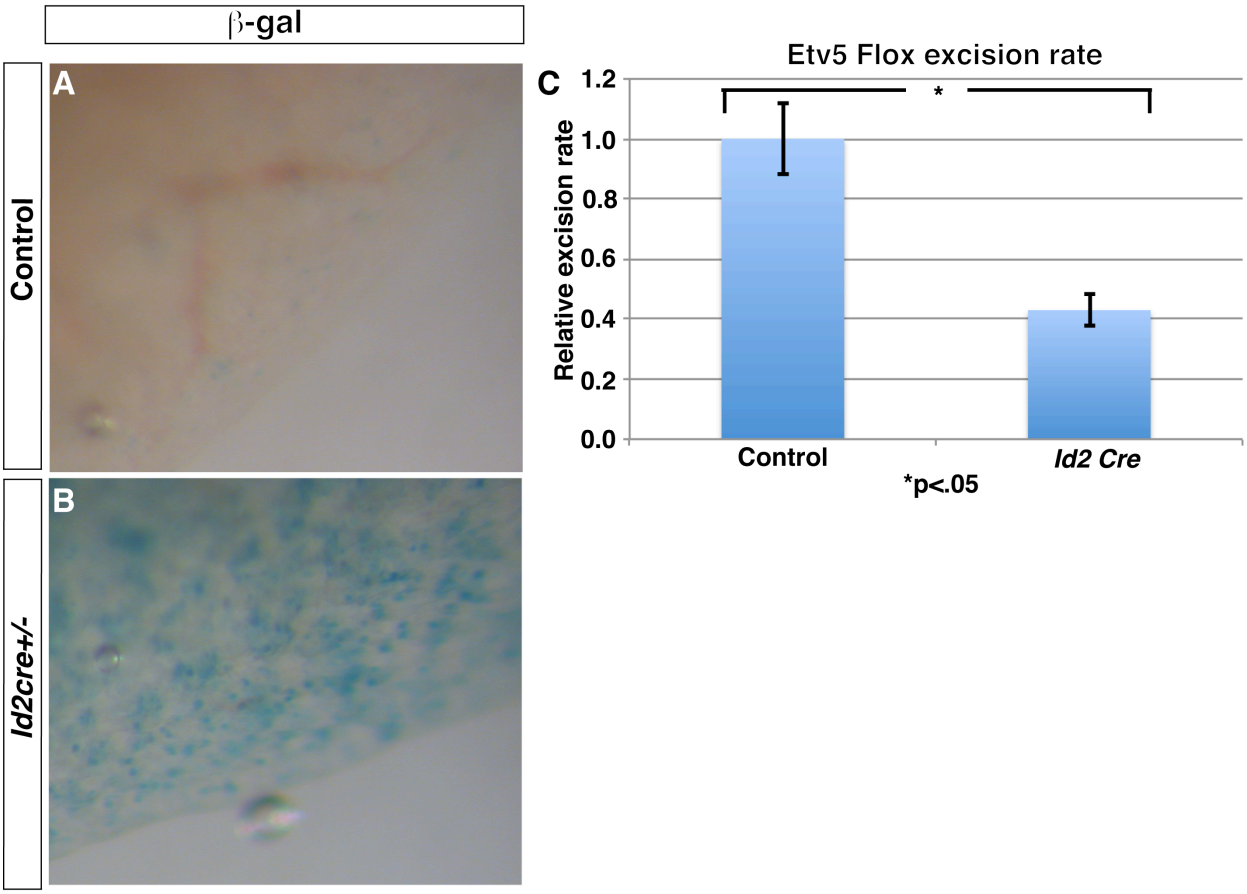

Figure 9. Conditional inactivation of the *Etv4;5* in the postnatal lung does effect alveolar development.

(A-B) Representative H&E stained frozen sections from the alveolar regions of P28 control and *Etv4;5* conditional lungs. At P28 *Etv4;5* conditional mutant are not phenotypically different from controls (A-B). The alveolar complexity was quantified by measuring the mean linear intercept (MLI) as detailed in the materials/methods section (C). We observed no difference in the relative MLI of control and Etv4;5 conditional mice at P28 (N=4) (C). Data are presented as means (+SEM).

Figure 9. Conditional inactivation of the *Etv4;5* in the postnatal lung does effect alveolar development.

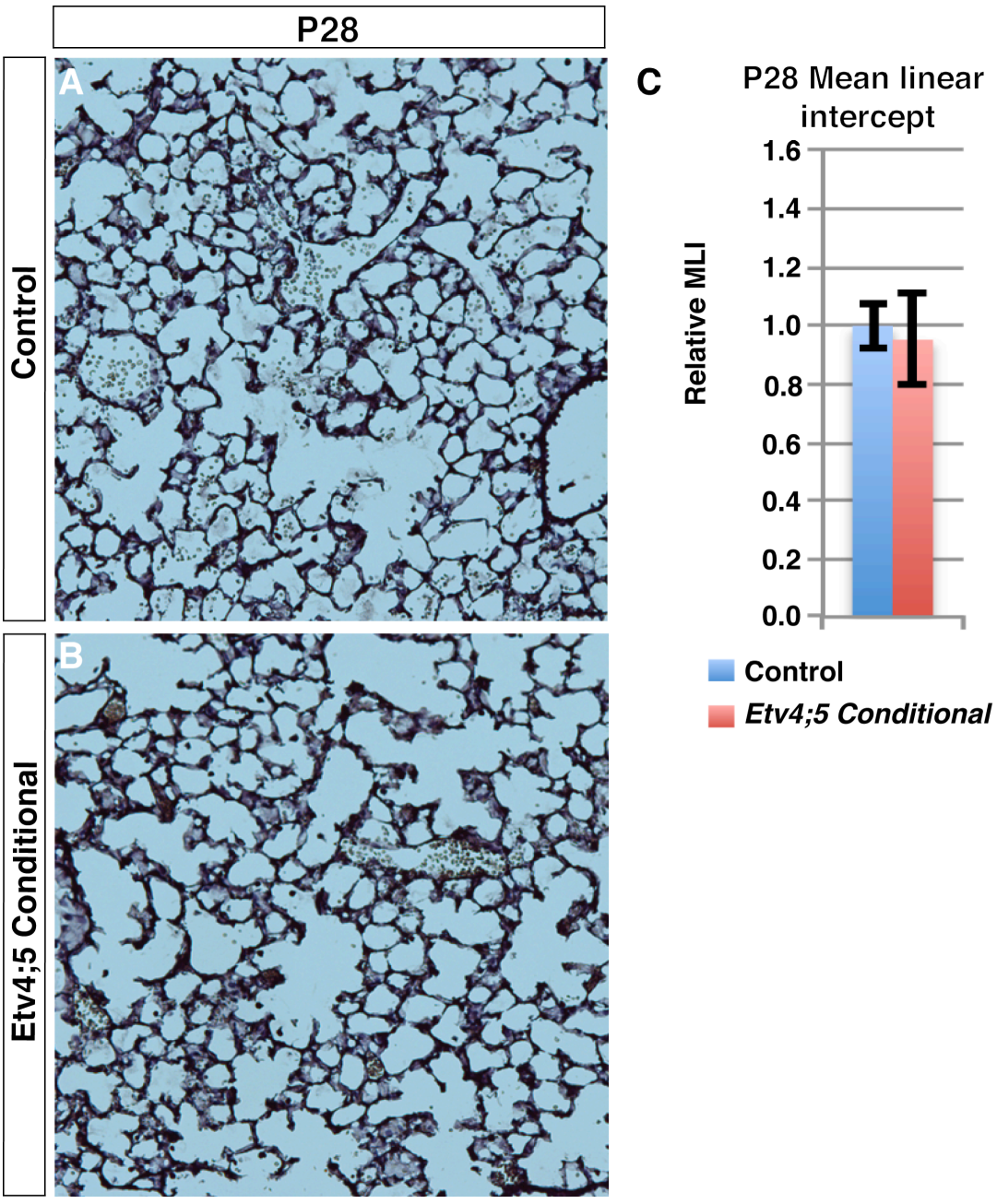

Appendix II: Identification of a novel allele of *Ift140*

Jamie Verheyden and John Herriges contributed equally to this appendix

Introduction:

Cilia are microtubule-based organelles that are highly conserved across most eukaryotic organisms (Pazour et al. 2003). In eukaryotes, the core of each cilium is a microtubule axonneme, which grows from a centriole-derived basal body. Each cilium is produced and maintained by the motor proteins, Kinesen and Dynein, and the intraflagellar transport (hereafter IFT) proteins, which interact with the motor proteins to allow for the transport of materials along the axoneme (Berbari et al. 2009). In eukaryotes, there are two major types of cilia, the motile cilia and the primary cilia. Motile cilia are found in a variety of tissue types, including the trachea and main bronchi of the lung, where they mediate the movement of extracellular materials like growth factors and mucus (Berbari et al. 2009). Primary cilia are largely immobile, and protrude from almost every cell in eukaryotes (Berbari et al. 2009, Novarino et al. 2011). Traditionally, primary cilia were thought to be vestigial organelles; however, recent findings have demonstrated that the primary cilia are critical for embryonic development.

One of the methods through which cilia control embryonic development is by the regulating SHH signaling (Berbari et al. 2009). The SHH signaling pathway is a critical mediator of embryonic development, where it regulates the patterning of tissues like the lung and limb (Pepicelli et al. 1998; Harfe et al. 2004). Recent studies have demonstrated that several components of the SHH signaling pathway, including PTC, SMO, and GLI proteins localize to primary cilia (Berbari et al. 2009). The essential role that cilia play in mediating SHH signaling has been demonstrated in several mutant IFT mouse lines, which have disrupted ciliogenesis. In the neural tube, where SHH signaling mediates dorsal/ventral patterning, *Ift88* and *Ift172* mutant mice display a decrease in

SHH signaling, which results in the loss motor neurons (Huangfu et al 2003). Interestingly, in the limb, inhibiting ciliogenesis through the mutation of IFT proteins like, *Ift122*, *Ift144*, and *Ift140* increases SHH signaling (Qin et al. 2011;Ashe et al. 2012; Cauruna et al. 2013). The discrepancy in how IFT proteins can have a different affect on SHH signaling in different tissues is not fully understood, however recent studies have suggested the activation in SHH signaling in the limb is the result of a decrease in the ratio of GLI repressor to GLI activator proteins (Qin et al. 2011).

In this study we performed an ENU forward mutagenesis screen to identify novel genes that are involved in mouse development. Among the mutations that we identified was a novel mutation in the IFT gene *Ift140*. Here we begin to characterize the role of *Ift140* in embryonic patterning and the regulation of SHH signaling in the limb.

Results/Discussion:

Screen:

To identify novel genes involve embryonic development we performed a standard three-generation forward ENU mutagenesis screen. From this screen we were able to identify multiple lines that had a variety of reproducible phenotypes. 4834 was one of the lines in which we identified a reproducible phenotype. Mutant mice in line 4834 presented with a variety of external phenotypes including; a smaller size, preaxial polydactyly, exencephaly, and with partial penetrance cleft lip and cleft palate (Figure 1A,B). In the body cavity, 4834 mutants developed: a four lobed liver, a fusion of the right lung lobes, a smaller spleen, and with varying penetrance an abnormally shaped heart (Figure 1B). In addition to the phenotypes that were seen at P0, we found that the frequency of mutant pups was much lower than the expected 25%, with only 10% of the

pups displaying mutant phenotypes. This suggested that either a portion of the mutant embryos were aborted prior to birth, or that the phenotypes were partially penetrant. To test these hypotheses, we collected embryos from line 4834 at E11.5. At this stage we found that approximately 25% of the embryos were mutant (N=10/42), suggesting that the lower percentage of mutant pups we saw at P0 was due to premature abortion. Additionally, when 4834 litters were taken at E13.5, several of the mutant embryos were degraded, suggesting that the premature abortion begins between E11.5 and E13.5. From these data we concluded that line 4834 contained a mutation that resulted in a reproducible phenotype that could be further mapped.

Line 4834 represents a novel mutation in Ift140.

To map the mutation associated with line 4834 we used we used simple sequence repeat linkage mapping (SSRP). Within the genome, we found one SSRP marker that was linked to the mutant phenotype, D17MIT133, which is located near the centromere of chromosome 17 (Figure 2A-B). There were hundreds of genes associated with this marker; however the lung lobation, liver lobation, and polydactyly phenotypes we observed in line 4834 suggested that the mutation was affecting left-right pattern development. By narrowing down the list of genes in that region to factors that may mediate left-right patterning, we identified the IFT protein, *Ift140*. *Ift140* was strong candidate gene, as the phenotypes we observed in the 4834 mutant embryos strongly resembled the phenotypes reported in ENU mutant lines for the closely related IFT genes, *Ift144* and *Ift122* (Qin et al. 2011;Ashe et al. 2012). When we sequenced the *Ift140* transcript we identified that there was an adenine to guanine substitution in the

mutant embryos which resulted in a Histidine to Arginine shift at amino acid 70 (Figure 3A-C). Although Histidine and Arginine are both positively charged amino acids the program PolyPhen-2 predicted that this amino acid change would “probably be damaging” to the function of IFT140. Additionally, this amino acid lies within a WD40 domain of IFT140, and is very highly conserved, suggesting that it is a functionally important. The WD40 domain is involved in protein binding therefore it is likely that this mutation would affect the ability IFT140 to be involved in intraflagellar transport. Furthermore, after we identified this mutation in *Ift140*, another group published an ENU induced mutation of *Ift140*, which presented with similar phenotypes to what we see in line 4834 (Cauruna et al. 2013). Together these data demonstrate that line 4834 contains a novel mutation in *Ift140*, which is predicted to inhibit the normal function of IFT140 during development.

Ift140 mutant mice have altered SHH signaling in the limb.

One of the most prominent defects we observed in the 4834 mutant line is the preaxial polydactyly in both the hindlimbs and forelimbs (Figure 4A-D). Previous studies have demonstrated that alterations in the SHH signaling pathway can lead to preaxial polydactyly phenotype similar to what we see in line 4834 (Litingtung et al. 2002). In addition, during development, cilia have to shown to mediate the SHH signaling pathway (Qin et al. 2011). This raised that possibility that, SHH signaling may be altered in the 4834 mutant limb buds.

To test this hypothesis, we examined whether SHH signaling is altered in 4834 mutant limb buds. By *in situ* hybridization, we found that *Shh* was ectopically expressed

in the mutant hindlimbs and forelimbs (Figure 5A-D). Furthermore, we found that the expression domains of the SHH signaling readout, *Gli1* was also expanded in the anterior region of the forelimb and hindlimb (Figure 5E-H). Finally, we saw that expression of the *Shh* expression mediator dHand was expanded in the forelimb of the *If140* mutants, but not the hindlimb (Figure 5I-L) (Chartie et al. 2000). Interestingly, when we compared the expression changes that we observed in our *Ift140* line to what was shown in the published *Ift140* ENU line, there were a few differences. First, they saw a more expanded *Shh* expression domain in the forelimb than the hindlimb, while we see an equal expansion of *Shh* in both the hindlimb and the forelimb (Miller et al. 2013). Second, they see a more consistent change in *dHand* expression than we do in our mutation. The differences between the phenotypes seen in the two *Ift140* lines could be due a different levels of functionality of mutated IFT140 protein. Additionally, this could be due to the slight differences in the stages of the embryos were used.

Conclusions:

In this study we performed an ENU mutagenesis screen to identify novel genes involved in mouse development. We were able to identify a novel mutation in the intraflagellar transport protein *Ift140*. This mutation lies within a WD40 domain, suggesting that it would affect that ability of IFT140 to mediate transport within the cilia. Finally, our data suggests that the polydactyly in the hindlimb and forelimb are caused by a disruption in SHH signaling; however, more work would need to be done confirm this.

Materials and Methods:

Mice:

To identify novel genes involved in mouse development we performed a standard ENU mutagenesis screen. First, we mutagenized G0 C57Bl6 strain mice using ENU. Each mutagenized G0 male was outcrossed to FvB strain females, generating G1 male carriers. Next, we generated G2 carrier females by outcrossing the G1 males to FvB females. Finally the G2 females were backcrossed to the G1 male and their offspring (G3) were screened for phenotypic abnormalities at postnatal day zero (P0). The embryos used in these experiments were harvested from time-mated females, with noon the day of the vaginal plug counting as E0.5.

Sequencing:

Sequencing of line 4834 was performed using a standard Big Dye reaction.

RNA *in situ* Hybridization

RNA *in situ* hybridization was performed following a protocol that was adapted from previously published protocols (Wall and Hogan 1995; Abler et al. 2011; Herriges 2012). Briefly, wholemount tissues stored in methanol were rehydrated using PBS with 0.1% Tween (PBT). Tissues were then permeabilized using 10µg/ml proteinase K in PBT for 10 minutes. Tissues were fixed with 4% paraformaldehyde, 0.2% glutaraldehyde in PBT for 20 minutes. They were then washed and allowed to hybridize with probes at 70oC overnight. After the hybridization, tissues were washed three times, twenty minutes each in 2x SSC, 0.1% CHAPS, and then in 0.2x SSC, 0.1% CHAPS at 70oC. Tissues

were then washed in KTBT and blocked for 2 hours in 2% blocking solution (Roche) and 20% heat inactivated sheep serum (Sigma) in KTBT at room temperature. The tissues were then incubated overnight at 4˚C in the primary antibody, AP conjugated α-DIG, Fab fragment (Roche) at a dilution of 1:2000 using 2% blocking solution and 20% heat inactivated sheep serum in KTBT. The tissues were then washed 5 times, 1hour each in KTBT at room temperature. Following this, the tissues were washed twice, 5 minutes each with 0.1% Tween, 1mM Levamisole in ddH2O. Finally the tissues were stained in BM purple (Roche) containing 0.1% Tween and 1mM levamisole. The staining was carried out for varying amount of time depending on the probes until desired intensity, from 30 minutes to 8 hours.

Skeletal prep:

Skeletal preparations were performed using Alcian Blue and Alizarin Red and a standard protocol.

Figures:

Figure 1: Line 4834 presents with a variety of phenotypes.

(A) Mutant embryos at P0 and E11.5 present with a wide variety of phenotypes. Including preaxial polydactyly, abnormal somite development, and exencephaly. (B) A complete list of the phenotypes associated with line 4834 and their penetrance.

Figure 1: Line 4834 presents with a variety of phenotypes

A

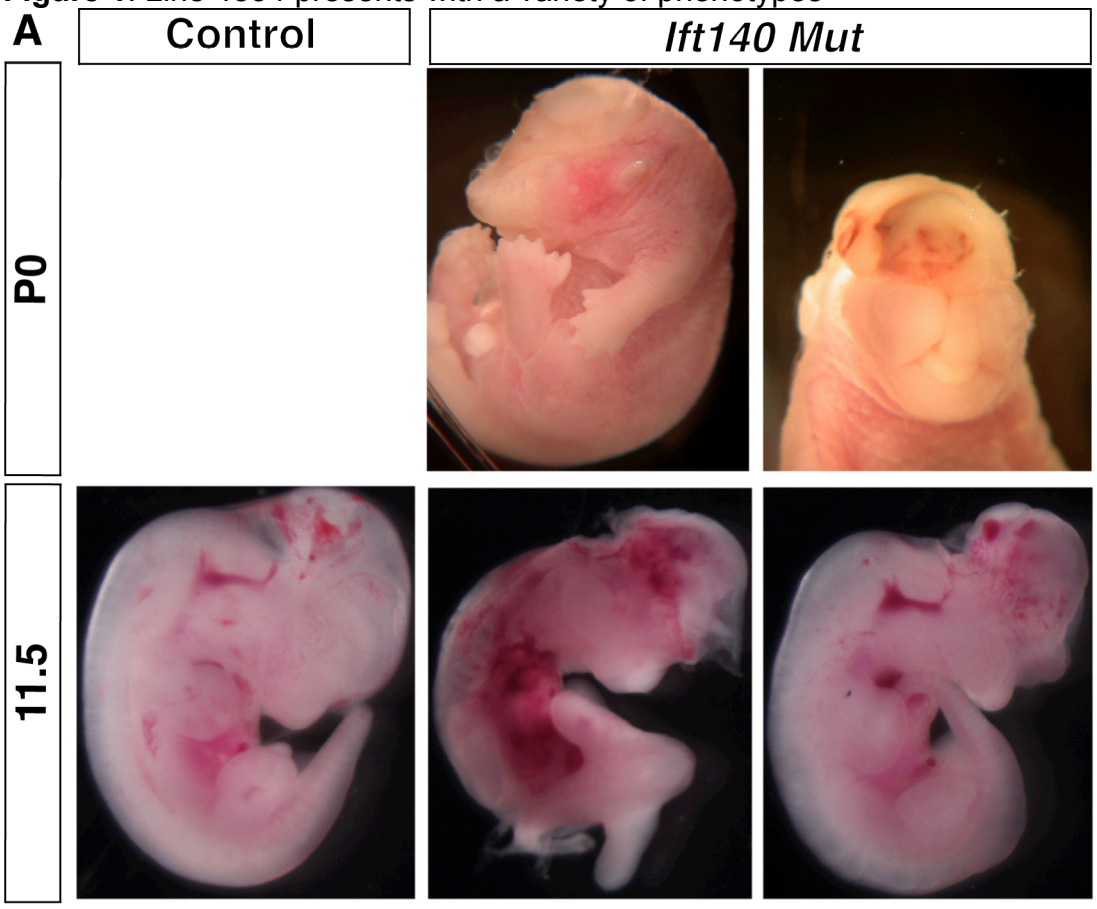

B

Phenotype	Penetrance
Preaxial Polydactyly	100% (N=10/10)
Four lobed liver	100% (N=10/10)
Exencephaly	100% (N=10/10)
Small Spleen	100% (N=5/5)
Fusion of right lung lobes	100% (N=5/5)
Disrupted somite development*	100% (N=7/7)
Cleft Palate	30% (N=3/10)
Cleft Lip	40% (N=4/10)
Abnormal heart shape	60% (N= 6/10)

*Only examined in embryonic samples

Figure 2: SSRP mapping revealed that the mutation in Line 4834 mapped to chromosome 17.

In line 4834 we performed SSRP mapping.(A) The only SSRP marker that was 100% homozygous Bl6 (B) in all of the mutant embryos was D17Mit133. The surrounding markers D17Mit106 and D17MIT9 were both mostly Bl6 (B); however, some mutants were Hets (H)for Bl6 and FvB at those markers. (B) Marker D17MIT133 is close to the centromere of chromosome 17 and is associated with hundreds of genes. The graphics in 2B were modified from the MGI database.

Figure 2: SSRP mapping revealed that the mutation in Line 4834 mapped to chromosome 17.

A

Embryo #	D17Mit133	D17Mit106	D17Mit9
9887-1	B	B	B
9889-2	B	B	B
9890-1	B	B	B
9890-2	B	H	H
8276-1	B	H	H
8447-1	B	B	
8447-2	B	B	

B

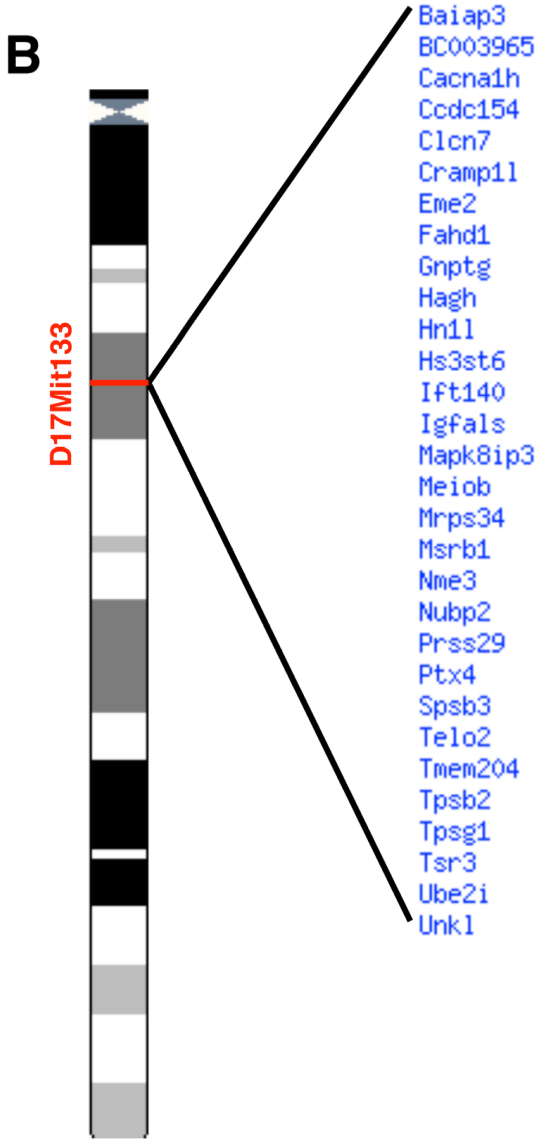

Figure 3. Line 4834 contains a mutation in *Ift140* that results in an amino acid change at amino acid seventy.

(A) Big dye sequencing revealed that line 4834 contains a C-A mutation. (B) This results in a Histidine to Arginine change at amino acid 70 on Ift40. This Histidine lies within a WD40 domain and is highly conserved.

Figure 3. Line 4834 contains a mutation in *Ift140* that results in an amino acid change at amino acid seventy.

A

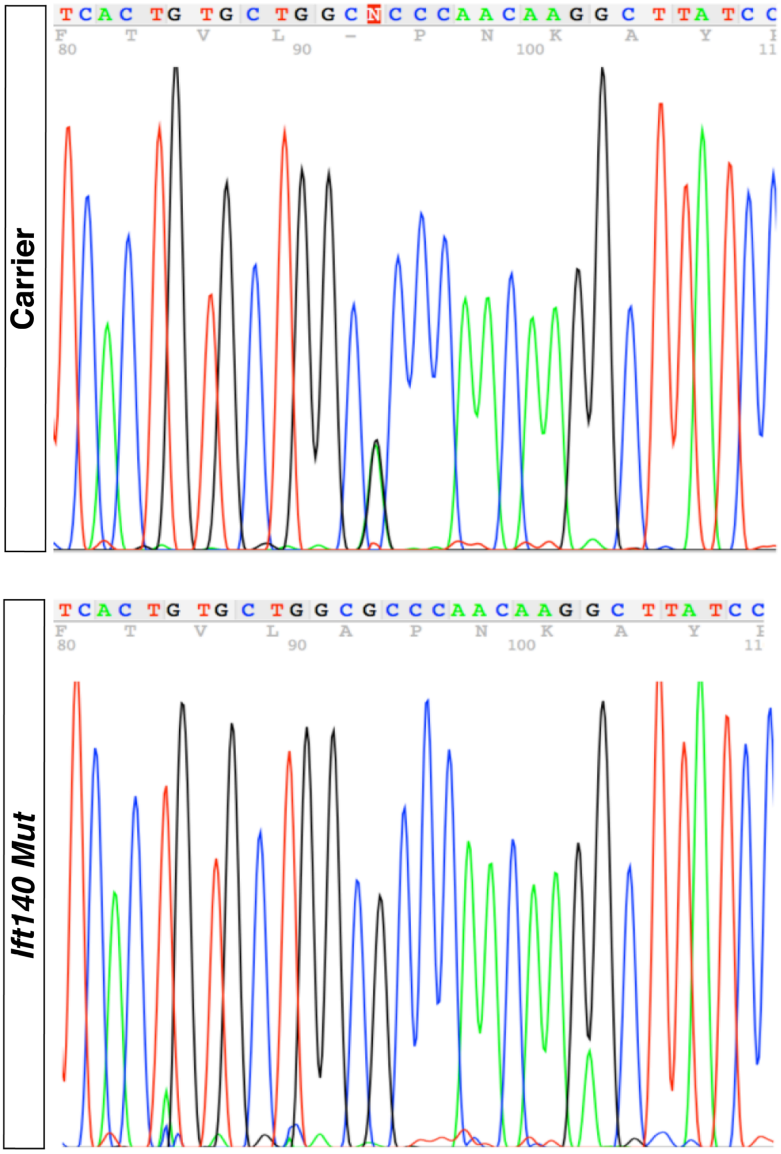

B

Species	Amino Acid Sequence
Mouse	HIERSFQATSLCWHPTRLILAIGW
Human	HVERPFRVASLCWHPTRLVLAVGW
Cow	HVERSFRVTCLCWHPTRLILAIGW
Chicken	HIERSFQVTSLSWHPSRLILAAGW
Zebrafish	HVERGFSPSLLQWHPNKPLLAVGW
Opossum	HIERSFRAMSLSWHPTRMILAIGW
Xenopus	QIKRTSHPTVLSWHPTKRTLVTGW
4834 Line	HIERSFQATSLCWRPTRLILAIGW

Figure 4: *Ift140* mutant mice develop preaxial polydactyly in both the hindlimbs and the forelimbs.

At P0, control pups contain five digits in the forelimb (A). *Ift140* Mutant embryos develop preaxial polydactyly in the forelimbs by P0 (C). At P0, control pups contain five digits in the hindlimb (C). *Ift140* Mutant embryos develop preaxial polydactyly in the hindlimbs by P0 (D).

Figure 4: *Ift140* mutant mice develop preaxial polydactyly in both the hindlimbs and the forelimbs.

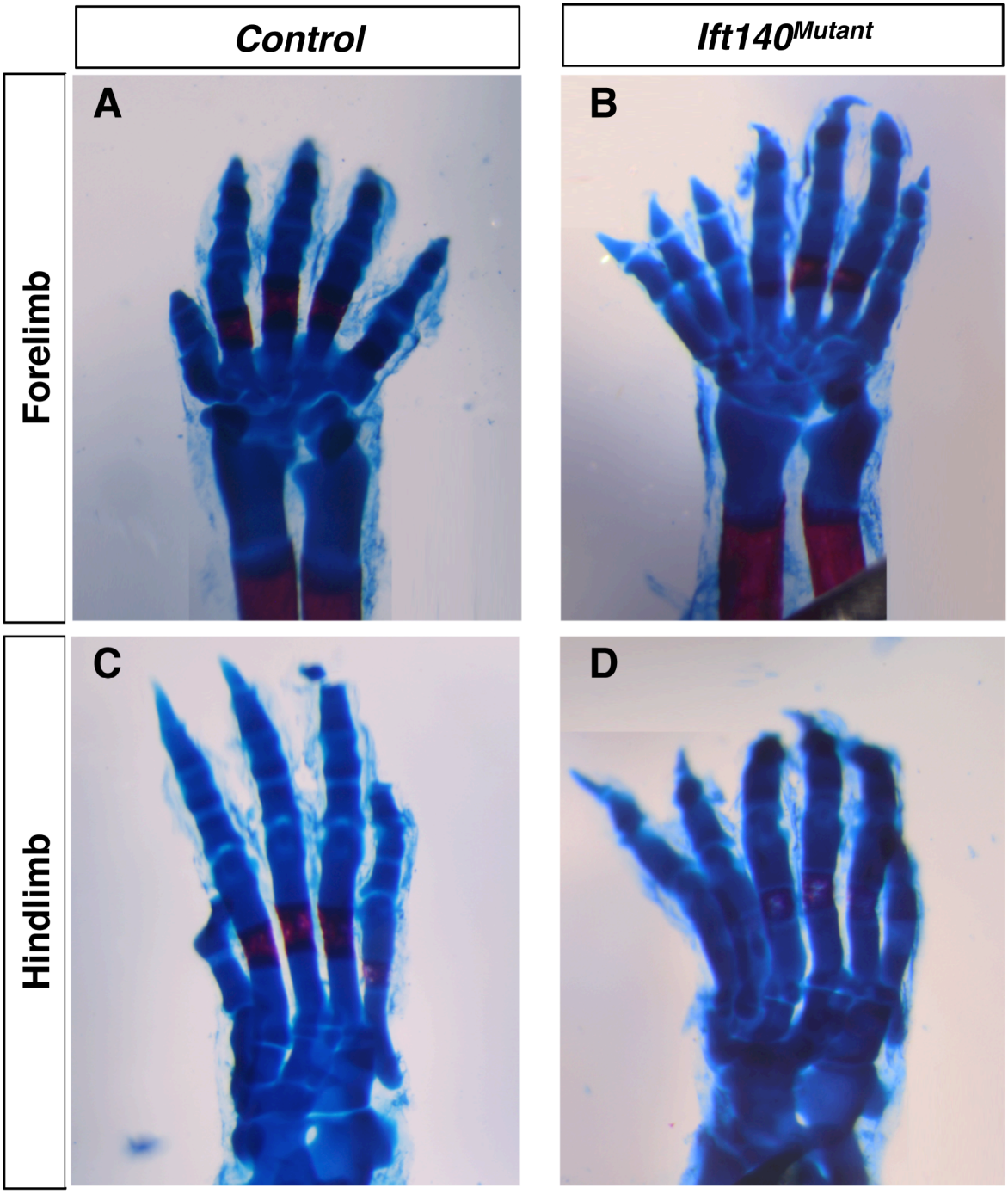

Figure 5: SHH signaling is disrupted in the *Ift140* mutant limbs.

(A-L) Representative RNA *in situ* hybridization E11.25-E11.5 limb buds. At E11.5, the *Ift140* mutant limb shows ectopic Shh expression in the anterior region (top) of the forelimb and hindlimb (A-D). The Gli1 expression domain appears to be partially expanded in the forelimb of the *Ift140* mutant (E,F), but not in the hindlimb (G,H). The *dHand* expression domain is also expanded in the forelimb (I,J), but not the hindlimb (K,L).

Figure 5: SHH signaling is disrupted in the *Ift140* mutant limbs.

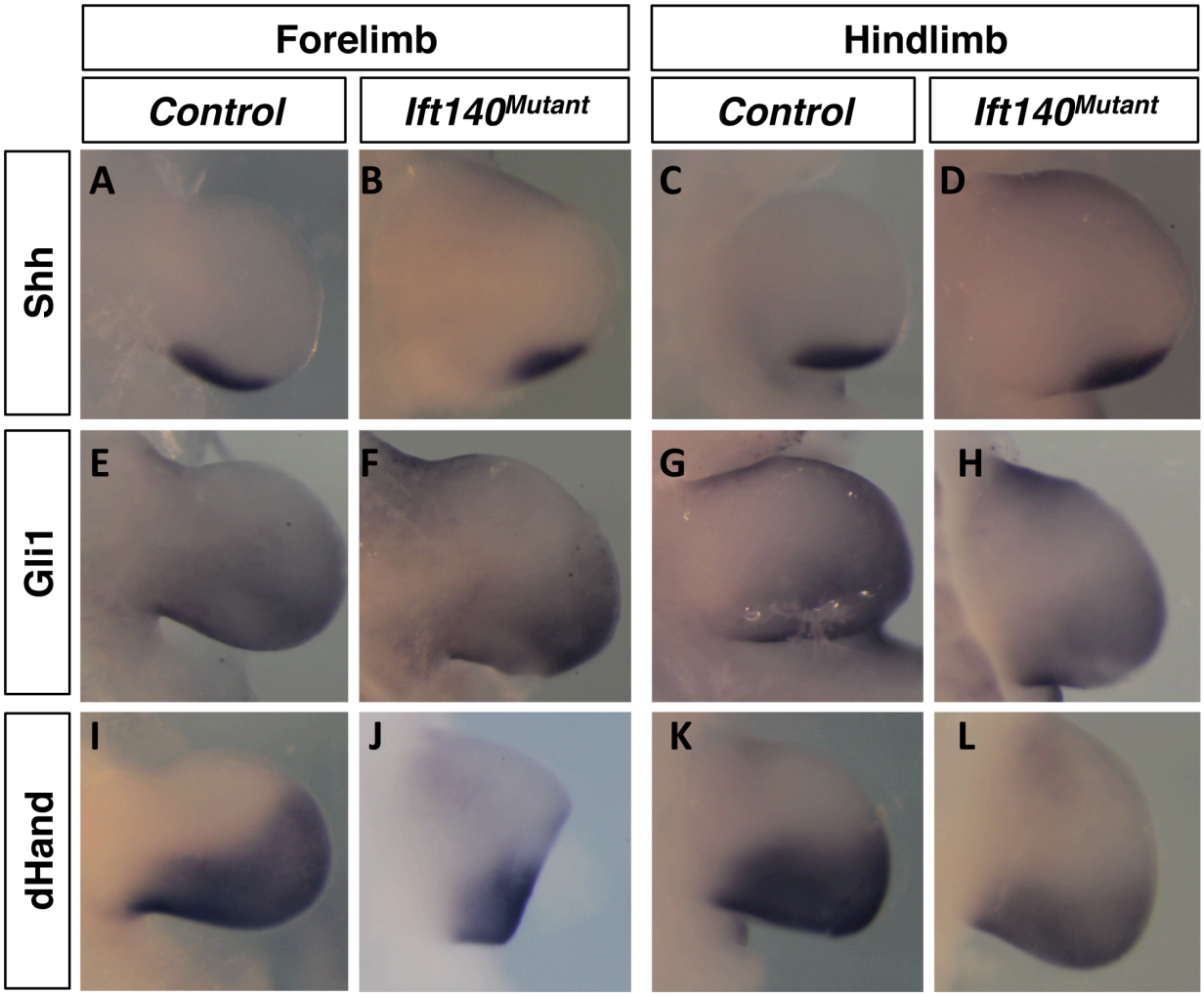

References:

Abler LL, Mansour SL, Sun X. 2009. Conditional gene inactivation reveals roles for Fgf10 and Fgfr2 in establishing a normal pattern of epithelial branching in the mouse Cirulis lung. Dev Dyn. 238(8):1999-2013

Abler LL, Mehta V, Keil KP, Joshi PS, Flucus CL, Hardin HA, Schmitz CT, Vezina CM. 2011. A high throughput in situ hybridization method to characterize mRNA expression patterns in the fetal mouse lower urogenital tract. J Vis Exp. (54), e2912.

Arber S, Han B, Mendelsohn M, Smith M, Jessell TM, Sockanathan S. 1999. Requirement for the homeobox gene Hb9 in the consolidation of motor neuron identity. Neuron 23:659-674.

Albig AR, Roy TG, Becenti DJ, Schiemann WP. 2007. Transcriptase analysis of endothelial cell gene expression induced by growth on matrigel matrices: identification and characterization of MAGP-2 and lumican as novel regulators of angiogenesis. Angiogenesis.10(3):197-216.

Anderson MJ, Naiche LA, Wilson CP, Elder C, Swing DA, Lewandoski M. 2013.TCreERT2, a transgenic mouse line for temporal control of Cre-mediated recombination in lineages emerging from the primitive streak or tail bud. PLoS One. 30;8(4):e62479.

Ashe A, Butterfield NC, Town L, Courtney AD, Cooper AN, Ferguson C, Barry R, Olsson F, Liem KF Jr, Parton RG, Wainwright BJ, Anderson KV, Whitelaw E, Wicking C. 2012. Mutations in mouse Ift144 model the craniofacial, limb and rib defects in skeletal ciliopathies. Hum Mol Genet. 2012 Apr 15;21(8):1808-23.

Aubin J, Lemieux M, Tremblay M, Bérard J, Jeannotte L. 1997. Early postnatal lethality in Hoxa-5 mutant mice is attributable to respiratory tract defects. Dev Biol 192:432-445.

Auden A, Caddy J, Wilanowski T, Ting SB, Cunningham JM, Jane SM. 2006. Spatial and temporal expression of the Grainyhead-like transcription factor family during murine development. Gene Expr Patterns 6:964-970.

Ayadi A, Zheng H, Sobieszczuk P, Buchwalter G, Moerman P, Alitalo K, Wasylyk B. 2001. Net-targeted mutant mice develop a vascular phenotype and up-regulate egr-1. EMBO J 20:5139-5152.

Badesch DB, Lee PD, Parks WC, Stenmark KR. Insulin-like growth factor I stimulates elastin synthesis by bovine pulmonary arterial smooth muscle cells. Biochem Biophys Res Commun 1989;160:382–387

Barbacci E, Reber M, Ott MO, Breillat C, Huetz F, Cereghini S. 1999. Variant hepatocyte nuclear factor 1 is required for visceral endoderm specification.

Development 126:4795-4805.

Becker MB, Zülch A, Bosse A, Gruss P. 2001. Irx1 and Irx2 expression in early lung development. Mech Dev 106:155-158.

Beenken A, Mohammadi M. 2009. The FGF family: biology, pathophysiology and therapy. Nat Rev Drug Discov. 2009 Mar;8(3):235-53.

Bellusci S, Henderson R, Winnier G, Oikawa T, Hogan BL. 1996. Evidence from normal expression and targeted misexpression that bone morphogenetic protein (Bmp-4) plays a role in mouse embryonic lung morphogenesis. Development 122:1693-1702.

Bellusci S, Furuta Y, Rush MG, Henderson R, Winnier G, Hogan BL. 1997. Involvement of Sonic hedgehog (Shh) in mouse embryonic lung growth and morphogenesis. Development. 1997 Jan;124(1):53-63.

Bellusci S, Grindley J, Emoto H, Itoh N, Hogan BL. 1997. Fibroblast growth factor 10 (FGF10) and branching morphogenesis in the embryonic mouse lung. Development 124: 4867–4878.

Benjamin JT, Smith RJ, Halloran BA, Day TJ, Kelly DR, Prince LS. 2007. FGF-10 is decreased in bronchopulmonary dysplasia and suppressed by Toll-like receptor activation. Am J Physiol Lung Cell Mol Physiol.;292(2):L550-8.

Berbari NF, O'Connor AK, Haycraft CJ, Yoder BK. 2009. The primary cilium as a complex signaling center. Curr Biol. 19(13):R526-35.

Bermingham JR, Scherer SS, O'Connell S, Arroyo E, Kalla KA, Powell FL, Rosenfeld MG. 1996. Tst-1/Oct-6/SCIP regulates a unique step in peripheral myelination and is required for normal respiration. Genes Dev 10:1751-1762.

Bermingham JR, Shumas S, Whisenhunt T, Sirkowski EE, O'Connell S, Scherer SS, Rosenfeld MG. 2002. Identification of genes that are downregulated in the absence of the POU domain transcription factor pou3f1 (Oct-6, Tst-1, SCIP) in sciatic nerve. J Neurosci 22:10217-10231.

Bi W, Huang W, Whitworth DJ, Deng JM, Zhang Z, Behringer RR, de Crombrugghe B. 2001. Haploinsufficiency of Sox9 results in defective cartilage primordia and premature skeletal mineralization. Proc Natl Acad Sci U S A 98:6698-6703.

Boglev Y, Wilanowski T, Caddy J, Parekh V, Auden A, Darido C, Hislop NR, Cangkrama M, Ting SB, Jane SM. 2011. The unique and cooperative roles of the Grainy head-like transcription factors in epidermal development reflect unexpected target gene specificity. Dev Biol 349:512-522.

Bosse A, Zülch A, Becker MB, Torres M, Gómez-Skarmeta JL, Modolell J, Gruss P.

1997. Identification of the vertebrate Iroquois homeobox gene family with overlapping expression during early development of the nervous system. Mech Dev 69:169-181.

Boström H, Willetts K, Pekny M, Levéen P, Lindahl P, Hedstrand H, Pekna M, Hellström M, Gebre-Medhin S, Schalling M, Nilsson M, Kurland S, Törnell J, Heath JK, Betsholtz C. 1996. PDGF-A signaling is a critical event in lung alveolar myofibroblast development and alveogenesis. Cell. 85 863-73.

Boucherat O, Franco-Montoya ML, Thibault C, Incitti R, Chailley-Heu B, Delacourt C, Bourbon JR. 2007. Gene expression profiling in lung fibroblasts reveals new players in alveolarization. Physiol Genomics. 32:128-41.

Bourbon J, Boucherat O, Chailley-Heu B, Delacourt C. 2005. Control mechanisms of lung alveolar development and their disorders in bronchopulmonary dysplasia. Pediatr. Res. 57,38R -46R.

Cañadas V, Vilacosta I, Bruna I, Fuster V. 2010. Marfan syndrome. Part 1: pathophysiology and diagnosis. Nat Rev Cardiol. 7:256-65.

Cardoso WV, Lu J. 2006. Regulation of early lung morphogenesis: questions, facts and controversies. Development 133: 1611–1624.

Cardoso WV. 1995. Transcription factors and pattern formation in the developing lung. Am J Physiol 269:L429-442.

Cardoso WV, Whitsett JA. 2008. Resident cellular components of the lung: developmental aspects. Proc Am Thorac Soc 5:767-771.

Carta L, Pereira L, Arteaga-Solis E, Lee-Arteaga SY, Lenart B, Starcher B, Merkel CA, Sukoyan M, Kerkis A, Hazeki N, Keene DR, Sakai LY, Ramirez F. 2006. Fibrillins 1 and 2 perform partially overlapping functions during aortic development. J Biol Chem. 281:8016-23.

Caruana G, Farlie PG, Hart AH, Bagheri-Fam S, Wallace MJ, Dobbie MS, Gordon CT, Miller KA, Whittle B, Abud HE, Arkell RM, Cole TJ, Harley VR, Smyth IM, Bertram JF. 2013. Genome-wide ENU mutagenesis in combination with high density SNP analysis and exome sequencing provides rapid identification of novel mouse models of developmental disease. PLoS One. 8(3):e55429.

Carver EA, Jiang R, Lan Y, Oram KF, Gridley T. 2001. The mouse snail gene encodes a key regulator of the epithelial-mesenchymal transition. Mol Cell Biol 21:8184-8188.

Cermenati S, Moleri S, Cimbro S, Corti P, Del Giacco L, Amodeo R, Dejana E, Koopman P, Cotelli F, Beltrame M. 2008. Sox18 and Sox7 play redundant roles in vascular development. Blood 111:2657-2666.

Chapman DL, Garvey N, Hancock S, Alexiou M, Agulnik SI, Gibson-Brown JJ, Cebra-Thomas J, Bollag RJ, Silver LM, Papaioannou VE. 1996. Expression of the T-box family genes, Tbx1-Tbx5, during early mouse development. Dev Dyn 206:379-390.

Charité J, McFadden DG, Olson EN. 2000. The bHLH transcription factor dHAND controls Sonic hedgehog expression and establishment of the zone of polarizing activity during limb development. Development.127(11):2461-70.

Chatonnet F, Thoby-Brisson M, Abadie V, Domínguez del Toro E, Champagnat J, Fortin G. 2002. Early development of respiratory rhythm generation in mouse and chick. Respir Physiol Neurobiol 131:5-13.

Chen C, Ouyang W, Grigura V, Zhou Q, Carnes K, Lim H, Zhao GQ, Arber S, Kurpios N, Murphy TL, Cheng AM, Hassell JA, Chandrashekar V, Hofmann MC, Hess RA, Murphy KM. 2005. ERM is required for transcriptional control of the spermatogonial stem cell niche. Nature 436:1030-1034.

Chen ZH, Kim HP, Sciurba FC, Lee SJ, Feghali-Bostwick C, Stolz DB, Dhir R, Landreneau RJ, Schuchert MJ, Yousem SA, Nakahira K, Pilewski JM, Lee JS, Zhang Y, Ryter SW, Choi AM. 2008. Egr-1 regulates autophagy in cigarette smoke-induced chronic obstructive pulmonary disease. PLoS One 3:e3316.

Chen L, Acciani T, Le Cras T, Lutzko C, Perl AK. 2012. Dynamic regulation of platelet-derived growth factor receptor α expression in alveolar fibroblasts during realveolarization. Am J Respir Cell Mol Biol. 47(4):517-27.

Chen JK, Taipale J, Young KE, Maiti T, Beachy PA. 2002. Small molecule modulation of Smoothened activity. Proc Natl Acad Sci U S A. 99(22):14071-6.

Choi JS, Zheng LT, Ha E, Lim YJ, Kim YH, Wang YP, Lim Y. 2006. Comparative genomic hybridization array analysis and real-time PCR reveals genomic copy number alteration for lung adenocarcinomas. Lung 184:355-362.

Chokas AL, Trivedi CM, Lu MM, Tucker PW, Li S, Epstein JA, Morrisey EE. 2010. Foxp1/2/4-NuRD interactions regulate gene expression and epithelial injury response in the lung via regulation of interleukin-6. J Biol Chem 285:13304-13313.

Chong JL, Wenzel PL, Sáenz-Robles MT, Nair V, Ferrey A, Hagan JP, Gomez YM, Sharma N, Chen HZ, Ouseph M, Wang SH, Trikha P, Culp B, Mezache L, Winton DJ, Sansom OJ, Chen D, Bremner R, Cantalupo PG, Robinson ML, Pipas JM, Leone G. 2009. E2f1-3 switch from activators in progenitor cells to repressors in differentiating cells. Nature 462:930-934.

Chotteau-LelieAvre, et al. (1997) Differential expression patterns of the PEA3group transcription factors through murine embryonic development. Oncogene. 15, 937-52

Christoffels VM, Keijser AG, Houweling AC, Clout DE, Moorman AF. 2000. Patterning the embryonic heart: identification of five mouse Iroquois homeobox genes in the developing heart. Dev Biol 224:263-274.

Cirulis JT, Bellingham CM, Davis EC, Hubmacher D, Reinhardt DP, Mecham RP,et al. 2008 Fibrillins, fibulins, and matrix-associated glycoprotein modulate the kinetics and morphology of in vitro self-assembly of a recombinant elastin-likepolypeptide. Biochemistry;47:12601–13.

Coffinier C, Gresh L, Fiette L, Tronche F, Schütz G, Babinet C, Pontoglio M, Yaniv M, Barra J. 2002. Bile system morphogenesis defects and liver dysfunction upon targeted deletion of HNF1beta. Development 129:1829-1838.

Coffinier C, Thépot D, Babinet C, Yaniv M, Barra J. 1999. Essential role for the homeoprotein vHNF1/HNF1beta in visceral endoderm differentiation. Development 126:4785-4794.

Cohen DR, Cheng CW, Cheng SH, Hui CC. 2000. Expression of two novel mouse Iroquois homeobox genes during neurogenesis. Mech Dev 91:317-321.

Cohen ED, Ihida-Stansbury K, Lu MM, Panettieri RA, Jones PL, Morrisey EE. 2009. Wnt signaling regulates smooth muscle precursor development in the mouse lung via a tenascin C/PDGFR pathway. J Clin Invest 119:2538-2549.

Colvin JS, White AC, Pratt SJ, Ornitz DM. 2001. Lung hypoplasia and neonatal death in Fgf9-null mice identify this gene as an essential regulator of lung mesenchyme. Development. 128:2095-106.

Combs MD, Knutsen RH, Broekelmann TJ, Toennies HM, Brett TJ, Miller CA, Kober DL, Craft CS, Atkinson JJ, Shipley JM, Trask BC, Mecham RP. 2013, Microfibril-associated glycoprotein 2 (MAGP2) loss of function has pleiotropic effects in vivo. J Biol Chem. 288:28869-80.

Compernolle V, Brusselmans K, Franco D, Moorman A, Dewerchin M, Collen D, Carmeliet P. 2003. Cardia bifida, defective heart development and abnormal neural crest migration in embryos lacking hypoxia-inducible factor-1alpha. Cardiovasc Res 60:569-579.

Coward WR, Saini G, Jenkins G. 2010. The pathogenesis of idiopathic pulmonary fibrosis. Ther Adv Respir Dis 4:367-388.

Davenport TG, Jerome-Majewska LA, Papaioannou VE. 2003. Mammary gland, limb and yolk sac defects in mice lacking Tbx3, the gene mutated in human ulnar mammary syndrome. Development 130:2263-2273.

Dabovic B, Chen Y, Choi J, Davis EC, Sakai LY, Todorovic V, Vassallo M, Zilberberg L, Singh A, Rifkin DB. 2011. Control of lung development by latent TGF-β binding proteins. J Cell Physiol. 226(6):1499-509.

Davidson JM, Zoia O, Liu JM. Modulation of transforming growth factor-b1 stimulated elastin and collagen production and proliferation in porcine vascular smooth muscle cells and skin fibroblasts by basic fibroblast growth factor, transforming growth factor–a, and insulinlike growth factor–I. J Cell Physiol 1993;155:149–156.

De Langhe SP, Carraro G, Tefft D, Li C, Xu X, Chai Y, Minoo P, Hajihosseini MK, Drouin J, Kaartinen V, Bellusci S. 2008. Formation and differentiation of multiple mesenchymal lineages during lung development is regulated by beta-catenin signaling. PLoS One 3:e1516.

de Launoit Y, Audette M, Pelczar H, Plaza S, Baert JL. 1998. The transcription of the intercellular adhesion molecule-1 is regulated by Ets transcription factors. Oncogene. 1998 Apr 23;16(16):2065-73.

Del Moral PM, De Langhe SP, Sala FG, Veltmaat JM, Tefft D, Wang K, Warburton D, Bellusci S. 2006. Differential role of FGF9 on epithelium and mesenchyme in mouse embryonic lung. Dev Biol 293: 77–89.

DeLisser HM, Helmke BP, Cao G, Egan PM, Taichman D, Fehrenbach M, Zaman A, Cui Z, Mohan GS, Baldwin HS, Davies PF, Savani RC. 2006. Loss of PECAM-1 function impairs alveolarization. J Biol Chem. 281(13):8724-31

De Moerlooze L, Spencer-Dene B, Revest J, Hajihosseini M, Rosewell I, Dickson C. 2000. An important role for the IIIb isoform of fibroblast growth factor receptor 2 (FGFR2) in mesenchymal-epithelial signalling during mouse organogenesis. Development 127: 483–492.

Denaxa M, Sharpe PT, Pachnis V. 2009. The LIM homeodomain transcription factors Lhx6 and Lhx7 are key regulators of mammalian dentition. Dev Biol 333:324-336.

Desmazières A, Decker L, Vallat JM, Charnay P, Gilardi-Hebenstreit P. 2008. Disruption of Krox20-Nab interaction in the mouse leads to peripheral neuropathy with biphasic evolution. J Neurosci 28:5891-5900.

Diez-Roux G, Banfi S, Sultan M, Geffers L, Anand S, Rozado D, Magen A, Canidio E, Pagani M, Peluso I, Lin-Marq N, Koch M, Bilio M, Cantiello I, Verde R, De Masi C, Bianchi SA, Cicchini J, Perroud E, Mehmeti S, Dagand E, Schrinner S, Nürnberger A, Schmidt K, Metz K, Zwingmann C, Brieske N, Springer C, Hernandez AM, Herzog S, Grabbe F, Sieverding C, Fischer B, Schrader K, Brockmeyer M, Dettmer S, Helbig C, Alunni V, Battaini MA, Mura C, Henrichsen CN, Garcia-Lopez R, Echevarria D, Puelles E, Garcia-Calero E, Kruse S, Uhr M, Kauck C, Feng G, Milyaev N, Ong CK, Kumar L, Lam M, Semple CA, Gyenesei A, Mundlos S, Radelof U, Lehrach H, Sarmientos P,

Reymond A, Davidson DR, Dollé P, Antonarakis SE, Yaspo ML, Martinez S, Baldock RA, Eichele G, Ballabio A. 2011. A high-resolution anatomical atlas of the transcriptome in the mouse embryo. PLoS Biol 9:e1000582.

Dobbs LG, Johnson MD, Vanderbilt J, Allen L, Gonzalez R.. 2010. The great big alveolar TI cell: evolving concepts and paradigms. Cell Physiol Biochem. 25, 55-62.

Domenga V, Fardoux P, Lacombe P, Monet M, Maciazek J, Krebs LT, Klonjkowski B, Berrou E, Mericskay M, Li Z, Tournier-Lasserve E, Gridley T, Joutel A. 2004. Notch3 is required for arterial identity and maturation of vascular smooth muscle cells. Genes Dev 18:2730-2735.

Domyan ET, Ferretti E, Throckmorton K, Mishina Y, Nicolis SK, Sun X. 2011. Signaling through BMP receptors promotes respiratory identity in the foregut via repression of Sox2. Development 138:971-981.

Domyan ET, Sun X. 2011. Patterning and plasticity in development of the respiratory lineage. Dev Dyn 240:477-485.

Donner AL, Episkopou V, Maas RL. 2007. Sox2 and Pou2f1 interact to control lens and olfactory placode development. Dev Biol 303:784-799.

Dunn TL, Mynett-Johnson L, Wright EM, Hosking BM, Koopman PA, Muscat GE. 1995. Sequence and expression of Sox-18 encoding a new HMG-box transcription factor. Gene 161:223-225.

Eblaghie MC, Reedy M, Oliver T, Mishina Y, Hogan BL. 2006. Evidence that autocrine signaling through Bmpr1a regulates the proliferation, survival and morphogenetic behavior of distal lung epithelial cells. Dev Biol 291:67-82.

Elluru RG, Whitsett JA. 2004. Potential role of Sox9 in patterning tracheal cartilage ring formation in an embryonic mouse model. Arch Otolaryngol Head Neck Surg 130:732-736.

Eswarakumar VP, Lax I, Schlessinger J. 2005. Cellular signaling by fibroblast growth factor receptors. Cytokine Growth Factor Rev. 16(2):139-49.

Faedo A, Tomassy GS, Ruan Y, Teichmann H, Krauss S, Pleasure SJ, Tsai SY, Tsai MJ, Studer M, Rubenstein JL. 2008. COUP-TFI coordinates cortical patterning, neurogenesis, and laminar fate and modulates MAPK/ERK, AKT, and beta-catenin signaling. Cereb Cortex 18:2117-2131.

Fajas L, Landsberg RL, Huss-Garcia Y, Sardet C, Lees JA, Auwerx J. 2002. E2Fs regulate adipocyte differentiation. Dev Cell 3:39-49.

Fischer A, Steidl C, Wagner TU, Lang E, Jakob PM, Friedl P, Knobeloch KP, Gessler M.

2007. Combined loss of Hey1 and HeyL causes congenital heart defects because of impaired epithelial to mesenchymal transition. Circ Res 100:856-863.

Fischer E, Legue E, Doyen A, Nato F, Nicolas JF, Torres V, Yaniv M, Pontoglio M. 2006. Defective planar cell polarity in polycystic kidney disease. Nat Genet 38:21-23.

Firulli BA1, Krawchuk D, Centonze VE, Vargesson N, Virshup DM, Conway SJ, Cserjesi P, Laufer E, Firulli AB. (2005). Altered Twist1 and Hand2 dimerization is associated with Saethre-Chotzen syndrome and limb abnormalities. Nat. Genet. 37, 373-381.

Fragkouli A, van Wijk NV, Lopes R, Kessaris N, Pachnis V. 2009. LIM homeodomain transcription factor-dependent specification of bipotential MGE progenitors into cholinergic and GABAergic striatal interneurons. Development 136:3841-3851.

Francois M, Koopman P, Beltrame M. 2010. SoxF genes: Key players in the development of the cardio-vascular system. Int J Biochem Cell Biol 42:445-448.

Franco-Montoya ML, Boucherat O, Thibault C, Chailley-Heu B, Incitti R, Delacourt C, Bourbon JR. 2011. Profiling target genes of FGF18 in the postnatal mouse lung: possible relevance for alveolar development. Physiol Genomics.43(21):1226-40.

Ghazvini M, Mandemakers W, Jaegle M, Piirsoo M, Driegen S, Koutsourakis M, Smit X, Grosveld F, Meijer D. 2002. A cell type-specific allele of the POU gene Oct-6 reveals Schwann cell autonomous function in nerve development and regeneration. EMBO J 21:4612-4620.

Gialmanidis IP, Bravou V, Amanetopoulou SG, Varakis J, Kourea H, Papadaki H. 2009. Overexpression of hedgehog pathway molecules and FOXM1 in non-small cell lung carcinomas. Lung Cancer 66:64-74.

Gobin AS, West JL. 2003. Val-ala-pro-gly, an elastin-derived non-integrin ligand: smooth muscle cell adhesion and specificity. J Biomed Mater Res A. 67:255-9.

Gontan C, de Munck A, Vermeij M, Grosveld F, Tibboel D, Rottier R. 2008. Sox2 is important for two crucial processes in lung development: branching morphogenesis and epithelial cell differentiation. Dev Biol 317:296-309.

Goss AM, Tian Y, Cheng L, Yang J, Zhou D, Cohen ED, Morrisey EE. 2011. Wnt2 signaling is necessary and sufficient to activate the airway smooth muscle program in the lung by regulating myocardin/Mrtf-B and Fgf10 expression. Dev Biol 356:541-552.

Goss AM, Tian Y, Tsukiyama T, Cohen ED, Zhou D, Lu MM, Yamaguchi TP, Morrisey EE. 2009. Wnt2/2b and beta-catenin signaling are necessary and sufficient to specify lung progenitors in the foregut. Dev Cell 17:290-298.

Gray PA. 2008. Transcription factors and the genetic organization of brain stem

respiratory neurons. J Appl Physiol 104:1513-1521.

Gray PA, Fu H, Luo P, Zhao Q, Yu J, Ferrari A, Tenzen T, Yuk DI, Tsung EF, Cai Z, Alberta JA, Cheng LP, Liu Y, Stenman JM, Valerius MT, Billings N, Kim HA, Greenberg ME, McMahon AP, Rowitch DH, Stiles CD, Ma Q. 2004. Mouse brain organization revealed through direct genome-scale TF expression analysis. Science 306:2255-2257.

Grier DG, Thompson A, Lappin TR, Halliday HL. 2009. Quantification of Hox and surfactant protein-B transcription during murine lung development. Neonatology 96:50-60.

Guseh JS, Bores SA, Stanger BZ, Zhou Q, Anderson WJ, Melton DA, Rajagopal J. 2009. Notch signaling promotes airway mucous metaplasia and inhibits alveolar development. Development 136:1751-1759.

Hallaq H, Pinter E, Enciso J, McGrath J, Zeiss C, Brueckner M, Madri J, Jacobs HC, Wilson CM, Vasavada H, Jiang X, Bogue CW. 2004. A null mutation of Hhex results in abnormal cardiac development, defective vasculogenesis and elevated Vegfa levels. Development 131:5197-5209.

Harrison KA, Thaler J, Pfaff SL, Gu H, Kehrl JH. 1999. Pancreas dorsal lobe agenesis and abnormal islets of Langerhans in Hlxb9-deficient mice. Nat Genet 23:71-75.

Hamilton TG, Klinghoffer RA, Corrin PD, Soriano P. 2003. Evolutionary divergence of platelet-derived growth factor alpha receptor signaling mechanisms. Mol Cell Biol.23(11):4013-25.

Harfe BD, Scherz PJ, Nissim S, Tian H, McMahon AP, Tabin CJ. 2004. Evidence for an expansion-based temporal Shh gradient in specifying vertebrate digit identities. Cell. 2004. 118(4):517-28.

Harris KS, Zhang Z, McManus MT, Harfe BD, Sun X. 2006. Dicer function is essential for lung epithelium morphogenesis. Proc Natl Acad Sci U S A. 103(7):2208-13.

Herriges JC, Yi L, Hines EA, Harvey JF, Xu G, Gray PA, Ma Q, Sun X. 2012. Genome-scale study of transcription factor expression in the branching mouse lung. Dev Dyn. 2012.9:1432-53.

Hisa T, Spence SE, Rachel RA, Fujita M, Nakamura T, Ward JM, Devor-Henneman DE, Saiki Y, Kutsuna H, Tessarollo L, Jenkins NA, Copeland NG. 2004. Hematopoietic, angiogenic and eye defects in Meis1 mutant animals. EMBO J 23:450-459.

Hoodless PA, Pye M, Chazaud C, Labbé E, Attisano L, Rossant J, Wrana JL. 2001. FoxH1 (Fast) functions to specify the anterior primitive streak in the mouse. Genes Dev 15:1257-1271.

Hokuto I, Perl AK, Whitsett JA. 2003. Prenatal, but not postnatal, inhibition of fibroblast growth factor receptor signaling causes emphysema. J Biol Chem;278:415–421.

Hosking B, François M, Wilhelm D, Orsenigo F, Caprini A, Svingen T, Tutt D, Davidson T, Browne C, Dejana E, Koopman P. 2009. Sox7 and Sox17 are strain-specific modifiers of the lymphangiogenic defects caused by Sox18 dysfunction in mice. Development 136:2385-2391.

Houweling AC, Dildrop R, Peters T, Mummenhoff J, Moorman AF, Rüther U, Christoffels VM. 2001. Gene and cluster-specific expression of the Iroquois family members during mouse development. Mech Dev 107:169-174.

Huangfu D, Liu A, Rakeman AS, Murcia NS, Niswander L, Anderson KV. 2003. Hedgehog signalling in the mouse requires intraflagellar transport proteins. Nature.;426(6962):83-7.

Hung JJ, Yang MH, Hsu HS, Hsu WH, Liu JS, Wu KJ. 2009. Prognostic significance of hypoxia-inducible factor-1alpha, TWIST1 and Snail expression in resectable non-small cell lung cancer. Thorax 64:1082-1089.

Ido A, Miura Y, Watanabe M, Sakai M, Inoue Y, Miki T, Hashimoto T, Morinaga T, Nishi S, Tamaoki T. 1996. Cloning of the cDNA encoding the mouse ATBF1 transcription factor. Gene 168:227-231.

Ingraham CR, Kinoshita A, Kondo S, Yang B, Sajan S, Trout KJ, Malik MI, Dunnwald M, Goudy SL, Lovett M, Murray JC, Schutte BC. 2006. Abnormal skin, limb and craniofacial morphogenesis in mice deficient for interferon regulatory factor 6 (Irf6). Nat Genet 38:1335-1340.

Irrthum A, Devriendt K, Chitayat D, Matthijs G, Glade C, Steijlen PM, Fryns JP, Van Steensel MA, Vikkula M. 2003. Mutations in the transcription factor gene SOX18 underlie recessive and dominant forms of hypotrichosis-lymphedema-telangiectasia. Am J Hum Genet 72:1470-1478.

Ito T, Arimitsu N, Takeuchi M, Kawamura N, Nagata M, Saso K, Akimitsu N, Hamamoto H, Natori S, Miyajima A, Sekimizu K. 2006. Transcription elongation factor S-II is required for definitive hematopoiesis. Mol Cell Biol 26:3194-3203.

Iyer NV, Kotch LE, Agani F, Leung SW, Laughner E, Wenger RH, Gassmann M, Gearhart JD, Lawler AM, Yu AY, Semenza GL. 1998. Cellular and developmental control of O2 homeostasis by hypoxia-inducible factor 1 alpha. Genes Dev 12:149-162.

Jayachandran A, Königshoff M, Yu H, Rupniewska E, Hecker M, Klepetko W, Seeger W, Eickelberg O. 2009. SNAI transcription factors mediate epithelial-mesenchymal transition in lung fibrosis. Thorax 64:1053-1061.

Jen Y, Manova K, Benezra R. 1996. Expression patterns of Id1, Id2, and Id3 are highly related but distinct from that of Id4 during mouse embryogenesis. Dev Dyn 207:235-252.

Joza S, Wang J, Tseu I, Ackerley C, Post M. 2013. Fetal, but not postnatal, deletion of semaphorin-neuropilin-1 signaling affects murine alveolar development. Am J Respir Cell Mol Biol. 49(4):627-36

Junhao Mao, Edwina McGlinn, Peng Huang, Clifford J. Tabin, Andrew P. McMahon. 2009. Fgf-Dependent Etv4/5 Activity Is Required for Posterior Restriction of Sonic hedgehog and Promoting Outgrowth of the Vertebrate Limb. Dev Cell. 16: 600-606.

Kaeser MD, Aslanian A, Dong MQ, Yates JR, Emerson BM. 2008. BRD7, a novel PBAF-specific SWI/SNF subunit, is required for target gene activation and repression in embryonic stem cells. J Biol Chem 283:32254-32263.

Kaestner KH, Lee KH, Schlöndorff J, Hiemisch H, Monaghan AP, Schütz G. 1993. Six members of the mouse forkhead gene family are developmentally regulated. Proc Natl Acad Sci U S A 90:7628-7631.

Kalin TV, Wang IC, Meliton L, Zhang Y, Wert SE, Ren X, Snyder J, Bell SM, Graf L, Whitsett JA, Kalinichenko VV. 2008. Forkhead Box m1 transcription factor is required for perinatal lung function. Proc Natl Acad Sci U S A 105:19330-19335.

Karvonen HM, Lehtonen ST, Harju T, Sormunen RT, Lappi-Blanco E, Mäkinen JM, Laitakari K, Johnson S, Kaarteenaho RL. Myofibroblast expression in airways and alveoli is affected by smoking and COPD. 2013. Respir Res. 11;14:84.

Keijzer R, van Tuyl M, Meijers C, Post M, Tibboel D, Grosveld F, Koutsourakis M. 2001. The transcription factor GATA6 is essential for branching morphogenesis and epithelial cell differentiation during fetal pulmonary development. Development 128:503-511.

Keng VW, Yagi H, Ikawa M, Nagano T, Myint Z, Yamada K, Tanaka T, Sato A, Muramatsu I, Okabe M, Sato M, Noguchi T. 2000. Homeobox gene Hex is essential for onset of mouse embryonic liver development and differentiation of the monocyte lineage. Biochem Biophys Res Commun 276:1155-1161.

Khoor A, Stahlman MT, Gray ME, Whitsett JA. 1994. Temporal-spatial distribution of SP-B and SP-C proteins and mRNAs in developing respiratory epithelium of human lung. J Histochem Cytochem. 1994. 42(9):1187-99.

Kim CF, Jackson EL, Woolfenden AE, Lawrence S, Babar I, Vogel S, Crowley D, Bronson RT, Jacks T. 2005a. Identification of bronchioalveolar stem cells in normal lung and lung cancer. Cell 121:823-835.

Kim IM, Ramakrishna S, Gusarova GA, Yoder HM, Costa RH, Kalinichenko VV. 2005b. The forkhead box m1 transcription factor is essential for embryonic development of pulmonary vasculature. J Biol Chem 280:22278-22286.

Kim KK, Kugler MC, Wolters PJ, Robillard L, Galvez MG, Brumwell AN, Sheppard D, Chapman HA. 2006. Alveolar epithelial cell mesenchymal transition develops in vivo during pulmonary fibrosis and is regulated by the extracellular matrix. Proc Natl Acad Sci U S A 103:13180-13185.

Kim TS, Kawaguchi M, Suzuki M, Jung CG, Asai K, Shibamoto Y, Lavin MF, Khanna KK, Miura Y. 2010. The ZFHX3 (ATBF1) transcription factor induces PDGFRB, which activates ATM in the cytoplasm to protect cerebellar neurons from oxidative stress. Dis Model Mech 3:752-762.

Kinkead R, LeBlanc M, Gulemetova R, Lalancette-Hébert M, Lemieux M, Mandeville I, Jeannotte L. 2004. Respiratory adaptations to lung morphological defects in adult mice lacking Hoxa5 gene function. Pediatr Res 56:553-562.

Kitamura K, Miura H, Miyagawa-Tomita S, Yanazawa M, Katoh-Fukui Y, Suzuki R, Ohuchi H, Suehiro A, Motegi Y, Nakahara Y, Kondo S, Yokoyama M. 1999. Mouse Pitx2 deficiency leads to anomalies of the ventral body wall, heart, extra- and periocular mesoderm and right pulmonary isomerism. Development 126:5749-5758.

Kofron M, Puck H, Standley H, Wylie C, Old R, Whitman M, Heasman J. 2004. New roles for FoxH1 in patterning the early embryo. Development 131:5065-5078.

Kondo S, Schutte BC, Richardson RJ, Bjork BC, Knight AS, Watanabe Y, Howard E, de Lima RL, Daack-Hirsch S, Sander A, McDonald-McGinn DM, Zackai EH, Lammer EJ, Aylsworth AS, Ardinger HH, Lidral AC, Pober BR, Moreno L, Arcos-Burgos M, Valencia C, Houdayer C, Bahuau M, Moretti-Ferreira D, Richieri-Costa A, Dixon MJ, Murray JC. 2002. Mutations in IRF6 cause Van der Woude and popliteal pterygium syndromes. Nat Genet 32:285-289.

Kranenburg AR, De Boer WI, Van Krieken JH, Mooi WJ, Walters JE, Saxena PR, Sterk PJ, Sharma HS. 2002. Enhanced expression of fibroblast growth factors and receptor FGFR-1 during vascular remodeling in chronic obstructive pulmonary disease. Am J Respir Cell Mol Biol. 278:415-21.

Kranenburg AR, Willems-Widyastuti A, Mooi WJ, Saxena PR, Sterk PJ, de Boer WI, Sharma HS. 2005. Chronic obstructive pulmonary disease is associated with enhanced bronchial expression of FGF-1, FGF-2, and FGFR-1. J Pathol. 206:28-38.

Kumar R, Reynolds DM, Shevchenko A, Goldstone SD, Dalton S. 2000. Forkhead transcription factors, Fkh1p and Fkh2p, collaborate with Mcm1p to control transcription required for M-phase. Curr Biol 10:896-906.

Kumar VH, Lakshminrusimha S, El Abiad MT, Chess PR, Ryan RM. 2005. Growth factors in lung development. Adv Clin Chem. 40:261-316

Kuure S, Chi X, Lu B, Costantini F. 2010. The transcription factors Etv4 and Etv5 mediate formation of the ureteric bud tip domain during kidney development. Development. 2010 Jun;137(12):1975-9.

Laing MA, Coonrod S, Hinton BT, Downie JW, Tozer R, Rudnicki MA, Hassell JA. 2000. Male sexual dysfunction in mice bearing targeted mutant alleles of the PEA3 ets gene. Mol Cell Biol. 2000 Dec;20(24):9337-45.

Lazarus A, Del-Moral PM, Ilovich O, Mishani E, Warburton D, Keshet E. 2011. A perfusion-independent role of blood vessels in determining branching stereotypy of lung airways. Development 138:2359-2368.

Lazzaro D, Price M, de Felice M, Di Lauro R. 1991. The transcription factor TTF-1 is expressed at the onset of thyroid and lung morphogenesis and in restricted regions of the foetal brain. Development 113:1093-1104.

Le N, Nagarajan R, Wang JY, Svaren J, LaPash C, Araki T, Schmidt RE, Milbrandt J. 2005. Nab proteins are essential for peripheral nervous system myelination. Nat Neurosci 8:932-940.

Lebel M, Agarwal P, Cheng CW, Kabir MG, Chan TY, Thanabalasingham V, Zhang X, Cohen DR, Husain M, Cheng SH, Bruneau BG, Hui CC. 2003. The Iroquois homeobox gene Irx2 is not essential for normal development of the heart and midbrain-hindbrain boundary in mice. Mol Cell Biol 23:8216-8225.

Lee CG, Cho SJ, Kang MJ, Chapoval SP, Lee PJ, Noble PW, Yehualaeshet T, Lu B, Flavell RA, Milbrandt J, Homer RJ, Elias JA. 2004. Early growth response gene 1-mediated apoptosis is essential for transforming growth factor beta1-induced pulmonary fibrosis. J Exp Med 200:377-389.

Leimeister C, Schumacher N, Steidl C, Gessler M. 2000. Analysis of HeyL expression in wild-type and Notch pathway mutant mouse embryos. Mech Dev 98:175-178.

Lemaire, R., Bayle, J., Mecham, R. P., and Lafyatis, R. (2007)Microfibril-associated MAGP-2 stimulates elastic fiber assembly. *J. Biol. Chem.* 282, 800-808

Li C, Hu L, Xiao J, Chen H, Li JT, Bellusci S, Delanghe S, Minoo P. 2005. Wnt5a regulates Shh and Fgf10 signaling during lung development. Dev Biol 287:86-97.

Li C, Xiao J, Hormi K, Borok Z, Minoo P. 2002. Wnt5a participates in distal lung morphogenesis. Dev Biol 248:68-81.

Li H, Edlund H. 2001. Persistent expression of Hlxb9 in the pancreatic epithelium

impairs pancreatic development. Dev Biol 240:247-253.

Li Y, Gordon J, Manley NR, Litingtung Y, Chiang C. 2008. Bmp4 is required for tracheal formation: a novel mouse model for tracheal agenesis. Dev Biol 322:145-155.

Li Y, Zhang H, Choi SC, Litingtung Y, Chiang C. 2004. Sonic hedgehog signaling regulates Gli3 processing, mesenchymal proliferation, and differentiation during mouse lung organogenesis. Dev Biol 270:214-231.

Lim L, Kalinichenko VV, Whitsett JA, Costa RH. 2002. Fusion of lung lobes and vessels in mouse embryos heterozygous for the forkhead box f1 targeted allele. Am J Physiol Lung Cell Mol Physiol 282:L1012-1022.

Lin, S., A. K. Perl, et al. (2006). "Erm/thyroid transcription factor 1 interactions modulate surfactant protein C transcription." J Biol Chem 281(24): 16716-26.

Lindahl P, Karlsson L, Hellström M, Gebre-Medhin S, Willetts K, Heath JK, Betsholtz C. 1997. Alveogenesis failure in PDGF-A-deficient mice is coupled to lack of distal spreading of alveolar smooth muscle cell progenitors during lung development. Development 124, 3943-53.

Liodis P, Denaxa M, Grigoriou M, Akufo-Addo C, Yanagawa Y, Pachnis V. 2007. Lhx6 activity is required for the normal migration and specification of cortical interneuron subtypes. J Neurosci 27:3078-3089.

Litingtung Y, Dahn RD, Li Y, Fallon JF, Chiang C. 2002. Shh and Gli3 are dispensable for limb skeleton formation but regulate digit number and identity. Nature. 418(6901):979-83.

Liu C, Liu W, Lu MF, Brown NA, Martin JF. 2001. Regulation of left-right asymmetry by thresholds of Pitx2c activity. Development 128:2039-2048.

Liu C, Morrisey EE, Whitsett JA. 2002. GATA-6 is required for maturation of the lung in late gestation. Am J Physiol Lung Cell Mol Physiol 283:L468-475.

Liu Y, Hogan BL. 2002. Differential gene expression in the distal tip endoderm of the embryonic mouse lung. Gene Expr Patterns 2:229-233.

Liu Y, Jiang H, Crawford HC, Hogan BL. 2003. Role for ETS domain transcription factors Pea3/Erm in mouse lung development. Dev Biol 261:10-24.

Liu X, Zhao Y, Gao J, Pawlyk B, Starcher B, Spencer JA, Yanagisawa H, Zuo J, Li T. 2004. Elastic fiber homeostasis requires lysyl oxidase-like 1 protein. Nat Genet. 2004. 36(2):178-82.

Lowery JW, Frump AL, Anderson L, DiCarlo GE, Jones MT, de Caestecker MP. 2010.

ID family protein expression and regulation in hypoxic pulmonary hypertension. Am J Physiol Regul Integr Comp Physiol 299:R1463-1477.

Lu BC, Cebrian C, Chi X, Kuure S, Kuo R, Bates CM, Arber S, Hassell J, MacNeil L, Hoshi M, Jain S, Asai N, Takahashi M, Schmidt-Ott KM, Barasch J, D'Agati V, Costantini F. 2009. Etv4 and Etv5 are required downstream of GDNF and Ret for kidney branching morphogenesis. Nat Genet. 41(12):1295-302.

Lu MF, Pressman C, Dyer R, Johnson RL, Martin JF. 1999. Function of Rieger syndrome gene in left-right asymmetry and craniofacial development. Nature 401:276-278.

Lu MM, Li S, Yang H, Morrisey EE. 2002. Foxp4: a novel member of the Foxp subfamily of winged-helix genes co-expressed with Foxp1 and Foxp2 in pulmonary and gut tissues. Mech Dev 119 Suppl 1:S197-202.

Lu X, Meng X, Morris CA, Keating MT. 1998. A novel human gene, WSTF, is deleted in Williams syndrome. Genomics 54:241-249.

Lufkin T, Dierich A, LeMeur M, Mark M, Chambon P. 1991. Disruption of the Hox-1.6 homeobox gene results in defects in a region corresponding to its rostral domain of expression. Cell 66:1105-1119.

Lyden D, Young AZ, Zagzag D, Yan W, Gerald W, O'Reilly R, Bader BL, Hynes RO, Zhuang Y, Manova K, Benezra R. 1999. Id1 and Id3 are required for neurogenesis, angiogenesis and vascularization of tumour xenografts. Nature 401:670-677.

Lü J, Izvolsky KI, Qian J, Cardoso WV. 2005. Identification of FGF10 targets in the embryonic lung epithelium during bud morphogenesis. J Biol Chem 280:4834-4841.

Lü J, Qian J, Izvolsky KI, Cardoso WV. 2004. Global analysis of genes differentially expressed in branching and non-branching regions of the mouse embryonic lung. Dev Biol 273:418-435.

Maeda Y, Davé V, Whitsett JA. 2007. Transcriptional control of lung morphogenesis. Physiol Rev 87:219-244.

Mahlapuu M, Enerbäck S, Carlsson P. 2001. Haploinsufficiency of the forkhead gene Foxf1, a target for sonic hedgehog signaling, causes lung and foregut malformations. Development 128:2397-2406.

Mandeville I, Aubin J, LeBlanc M, Lalancette-Hébert M, Janelle MF, Tremblay GM, Jeannotte L. 2006. Impact of the loss of Hoxa5 function on lung alveogenesis. Am J Pathol 169:1312-1327.

Mariani TJ, Reed JJ, Shapiro SD. Expression profiling of the developing mouse lung: insights into the establishment of the extracellular matrix. Am J Respir Cell Mol Biol 2002;26:541–548.

Martis PC, Whitsett JA, Xu Y, Perl AK, Wan H, Ikegami M. 2006. C/EBPalpha is required for lung maturation at birth. Development 133:1155-1164.

Matis C, Oury F, Remacle S, Lampe X, Gofflot F, Picard JJ, Rijli FM, Rezsohazy R. 2007. Identification of Lmo1 as part of a Hox-dependent regulatory network for hindbrain patterning. Dev Dyn 236:2675-2684.

McGowan SE, Grossmann RE, Kimani PW, Holmes AJ. 2008. Platelet-derived growth factor receptor-alpha-expressing cells localize to the alveolar entry ring and have characteristics of myofibroblasts during pulmonary alveolar septal formation. Anat Rec (Hoboken). 2008 Dec;291(12):1649-61.

McGrath EE, Blades Z, Anderson PB. 2010. Chylothorax: aetiology, diagnosis and therapeutic options. Respir Med 104:1-8.

Merrilees MJ, Ching PS, Beaumont B, Hinek A, Wight TN, Black PN. 2008. Changes in elastin, elastin binding protein and versican in alveoli in chronic obstructive pulmonary disease. Respir Res. 18;9:41.

Metzger DE, Stahlman MT, Shannon JM. 2008a. Misexpression of ELF5 disrupts lung branching and inhibits epithelial differentiation. Dev Biol 320:149-160.

Metzger DE, Xu Y, Shannon JM. 2007. Elf5 is an epithelium-specific, fibroblast growth factor-sensitive transcription factor in the embryonic lung. Dev Dyn 236:1175-1192.

Metzger RJ, Klein OD, Martin GR, Krasnow MA. 2008b. The branching programme of mouse lung development. Nature 453:745-750.

Miller KA, Ah-Cann CJ, Welfare MF, Tan TY, Pope K, Caruana G, Freckmann ML, Savarirayan R, Bertram JF, Dobbie MS, Bateman JF, Farlie PG. 2013. Cauli: a mouse strain with an Ift140 mutation that results in a skeletal ciliopathy modelling Jeune syndrome. PLoS Genet. 2013 Aug;9(8):e1003746.

Min H, Danilenko DM, Scully SA, Bolon B, Ring BD, Tarpley JE, DeRose M, Simonet WS. 1998. Fgf-10 is required for both limb and lung development and exhibits striking functional similarity to Drosophila branchless. Genes Dev 12: 3156–3161.

Minoo P, Hamdan H, Bu D, Warburton D, Stepanik P, deLemos R. 1995. TTF-1 regulates lung epithelial morphogenesis. Dev Biol 172:694-698.

Minoo P, Hu L, Xing Y, Zhu NL, Chen H, Li M, Borok Z, Li C. 2007. Physical and functional interactions between homeodomain NKX2.1 and winged helix/forkhead

FOXA1 in lung epithelial cells. Mol Cell Biol 27:2155-2165.

Minoo P, Su G, Drum H, Bringas P, Kimura S. 1999. Defects in tracheoesophageal and lung morphogenesis in Nkx2.1(-/-) mouse embryos. Dev Biol 209:60-71.

Miyazono K, Miyazawa K. 2002. Id: a target of BMP signaling. Sci STKE 2002:pe40.

Moens CB, Selleri L. 2006. Hox cofactors in vertebrate development. Dev Biol 291:193-206.

Mohan B, Mittal CM. 2011. Supravalvular aortic stenosis in William's syndrome. Ann Pediatr Cardiol 4:213-214.

Mollard R, Dziadek M. 1997. Homeobox genes from clusters A and B demonstrate characteristics of temporal colinearity and differential restrictions in spatial expression domains in the branching mouse lung. Int J Dev Biol 41:655-666.

Morimoto M, Liu Z, Cheng HT, Winters N, Bader D, Kopan R. 2010. Canonical Notch signaling in the developing lung is required for determination of arterial smooth muscle cells and selection of Clara versus ciliated cell fate. J Cell Sci 123:213-224.

Morrisey EE and Hogan BL. 2010. Preparing for the first breath: genetic and cellular mechanisms in lung development. Dev Cell. 18:8-23.

Motoyama J, Heng H, Crackower MA, Takabatake T, Takeshima K, Tsui LC, Hui C. 1998. Overlapping and non-overlapping Ptch2 expression with Shh during mouse embryogenesis. Mech Dev 78:81-84.

Mund SI, Stampanoni M, Schittny JC. 2008. Developmental alveolarization of the mouse lung. Dev Dyn 237:2108-2116.

Murakami T, Kondo S, Ogata M, Kanemoto S, Saito A, Wanaka A, Imaizumi K. 2006. Cleavage of the membrane-bound transcription factor OASIS in response to endoplasmic reticulum stress. J Neurochem 96:1090-1100.

Murakami T, Saito A, Hino S, Kondo S, Kanemoto S, Chihara K, Sekiya H, Tsumagari K, Ochiai K, Yoshinaga K, Saitoh M, Nishimura R, Yoneda T, Kou I, Furuichi T, Ikegawa S, Ikawa M, Okabe M, Wanaka A, Imaizumi K. 2009. Signalling mediated by the endoplasmic reticulum stress transducer OASIS is involved in bone formation. Nat Cell Biol 11:1205-1211.

Muthusamy N, Barton K, Leiden JM. 1995. Defective activation and survival of T cells lacking the Ets-1 transcription factor. Nature 377:639-642.

Nagata M, Ito T, Arimitsu N, Koyama H, Sekimizu K. 2009. Transcription arrest relief by S-II/TFIIS during gene expression in erythroblast differentiation. Genes Cells 14:371-

380.

Nakagawa O, McFadden DG, Nakagawa M, Yanagisawa H, Hu T, Srivastava D, Olson EN. 2000. Members of the HRT family of basic helix-loop-helix proteins act as transcriptional repressors downstream of Notch signaling. Proc Natl Acad Sci U S A 97:13655-13660.

Neptune ER, Frischmeyer PA, Arking DE, Myers L, Bunton TE, Gayraud B, Ramirez F, Sakai LY, Dietz HC. (2003) Dysregulation of TGF-B activation contributes to pathogenesis in Marfan syndrome Nature Genetics; 33: 407 – 411

Novarino G, Akizu N, Gleeson JG 2011. Modeling human disease in humans: the ciliopathies. Cell;147(1):70-9.

Okubo T, Hogan BL. 2004. Hyperactive Wnt signaling changes the developmental potential of embryonic lung endoderm. J Biol 3:11.

Oosterwegel M, van de Wetering M, Timmerman J, Kruisbeek A, Destree O, Meijlink F, Clevers H. 1993. Differential expression of the HMG box factors TCF-1 and LEF-1 during murine embryogenesis. Development 118:439-448.

Ormestad M, Astorga J, Landgren H, Wang T, Johansson BR, Miura N, Carlsson P. 2006. Foxf1 and Foxf2 control murine gut development by limiting mesenchymal Wnt signaling and promoting extracellular matrix production. Development 133:833-843.

Ornitz DM, Xu J, Colvin JS, McEwen DG, MacArthur CA, Coulier F, Gao G, Goldfarb M. 1996. Receptor specificity of the fibroblast growth factor family. J Biol Chem. 1996 Jun 21;271(25):15292-7.

Orr-Urtreger A, Bedford MT, Burakova T, Arman E, Zimmer Y, Yayon A, Givol D, Lonai P. 1993. Developmental localization of the splicing alternatives of fibroblast growth factor receptor-2 (FGFR2). Dev Biol. (2):475

Ott EB, van den Akker NM, Sakalis PA, Gittenberger-de Groot AC, Te Velthuis AJ, Bagowski CP. 2008. The lim domain only protein 7 is important in zebrafish heart development. Dev Dyn 237:3940-3952.

Oya H, Yokoyama A, Yamaoka I, Fujiki R, Yonezawa M, Youn MY, Takada I, Kato S, Kitagawa H. 2009. Phosphorylation of Williams syndrome transcription factor by MAPK induces a switching between two distinct chromatin remodeling complexes. J Biol Chem 284:32472-32482.

Padela S, Yi M, Cabacungan J, Shek S, Belcastro R, Masood A, Jankov RP, Tanswell AK. 2008. A critical role for fibroblast growth factor-7 during early alveolar formation in the neonatal rat. Pediatr Res. 63:232-8.

Pan L, Sato S, Frederick JP, Sun XH, Zhuang Y. 1999. Impaired immune responses and B-cell proliferation in mice lacking the Id3 gene. Mol Cell Biol 19:5969-5980.

Park KS, Wells JM, Zorn AM, Wert SE, Laubach VE, Fernandez LG, Whitsett JA. 2006a. Transdifferentiation of ciliated cells during repair of the respiratory epithelium. Am J Respir Cell Mol Biol 34:151-157.

Park KS, Wells JM, Zorn AM, Wert SE, Whitsett JA. 2006b. Sox17 influences the differentiation of respiratory epithelial cells. Dev Biol 294:192-202.

Park WY, Miranda B, Lebeche D, Hashimoto G, Cardoso WV.. 1998.FGF-10 is a chemotactic factor for distal epithelial buds during lung development. Dev Biol. 1998 Sep 15;201(2):125-34.

Patel D, Vandromme SE, Reid ME, Taite LJ. 2012. Synergistic activity of αvβ3 integrins and the elastin binding protein enhance cell-matrix interactions on bioactive hydrogel surfaces. Biomacromolecules. 13:1420-8.
Pazour GJ, Witman GB. 2003. The vertebrate primary cilium is a sensory organelle. Curr Opin Cell Biol. 15(1):105-10.

Peoples RJ, Cisco MJ, Kaplan P, Francke U. 1998. Identification of the WBSCR9 gene, encoding a novel transcriptional regulator, in the Williams-Beuren syndrome deletion at 7q11.23. Cytogenet Cell Genet 82:238-246.

Pepicelli CV, Lewis PM, McMahon AP. 1998. Sonic hedgehog regulates branching morphogenesis in the mammalian lung. Curr Biol 8:1083-1086.

Pereira FA, Qiu Y, Zhou G, Tsai MJ, Tsai SY. 1999. The orphan nuclear receptor COUP-TFII is required for angiogenesis and heart development. Genes Dev 13:1037-1049.

Perl AK, Kist R, Shan Z, Scherer G, Whitsett JA. 2005. Normal lung development and function after Sox9 inactivation in the respiratory epithelium. Genesis 41:23-32.

Post M, Souza P, Liu J, Tseu I, Wang J, Kuliszewski M, Tanswell AK. 1996. Keratinocyte growth factor and its receptor are involved in regulating early lung branching. Development.122:3107-15.

Pyrgaki C, Liu A, Niswander L. 2011. Grainyhead-like 2 regulates neural tube closure and adhesion molecule expression during neural fold fusion. Dev Biol 353:38-49.

Qi Y, Ranish JA, Zhu X, Krones A, Zhang J, Aebersold R, Rose DW, Rosenfeld MG, Carrière C. 2008. Atbf1 is required for the Pit1 gene early activation. Proc Natl Acad Sci U S A 105:2481-2486.

Qin J, Lin Y, Norman RX, Ko HW, Eggenschwiler JT. 2011. Intraflagellar transport protein 122 antagonizes Sonic Hedgehog signaling and controls ciliary localization of pathway components. Proc Natl Acad Sci U S A.108(4):1456-61.

Qiu Y, Pereira FA, DeMayo FJ, Lydon JP, Tsai SY, Tsai MJ. 1997. Null mutation of mCOUP-TFI results in defects in morphogenesis of the glossopharyngeal ganglion, axonal projection, and arborization. Genes Dev 11:1925-1937.

Quaggin SE, Schwartz L, Cui S, Igarashi P, Deimling J, Post M, Rossant J. 1999. The basic-helix-loop-helix protein pod1 is critically important for kidney and lung organogenesis. Development 126:5771-5783.

Que J, Choi M, Ziel JW, Klingensmith J, Hogan BL. 2006. Morphogenesis of the trachea and esophagus: current players and new roles for noggin and Bmps. Differentiation 74:422-437.

Que J, Luo X, Schwartz RJ, Hogan BL. 2009. Multiple roles for Sox2 in the developing and adult mouse trachea. Development 136:1899-1907.

Que J, Okubo T, Goldenring JR, Nam KT, Kurotani R, Morrisey EE, Taranova O, Pevny LH, Hogan BL. 2007. Multiple dose-dependent roles for Sox2 in the patterning and differentiation of anterior foregut endoderm. Development 134:2521-2531.

Que J, Wilm B, Hasegawa H, Wang F, Bader D, Hogan BL. 2008. Mesothelium contributes to vascular smooth muscle and mesenchyme during lung development. Proc Natl Acad Sci U S A 105:16626-16630.

Rampalli S, Li L, Mak E, Ge K, Brand M, Tapscott SJ, Dilworth FJ. 2007. p38 MAPK signaling regulates recruitment of Ash2L-containing methyltransferase complexes to specific genes during differentiation. Nat Struct Mol Biol 14:1150-1156.

Rauch T, Wang Z, Zhang X, Zhong X, Wu X, Lau SK, Kernstine KH, Riggs AD, Pfeifer GP. 2007. Homeobox gene methylation in lung cancer studied by genome-wide analysis with a microarray-based methylated CpG island recovery assay. Proc Natl Acad Sci U S A 104:5527-5532.

Rawlins EL, Clark CP, Xue Y, Hogan BL. 2009. The Id2+ distal tip lung epithelium contains individual multipotent embryonic progenitor cells. Development 136:3741-3745.

Rawlins EL, Hogan BL. 2006. Epithelial stem cells of the lung: privileged few or opportunities for many? Development 133:2455-2465.

Reines D, Conaway JW, Conaway RC. 1996. The RNA polymerase II general elongation factors. Trends Biochem Sci 21:351-355.

Restivo G, Nguyen BC, Dziunycz P, Ristorcelli E, Ryan RJ, Özuysal Ö, Di Piazza M, Radtke F, Dixon MJ, Hofbauer GF, Lefort K, Dotto GP. 2011. IRF6 is a mediator of Notch pro-differentiation and tumour suppressive function in keratinocytes. EMBO J 30:4571-4585.

Rezvani M, Wilde J, Vitt P, Mailaparambil B, Grychtol R, Krueger M, Heinzmann A. 2013. Association of a FGFR-4 gene polymorphism with bronchopulmonary dysplasia and neonatal respiratory distress. Dis Markers. 35(6):633-40.

Riby DM, Porter MA. 2010. Williams syndrome. Adv Child Dev Behav 39:163-209.

Rifat Y, Parekh V, Wilanowski T, Hislop NR, Auden A, Ting SB, Cunningham JM, Jane SM. 2010. Regional neural tube closure defined by the Grainy head-like transcription factors. Dev Biol 345:237-245.

Rnjak J, Li Z, Maitz PK, Wise SG, Weiss AS. 2009. Primary human dermal fibroblast interactions with open weave three-dimensional scaffolds prepared from synthetic human elastin. Biomaterials. 30:6469-77.

Rock JR, Barkauskas CE, Cronce MJ, Xue Y, Harris JR, Liang J, Noble PW, Hogan BL. 2011. Multiple stromal populations contribute to pulmonary fibrosis without evidence for epithelial to mesenchymal transition. Proc Natl Acad Sci U S A 108:E1475-1483.

Rollin J, Bléchet C, Régina S, Tenenhaus A, Guyétant S, Gidrol X. 2009. The intracellular localization of ID2 expression has a predictive value in non small cell lung cancer. PLoS One 4:e4158.

Sagai, T, et al. (2009). A cluster of three long-range enhancers directs regionalShh expression in the epithelial linings. Development. 136, 1665-74.

Saini Y, Harkema JR, LaPres JJ. 2008. HIF1alpha is essential for normal intrauterine differentiation of alveolar epithelium and surfactant production in the newborn lung of mice. J Biol Chem 283:33650-33657.

Sakamoto Y, Hara K, Kanai-Azuma M, Matsui T, Miura Y, Tsunekawa N, Kurohmaru M, Saijoh Y, Koopman P, Kanai Y. 2007. Redundant roles of Sox17 and Sox18 in early cardiovascular development of mouse embryos. Biochem Biophys Res Commun 360:539-544.

Sawaya PL, Stripp BR, Whitsett JA, Luse DS. 1993. The lung-specific CC10 gene is regulated by transcription factors from the AP-1, octamer, and hepatocyte nuclear factor 3 families. Mol Cell Biol 13:3860-3871.

Semenza GL. 2001a. HIF-1 and mechanisms of hypoxia sensing. Curr Opin Cell Biol 13:167-171.

Semenza GL. 2001b. Hypoxia-inducible factor 1: control of oxygen homeostasis in health and disease. Pediatr Res 49:614-617.

Serrano AG, Pérez-Gil J. 2006. Protein-lipid interactions and surface activity in the pulmonary surfactant system. Chem Phys Lipids.141(1-2):105-18

Sekine K, Ohuchi H, Fujiwara M, Yamasaki M, Yoshizawa T, Sato T, Yagishita N, Matsui D, Koga Y, Itoh N, Kato S. 1999. Fgf10 is essential for limb and lung formation. Nat Genet 21: 138–141.

Sharma N, Timmers C, Trikha P, Saavedra HI, Obery A, Leone G. 2006. Control of the p53-p21CIP1 Axis by E2f1, E2f2, and E2f3 is essential for G1/S progression and cellular transformation. J Biol Chem 281:36124-36131.

Shi W, Chen F, Cardoso WV. 2009. Mechanisms of lung development: contribution to adult lung disease and relevance to chronic obstructive pulmonary disease. Proc Am Thorac Soc 6:558-563.

Shin JH, Ko HS, Kang H, Lee Y, Lee YI, Pletinkova O, Troconso JC, Dawson VL, Dawson TM. 2011. PARIS (ZNF746) repression of PGC-1α contributes to neurodegeneration in Parkinson's disease. Cell 144:689-702.

Shu W, Lu MM, Zhang Y, Tucker PW, Zhou D, Morrisey EE. 2007. Foxp2 and Foxp1 cooperatively regulate lung and esophagus development. Development 134:1991-2000.

Shu W, Yang H, Zhang L, Lu MM, Morrisey EE. 2001. Characterization of a new subfamily of winged-helix/forkhead (Fox) genes that are expressed in the lung and act as transcriptional repressors. J Biol Chem 276:27488-27497.

Silvestri C, Narimatsu M, von Both I, Liu Y, Tan NB, Izzi L, McCaffery P, Wrana JL, Attisano L. 2008. Genome-wide identification of Smad/Foxh1 targets reveals a role for Foxh1 in retinoic acid regulation and forebrain development. Dev Cell 14:411-423.

Sosic D; Richardson JA; Yu K; Ornitz DM; Olson EN. 2003. Twist regulates cytokine gene expression through a negative feedback loop that represses NF-kappaB activity. Cell 112(2):169-80.

Srisuma S, Bhattacharya S, Simon DM, Solleti SK, Tyagi S, Starcher B, Mariani TJ. 2010. Fibroblast growth factor receptors control epithelial-mesenchymal interactions necessary for alveolar elastogenesis. Am J Respir Crit Care Med 181:838-850.

Starcher B, d'Azzo A, Keller PW, Rao GK, Nadarajah D, Hinek A. 2008. Neuraminidase-1 is required for the normal assembly of elastic fibers. Am J Physiol Lung Cell Mol Physiol. 295: L637-47.

Steward MM, Lee JS, O'Donovan A, Wyatt M, Bernstein BE, Shilatifard A. 2006.

Molecular regulation of H3K4 trimethylation by ASH2L, a shared subunit of MLL complexes. Nat Struct Mol Biol 13:852-854.

Stoller JZ, Huang L, Tan CC, Huang F, Zhou DD, Yang J, Gelb BD, Epstein JA. 2010. Ash2l interacts with Tbx1 and is required during early embryogenesis. Exp Biol Med (Maywood) 235:569-576.

Stopka T, Skoultchi AI. 2003. The ISWI ATPase Snf2h is required for early mouse development. Proc Natl Acad Sci U S A 100:14097-14102.

Stryke D, Kawamoto M, Huang CC, Johns SJ, King LA, Harper CA, Meng EC, Lee RE, Yee A, L'Italien L, Chuang PT, Young SG, Skarnes WC, Babbitt PC, Ferrin TE. 2003. BayGenomics: a resource of insertional mutations in mouse embryonic stem cells. Nucleic Acids Res 31:278-281.

Su N, Xu X, Li C, He Q, Zhao L, Li C, Chen S, Luo F, Yi L, Du X, Huang H, Deng C, Chen L. 2010. Generation of Fgfr3 conditional knockout mice. Int J Biol Sci.;6(4):327-32.

Sum EY, O'Reilly LA, Jonas N, Lindeman GJ, Visvader JE. 2005. The LIM domain protein Lmo4 is highly expressed in proliferating mouse epithelial tissues. J Histochem Cytochem 53:475-486.

Sun J, Chen H, Chen C, Whitsett JA, Mishina Y, Bringas P, Ma JC, Warburton D, Shi W. 2008. Prenatal lung epithelial cell-specific abrogation of Alk3-bone morphogenetic protein signaling causes neonatal respiratory distress by disrupting distal airway formation. Am J Pathol 172:571-582.

Swirnoff AH, Apel ED, Svaren J, Sevetson BR, Zimonjic DB, Popescu NC, Milbrandt J. 1998. Nab1, a corepressor of NGFI-A (Egr-1), contains an active transcriptional repression domain. Mol Cell Biol 18:512-524.

Tamplin OJ, Kinzel D, Cox BJ, Bell CE, Rossant J, Lickert H. 2008. Microarray analysis of Foxa2 mutant mouse embryos reveals novel gene expression and inductive roles for the gastrula organizer and its derivatives. BMC Genomics 9:511.

Tan CC, Walsh MJ, Gelb BD. 2009. Fgfr3 is a transcriptional target of Ap2delta and Ash2l-containing histone methyltransferase complexes. PLoS One 4:e8535.

Tang N, Marshall WF, McMahon M, Metzger RJ, Martin GR. 2011. Control of mitotic spindle angle by the RAS-regulated ERK1/2 pathway determines lung tube shape. Science. 333:342-5

ten Dijke P, Korchynskyi O, Valdimarsdottir G, Goumans MJ. 2003. Controlling cell fate by bone morphogenetic protein receptors. Mol Cell Endocrinol 211:105-113.

Tian H, McKnight SL, Russell DW. 1997. Endothelial PAS domain protein 1 (EPAS1), a transcription factor selectively expressed in endothelial cells. Genes Dev 11:72-82.

Tian J, Mahmood R, Hnasko R, Locker J. 2006. Loss of Nkx2.8 deregulates progenitor cells in the large airways and leads to dysplasia. Cancer Res 66:10399-10407.

Tian Y, Zhang Y, Hurd L, Hannenhalli S, Liu F, Lu MM, Morrisey EE. 2011. Regulation of lung endoderm progenitor cell behavior by miR302/367. Development 138:1235-1245.

Tiozzo C, De Langhe S, Yu M, Londhe VA, Carraro G, Li M, Li C, Xing Y, Anderson S, Borok Z, Bellusci S, Minoo P. 2009. Deletion of Pten expands lung epithelial progenitor pools and confers resistance to airway injury. Am J Respir Crit Care Med. 180:701-12.

Tompkins DH, Besnard V, Lange AW, Wert SE, Keiser AR, Smith AN, Lang R, Whitsett JA. 2009. Sox2 is required for maintenance and differentiation of bronchiolar Clara, ciliated, and goblet cells. PLoS One 4:e8248.

Tsai SY, Opavsky R, Sharma N, Wu L, Naidu S, Nolan E, Feria-Arias E, Timmers C, Opavska J, de Bruin A, Chong JL, Trikha P, Fernandez SA, Stromberg P, Rosol TJ, Leone G. 2008. Mouse development with a single E2F activator. Nature 454:1137-1141.

Tsao PN, Chen F, Izvolsky KI, Walker J, Kukuruzinska MA, Lu J, Cardoso WV. 2008. Gamma-secretase activation of notch signaling regulates the balance of proximal and distal fates in progenitor cells of the developing lung. J Biol Chem 283:29532-29544.

Tsao PN, Vasconcelos M, Izvolsky KI, Qian J, Lu J, Cardoso WV. 2009. Notch signaling controls the balance of ciliated and secretory cell fates in developing airways. Development 136:2297-2307.

Tse E, Smith AJ, Hunt S, Lavenir I, Forster A, Warren AJ, Grutz G, Foroni L, Carlton MB, Colledge WH, Boehm T, Rabbitts TH. 2004. Null mutation of the Lmo4 gene or a combined null mutation of the Lmo1/Lmo3 genes causes perinatal lethality, and Lmo4 controls neural tube development in mice. Mol Cell Biol 24:2063-2073.

Tseng BS, Cavin ST, Booth FW, Olson EN, Marin MC, McDonnell TJ, Butler IJ. 2000. Pulmonary hypoplasia in the myogenin null mouse embryo. Am J Respir Cell Mol Biol 22:304-315.

Turino GM, Ma S, Lin YY, Cantor JO, Luisetti M. 2011. Matrix elastin: a promising biomarker for chronic obstructive pulmonary disease. Am J Respir Crit Care Med. 184(6):637-41

Turner N, Grose R. 2010. Fibroblast growth factor signalling: from development to cancer. Nat Rev Cancer. 10(2):116-29.

Umehara T, Kida S, Hasegawa S, Fujimoto H, Horikoshi M. 1997. Restricted expression of a member of the transcription elongation factor S-II family in testicular germ cells during and after meiosis. J Biochem 121:598-603.

Usui H, Shibayama M, Ohbayashi N, Konishi M, Takada S, Itoh N. 2004. Fgf18 is required for embryonic lung alveolar development. Biochem Biophys Res Commun. 322:887-92.

van Genderen C, Okamura RM, Fariñas I, Quo RG, Parslow TG, Bruhn L, Grosschedl R. 1994. Development of several organs that require inductive epithelial-mesenchymal interactions is impaired in LEF-1-deficient mice. Genes Dev 8:2691-2703.

van Tuyl M, Liu J, Groenman F, Ridsdale R, Han RN, Venkatesh V, Tibboel D, Post M. 2006. Iroquois genes influence proximo-distal morphogenesis during rat lung development. Am J Physiol Lung Cell Mol Physiol 290:L777-L789.

Vargova J, Vargova K, Skoultchi AI, Stopka T. 2009. Nuclear localization of ISWI ATPase Smarca5 (Snf2h) in mouse. Front Biosci (Elite Ed) 1:553-559.

Vellanki RN, Zhang L, Guney MA, Rocheleau JV, Gannon M, Volchuk A. 2010. OASIS/CREB3L1 induces expression of genes involved in extracellular matrix production but not classical endoplasmic reticulum stress response genes in pancreatic beta-cells. Endocrinology 151:4146-4157.

Verdeguer F, Le Corre S, Fischer E, Callens C, Garbay S, Doyen A, Igarashi P, Terzi F, Pontoglio M. 2010. A mitotic transcriptional switch in polycystic kidney disease. Nat Med 16:106-110.

Vincent T, Neve EP, Johnson JR, Kukalev A, Rojo F, Albanell J, Pietras K, Virtanen I, Philipson L, Leopold PL, Crystal RG, de Herreros AG, Moustakas A, Pettersson RF, Fuxe J. 2009. A SNAIL1-SMAD3/4 transcriptional repressor complex promotes TGF-beta mediated epithelial-mesenchymal transition. Nat Cell Biol 11:943-950.

Visel A, Thaller C, Eichele G. 2004. GenePaint.org: an atlas of gene expression patterns in the mouse embryo. Nucleic Acids Res 32:D552-556.

von Both I, Silvestri C, Erdemir T, Lickert H, Walls JR, Henkelman RM, Rossant J, Harvey RP, Attisano L, Wrana JL. 2004. Foxh1 is essential for development of the anterior heart field. Dev Cell 7:331-345.

Volckaert T, Campbell A, Dill E, Li C, Minoo P, De Langhe S. 2013. Localized Fgf10 expression is not required for lung branching morphogenesis but prevents differentiation of epithelial progenitors. Development. 18:3731-42.

Vrhovski B, Weiss AS. Biochemistry of tropoelastin. Eur J Biochem 1998;258: 1–18.

Wagenseil and Mecham. 2007. New insights into elastic fiber assembly. Birth Defects Res C Embryo Today. 81(4):229-40.

Wall NA, Hogan BL. 1995. Expression of bone morphogenetic protein-4 (BMP-4), bone morphogenetic protein-7 (BMP-7), fibroblast growth factor-8 (FGF-8) and sonic hedgehog (SHH) during branchial arch development in the chick. Mech Dev 53:383-392.

Wan H, Dingle S, Xu Y, Besnard V, Kaestner KH, Ang SL, Wert S, Stahlman MT, Whitsett JA. 2005. Compensatory roles of Foxa1 and Foxa2 during lung morphogenesis. J Biol Chem 280:13809-13816.

Wan H, Kaestner KH, Ang SL, Ikegami M, Finkelman FD, Stahlman MT, Fulkerson PC, Rothenberg ME, Whitsett JA. 2004a. Foxa2 regulates alveolarization and goblet cell hyperplasia. Development 131:953-964.

Wan H, Xu Y, Ikegami M, Stahlman MT, Kaestner KH, Ang SL, Whitsett JA. 2004b. Foxa2 is required for transition to air breathing at birth. Proc Natl Acad Sci U S A 101:14449-14454.

Wang IC, Zhang Y, Snyder J, Sutherland MJ, Burhans MS, Shannon JM, Park HJ, Whitsett JA, Kalinichenko VV. 2010. Increased expression of FoxM1 transcription factor in respiratory epithelium inhibits lung sacculation and causes Clara cell hyperplasia. Dev Biol 347:301-314.

Wang T, Tamakoshi T, Uezato T, Shu F, Kanzaki-Kato N, Fu Y, Koseki H, Yoshida N, Sugiyama T, Miura N. 2003. Forkhead transcription factor Foxf2 (LUN)-deficient mice exhibit abnormal development of secondary palate. Dev Biol 259:83-94.

Wang VE, Schmidt T, Chen J, Sharp PA, Tantin D. 2004. Embryonic lethality, decreased erythropoiesis, and defective octamer-dependent promoter activation in Oct-1-deficient mice. Mol Cell Biol 24:1022-1032.

Wang X, Pasolli HA, Williams T, Fuchs E. 2008. AP-2 factors act in concert with Notch to orchestrate terminal differentiation in skin epidermis. J Cell Biol 183:37-48.

Wang ZM, Yang H, Livingston DM. 1998. Endogenous E2F-1 promotes timely G0 exit of resting mouse embryo fibroblasts. Proc Natl Acad Sci U S A 95:15583-15586.

Warburton D, El-Hashash A, Carraro G, Tiozzo C, Sala F, Rogers O, De Langhe S, Kemp PJ, Riccardi D, Torday J, Bellusci S, Shi W, Lubkin SR, Jesudason E. 2010. Lung organogenesis. Curr Top Dev Biol 90:73-158.

Warburton D, Schwarz M, Tefft D, Flores-Delgado G, Anderson KD, Cardoso WV. 2000. The molecular basis of lung morphogenesis. Mech Dev 92:55-81.

Weaver M, Yingling JM, Dunn NR, Bellusci S, Hogan BL. 1999. Bmp signaling regulates proximal-distal differentiation of endoderm in mouse lung development. Development 126:4005-4015.

Wei G, Srinivasan R, Cantemir-Stone CZ, Sharma SM, Santhanam R, Weinstein M, Muthusamy N, Man AK, Oshima RG, Leone G, Ostrowski MC. 2009. Ets1 and Ets2 are required for endothelial cell survival during embryonic angiogenesis. Blood 114:1123-1130.

Wei GH, Badis G, Berger MF, Kivioja T, Palin K, Enge M, Bonke M, Jolma A, Varjosalo M, Gehrke AR, Yan J, Talukder S, Turunen M, Taipale M, Stunnenberg HG, Ukkonen E, Hughes TR, Bulyk ML, Taipale J. 2010. Genome-wide analysis of ETS-family DNA-binding in vitro and in vivo. EMBO J. 29(13):2147-60.

Weinstein M, Xu X, Ohyama K, Deng CX. 1998. FGFR-3 and FGFR-4 function cooperatively to direct alveogenesis in the murine lung. Development 125:3615-3623.

Wendel DP, Taylor DG, Albertine KH, Keating MT, Li DY. 2000. Impaired distal airway development in mice lacking elastin. Am J Respir Cell Mol Biol. 23(3):320-6

Werling U, Schorle H. 2002. Transcription factor gene AP-2 gamma essential for early murine development. Mol Cell Biol 22:3149-3156.

Werth M, Walentin K, Aue A, Schönheit J, Wuebken A, Pode-Shakked N, Vilianovitch L, Erdmann B, Dekel B, Bader M, Barasch J, Rosenbauer F, Luft FC, Schmidt-Ott KM. 2010. The transcription factor grainyhead-like 2 regulates the molecular composition of the epithelial apical junctional complex. Development 137:3835-3845.

Whitsett JA, Matsuzaki Y. 2006. Transcriptional regulation of perinatal lung maturation. Pediatr Clin North Am 53:873-887, viii.

Whitsett JA, Weaver TE. 2002. Hydrophobic surfactant proteins in lung function and disease. N Engl J Med 347:2141-2148.

WILLIAMS JC, BARRATT-BOYES BG, LOWE JB. 1961. Supravalvular aortic stenosis. Circulation 24:1311-1318.

Wind M, Reines D. 2000. Transcription elongation factor SII. Bioessays 22:327-336.

Winger Q, Huang J, Auman HJ, Lewandoski M, Williams T. 2006. Analysis of transcription factor AP-2 expression and function during mouse preimplantation development. Biol Reprod 75:324-333.

Xu B, Qu X, Gu S, Doughman YQ, Watanabe M, Dunwoodie SL, Yang YC. 2008. Cited2 is required for fetal lung maturation. Dev Biol 317:95-105.

Xu Q; Tam M; Anderson SA. 2008. Fate mapping Nkx2.1-lineage cells in the mouse telencephalon. J Comp Neurol 506(1):16-29.

Yamamoto H, Flannery ML, Kupriyanov S, Pearce J, McKercher SR, Henkel GW, Maki RA, Werb Z, Oshima RG. 1998. Defective trophoblast function in mice with a targeted mutation of Ets2. Genes Dev 12:1315-1326.

Yamamoto M, Mine N, Mochida K, Sakai Y, Saijoh Y, Meno C, Hamada H. 2003. Nodal signaling induces the midline barrier by activating Nodal expression in the lateral plate. Development 130:1795-1804.

Yamashita T, Ohneda O, Nagano M, Iemitsu M, Makino Y, Tanaka H, Miyauchi T, Goto K, Ohneda K, Fujii-Kuriyama Y, Poellinger L, Yamamoto M. 2008. Abnormal heart development and lung remodeling in mice lacking the hypoxia-inducible factor-related basic helix-loop-helix PAS protein NEPAS. Mol Cell Biol 28:1285-1297.

Yamauchi T, Yamauchi J, Kuwata T, Tamura T, Yamashita T, Bae N, Westphal H, Ozato K, Nakatani Y. 2000. Distinct but overlapping roles of histone acetylase PCAF and of the closely related PCAF-B/GCN5 in mouse embryogenesis. Proc Natl Acad Sci U S A 97:11303-11306.

Yang H, Lu MM, Zhang L, Whitsett JA, Morrisey EE. 2002. GATA6 regulates differentiation of distal lung epithelium. Development 129:2233-2246.

Yanagisawa H, Schluterman MK, Brekken RA. 2009. Fibulin-5, an integrin-binding matricellular protein: its function in development and disease. J Cell Commun Signal. 3 :337-47.

Yates LL, Schnatwinkel C, Murdoch JN, Bogani D, Formstone CJ, Townsend S, Greenfield A, Niswander LA, Dean CH. 2010. The PCP genes Celsr1 and Vangl2 are required for normal lung branching morphogenesis. Hum Mol Genet 19:2251-2267.

Yeo GC, Keeley FW, Weiss AS. 2011. Coacervation of tropoelastin. Adv Colloid Interface Sci. 167:94-103.

Yi L, Domyan ET, Lewandoski M, Sun X. 2009. Fibroblast growth factor 9 signaling inhibits airway smooth muscle differentiation in mouse lung. Dev Dyn. 238:123-37

Yi M, Belcastro R, Shek S, Luo D, Post M, Tanswell AK. 2006. Fibroblast growth factor-2 and receptor-1alpha(IIIc) regulate postnatal rat lung cell apoptosis. Am J Respir Crit Care Med. 174: 581-9.

Yin Y, Wang F, Ornitz DM. 2011. Mesothelial- and epithelial-derived FGF9 have distinct functions in the regulation of lung development. Development. 138(15):3169-77.

Yokota Y, Mansouri A, Mori S, Sugawara S, Adachi S, Nishikawa S, Gruss P. 1999. Development of peripheral lymphoid organs and natural killer cells depends on the helix-loop-helix inhibitor Id2. Nature 397:702-706.

Yoshimura K, Kitagawa H, Fujiki R, Tanabe M, Takezawa S, Takada I, Yamaoka I, Yonezawa M, Kondo T, Furutani Y, Yagi H, Yoshinaga S, Masuda T, Fukuda T, Yamamoto Y, Ebihara K, Li DY, Matsuoka R, Takeuchi JK, Matsumoto T, Kato S. 2009. Distinct function of 2 chromatin remodeling complexes that share a common subunit, Williams syndrome transcription factor (WSTF). Proc Natl Acad Sci U S A 106:9280-9285.

You LR, Takamoto N, Yu CT, Tanaka T, Kodama T, Demayo FJ, Tsai SY, Tsai MJ. 2005. Mouse lacking COUP-TFII as an animal model of Bochdalek-type congenital diaphragmatic hernia. Proc Natl Acad Sci U S A 102:16351-16356.

Yu S, Poe B, Schwarz M, Elliot SA, Albertine KH, Fenton S, Garg V, Moon AM. 2010. Fetal and postnatal lung defects reveal a novel and required role for Fgf8 in lung development. Dev Biol. 2010 Nov 1;347(1):92-108.

Zhang Y, Goss AM, Cohen ED, Kadzik R, Lepore JJ, Muthukumaraswamy K, Yang J, DeMayo FJ, Whitsett JA, Parmacek MS, Morrisey EE. 2008. A Gata6-Wnt pathway required for epithelial stem cell development and airway regeneration. Nat Genet 40:862-870.

Zhang Z, Verheyden JM, Hassell JA, Sun X. 2009. FGF-regulated Etv genes are essential for repressing Shh expression in mouse limb buds. Dev. Cell 16:607-13

Zhang Z, Sui P, Dong A, Hassell J, Cserjesi P, Chen YT, Behringer RR, Sun X. 2010. Preaxial polydactyly: interactions among ETV, TWIST1 and HAND2 control anterior-posterior patterning of the limb. Development. 137:3417-26

Zheng H, Wasylyk C, Ayadi A, Abecassis J, Schalken JA, Rogatsch H, Wernert N, Maira SM, Multon MC, Wasylyk B. 2003. The transcription factor Net regulates the angiogenic switch. Genes Dev 17:2283-2297.

Zhou J, Chehab R, Tkalcevic J, Naylor MJ, Harris J, Wilson TJ, Tsao S, Tellis I, Zavarsek S, Xu D, Lapinskas EJ, Visvader J, Lindeman GJ, Thomas R, Ormandy CJ, Hertzog PJ, Kola I, Pritchard MA. 2005. Elf5 is essential for early embryogenesis and mammary gland development during pregnancy and lactation. EMBO J 24:635-644.